Re_2O_7-MEDIATED SPIROCYCLIC ETHER SYNTHESIS FROM ACYCLIC PRECURSORS: SYNTHESIS AND H_2O_2-MEDIATED TARGETED CELLULAR RELEASE OF A PEDERIN ANALOGUE

by

Cephas Ofoe Dodzi Afeke

B.Sc. (Hons.) Chemistry, University of Ghana, 2009

M.S. Youngstown State University, 2015

Submitted to the Graduate Faculty of the

Kenneth P. Dietrich School of Arts and Sciences in partial fulfillment

of the requirements for the degree of

Doctor of Philosophy

University of Pittsburgh

2021

UNIVERSITY OF PITTSBURGH

DIETRICH SCHOOL OF ARTS AND SCIENCES

This dissertation was presented

By

Cephas Ofoe Dodzi Afeke

It was defended on

July 23rd, 2021

and approved by

Dr. Kazunori Koide, Professor, Department of Chemistry

Dr. Kabirul Islam, Assistant Professor, Department of Chemistry

Dr. Donna Huryn, Professor, Department of Pharmaceutical Sciences

Dissertation Director: Dr. Paul Floreancig, Professor, Department of Chemistry

Re_2O_7-MEDIATED SPIROCYCLIC ETHER SYNTHESIS FROM ACYCLIC PRECURSORS: SYNTHESIS AND H_2O_2-MEDIATED TARGETED CELLULAR RELEASE OF A PEDERIN ANALOGUE

Cephas Ofoe Dodzi Afeke, PhD

University of Pittsburgh, 2021

The synthesis of spirocyclic ethers from acyclic precursors bearing ketones that are flanked by an allylic alcohol and an alkene in the presence of Re_2O_7 via a sequence of allylic alcohol transposition, oxocarbenium ion formation, and Prins cyclization is described. The method is atom economical and results in significant increases in molecular complexity, with multiple stereocenters being set relative to a stereocenter in the substrate.

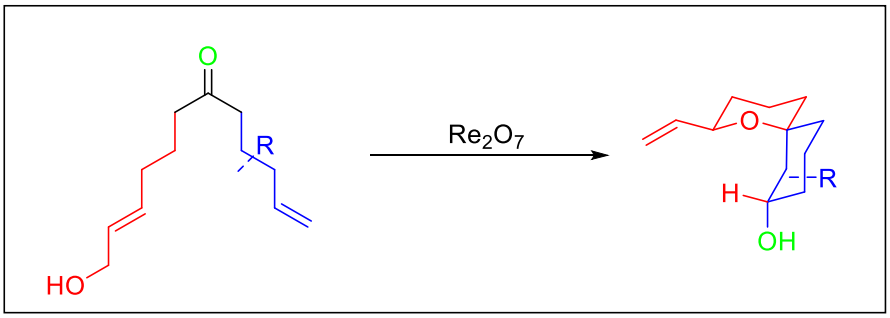

The use of self-immolative linkers in stimulus-responsive release of organic molecules and biological effectors demonstrate utility for the development of prodrugs and other therapeutics. This project describes the total synthesis of a pederin analogue (10-demethoxy-13-*O*-methyl pederin) which has shown cytotoxicity towards a number of cancer cells. Subsequent borylation of the analogue at the *C7*-hydroxy substituent via a new borylation strategy afforded a small molecule biological agent which leverages the unique hydrogen peroxide environment of cells

under oxidative stress to release the cytotoxic pederin analogue, thereby providing an opportunity for future advancements in anticancer therapy.

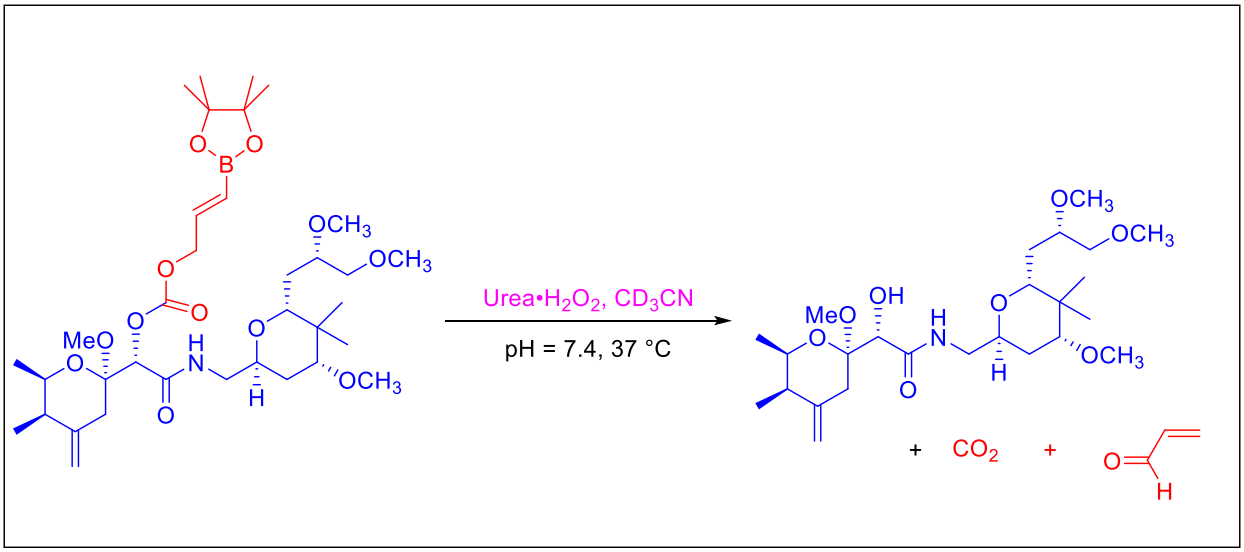

TABLE OF CONTENTS

ACKNOWLEDGEMENTS xiv

1.0 Re_2O_7-MEDIATED SPIROCYCLIC ETHER SYNTHESIS FROM ACYCLIC PRECURSORS 1

1.1 Introduction 1

1.1.1 Review of the synthesis of spirocyclic compounds 2

1.1.1.1 Iodine-mediated spirocycle formation 2

1.1.1.2 Acid/base-promoted spirocycle formation 3

1.1.1.3 Biologically active natural products 5

1.1.1.4 Acid-catalyzed intramolecular S_N1 oxaspirocyclization 5

1.1.1.5 Spirocyclization oxocarbenium ion-initiated pinacol rearrangement 6

1.2 Rhenium(VII) Oxide Chemistry 7

1.2.1 Re_2O_7-catalyzed lactol formation Leucascandrolide A total synthesis 8

1.2.2 Formation of bridged and spirocyclic ketals 8

1.2.3 Epoxide trapping mechanism in the formation of tetrahydropyran rings 9

1.2.4 Heterocycle formation via traceless trapping groups 10

1.2.5 Functional group tolerance and competitive termination by π-nucleophile. 11

1.2.6 Re_2O_7-catalyzed Prins reaction 13

1.2.7 Problem statement & research objective 14

1.3 Results and Discussion 14

1.4 Conclusion 28

1.5 Experimental 29

1.5.1 General information 29

1.5.2 General procedure for Re2O7-catalyzed spirocycle formation 30

1.5.3 General procedure for reaction optimization.....34

1.5.4 General procedure for conversion studies (kinetic experiment) 34

1.5.5 Determination of stereochemistry at quaternary stereocenter.....35

1.5.5.1 Procedure for oxidation of (6) and (7) 35

1.5.5.2 Procedure for hydrazone preparation for X-ray studies 36

2.0 SYNTHESIS AND H2O2-MEDIATED TARGETED CELLULAR RELEASE OF A PEDERIN ANALOGUE..... 53

2.1 Introduction 53

2.2 The Role of Boron in Drug Design..... 54

2.2.1 Boronate-based small molecules for H2O2-mediated molecular release.....55

2.2.2 Research objectives 59

2.3 Results and Discussion..... 62

2.3.1 Total synthesis of a pederin analogue 62

2.3.2 Borylation of pederin analogue.....66

2.3.3 Pederin analogue release and cell viability studies 68

2.4 Conclusion..... 74

2.5 Experimental..... 74

2.5.1 General information 74

2.5.2 Pederin analogue synthesis.....75

2.5.3 Boronate breakdown – ^{1}H NMR study 89

2.5.3.1 ^{1}H NMR sample preparation 89

2.5.3.2 Procedure for monitoring pederin breakdown of pederin analogue 2.36 89

APPENDIX A (SPECTROSCOPIC DATA FOR CHAPTER 1) 90

APPENDIX B (SPECTROSCOPIC DATA FOR CHAPTER 2) 152

BIBLIOGRAPHY 170

LIST OF TABLES

Table 1.1 Optimization study for spirocycle formation 19

LIST OF FIGURES

Figure 1.1 Representative bio-active spiroketals 5

Figure 1.2 X-ray crystal structure of derived hydrazone from 11 18

Figure 1.3 Diastereocontrol as a function of conversion 20

Figure 2.1 Boron-containing drugs approved by FDA..... 55

Figure 2.2 Structure of pederin 60

Figure 2.3 A) Proposed pederin analogue as biological effector B) Similar less potent analogue 61

Figure 2.4 Evaluation of cytotoxicity of pederin analogues and doxorubicin 70

Figure 2.5 1H NMR analysis of pederin boronate breakdown..... 71

Figure 2.6 Breakdown of pederin boronate 2.36 over time..... 72

Figure 2.7 Biological evaluation of pederin-boronate 2.36 73

Figure 2.8 Evaluation of boronate release in HeLa cells stimulated with paraquat..... 73

LIST OF SCHEMES

Scheme 1.1 Oxidative spirocyclization of para-substituted phenol to spirodienone 3

Scheme 1.2 Oxidative spirocyclization of p-substituted phenolic substrate to aculeatin A & B 3

Scheme 1.3 Base-catalyzed cyclization in the synthesis of (±)-acorone and (±)-isoacorone ... 4

Scheme 1.4 Spirocyclization in the synthesis of Hinesol 4

Scheme 1.5 Amberlyst-15-catalyzed oxaspirocyclization in synthesis of thespirane and analogue. 6

Scheme 1.6 Synthesis of naturally occurring spirocyclic ethers via oxocarbenium ion initiated pinacol rearrangement 7

Scheme 1.7 Re_2O_7-mediated allylic alcohol transposition and lactol formation 8

Scheme 1.8 Formation of bridged and spirocyclic ketals 9

Scheme 1.9 Mechanism for epoxide trapping 30 10

Scheme 1.10 Top - Transposition, trapping, ionization and nucleophilic termination sequence. Bottom - An analysis of competitive processes for relative diastereocontrol. a = isomerization, b = cyclization, c = ionization, d = termination 11

Scheme 1.11 Functional group tolerance of the traceless trapping reaction 12

Scheme 1.12 Formation of spirocyclic products 12

Scheme 1.13 Plausible mechanism for the formation of spirocyclic products 13

Scheme 1.14 Re(VII) catalyzed Prins cyclization 13

Scheme 1.15 Preparation of 5 16

Scheme 1.16 Spirocyclic ether formation 17

Scheme 1.17 Preparation of 12 21

Scheme 1.18 Relative stereocontrol from a chiral substrate 22

Scheme 1.19 Preparation of substrate 18 23

Scheme 1.20 Diminished stereocontrol via allylic 1,2-strain 24

Scheme 1.21 Influence of stereocenters on the cyclohexane ring system 24

Scheme 1.22 Effect of incorporating a substituent into the cyclohexane subunit 25

Scheme 1.23 Alkyne nucleophile in cyclization reaction 26

Scheme 1.24 1,1-Disubstituted alkene in cyclization reaction 27

Scheme 1.25 (Z) alkene substrate in cyclization reaction 27

Scheme 1.26 (E) alkene substrate leading to dehydration 28

Scheme 2.1 Fluorophore release through aryl boronate oxidation and 1,6-elimination 55

Scheme 2.2 Boronate probe in H_2O_2-mediated reporter signal release 56

Scheme 2.3 Synthesis and degradation of Oxi-DEX 57

Scheme 2.4 Peroxide-mediated alcohol release from α-alkoxy carbamate 58

Scheme 2.5 A) Molecular release in the presence of H_2O_2. B) Synthesis of α-boryl ethers and related structures 59

Scheme 2.6 Retrosynthetic analysis of pederin analogue 62

Scheme 2.7 Synthesis of keto alcohol 22 63

Scheme 2.8 Synthesis of nitrile 2.20 from keto alcohol 2.22 63

Scheme 2.9 Preparation of 2.27 64

Scheme 2.10 Synthesis of pederic acid fragment 2.19 65

Scheme 2.11 Completion of the synthesis of analogue 2.18 66

Scheme 2.12 Unsuccessful initial attempt at borylation 67

Scheme 2.13 α-alkoxy carbamate synthesis 67

Scheme 2.14 Preparation of borylated pederin analogue 2.36 and negative 2.34 control from 2.18..... 68

Scheme 2.15 Boronate linker cleavage from compound 2.36..... 71

ACKNOWLEDGEMENTS

I would like to thank my research advisor, Prof. Paul Floreancig, for accepting me into his research group and offering the mentorship that I enjoyed throughout my period of study in Pittsburgh. I could certainly not have completed my degree without his support and encouragement. I would like to thank my dissertation committee members Prof. Kazunori Koide, Prof. Kabirul Islam and Prof. Donna Huryn for all their feedback and for accepting to be on my committee.

I would like to personally thank all of my colleagues from the Floreancig lab for being a great learning partners and friends. My experiences with you have shaped my life entirely and I am truly grateful.

I would also like to thank Prof. Alex Deiters and Prof. Tara Meyer for their support and also Amy Ryan of the Deiters' lab for her support and experience in the course of the drug delivery project. This dissertation document would not be complete without data from biological studies that she carried out.

Finally, I wish to thank my family for all the love and outstanding support throughout this journey. It has always never been easy but their belief and encouragement have been wonderful and have made this journey worthwhile.

1.0 Re_2O_7-MEDIATED SPIROCYCLIC ETHER SYNTHESIS FROM ACYCLIC PRECURSORS

1.1 Introduction

The advantage of structural complexity with respect to target selectivity is revealed in recent surveys[1] of compounds at the various stages of drug discovery, highlighting the importance of developing new methods to increase complexity.[2] Numerous metrics can be used to assess molecular complexity. Allu and co-workers[3] proposed a simple and flexible metric to calculate molecular complexity, which is aimed at lowering the correlation with molecular weight. Results based on over 260,000 molecules indicate that the synthetic and molecular complexity (SMCM) score is the least correlated to molecular weight, when compared to two other known complexity measures by Baron and Chanon[4] as well as Bertz and co-workers.[5] However, the intuitive approach reported by Whitlock[6] provides a simple guide for determining the change in complexity in a reaction. In this approach, Whitlock used the number of rings, unsaturated bonds, heteroatoms, and chiral centers to calculate the complexity of natural products. Our group has used these metrics to guide a program directed toward the rapid generation of spirocyclic and bridged bicyclic acetals from structurally simple precursors. Xun Han's work in spiroacetal formation through telescoped cycloaddition and carbon–hydrogen bond functionalization,[7] Peh's convergent one-pot oxidative [*n + 1*] approaches to spiroacetal synthesis,[8] Hanna's diverted total synthesis of potent and rapidly accessible Bistramide analogues[9] as well as Caplan's total synthesis of Divergolide E and H[10] highlight these efforts. This dissertation describes a new rearrangement reaction that results in the

formation of structurally complex spirocyclic ethers from acyclic precursors, in which two rings and up to four stereocenters are generated.

1.1.1 Review of the synthesis of spirocyclic compounds

Spirocycles are common components in many biologically active compounds.[11] Their structural rigidity allows for the orientation of functional groups in unique spatial arrangements, and when used appropriately, spirocyclization provides an excellent way to enforce the desired conformation for ligand–protein binding.[12] Furthermore, conformational restriction may reduce off-target activities.[13] The structural complexity of spirocycles also lends inspiration to synthetic chemists in developing new approaches for accessing these scaffolds.[14]

1.1.1.1 Iodine-mediated spirocycle formation

Ley and co-workers used a polymeric (diacetoxyiodo)benzene (PIDA) reagent to achieve the synthesis of the spirocyclic core of natural product *(+)*-epidihydromaritidine (Scheme 1.1). In this report, para-substituted phenol (I) was cyclized to spirodienone (II) using polymer supported (diacetoxy)iodobenzene reagent. The desired product was obtained in 70% yield without conventional work-up procedure and purification by chromatographic technique. Furthermore, the synthesized spirocyclic compound (II) was converted into the alkaloid (+)-epidihydromaritidine (III) in three chemical steps.[15]

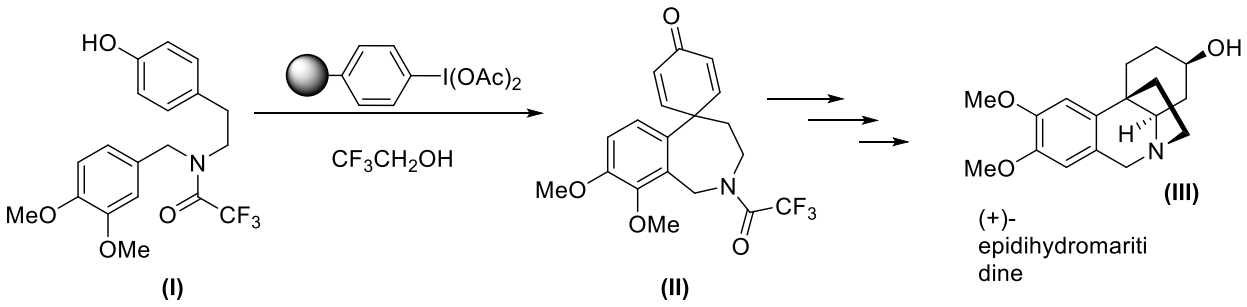

Scheme 1.1 Oxidative spirocyclization of para-substituted phenol to spirodienone

Similarly, Marco and co-workers reported the synthesis of naturally occurring spiroacetals aculeatin A and B with the use of [Bis(trifluoroacetoxy)iodo]benzene (PIFA) as an electrophile (IV) in one step during their synthesis. (Scheme 1.2).[16]

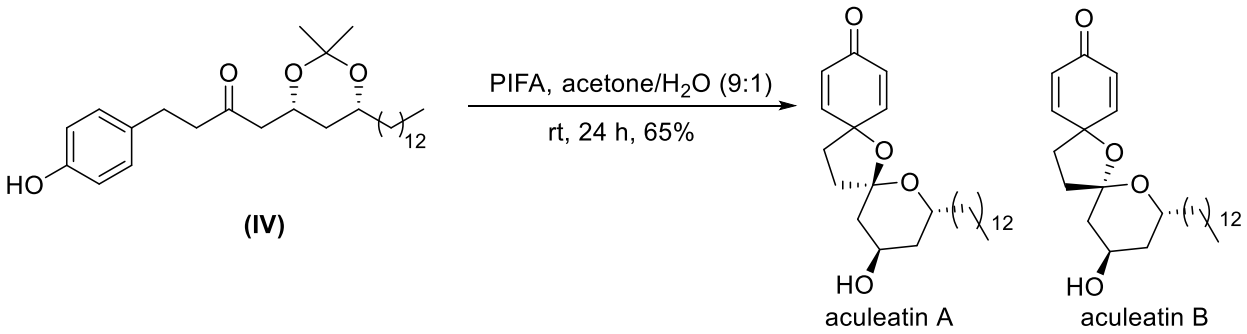

Scheme 1.2 Oxidative spirocyclization of p-substituted phenolic substrate to aculeatin A & B

1.1.1.2 Acid/base-promoted spirocycle formation

The Dolby group accomplished the synthesis of (±)-acorone from 4-methyl-3-cyclohexene carboxaldehyde (V) using an intramolecular base-catalyzed (NaOEt in ethanol) aldol cyclization.[17] A similar method reported by Martin et al. in 1978 used base-promoted aldol cyclo-condensation to synthesize racemic acorone (Scheme 1.3).[18]

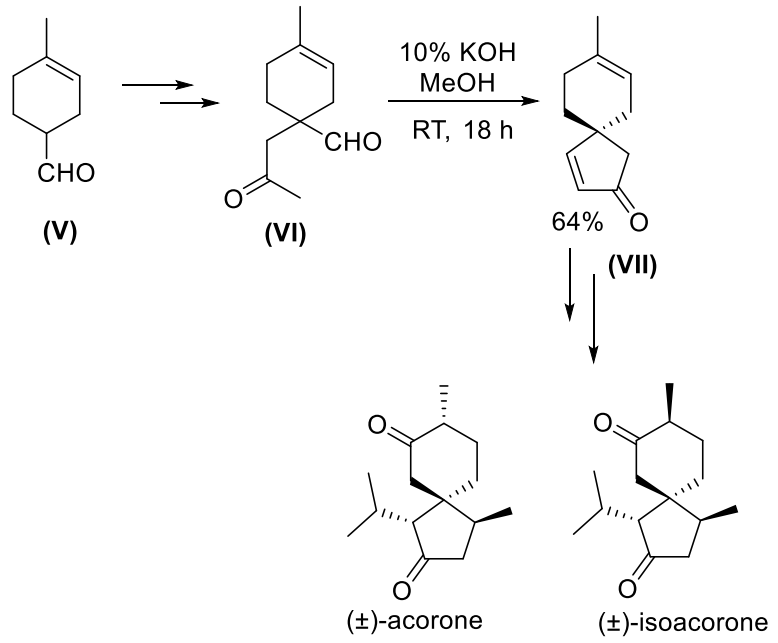

Scheme 1.3 Base-catalyzed cyclization in the synthesis of (±)-acorone and (±)-isoacorone

Deslongchamps and co-workers also embarked on the synthesis of agarospirol and hinesol from a ketoester (VIII) in which the common spirocyclic core (XI) of the compounds was accessed by treatment of a cyclopropane intermediate (IX) with acid (Scheme 1.4).[19]

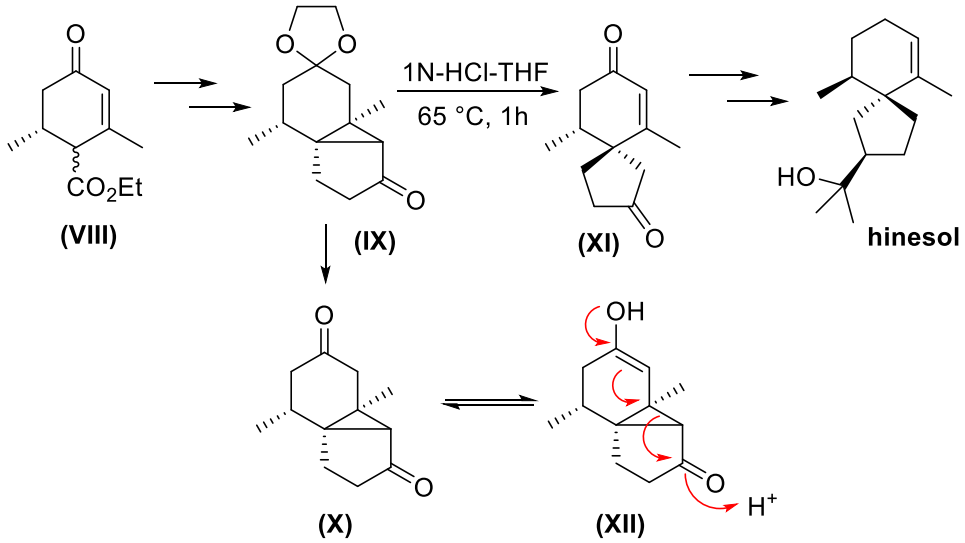

Scheme 1.4 Spirocyclization in the synthesis of Hinesol

1.1.1.3 Biologically active natural products

Spiroacetals are frequently found in biologically active natural products[20] and as such are increasingly being used as scaffolds in high throughput chemistry for drug discovery (Figure 1.1).

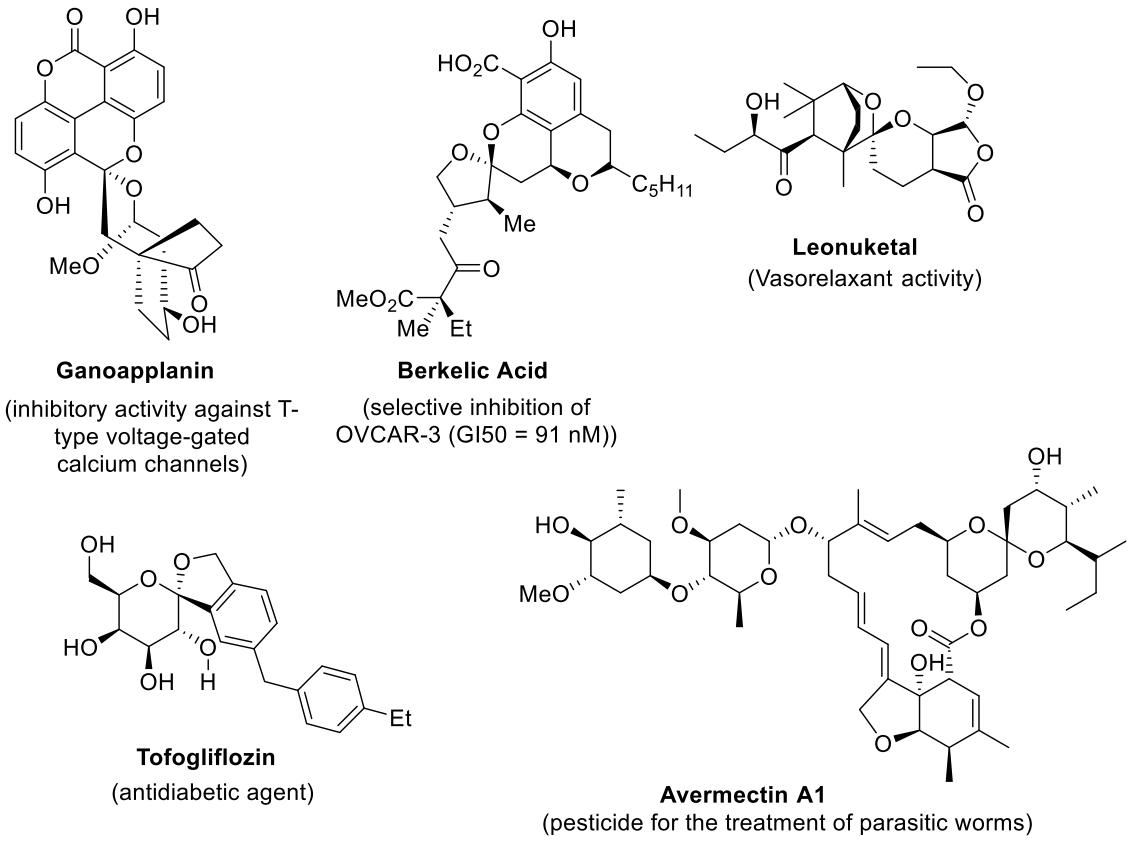

Figure 1.1 Representative bio-active spiroketals

Spirocyclic ethers, while less common, provide a similar geometry and rigidity and are not susceptible to acid-mediated ring opening, suggesting that these structures could be useful entries in lead-generation efforts.[21]

1.1.1.4 Acid-catalyzed intramolecular S_N1 oxaspirocyclization

Notable amongst these efforts is the methodology by Young and co-workers describing an Amberlyst-15-catalyzed intramolecular S_N1' oxaspirocyclization of allylic alcohols providing

spirocyclic ethers in quantitative yields. This method has also been applied to the total synthesis of theaspirane and theaspirone (Scheme 1.5).[22] The synthesis commenced by selective reduction of the α,β-unsaturated bond in β-ionine (XVI) using triphenyltin hydride to give a ketone intermediate (XIII) with a C-C single bond. Subsequent oxidation of the allylic methylene group of the ketone intermediate (XIII) with *tert*-butyl hydroperoxide and catalytic amount of chromic anhydride, followed by Luche reduction of the enone gave the diol (XIV). Amberlyst-15-catalyzed S_N1' oxaspirocyclization finally converted the secondary allylic alcohol into theaspirane (XV) in 95% yield, which by allylic oxidation afforded theaspirone (XVII) in 67% yield.

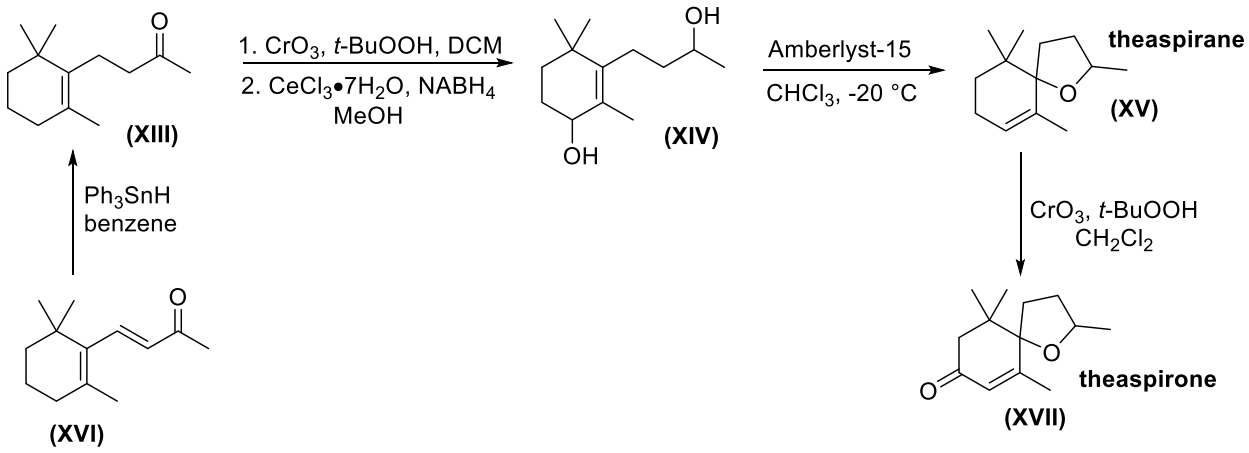

Scheme 1.5 Amberlyst-15-catalyzed oxaspirocyclization in synthesis of thespirane and analogue.

1.1.1.5 Spirocyclization via oxocarbenium ion-initiated pinacol rearrangement

Paquette and co-workers described the preparation of the natural products dactyloxene B and C in seven steps from a common chiral intermediate **XX** (Scheme 1.6).[23] The synthesis involved the nucleophilic addition of a substituted dihydrofuran (XVIII) into *trans*-2,3-dimethylcyclopentanone (XIX). The product of this reaction (XX) was then treated with Dowex-50× 4-400 resin for two days to provide the desired chromatographically separable spirocyclic

ketone intermediates **XXI** and **XXII** in 63% combined yield. These intermediates were further functionalized in a few steps to obtain the natural products.

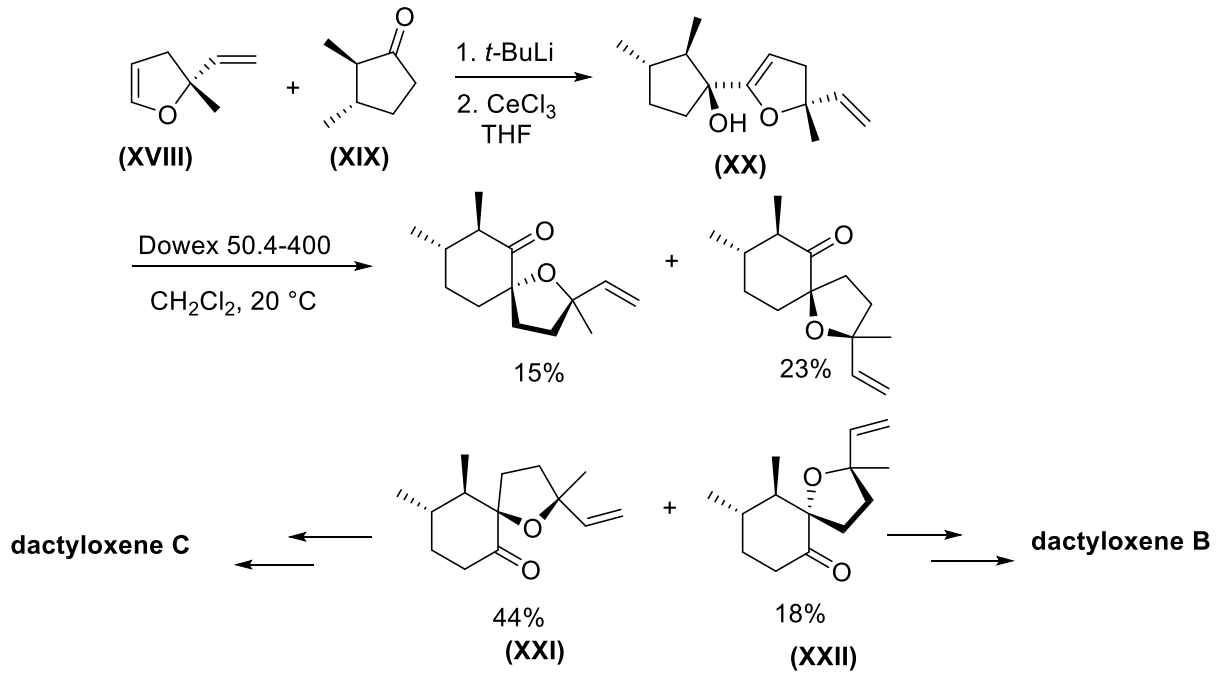

Scheme 1.6 Synthesis of naturally occurring spirocyclic ethers via oxocarbenium ion initiated pinacol rearrangement

1.2 Rhenium(VII) Oxide Chemistry

Since the original report by Osborn and co-workers on the use of rhenium(VII) oxide in the 1,3-transposition of allyl alcohols[24], the methodology has widely been studied and applied for the transposition of a variety of 1°, 2° and 3° allylic alcohols in the synthesis of useful organic molecules and synthetic intermediates.[25,26]

1.2.1 Re_2O_7-catalyzed lactol formation Leucascandrolide A total synthesis

Jung and co-workers embarked on the total synthesis of leucascandrolide A macrolactone, in which one of the later steps required allylic alcohol transposition prior to the macrolide formation.[27] They postulated that the desired transposed product would be formed preferentially under equilibrating conditions due to the capacity of the transposed alcohol to engage in hydrogen bonding with the tetrahydropyran ether, and in consideration of the report by Kozmin and co-workers[28] of the unexpected stability of the leucascandrolide macrolactol, for its potential to add into the pendent C_1 carbonyl group. Subjecting the untransposed alcohol (**1b**) to Re_2O_7 in Et_2O gave the desired lactol product in 69% yield (Scheme 1.7).

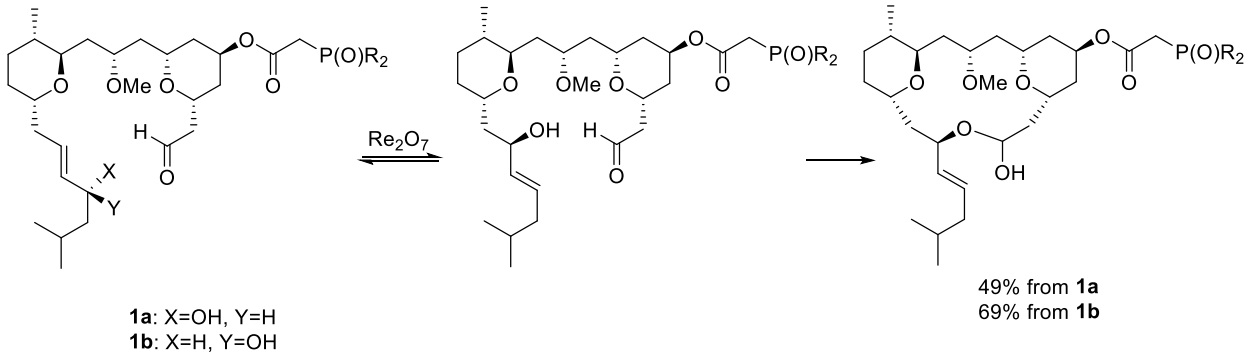

Scheme 1.7 Re_2O_7-mediated allylic alcohol transposition and lactol formation

1.2.2 Formation of bridged and spirocyclic ketals

Xie and co-workers demonstrated that the experimentally facile sequence of Re_2O_7-mediated allylic alcohol isomerization followed by nucleophilic addition into an oxocarbenium ion can be used to generate stereocenters with high levels of thermodynamic control[29]. They concluded that stereocontrol is maximized when the energetic difference between diastereomeric

products is sufficient to create a strong preference, when reversibility in the cyclization reaction is facilitated by increasing the stability of the oxocarbenium ion intermediate, and when stereochemical scrambling is promoted by increasing the substitution on the intermediate allyl cation. Applying these principles to more complex substrates led to the syntheses of bridged and spirocyclic ketals with good to excellent levels of stereocontrol (Scheme 1.8).

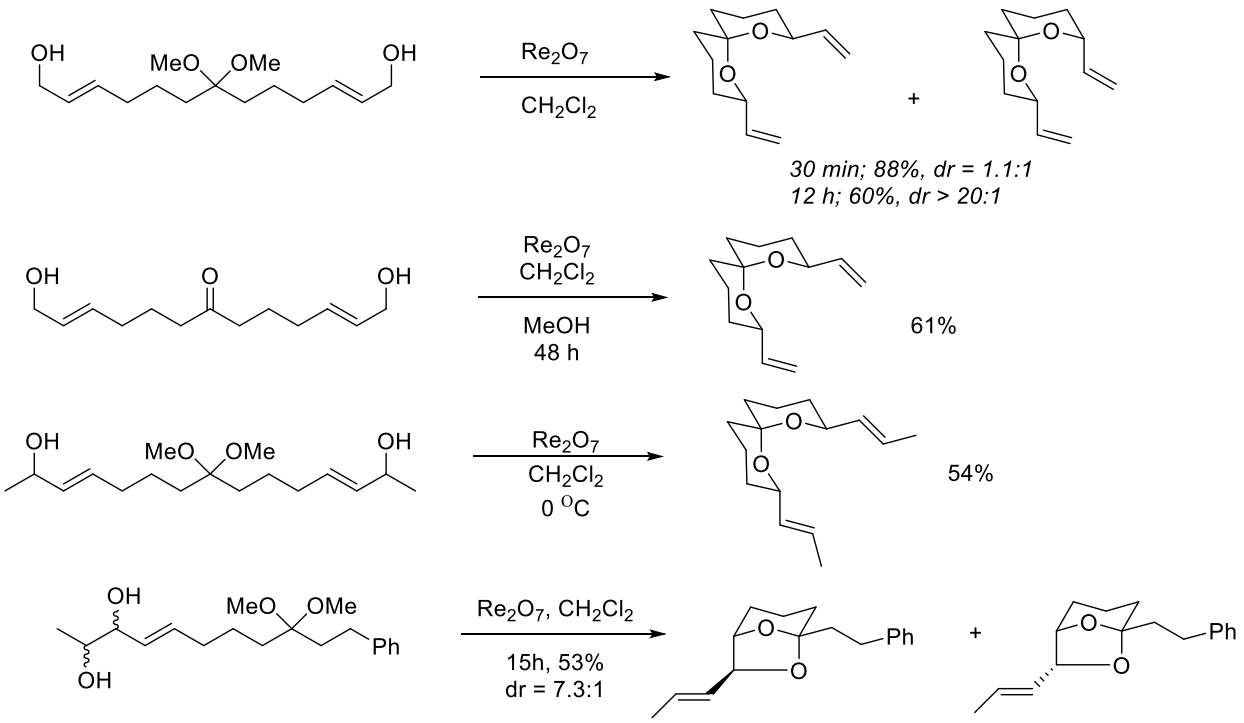

Scheme 1.8 Formation of bridged and spirocyclic ketals

1.2.3 Epoxide trapping mechanism in the formation of tetrahydropyran rings

Xie and co-workers also demonstrated that epoxide cascade reactions can be initiated by rhenium(VII) oxide mediated allylic alcohol transposition reactions. These transformations are possible because rhenium oxide has dual roles as a transposition catalyst and as an acid that

enhances the electrophilicity of the epoxide group and promotes product ionization, thereby allowing thermodynamically controlled stereochemical equilibration (Scheme 1.9).[30]

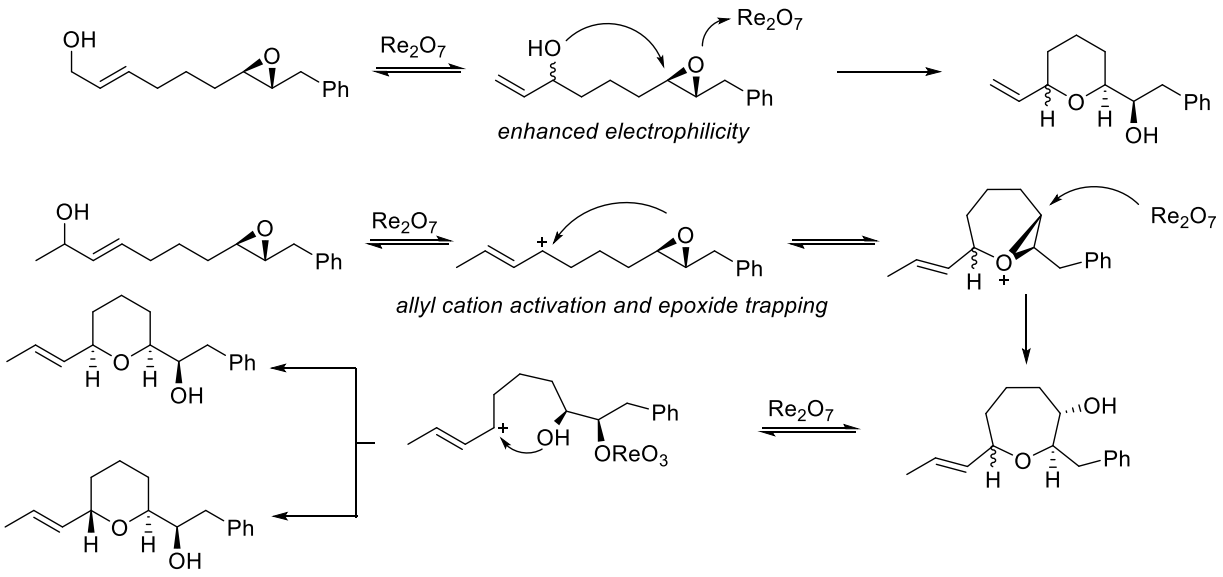

Scheme 1.9 Mechanism for epoxide trapping 30

1.2.4 Heterocycle formation via traceless trapping groups

Previous studies into the utility of Re_2O_7 in heterocycle synthesis leave vestiges of the electrophiles from the starting substrates in the final product, leading Xie and co-workers to subsequently demonstrate an approach to heterocycle synthesis via Re_2O_7 a cascade sequence of allylic alcohol transposition, intramolecular trapping, ionization and intermolecular termination, involving the use of traceless electrophiles. Aldehydes and ketones act as trapping groups, and silanes, π-nucleophiles and alcohols act as terminating agents in the formation of various tetrahydrofuran and tetrahydropyran products. (Scheme 1.10).[31] They concluded, work that relative stereochemistry of reactions with chiral substrates could be achieved by manipulating the

rates of transposition and termination (i.e. high stereocontrol can be achieved when the rate of transposition is high, and the rate of termination is low).

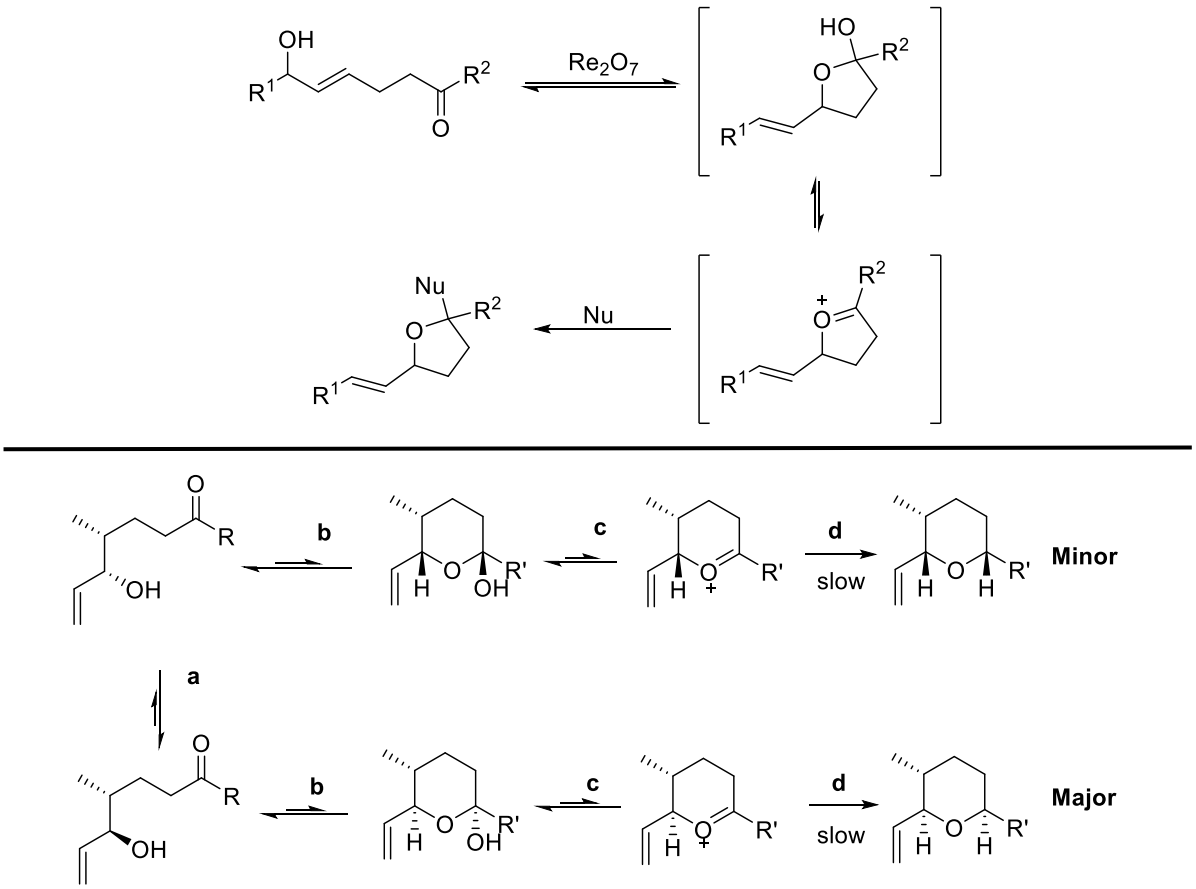

Scheme 1.10 Top - Transposition, trapping, ionization and nucleophilic termination sequence. Bottom - An analysis of competitive processes for relative diastereocontrol. a = isomerization, b = cyclization, c = ionization, d = termination

1.2.5 Functional group tolerance and competitive termination by π-nucleophile

Xie established tolerance of this reaction with a variety of functional groups including esters, bromides and alkenes (Scheme 1.11).[31]

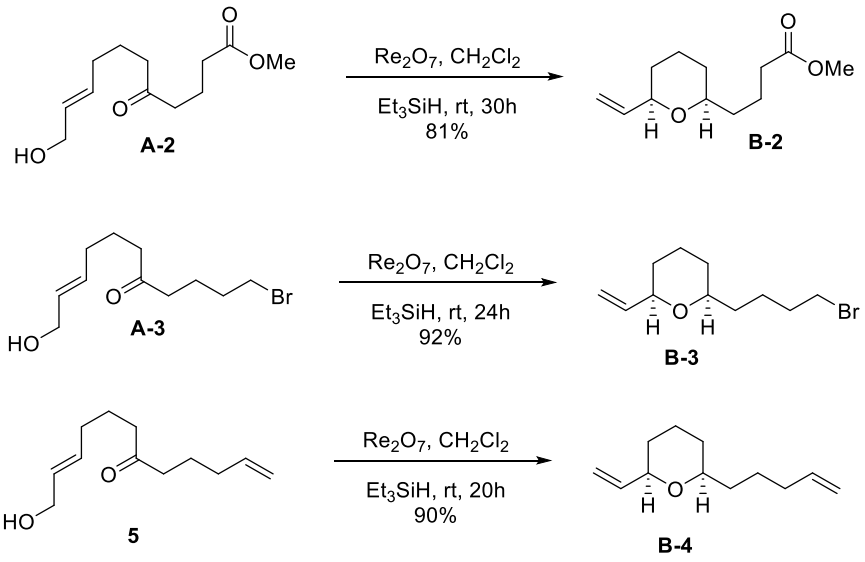

Scheme 1.11 Functional group tolerance of the traceless trapping reaction

However, upon screening the alkene substrate **A-4** under the conditions for the bimolecular reaction, Xie and co-workers observed the formation of spirocyclic ether side products (<10%) which were identified as **6** and **7** in addition to the expected product **B-4**. Substrate **A-4**, when exposed to Re_2O_7 without the addition of Et_3SiH, delivered a combined yield of 91% of **6** and **7** in a 2.5:1 ratio (Scheme 1.12).[32] Hence establishing the fact that the intermolecular trapping by Et_3SiH is much faster than intramolecular trapping by an alkene.

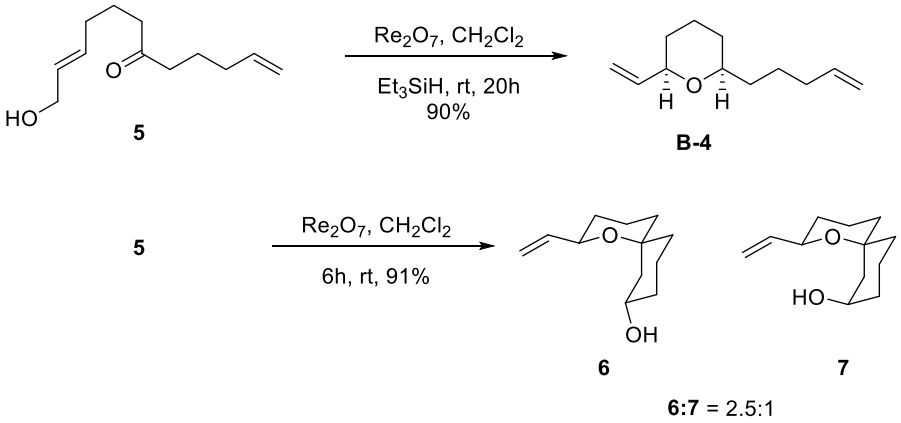

Scheme 1.12 Formation of spirocyclic products

Xie postulated that the formation of **6** and **7** occurs through a Prins[32,33] cyclization reaction between the pendent alkene and the oxocarbenium ion intermediate via a possible mechanism in Scheme 1.13, with perrhenate ion or traces of water quenching the resultant carbocation.

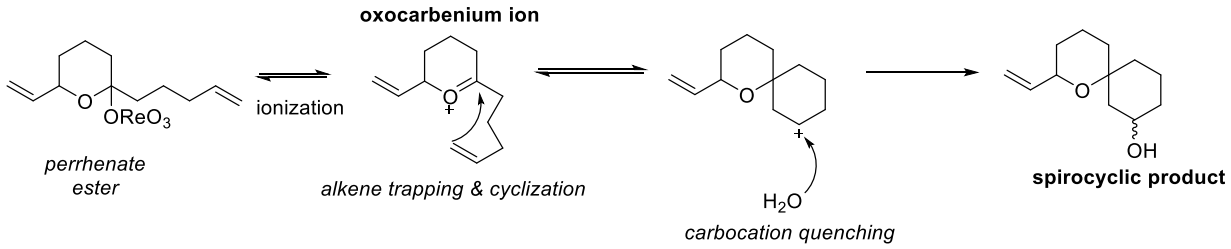

Scheme 1.13 Plausible mechanism for the formation of spirocyclic products

1.2.6 Re_2O_7-catalyzed Prins reaction

This interesting result bears similarity with the report by Rychnovsky and co-workers of Prins cyclization reactions catalyzed by Re(VII) complexes (Scheme 1.14).[34]

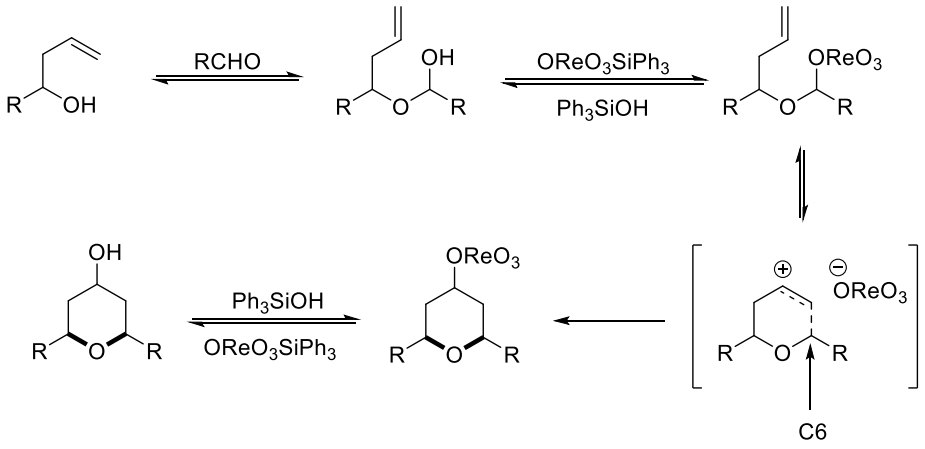

Scheme 1.14 Re(VII) catalyzed Prins cyclization

In their study, activation was achieved via the formation of perrhenate ester from the hemiacetal, and solvolysis of the ester to form a tight ion pair intermediate with the pendent alkene adding into the carbocation and leading to cyclization and hydroxy-substituted THP formation.

1.2.7 Problem statement & research objective

Despite the enormous efforts over the last few years in developing stereoselective methods for the synthesis of complex structures, the regio and stereocontrolled generation of tertiary carbon centers continue to be an important goal in organic synthesis and particularly so in the formation of spirocyclic scaffolds.[35]

The objective of this research, motivated by Xie's observation of the formation of spirocyclic products with Re_2O_7 in the absence of an external nucleophilic quencher in the bimolecular reaction, is to explore the unimolecular Re_2O_7-catalyzed pathway as a viable synthetic approach towards the formation of a variety of spirocycles from acyclic precursors. This research also seeks to investigate the level of control that existing stereocenters in the acyclic precursors have on the generation of new stereocenters in the spirocyclic products.

1.3 Results and Discussion

We began with the synthesis of compound **5**, which was the substrate used by Xie in his work that generated the spirocyclic ether. Olefin cross metathesis between 5-bromo-1-pentene and *cis*-2-butene-1,4-diol catalyzed by the second-generation Grubbs-Hoveyda catalyst and subsequent alcohol protection afforded the allyl alcohol **S2**. Lithium-halogen exchange and

nucleophilic acyl substitution with the Weinreb amide followed by deprotection afforded compound **5** in 40% yield (Scheme 1.15). We also observed quantitative amounts of Wurtz coupling products as reason for the poor yield.

Subjecting substrate 5 to Re2O7 in CH2Cl2 at room temperature quickly and efficiently afforded spirocyclic ether 6 and its diastereomer 7 in 94% overall yield as a 4:1 mixture (Scheme 1.16). This transformation generates two rings and three stereocenters with good atom economy. The major isomer was the equatorial alcohol as determined by 1H NMR coupling constant as well as one-dimensional Nuclear Overhauser Effect (NOE) analyses, and the relative stereocontrol between the alkene-containing stereocenter and the fully substituted carbon was extremely high. We propose that the reaction proceeds through the formation of oxocarbenium ion 8, followed by Prins-type cyclization through a chair transition state with nucleophilic attack by the alkene from the stereoelectronically preferred axial trajectory, and perrhenate approach through an anti-addition pathway36 to generate perrhenate ester 9.

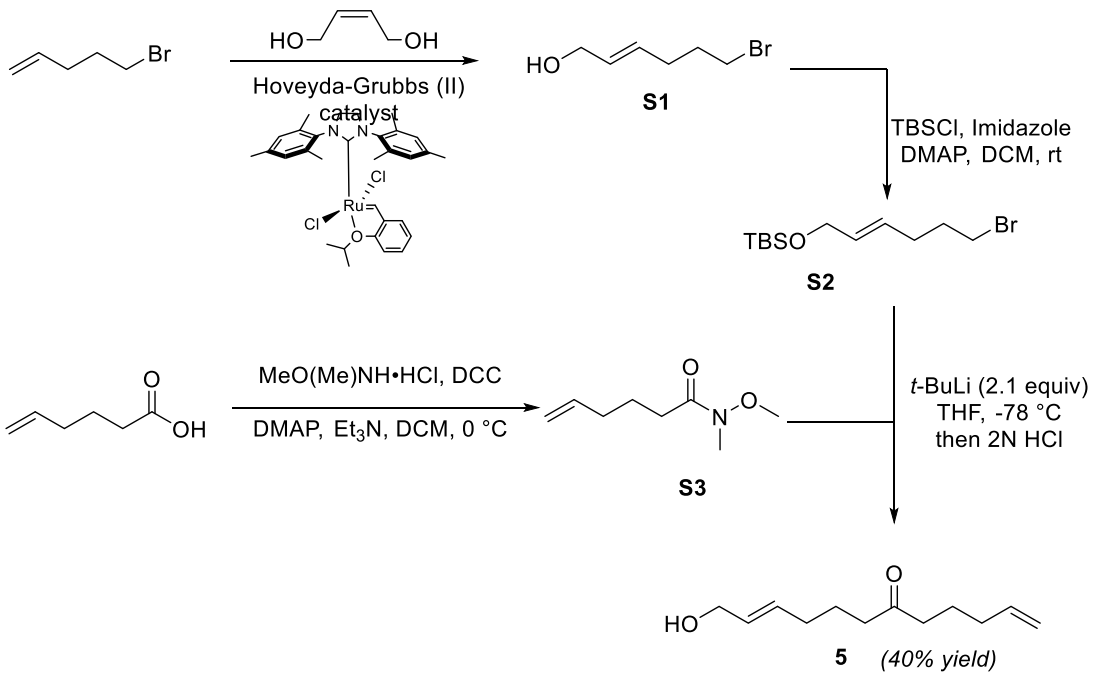

Scheme 1.15 Preparation of 5

Perrhenate ester cleavage with HOReO3 provides the major isomer while regenerating Re2O7. The formation of the minor isomer could either arise from a syn-addition in the Prins step37 or through the intermediacy of boat transition state 10. Independent oxidations of 6 and 7 produced the common ketone 11, in which the structure was confirmed by crystallographic analysis of the corresponding 2,4-dinitrophenylhydrazone (Figure 1.2),38 thereby confirming that epimeric alcohols were produced in this reaction.

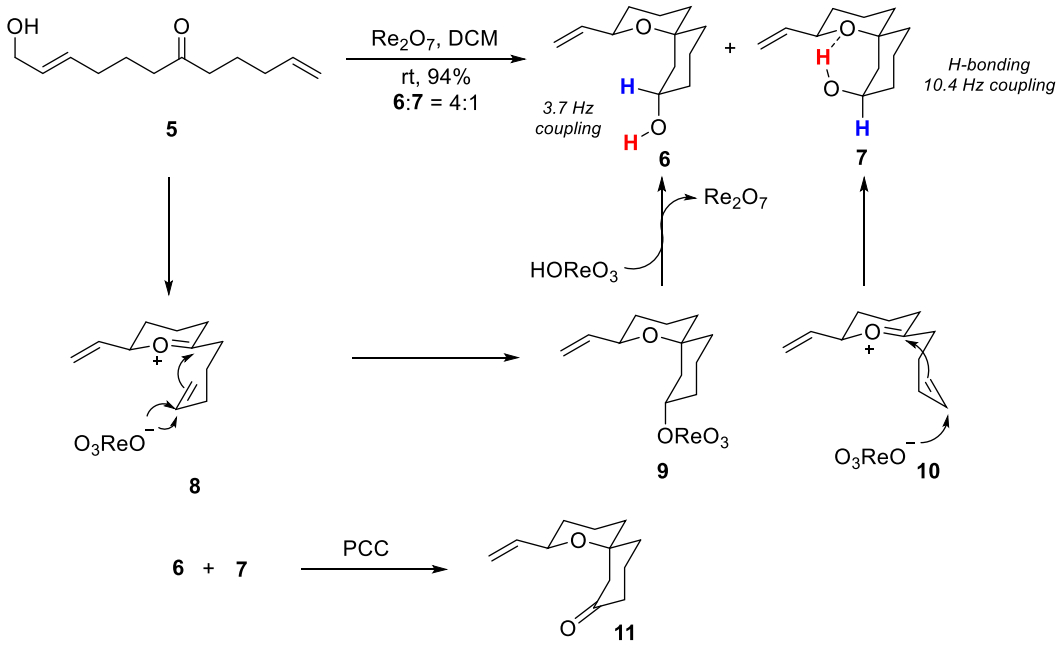

Scheme 1.16 Spirocyclic ether formation

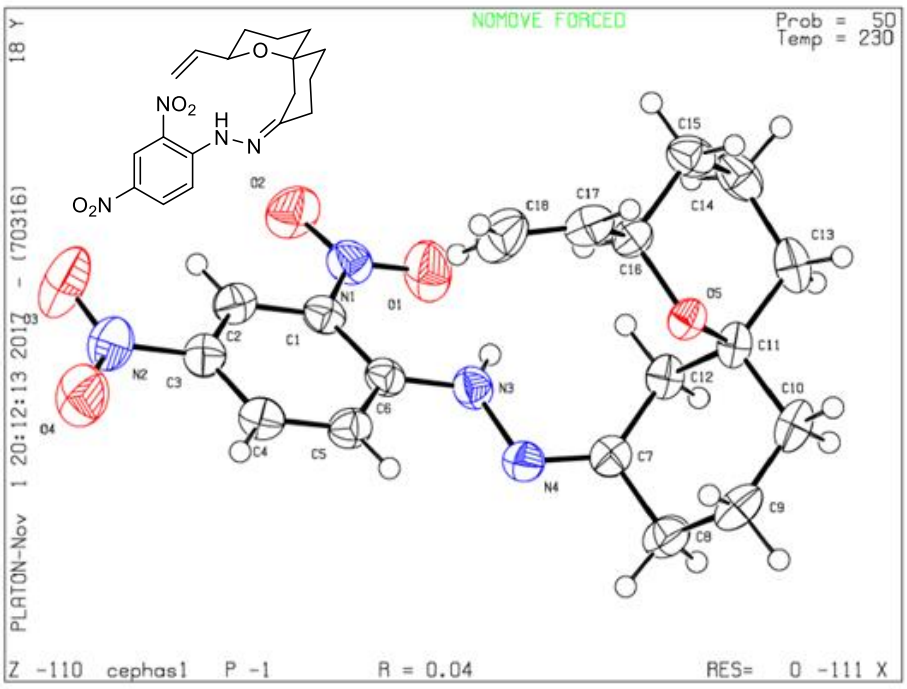

Reprinted with permission from {Afeke, C.; Xie, Y.; Floreancig, P. E., *Org. Lett.* **2019**, *21, 13*, 5064-5067.}. Copyright {2019} American Chemical Society."

Figure 1.2 X-ray crystal structure of derived hydrazone from 11

The ratio of diastereomers was minimally influenced by solvent polarity although solvents such as water, ethyl acetate, and diethyl ether were incompatible with the transformation (Table 1.1).

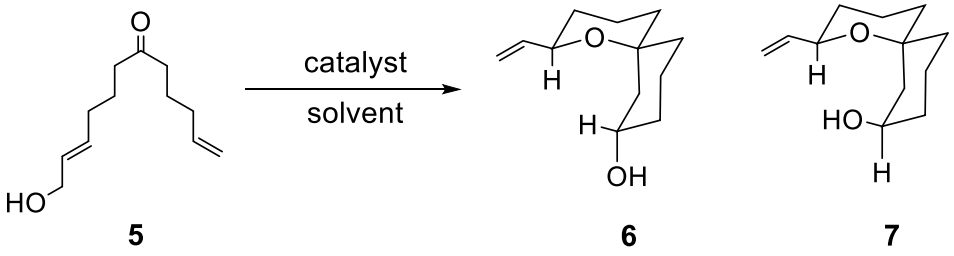

Table 1.1 Optimization study for spirocycle formation

No	Catalyst	Solvent	Temp (°C)	Time (h)	Yield (%)	d.r. (6:7)
1	$Re_2O_7 \cdot SiO_2$	DCM	rt	0.25	0	n/a
2	$Re_2O_7 \cdot SiO_2$	DCM	0	1	0	n/a
3	**Re_2O_7**	**DCM**	**rt**	**0.4**	**94**	**4:1**
4	Re_2O_7	DCM	rt	1.75	89	2:1
5	Re_2O_7	MeCN	rt	1	91	4:1
6	Re_2O_7	Hexanes	rt	1.5	32	4:1
7	Re_2O_7	$MeNO_2$	rt	2	53	4:1
8	Re_2O_7	Et_2O	rt	1	0	n/a
9	Re_2O_7	H_2O	rt	1	0	n/a
10	Re_2O_7	EtOAc	rt	1	0	n/a

We observed an erosion in the ratio of **6** to **7** at prolonged reaction times, ultimately leading to a 2:1 diastereomeric mixture. Monitoring the reaction progress by ^1H NMR in CD_2Cl_2 provided greater insights into the transformation. The reaction proceeded more slowly in the NMR experiment due to the diminished mixing of the sparingly soluble catalyst, thereby providing an opportunity to observe the diastereomeric ratios at lower conversions than those accessible in a standard reaction apparatus. This study showed that the initial diastereomeric ratio of **6/7** is greater than 11:1 and reduces with increased conversion (Figure 1.3), indicating that the Prins reaction initially proceeds from **8** to **9**, with the expected anti-addition to the alkene. Equilibration, presumably as the result of a retro-Prins reaction from **6** to **8** via intermediate **9**[34] though a simple substitution cannot be ruled out, is rapid and competitive with cyclization, as evidenced by the loss of stereoselectivity prior to starting material consumption. The axial alcohol **7** is

thermodynamically preferred due to its capacity to engage in hydrogen bonding (Scheme 1.16) with the tetrahydropyran ring. This is evidenced by a 10.4 Hz coupling between the alcohol proton and the methine proton at the alcohol stereocenter relative a 3.7 Hz coupling in the case of compound **6**.

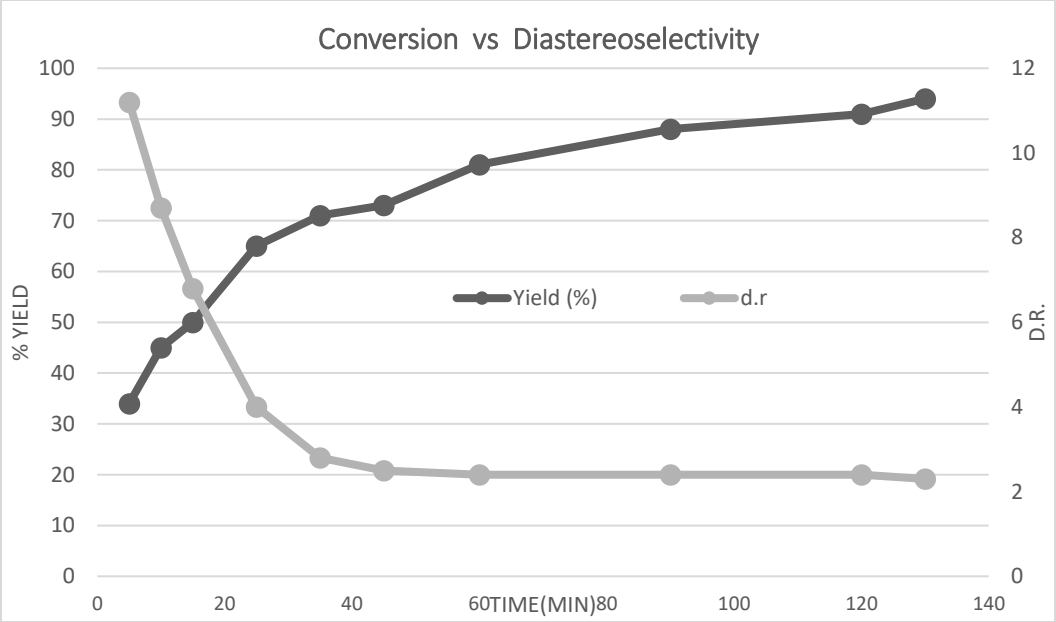

Figure 1.3 Diastereocontrol as a function of conversion

Having demonstrated the viability of the initial spirocyclization, we set out to determine the extent to which existing stereocenters in the substrate would influence the generation of newly formed stereogenic centers in the spirocyclic ether products. We envisioned that selectivity in this endeavor would be driven by faster equilibration of the stereocenters in the intermediates relative to the terminal Prins cyclization step. Substrate **12** was accessed in seven steps[38] starting with the *m*CPBA epoxidation of the tri-substituted alkene of β-citronellene, followed by cross metathesis with *cis*-2-butene-1,4-diol and resultant allyl alcohol protection. Oxidative epoxide cleavage with periodic acid to give an aldehyde intermediate was followed by the Grignard addition of the

pentene chain. Subsequent oxidation of the resultant secondary alcohol and silyl ether cleavage afforded compound **12** in 67% yield (Scheme 1.17).

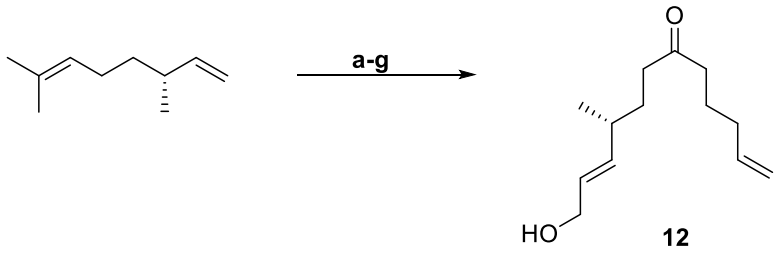

Reagents and conditions
a) *m*CPBA, CH_2Cl_2, 0 °C, 93%, b), *cis*-2-butene-1,4-diol, Hoveda-Grubbs II, CH_2Cl_2, rt, 26%
c) TBSCl, imidazole, DMAP, CH_2Cl_2, rt, 88%, d) H_5IO_6, CH_2Cl_2, 0 °C, 86%,
e) Mg, 5-bromo-1-pentene, THF, 73%, f) PCC, Celite, CH_2Cl_2, 81%, g) AcOH, THF, H_2O, rt, 67%.

Scheme 1.17 Preparation of 12

We postulated that non-stereoselective transposition, hemiacetal formation, and ionization will form oxocarbenium ions **13** and **14**. The oxocarbenium ions, and presumably their hemiacetal precursors, are in equilibrium because all steps are reversible. Thus, **13**, with the methyl and vinyl groups in equatorial orientations, should be the favored intermediate (Scheme 1.18). Xie and co-workers have previously observed in the bimolecular variants of this process that stereoselectivity improves as the rate of the final nucleophilic addition is lowered,[31] consistent with a model in which stereocontrol increases as the rate of equilibration becomes greater than the rate of nucleophilic addition. Thus, reactions proceed through the thermodynamically preferred oxocarbenium ion.

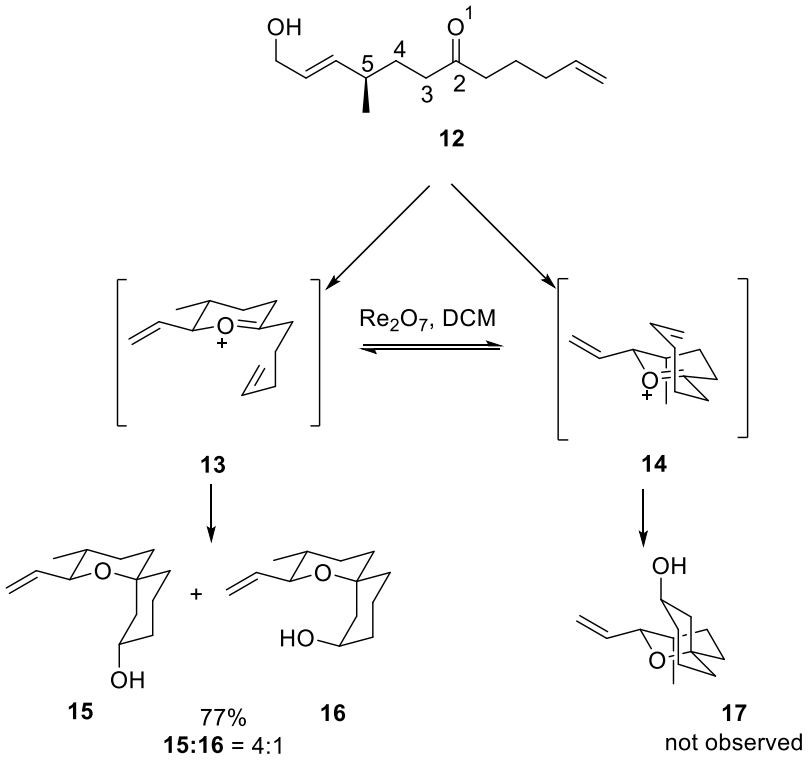

Scheme 1.18 Relative stereocontrol from a chiral substrate

Subjecting substrate **12** to Re_2O_7 demonstrated that equilibration is indeed faster than cyclization, with compounds **15** and **16** being the only observed stereoisomers in a 4:1 mixture. No products that contain the diastereomeric skeleton represented by **17** were isolated or observed thereby illustrating stereocontrol that is directed by the Curtin-Hammett kinetics.[39] As before, oxidation of the isomeric alcohols provided the same ketone, therefore proving that the spirocyclic scaffolds were the same for both isomers.

We prepared substrate **18** where the methyl substitution is incorporated at the C_4 position in ten total steps starting with the mono TBS protection of 3-methyl-1,5-pentanediol. Parikh-Doering oxidation followed by Horner-Wadsworth-Emmons olefination and DIBAL-H reduction of the resultant α,β-unsaturated ester afforded the allylic alcohol portion which was protected with *tert*-butyl diphenyl silane (TBDPS). Selective deprotection of the TBS ether followed by a

sequence of PCC oxidation, Grignard addition, oxidation and TBDPS ether cleavage afforded substrate **18** in 81% yield from the final step (Scheme 1.19).

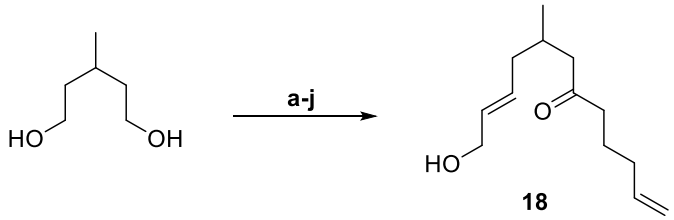

Reagents and conditions

a) TBSCl, NaH, THF, 0 °C, 58 %. b) $Py.SO_3$, DMSO, Et_3N, DCM 0 °C, 97%. c) NaH, $(MeO)_2P(O)CH_2C(O)OMe$, THF, 0 °C, 80% (87:13, ***E:Z***). d) DIBAL-H, THF, 0 °C, 98%. e) TBDPSCl, Imidazole, DCM, 0 °C, 92%. f) 1*N* HCl, THF, rt ,55%. g) PCC, Celite, DCM, rt, 83%. h) Mg, I_2, C_5H_9Br, THF, 0 °C 97%. i) PCC, Celite, DCM, rt, 98%. j) TBAF, THF, rt, 81%.

Scheme 1.19 Preparation of substrate 18

Subjecting substrate **18** to Re_2O_7 resulted in a spirocycle with excellent stereoinduction at the C_4 position. The methyl substituent orientates towards the equatorial position in both major and minor diasteromers with a 3.6:1 ratio of major and minor alcohols.

However, subjecting substrate **20**[38] with the methyl substitution at the C_3 position to Re_2O_7 led to diminished stereocontrol (Scheme 1.20) at the methyl stereocenter. Ambiguity at the alcohol stereocenter was eliminated via oxidation to give the two products **21** and **21a**. The erosion of stereoinduction from the 3-methyl substituent can be attributed to the destabilization of the conformation with an equatorially oriented methyl group in the intermediate oxocarbenium ion due to allylic 1,2-strain.[40]

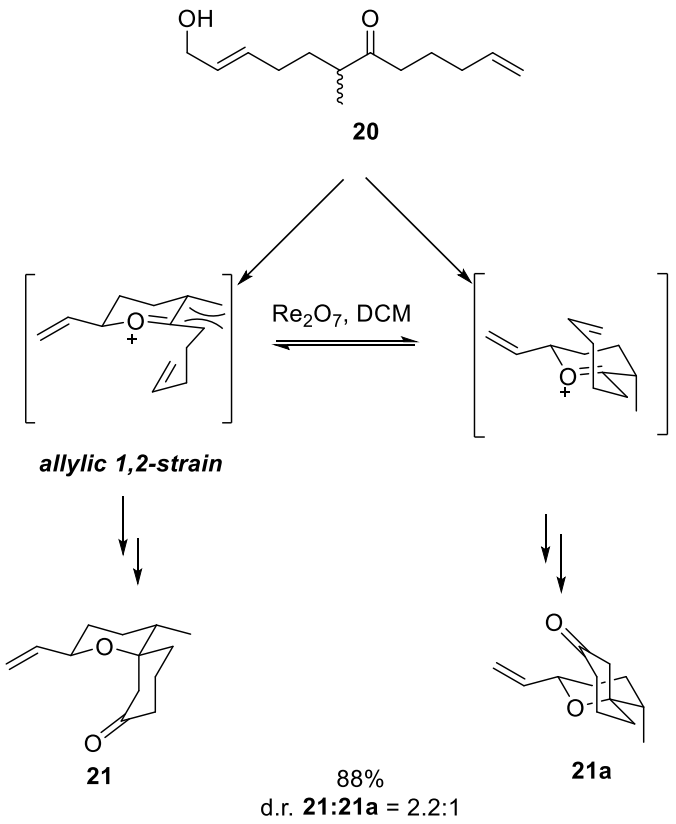

Scheme 1.20 Diminished stereocontrol via allylic 1,2-strain

We moved the methyl stereocenters onto the chain that leads to the cyclohexyl ring and the results observed were somewhat different (Scheme 1.21).

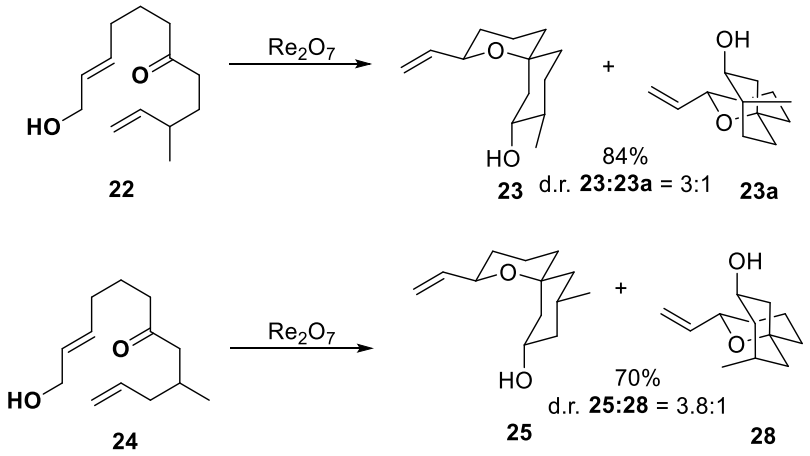

Scheme 1.21 Influence of stereocenters on the cyclohexane ring system

These examples produce diastereomeric mixtures, but the orientations of the methyl groups with respect to the ring system differ, while the hydroxy group is exclusively in an equatorial orientation (Scheme 1.21). These results show that an axially oriented methyl group in the transition state leading to the cyclohexyl ring slows the Prins reaction sufficiently to allow for stereochemical equilibration of the oxocarbenium ion, leading to a useful, albeit not perfect, level of stereocontrol. We postulate that the methyl groups in **22** and **24** promote cyclization through enhancing the population of the reactive conformer.[41] This is illustrated in Scheme 1.22, whereby **24** reacts to form oxocarbenium ions **26** and **27**, with **26** cyclizing rapidly to form **25**, and **27** cyclizing more slowly to form stereoisomer **28**. The lack of epimerization at alcohol stereocenter in this case can be explained by the conformationally induced rate increase in the Prins reaction and the slowed rate of retro-Prins reaction relative to the unsubstituted case, making the formation of **25** and **28** faster than stereochemical equilibration.

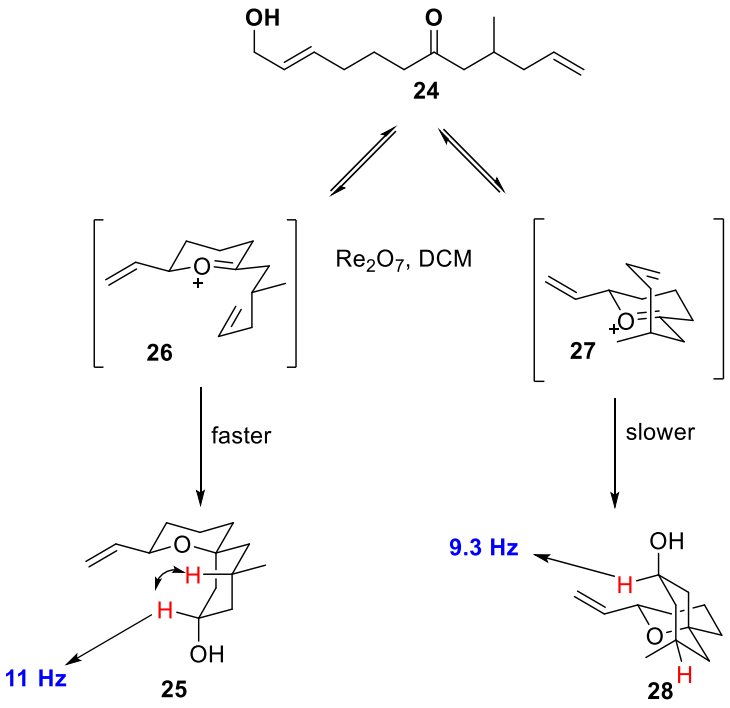

Scheme 1.22 Effect of incorporating a substituent into the cyclohexane subunit

The stereochemistry for **25** and **28** were determined by ^{1}H NMR coupling constant and one-dimentional Nuclear Overhauser Effect (1-D NOE) analyses, with the methine proton at the alcohol stereocenter found to have greater than 8 Hz coupling for both **25** and **28**, representing equatorial orientation of the alcohol in both compounds. 1-D NOE correlations observed between the methine protons at both stereocenters of the cyclohexyl ring of **25** indicated equatorial methyl orientation and the absence of such correlation in **28** suggests the opposite methyl stereochemistry.

This method is also compatible with various π-nucleophiles. Terminal alkyne substrate **29** cyclized to form ketones **11** and **30** in good chemical yield, but as a 1:1 mixture. This can be understood by the expected similarity in the thermodynamic stability of the isomeric products and the ease in which β-alkoxy ketones can proceed through ring opening and reclosure via an intermediate such as **31** (Scheme 1.23).

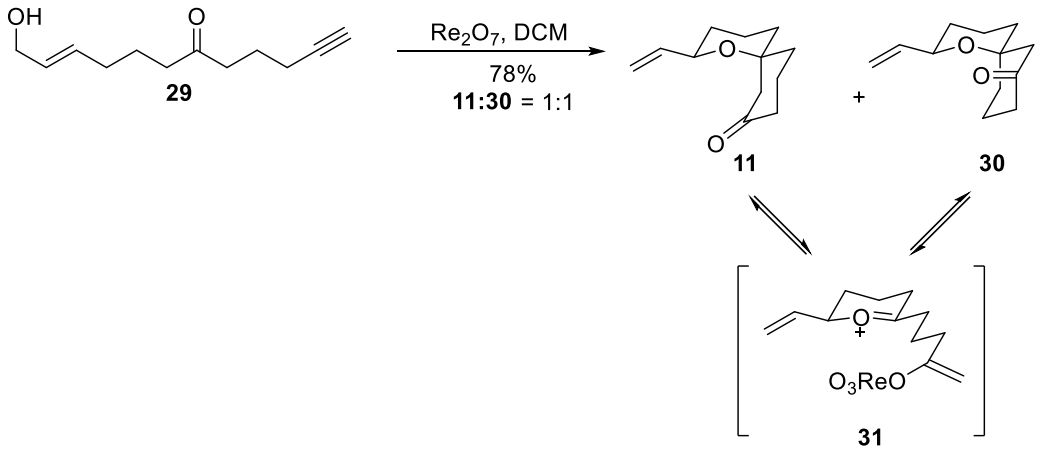

Scheme 1.23 Alkyne nucleophile in cyclization reaction

1,1-Disubstituted alkene **32** undergoes cyclization to yield tertiary alcohol **33**, accompanied by the dehydration product **34**. The dehydration product is derived from **33** rather than though an ene-type reaction with the oxocarbenium ion intermediate, as demonstrated by a time course study that showed a decreasing ratio of **33**/**34** over time, with **34** being the exclusive

spirocyclization product after 2.5 h. The formation of the tertiary alcohol as a single stereoisomer is consistent with the oxocarbenium ion that forms through the retro-Prins reaction being more strongly associated with the disubstituted alkene, leading to a favored pathway in which proton loss occurs in preference to stereochemical isomerization (Scheme 1.24).

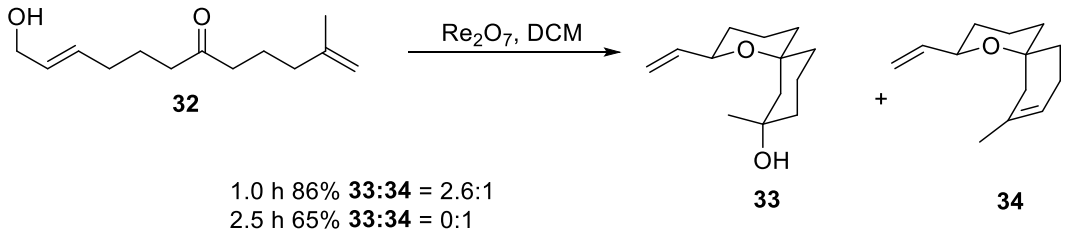

Scheme 1.24 1,1-Disubstituted alkene in cyclization reaction

Employing a prochiral nucleophile in these reactions leads to the generation of an additional stereocenter with high control, as seen with the conversion of (*Z*)-alkene substrate **35** to **36** and diastereomeric alcohol **37** (Scheme 1.25).

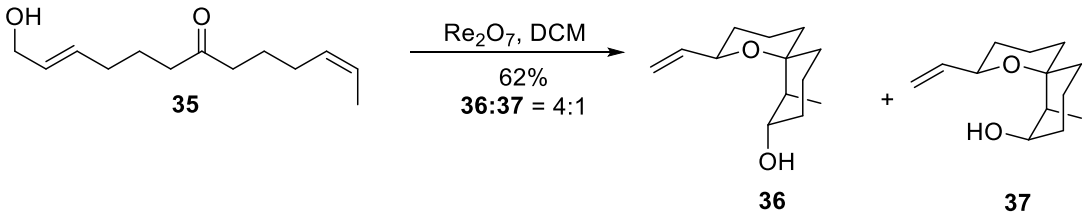

Scheme 1.25 (*Z*) alkene substrate in cyclization reaction

Thus, four new stereocenters can be created in this process with good to excellent levels of stereocontrol. Alcohols **36** and **37** undergo oxidation to form the same product indicating that, for this example, diastereomeric alcohols are formed from competitive *anti*- and *syn*-nucleophilic additions in the Prins step rather than through the intermediacy of a boat transition state. Dehydration of the allylic alcohol via an *E1* mechanism can be a significant competitive pathway if the Prins reaction is slow (not shown). This was observed during attempts to generate

cyclopentyl units, as poor orbital overlap slows the Prins cyclization, and when an (*E*)-alkene is used as a nucleophile, due to steric clashes with the tetrahydropyran in the transition state (Scheme 1.26).

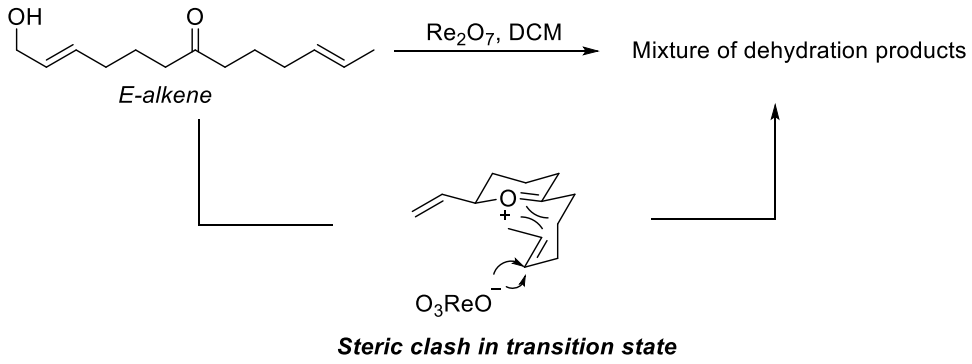

Scheme 1.26 (*E*) alkene substrate leading to dehydration

1.4 Conclusion

We have demonstrated that Re_2O_7 promotes the conversion of ketones that are flanked by an allylic alcohol an alkene to hydroxy-substituted spirocyclic ethers. These reactions significantly increase molecular complexity while demonstrating perfect atom economy. The transformation proceeds through an allylic alcohol isomerization followed by a dehydrative oxocarbenium ion formation and a Prins reaction. The carbon−carbon bond formation generally proceeds with excellent stereocontrol. The hydroxy group incorporation initially follows an anti-addition pathway, although the resulting alcohol isomerizes via a retro Prins pathway. Integrating a methyl group into the substrate delivers products good to excellent relative stereocontrol, indicating that stereochemical equilibration of the intermediate oxocarbenium ion is faster than the Prins reaction. Variations on the nucleophilic π-system allow for structural alterations of the product or the generation of additional stereocenters. The structurally rigid products and the potential for further

functionalization should prove to be useful in the design of new scaffolds for preparing biological screening libraries.

1.5 Experimental

1.5.1 General information

All reactions were performed in dry solvents under argon atmosphere using oven dried glassware unless otherwise specified. Dichloromethane was distilled over CaH_2 whereas diethyl ether and tetrahydrofuran solvents were distilled over sodium and benzophenone before use. Flash column chromatography with 60 Å silica gel and reagent grade solvents i.e. ethyl acetate, hexanes, diethyl ether or pentanes as eluent was performed to purify all compounds made. Analytical TLC was performed on E. Merck pre-coated (25 mm) silica gel 60 F_{-254} plates and visualized under UV (254 nm). High resolution and low-resolution mass spectra were collected on a VG 7070 spectrometer. IR spectra were obtained on a PerkinElmer FT-IR UATR spectrometer. ^{1}H NMR and ^{13}C NMR spectra were taken on a Bruker Avance 300 spectrometer at 300 MHz and 75 MHz respectively, a Bruker Avance 400 spectrometer at 400 MHz and 100 MHz, or a Bruker Avance 500 spectrometer at 500 MHz and 125 MHz and a Bruker Avance 600 MHz and 150 MHz as specified. The chemical shifts are reported in parts per million (ppm) on the delta (δ) scale. The solvent peak was used as a reference value, for ^{1}H NMR: $CHCl_3$ = 7.26 ppm, CH_2Cl_2 = 5.31 ppm, C_6H_6 = 7.16 ppm, for ^{13}C NMR: $CDCl_3$ = 77.2 ppm. Data are reported as follows: m = multiplet, s = singlet, d = doublet, t = triplet, q = quartet, pent = pentet, dd = doublet of doublets, dt = doublet of triplets, sext = sextet, sept = septet, oct = octet, dq = doublet of quartet, dp = doublet of pentet,

ddd = doublet of doublet of doublets, ddt = doublet of doublet of triplets, tt = triplet of triplet, br = broad.

1.5.2 General procedure for Re_2O_7-catalyzed spirocycle formation

To a solution of substrate (0.1 - 0.2 mmol) in DCM (0.5 – 1.5 mL), stirring at rt (unless otherwise noted) was added Re_2O_7 (3-6 mol %), and the mixture stirred until starting substrate was consumed. The reaction mixture was quenched with a few drops of pyridine, concentrated *in vacuo* and purified via flash column chromatography with 0 – 10% ethyl acetate in hexanes as eluent in gradient elution.

Preparation of (10E)-12-hydroxydodeca-1,10-dien-6-one (5)

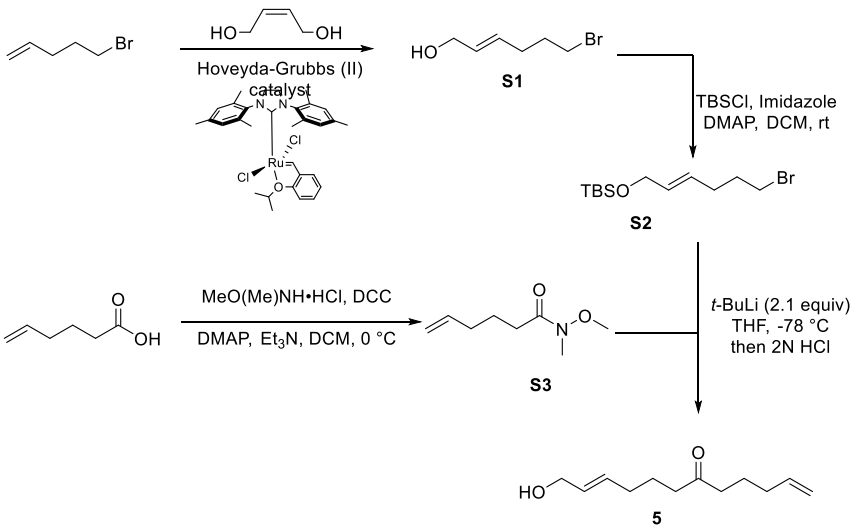

***(E)*-6-bromohex-2-en-1-ol (S1)**

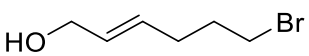

To a solution of *cis*-2-butene-1,4-diol (3.54 g, 40.2 mmol) and 5-bromo-1-pentene (3.0 g, 20.1 mmol) in DCM (10.0 mL) was added Hoveyda-Grubbs II catalyst (40 mg, 0.064 mmol) and the mixture stirred at rt for 16 h. The reaction mixture was concentrated

in vacuo and purified via flash column chromatography with 40% hexanes in ethyl acetate as eluent to yield 1.38 g (38.4%) of brown oil. ^{1}H NMR (300 MHz, $CDCl_3$): δ (ppm) 5.60-5.75 (m, 2H), 4.09 (d, *J* = 4.3 Hz, 2H), 3.41 (t, *J* = 6.7 Hz, 2H), 2.18-2.30 (m, 2H), 1.90-1.99 (m, 2H), 1.46 (s, 1H); ^{13}C NMR (75 MHz, $CDCl_3$): δ (ppm) 130.7, 130.5, 63.5, 33.1, 32.0, 30.5; HRMS (ESI) *m/z* calcd for $C_6H_{10}BrO$ $[M-H]^-$ 176.9915, found 176.9816.

***(E)-(*(6-bromohex-2-en-1-yl)oxy)(tert-butyl) dimethylsilane (S2)**

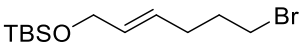

To a solution of **S1** (1.68 g, 9.38 mmol) and *tert*-butyl dimethyl silyl chloride (2.83 g, 18.8 mmol) in DCM (50 mL) was added imidazole (1.92 g, 28.1 mmol) and DMAP (0.12 g, 0.94 mmol) and the mixture stirred at rt for 3 h. The reaction was quenched with water and extracted with DCM, concentrated *in vacuo,* and purified via flash column chromatograpy with 10% ethyl acetate in hexanes to yield 2.46 g (89%) of colorless oil as product: ^{1}H NMR (300 MHz, $CDCl_3$): δ (ppm) 5.54-5.66 (m, 2H), 4.12 (d, *J* = 1.1 Hz, 2H), 3.40 (t, *J* = 6.7 Hz, 2H), 2.12-2.22 (m, 2H), 1.93 (pent, *J* = 6.8 Hz, 2H), 0.90 (s, 9H), 0.06 (s, 6H); ^{13}C NMR (75 MHz, $CDCl_3$): δ (ppm) 130.8, 128.7, 63.7, 33.1, 32.1, 30.5, 26.0, 18.4, -5.1; HRMS (ESI) *m/z* calcd for C12H24OSiBr $[M-H]^-$ 291.0780, found 291.0827.

N-methoxy-N-methylhex-5-enamide (S3)

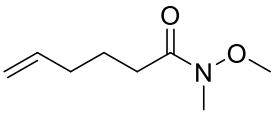

To a solution of 5-hexenoic acid (1.8 g, 14.1 mmol) in DCM (45 mL) at 0 °C was added *N,O*-dimethylhydroxylamine hydrochloride (1.65 g, 16.9 mmol), DCC (3.48 g, 16.9 mmol), DMAP (0.21 g, 1.69 mmol) and triethylamine (1.71 g, 16.9 mmol) and stirred until starting material was fully consumed. The reaction mixture was filtered through celite, washed

with 0.5 N HCl and extracted with DCM after which the crude product was purified via flash column chromatography with 20% ethyl acetate in hexanes and concentrated *in vacuo* to yield a pale-yellow oil (2.09 g, 87.3%): ^{1}H NMR (300 MHz, $CDCl_3$): δ (ppm) 5.70 (ddt, *J* = 17.1, 10.2, 7.1 Hz, 1H), 4.94 (dd, *J* = 17.2, 1.69 Hz), 4.88 (dd, *J* = 10.2, 1.5 Hz), 3.59 (s, 3H), 3.08 (s, 3H), 2.33 (t, *J* = 7.4 Hz, 2H), 2.02 (dt, *J* = 7.3, 7.0 Hz, 2H), 1.64 (pent, *J* = 7.7 Hz, 2H); ^{13}C NMR (75 MHz, $CDCl_3$): δ (ppm) 174.3, 138.0, 114.9, 61.1, 33.2, 32.1, 31.0, 23.6; HRMS (ESI) *m/z* calcd for $C_8H_{16}O_2N$ $[M+H]^+$ 158.1181, found 158.1175.

***(10E)*-12-hydroxydodeca-1,10-dien-6-one (5)**

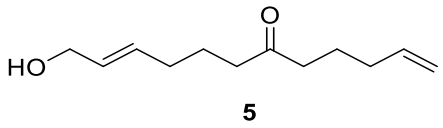

5

To an oven dried round bottom flask was added **S2** (1.86 g, 6.4 mmol) and diethyl ether (20 mL) and the solution was stirred at –78 °C. After 1 h of stirring, *tert*-butyllithium solution (1.7 M, 7.50 mL, 12.8 mmol) was added slowly and stirred for 0.25 h after which **S3** (1.0 g, 6.4 mmol) was added dropwise and stirred for an additional 0.5 h while maintaining the reaction at –78 °C. The reaction mixture was quenched with excess 2N HCl, extracted with diethyl ether and the crude product purified via chromatography with 20% ethyl acetate in hexanes to yield 0.5 g (40% yield) of colorless oil: ^{1}H NMR (500 MHz, $CDCl_3$): δ (ppm) 5.75 (ddt, *J* = 17.0, 10.2, 6.7 Hz, 1H), 5.60-5.68 (m, 2H), 5.00 (dd, *J* = 17.2, 1.2 Hz, 1H), 4.97 (dd, *J* = 10.2, 1.0 Hz, 1H), 4.08 (d, *J* = 3.1 Hz, 2H), 2.39 (t, *J* = 7.4 Hz, 4H), 2.04 (dt, *J* = 6.8, 6.3 Hz, 4H), 1.66 (pent, *J* = 7.4 Hz, 4H), 1.48 (s, 1H); ^{13}C NMR (125 MHz, $CDCl_3$): δ (ppm) 210.8, 138.0, 132.1, 129.8, 115.2, 63.6, 42.0, 41.9, 33.1, 31.6, 23.1, 22.8; HRMS (ESI) *m/z* calcd for $C_{12}H_{21}O_2$ $[M+H]^+$ 197.1536, found 197.1532. IR (thin film) cm^{-1}: 3408, 3114, 2930, 1708 1410, 1216, 1088, 970, 912.

(2*R*,6*R*,8*R*)-2-vinyl-1-oxaspiro [5.5]undecan-8-ol (6) and (2*R*,6*R*,8*S*)-2-vinyl-1-oxaspiro[5.5] undecane-8-ol (7).

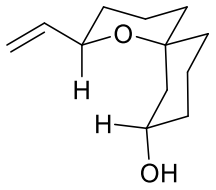

6

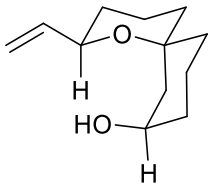

7

The general procedure for spirocycle synthesis was followed with **5** (20.0 mg, 0.1 mmol) and Re_2O_7 (3.0 mg, 0.006 mmol) in DCM (1.0 mL) for 25 mins at rt after which the crude mixture was purified with 10% ethyl acetate in hexanes via flash column chromatography to give 18.6 mg (93% yield) of product mixture **6** and **7** with diastereomeric ratio (d.r.) of 4:1 respectively. **Major (slower-eluting) Isomer (6):** ^{1}H NMR (400 MHz, $CDCl_3$): δ (ppm) 5.80 (ddd, *J* = 17.2, 10.5, 5.1 Hz, 1H), 5.20 (dt, *J* = 17.2, 1.6 Hz, 1H), 5.03, (dt, *J* = 10.5, 1.5 Hz, 1H), 4.04 (dt, *J* = 11.0, 5.4 Hz, 1H), 3.74 (tt, *J* = 11.0, 4.2 Hz, 1H), 2.68 (ddt, *J* = 13.5, 4.0, 2.6 Hz, 1H), 1.95 (d, *J* = 13.0 Hz, 1H), 1.71-1.84, (m, 2H), 1.64-1.67 (m, 2H), 1.52-1.58 (m, 2H), 1.36-1.44, (m, 2H), 1.30 (s, 1H) 1.15-1.28 (m, 3H), 0.87 (dd, *J* = 13.2, 10.9 Hz, 1H); ^{13}C NMR (100 MHz, $CDCl_3$): δ (ppm) 140.1, 114.0, 74.1, 70.1, 67.0, 39.1, 38.3, 36.1, 35.9, 31.4, 19.5, 19.2; HRMS (ESI) *m/z* calcd for $C_{12}H_{21}O_2$ $[M+H]^+$ 197.1536, found 197.1533; IR (thin film) cm^{-1}: 3399, 2946, 2861 1458 1265, 1020, 735. **Minor (faster-eluting) Isomer (7):** ^{1}H NMR (500 MHz, $CDCl_3$): δ (ppm) 5.79 (ddd, *J* = 17.2, 10.5, 5.8 Hz, 1H), 5.25 (dt, *J* = 17.2, 1.4 Hz, 1H), 5.07, (dt, *J* = 10.5, 1.4 Hz, 1H), 4.22 (ddd, *J* = 12.0, 5.7, 1.0 Hz, 1H), 3.95 (dp, *J* = 10.3, 3.5 Hz, 1H), 3.55 (d, *J* = 10.0 Hz, 1H), 2.48 (d, *J* = 14.0 Hz, 1H), 1.94-2.02, (m, 1H), 1.75-1.78 (m, 1H), 1.64-1.74 (m, 4H), 1.38-1.45, (m, 4H), 1.22-1.33 (m, 3H); ^{13}C NMR (125 MHz, $CDCl_3$): δ (ppm) 139.3, 115.0, 74.2, 71.6, 67.7, 39.8, 36.4, 33.3, 31.5, 19.4, 19.0, 15.9; HRMS (ESI) *m/z* calcd for $C_{12}H_{21}O_2$ $[M+H]^+$ 197.1536, found 197.1533; IR (thin film) cm^{-1}: 3402, 2927, 2872, 1463, 1263, 1077, 703.

1.5.3 General procedure for reaction optimization

The general protocol for spirocycle formation was followed with 10 mg (0.05 mmol) of **5** and catalyst (3 mol%) in 0.5 mL of each solvent listed and stirred at the respective temperature in a sealed 1-dram vial. The reaction mixture was quenched with a drop of pyridine, filtered through a plug of silica in a Fisherbrand 9-inch borosilicate Pasteur pipet column with 20% ethyl acetate in hexanes, and concentrated under reduced pressure to obtain total product yield. The concentrated mixture was then dissolved in $CDCl_3$ and analyzed with NMR spectroscopy for the diastereomeric ratio.

1.5.4 General procedure for conversion studies (kinetic experiment)

To a solution of **5** (10 mg, 0.05 mmol) in CD_2Cl_2 (0.2 mL) in a Wilmad 5 mm diameter, 7-inch borosilicate NMR tube was added 50 µL of 0.25 M solution of 1,4-difluorobenzene [(5.7 mg, 0.05 mmol) in CD_2Cl_2 (0.2 mL)] as internal standard. ^1H NMR spectrum was obtained on the sample with a Bruker Avance 600 MHz spectrometer at t=0, after which the sample was removed from the spectrometer, loaded with Re_2O_7 (2 mg, 0.004 mmol), shaken and inserted back into the spectrometer for analysis after 5 min. The removal of sample from spectrometer, vigorous shaking of the reaction mixture and re-insertion of the sample into the spectrometer and analysis for product yield and d.r. were repeated every 5 min for the first 25 min and then at 10 min intervals afterwards.

1.5.5 Determination of stereochemistry at quaternary stereocenter

1.5.5.1 Procedure for oxidation of (6) and (7)

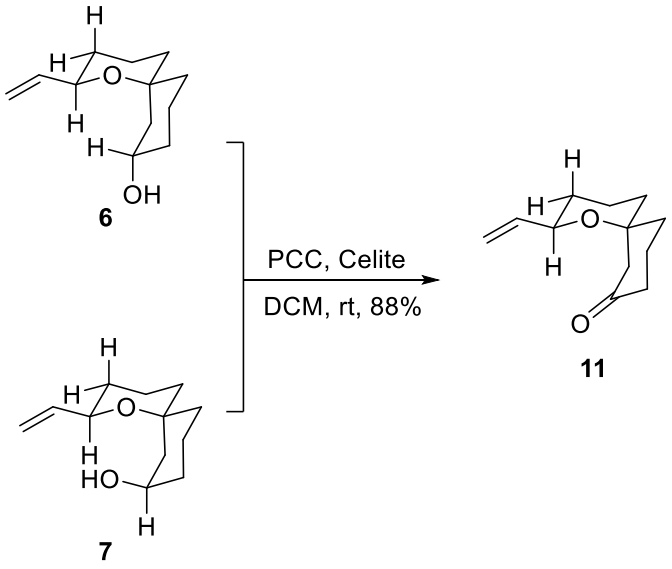

To a solution of a 1:1 mixture of **6** and **7** (40 mg, 0.2 mmol) in dichloromethane (2 mL) was added PCC (86 mg, 0.4 mmol) and Celite (0.1 g) and reaction stirred at rt for 15 min. The crude reaction mixture was then purified via flash column chromatography with 20% ethyl acetate in hexanes as eluent and the eluted fractions concentrated under reduced pressure to yield a colorless oil (35 mg, 88%) identified by NMR spectroscopy as a single ketone product with the same identity as compound **11**. ^{1}H NMR (500 MHz, $CDCl_3$): δ (ppm) 5.77 (ddd, *J* = 17.5, 10.6, 5.3 Hz, 1H), 5.17 (dt, *J* = 17.3, 1.6 Hz, 1H), 5.04 (dt, *J* = 10.6, 1.5 Hz, 1H), 4.04 (ddt, *J* = 11.2, 2.6, 1.1Hz, 1H), 2.96 (dt, *J* = 13.9, 1.6 Hz, 1H), 2.31-2.38 (m, 2H), 2.25-2.31 (m, 1H), 2.10-2.19 (m, 1H), 1.85-1.89 (m, 1H), 1.75-1.83 (m 2H), 1.63-1.70 (m, 3H), 1.56-1.59 (m, 1H), 1.39-1.45 (m, 1H), 1.20-1.42 (m, 1H); ^{13}C NMR (125 MHz, $CDCl_3$): δ (ppm) 210.0, 139.5, 114.6, 70.6, 46.4, 40.9, 38.9, 34.7, 31.1, 29.7, 20.5, 18.9.

1.5.5.2 Procedure for hydrazone preparation for X-ray studies

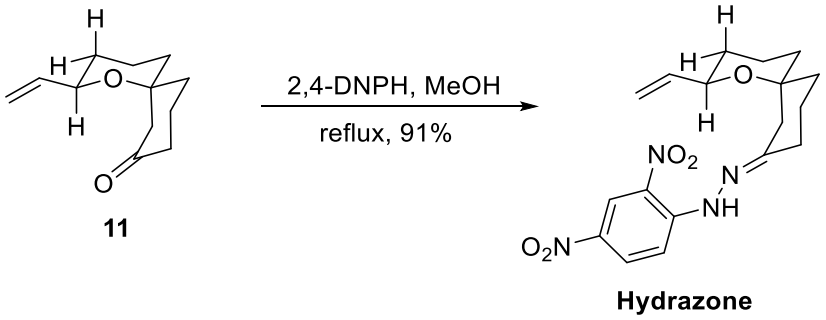

To a solution of **11** (30 mg, 0.15 mmol) in methanol (3 mL) was added 2,4-dinitrophenylhydrazine (61 mg, 0.31 mmol) and the mixture was refluxed under argon atmosphere until starting material **11** was fully consumed. The reaction mixture was concentrated and purified via flash column chromatography with 10% ethyl acetate in hexanes after which the eluted fractions were concentrated to yield a yellow-orange powdery precipitate (51 mg, 91%). The precipitate was then recrystallized via vapor diffusion by dissolving it in approximately 80 µL of ether in a 1-dram borosilicate glass vial and placing the vial in a larger 4-dram glass vial containing approximately 5 mL of pentane. The bigger vial containing the smaller 1-dram vial was capped tightly and allowed to sit for 96 h at room temperature for the recrystallized hydrazone to form. The regenerated crystals were dried under vacuum and analyzed with X-ray crystallography for the crystal structure of the derived hydrazone.

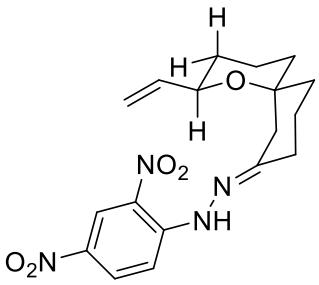

Hydrazone

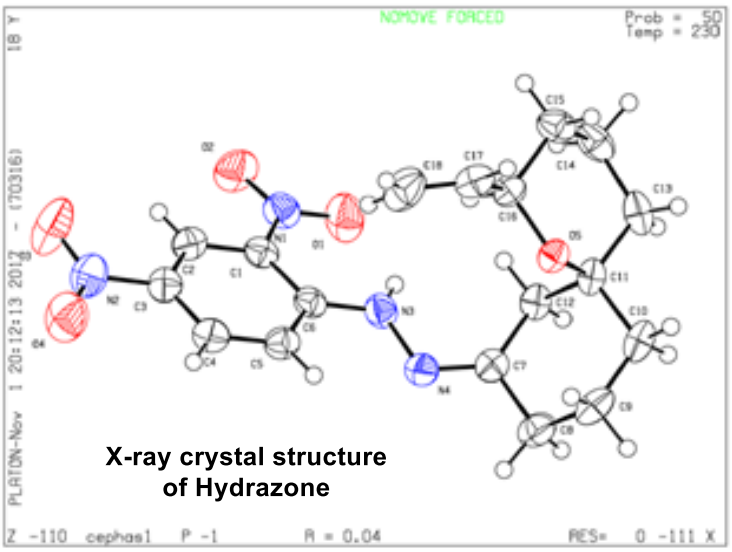

X-ray crystal structure of Hydrazone

"Reprinted with permission from {Afeke, C.; Xie, Y.; Floreancig, P. E., *Org. Lett.* **2019**, *21, 13*, 5064-5067.}. Copyright {2019} American Chemical Society."

Preparation of (9R,10E)-12-hydroxy-9-methyldodeca-1,10-dien-6-one (12)

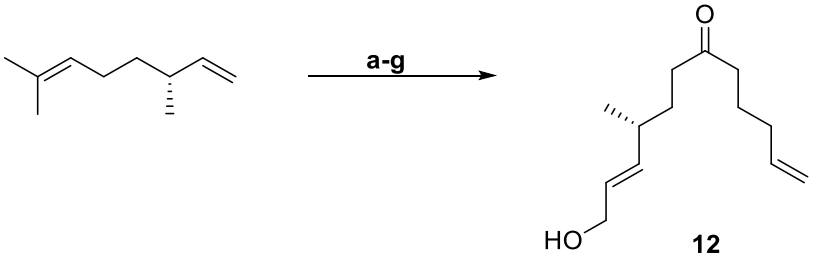

12

Reagents and conditions

a) *m*CPBA, CH_2Cl_2, 0 °C, 93%, b), *cis*-2-butene-1,4-diol, Hoveda-Grubbs II, CH_2Cl_2, rt, 26%
c) TBSCl, imidazole, DMAP, CH_2Cl_2, rt, 88%, d) H_5IO_6, CH_2Cl_2, 0 °C, 86%,
e) Mg, 5-bromo-1-pentene, THF, 73%, f) PCC, Celite, CH_2Cl_2, 81%, g) AcOH, THF, H_2O, rt, 67%.

(9*R*,10*E*)-12-hydroxy-9-methyldodeca-1,10-dien-6-one (12)

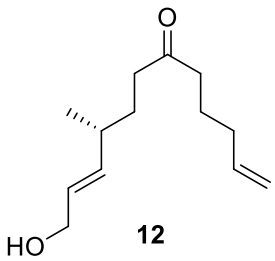

12

^{1}H NMR (400 MHz, $CDCl_3$): δ (ppm) 5.77 (ddt, *J* = 17.0, 10.2, 6.7 Hz, 1H), 5.60 (dt, *J* = 15.4, 5.4 Hz, 1H), 5.50 (dd, *J* = 15.1, 7.7 Hz, 1H), 4.95-5.03 (m, 2H), 4.09 (t, *J* = 4.6 Hz, 2H), 2.39 (t, *J* = 7.8 Hz, 2H), 2.37 (t, *J* = 7.8 Hz, 2H), 2.12 (sept, *J* = 7.0 Hz, 1H) 2.04 (qt, *J* = 7.0, 1.6 Hz, 2H), 1.66 (pent, *J* = 7.3 Hz, 2H), 1.48-1.59 (m, 2H), 1.32 (t, *J* = 5.6 Hz, 1H), 1.00 (d, *J* = 6.8 Hz, 3H); ^{13}C NMR (100 MHz, $CDCl_3$): δ (ppm) 211.1, 138.0, 137.9, 128.1, 115.2, 63.7, 42.0, 40.7, 36.2, 33.1,

30.4, 22.8, 20.5; HRMS (ESI) *m/z* calcd for $C_{13}H_{23}O_2$ $[M+H]^+$ 211.1693, found 211.1689; IR (thin film) cm^{-1}: 3406, 3107, 2927, 1709 1454, 1087, 971, 632.

(2*S*,3*R*,6*R*,8*S*)-3-methyl-2-vinyl-1-oxaspiro[5.5]undecan-8-ol (15) and (2*S*,3*R*,6*R*,8*R*)-3-methyl-2-vinyl-1-oxaspiro[5.5]undecan-8-ol (16)

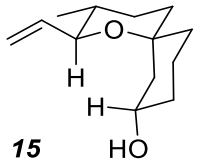

15

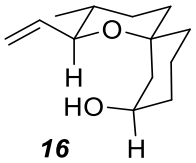

16

The general procedure for spirocycle synthesis was followed with **12** (15.0 mg, 0.1 mmol) and Re_2O_7 (2.0 mg, 0.004 mmol) in DCM (0.7 mL) for 10 mins at 0 °C. The reaction mixture was purified via flash column chromatography with 10% ethyl acetate in hexane and the eluted fractions concentrated *in vacuo* to give 11.6 mg (77% yield) of product mixture **15** and **16** with diastereomeric ratio of 4:1 respectively. **Major (slower-eluting) isomer (15)**: ^{1}H NMR (500 MHz, $CDCl_3$): δ (ppm) 5.77 (ddd, *J* = 17.2, 10.3, 6.8 Hz, 1H), 5.22 (d, *J* = 17.1, 1H), 5.12 (d, *J* = 10.4 Hz, 1H), 3.74 (tt, *J* = 10.9, 4.8Hz, 1H), 3.58 (dd, *J* = 10.1, 7.0 Hz, 1H), 2.66 (dd, *J* = 13.2, 1.8 Hz, 1H), 1.97 (d, *J* = 11.6 Hz, 1H) 1.72-1.81 (m. 1H), 1.52-1.63 (m, 4H), 1.38-1.50 (m, 3H), 1.24-1.33 (m, 4H), 0.82 (d, *J* = 6.6 Hz, 3H); ^{13}C NMR (125 MHz, $CDCl_3$): δ (ppm) 138.6, 116.5, 73.7, 67.1, 39.0, 38.3, 36.7, 36.0, 35.3, 28.1, 22.7, 19.6, 17.8; HRMS (ESI) *m/z* calcd for $C_{13}H_{23}O_2$ $[M+H]^+$ 211.1698, found 211.1691; IR (thin film) cm^{-1}: 3343, 2929, 2859, 1451, 1274, 1025, 920. **Minor (faster-eluting) isomer (16)**: ^{1}H NMR (500 MHz, $CDCl_3$): δ (ppm) 5.75 (ddd, *J* = 17.4, 10.3, 7.3 Hz, 1H), 5.28 (dd, *J* = 17.2, 1.0 Hz, 1H), 5.16 (dd, *J* = 10.4, 1.2 Hz, 1H), 3.95 (dp, *J* = 10.4, 3.7 Hz, 1H), 3.78 (dd, *J* = 9.7, 7.3 Hz, 1H), 3.53 (d, *J* = 9.0 Hz, 1H), 2.48 (d, *J* = 14.2 Hz, 1H), 1.88-2.06 (m, 2H), 1.63-1.78 (m, 2H), 1.41-1.51 (m, 3H), 1.38-1.42 (m, 3H), 1.30-1.37 (m, 2H), 0.83 (d, *J* = 6.4 Hz, 3H); ^{13}C NMR (125 MHz, $CDCl_3$): 137.9, 117.6, 78.6, 73.8, 67.7, 39.7, 37.0, 35.3,

34.0, 33.3, 27.9, 17.7, 16.0; HRMS (ESI) *m/z* calcd for $C_{13}H_{23}O_2$ $[M+H]^+$ 211.1698, found 211.1692; IR (thin film) cm^{-1}: 3336, 2925, 2853, 1453, 1025, 920.

Preparation of (E)-12-hydroxy-8-methyldodeca-1,10-dien-6-one (18)

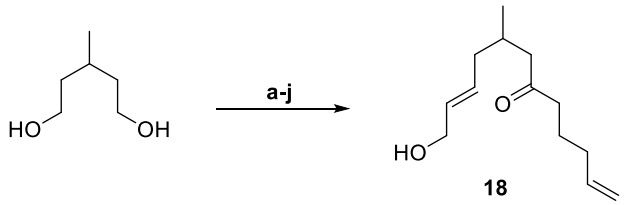

Reagents and conditions

a) TBSCl, NaH, THF, 0 °C, 58 %. b) $Py.SO_3$, DMSO, Et_3N, DCM 0 °C, 97%. c) NaH, $(MeO)_2P(O)CH_2C(O)OMe$, THF, 0 °C, 80% (87:13, ***E:Z***). d) DIBAL-H, THF, 0 °C, 98%. e) TBDPSCl, Imidazole, DCM, 0 °C, 92%. f) 1*N* HCl, THF, rt ,55%. g) PCC, Celite, DCM, rt, 83%. h) Mg, I_2, C_5H_9Br, THF, 0 °C 97%. i) PCC, Celite, DCM, rt, 98%. j) TBAF, THF, rt, 81%.

(*E*)-12-hydroxy-8-methyldodeca-1,10-dien-6-one (18)

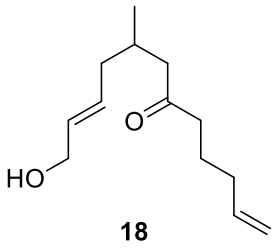

^{1}H NMR (500 MHz, $CDCl_3$): δ (ppm) 5.76 (ddt, *J* = 17.0, 10.2, 6.7 Hz, 1H), 5.63 (m, 2H), 5.00 (dq, *J* = 17.2, 1.7 Hz, 1H), 4.97 (ddt, *J* = 10.3, 2.0, 1.2 Hz, 1H), 4.09 (d, *J* = 3.6 Hz, 2H), 2.36-2.41 (m, 3H), 2.20 (dd, *J* = 16.0, 7.8 Hz, 1H), 2.10 (sept, *J* = 6.7 Hz, 1H), 2.01-2.07 (m, 2H), *1*.92-2.00 (m, 2H), 1.66 (pent, *J* = 7.4 Hz, 2H), 1.50 (br, 1H), 0.89 (d, *J* = 6.6 Hz, 3H); ^{13}C NMR (125 MHz, $CDCl_3$): δ (ppm) 210.7, 138.0, 131.1, 130.7, 115.2, 63.6, 49.5, 42.5, 39.5, 33.1, 29.1, 22.7, 19.8; HRMS (ESI) *m/z* calcd for $C_{13}H_{22}O_2Na$ $[M+Na]^+$ 233.1512, found 233.1505; IR (thin film) cm^{-1}: 3413, 2929, 1708, 1371, 912, 736.

(2*R*,4*R*,6*R*,8*S*)-4-methyl-2-vinyl-1-oxaspiro[5.5]undecan-8-ol (19) and (2*R*,4*R*,6*R*,8*R*)-4-methyl-2-vinyl-1-oxaspiro[5.5]undecan-8-ol (19a)

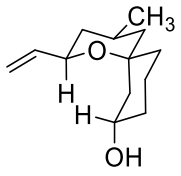

19

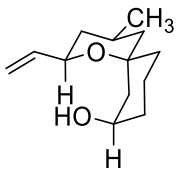

19a

The general procedure for spirocycle synthesis was followed with **18** (42 mg, 0.2 mmol) and Re_2O_7 (3 mg, 0.006 mmol) in DCM (1.0 mL) for 15 min at rt. The resultant mixture was purified via flash column chromatography using 0-20% ethyl acetate in hexanes as eluent in gradient elution and the eluted fractions concentrated *in vacuo* to give 32 mg (76% yield) of product mixture **19** and **19a** of d.r. of 3.6:1 with **19** as the major isomer. **Major (slower-eluting) isomer** (**19**) ^{1}H NMR (500 MHz, $CDCl_3$): δ (ppm) 5.81 (ddd, *J* = 17.3, 10.6, 5.2 Hz, 1H), 5.21 (dt, *J* = 17.5, 1.6 Hz, 1H), 5.04 (dt, *J* = 10.5, 1.6 Hz, 1H), 4.03 (dd, *J* = 11.5, 3.4 Hz, 1H), 3.75 (tt, *J* = 11.1, 4.2 Hz, 1H), 2.61 (d, *J* = 13.3 Hz, 1H), 1.98 (d, *J* = 13.5 Hz, 1H), 1.85-1.90 (m. 1H), 1.80 (qt, *J* = 13.3, 3.7Hz, 1H), 1.66 (d, *J* = 13.1 Hz, 1H), 1.52-1.56 (m, 2H), 1.44 (ddd, *J* = 13.5, 3.8, 1.7 Hz, 1H), 1.25 (td, *J* = 13.0, 4.1 Hz, 1H), 1.17 (qd, *J* = 13.2, 4.0 Hz, 1H), 0.98 (t, *J* = 12.8 Hz, 1H) 0.91 (dd, *J* = 13.2, 11.3 Hz, 1H), 0.89 (d, *J* = 6.1 Hz, 3H) 0.86 (t, *J* = 12.4 Hz, 1H), 0.84 (t, *J* = 12.4 Hz, 1H); ^{13}C NMR (125 MHz, $CDCl_3$): δ (ppm) 140.0, 114.1, 74.4, 70.2, 67.1, 45.1, 40.1, 39.1, 39.0, 36.0, 25.4, 22.5, 19.6; HRMS (ESI) *m/z* calcd for $C_{13}H_{23}O_2$ $[M+H]^+$ 211.1693, found 211.1690; IR (thin film) cm^{-1}: 3338, 2928 1480, 1263, 1020, 735. **Minor (faster-eluting) isomer** (**19a**) ^{1}H NMR (500 MHz, $CDCl_3$): δ (ppm) 5.80 (ddd, *J* = 17.2, 10.5, 5.8 Hz, 1H), 5.26 (dt, *J* = 17.3, 1.5 Hz, 1H), 5.08 (dt, *J* = 10.5, 1.3 Hz, 1H), 4.22 (dd, *J* = 11.4, 5.7, Hz, 1H), 3.94 (pent, *J* = 3.1 Hz, 1H), 2.43 (d, *J* = 14.3 Hz, 1H), 1.95-2.02 (m, 1H), 1.83-1.89 (m, 1H), 1.77(dd, *J* = 13.6, 3.5 Hz, 1H), 1.62-1.72 (m, 2H), 1.38-1.55 (m, 4H), 1.29 (d, *J* = 14.1 Hz, 1H), 1.18-1.26 (m, 1H), 0.90 (d, *J* = 6.6 Hz, 3H), 0.86-0.93 (m, 2H); ^{13}C NMR (125 MHz, $CDCl_3$): δ (ppm) 139.1, 115.1, 74.6, 71.7, 67.7, 45.4, 40.1, 39.8, 34.7, 33.3, 25.3, 22.3, 16.0; HRMS (ESI)

m/z calcd for $C_{13}H_{23}O_2$ $[M+H]^+$ 211.1693, found 211.1695; IR (thin film) cm^{-1}; 3420, 2927, 2868 1465, 1025, 920.

Preparation of (10E)-12-hydroxy-7-methyldodeca-1,10-dien-6-one (20)

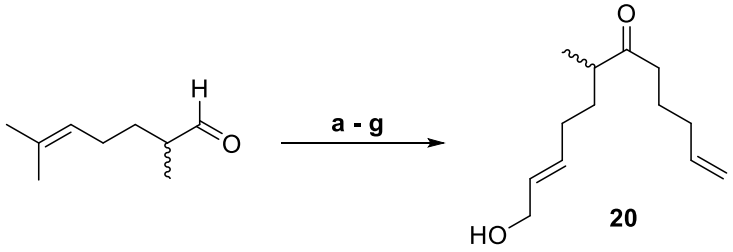

Reagents and conditions

a) *cis*-2-butene-1,4-diol, Hoveyda Grubbs II, DCM, rt, 21%. b) $(CH_3O)_3CH$, *p*-TsOH, MeOH, 0 °C, rt, 88%. c) PMBCl, NaH, Bu_4NI, THF, rt, 62%. d) *p*-TsOH, acetone, rt, 92%. e) 5-bromo-1-pentene, Mg, Et_2O 73%. f) PCC, Celite, DCM, 81%. g) 10% TFA in DCM, 65%.

(10*E*)-12-hydroxy-7-methyldodeca-1,10-dien-6-one (20)

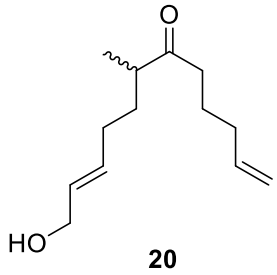

^{1}H NMR (400 MHz, $CDCl_3$): δ (ppm) 5.76 (ddt, *J* = 17.0, 10.2, 6.7 Hz, 1H), 5.63-5.65 (m, 2H), 4.96-5.04 (m, 2H), 4.08 (t, *J* = 3.2 Hz, 2H), 2.52 (sept, *J* = 6.7 Hz, 1H), 2.47 (dt, *J* = 17.2, 7.3 Hz, 1H), 2.41 (dt, *J* = 17.2, 7.3 Hz, 1H), 1.99-2.08 (m, 4H), 1.76 (dp, *J* = 8.8, 4.0 Hz, 1H), 1.66 (pent, *J* = 7.4 Hz, 2H), 1.35-1.44 (m, 1H), 1.31 (t, *J* = 5.3 Hz, 1H), 1.06 (d, *J* = 7.0 Hz, 3H); ^{13}C NMR (100 MHz, $CDCl_3$): 214.4, 138.1, 132.2, 129.6, 115.2, 63.6, 45.7, 40.3, 33.1, 32.1, 29.9, 22.6, 16.5; HRMS (ESI) *m/z* calcd for $C_{13}H_{23}O_2$ $[M+H]^+$ 211.1698, found 211.1694; IR (thin film) cm^{-1}: 3400, 2934, 1706, 1425, 1268, 1078, 923.

(2*R*,5*S*,6*S*)-5-methyl-2-vinyl-1-oxaspiro[5.5]undecan-8-one (21) and (2*S*,5*S*,6*R*)-5-methyl-2-vinyl-1-oxaspiro[5.5]undecan-8-one (21a)

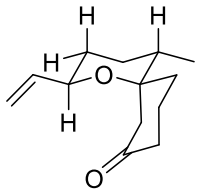

21

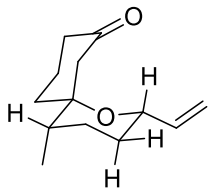

21a

The general procedure for spirocycle synthesis was followed with **20** (20.2 mg, 0.1 mmol) and Re_2O_7 (3.0 mg, 0.006 mmol) in DCM (1.2 mL) at rt for 10 min and the crude product mixture purified via flash column chromatography with 20% ethyl acetate in hexane. The eluted fractions were concentrated and immediately subjected to PCC (40.0 mg, 0.19 mmol) and Celite (40.0 mg) in DCM (1.0 mL) at rt for 15 minutes. The resultant crude mixture was then purified via flash column chromatography using 10 % ethyl acetate in hexanes to give 18 mg (88% yield over 2 steps) of product mixture **21** and **21a** with d.r. of 2.2:1 with **21** as the major diastereomer. ^{1}H NMR (600 MHz, $CDCl_3$) **Mixture of diastereomers** (**21** and **21a**): δ (ppm) 5.77 (ddd, *J* = 17.2, 10.5, 5.4 Hz, 0.3H), 5.74 (ddd, *J* = 17.3, 10.6, 5.0 Hz, 0.7H), 5.16 (dt, *J* = 17.3, 1.4 Hz, 0.3H), 5.15 (dt, *J* = 17.3, 1.6 Hz, 0.7H), 5.00-5.04 (m, 1H), 4.05-4.08 (m, 0.3H), 4.00-4.03 (m, 0.7H), 2.98 (dt, *J* = 13.8, 1.9 Hz, 0.3H), 2.85 (dt, *J* = 13.9, 2.4 Hz, 0.7H), 2.48 (d, *J* = 13.8 Hz, 0.3H), 2.23 (d, *J* = 13.9 Hz, 0.7H), 2.16-2.35 (m, 3H), 1.97-2.06 (m, 1H), 1.74-1.95 (m, 1H), 1.63-1.73 (m, 2H), 1.54-1.60 (m, 2H), 1.41-1.50 (m, 1H), 1.28-1.40 (m, 1H), 1.03 (d, *J* = 7.0 Hz, 0.9H), 0.89 (d, *J* = 6.7 Hz, 2.1H); ^{13}C NMR (150 MHz, $CDCl_3$) **Mixture of diastereomers** (**21** and **21a**): δ (ppm) 210.74, 210.34, 139.60, 139.31, 114.59, 114.43, 80.66, 78.93, 70.59, 70.13, 48.36, 41.30, 40.83, 40.78, 38.99, 35.73, 34.44, 32.79, 31.62, 27.74, 26.03, 25.63, 20.67, 20.47, 17.32, 14,24; HRMS (ESI) *m/z* calcd for $C_{13}H_{21}O_2$ $[M+H]^+$ 209.1542, found 209.1567.

Preparation of (3R,10E)-12-hydroxy-3-methyldodeca-1,10-dien-6-one (22)

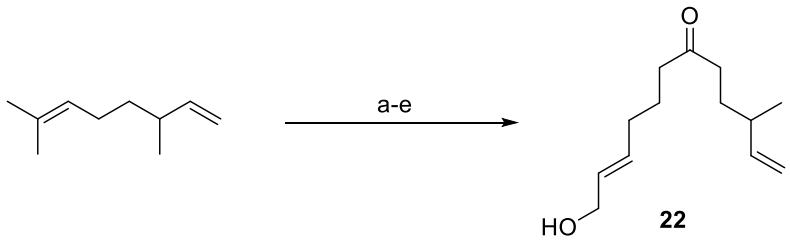

Reagents and conditions
a) *m*CPBA, DCM, 0 °C, 93%. b) PCC, H_5IO_6 , DCM, 0 °C, 75%.
c) MeNHOMe•HCl, DCC, DMAP, Et_3N, 71%. d) t-BuLi, **3**, -78 °C, 52%. e) AcOH, H_2O, 67%.

(3*R*,10*E*)-12-hydroxy-3-methyldodeca-1,10-dien-6-one (22)

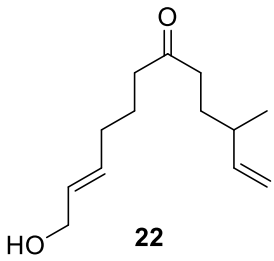

^{1}H NMR (500 MHz, $CDCl_3$): δ (ppm) 5.63-5.66 (m, 2H), 5.62 (ddd, *J* = 17.0, 10.3, 7.9 Hz, 1H), 4.96 (d, *J* = 17.0 Hz, 1H), 4.93 (d, *J* = 10.3 Hz, 1H), 4.09 (dd, *J* = 5.0, 4.7 Hz, 2H), 2.36-2.41 (m, 4H), 2.09 (sept, *J* = 7.4 Hz, 1H), 2.02-2.07 (m, 2H), 1.66 (pent, *J* = 7.4 Hz, 2H), 1.58-1.64 (m, 1H), 1.48-1.55 (m, 1H), 1.24-1.27 (m, 1H), 1.00 (d, *J* = 6.8 Hz, 3H); ^{13}C NMR (125 MHz, $CDCl_3$): 210.9, 143.8, 132.2, 129.8, 113.4, 63.7, 42.0, 40.6, 37.6, 31.6, 30.2, 23.1, 20.3; HRMS (ESI) *m/z* calcd for $C_{13}H_{23}O_2$ $[M+H]^+$ 211.1693, found 211.1694; IR (thin film) cm^{-1}: 3408, 2937, 1720, 1338, 1210, 1062, 941, 716.

(2*R*,6*S*,8*R*,9*R*)-9-methyl-2-vinyl-1-oxaspiro[5.5]undecan-8-ol (23) and (2*R*,6*S*,8*S*,9*R*)-9-methyl-2-vinyl-1-oxaspiro[5.5]undecan-8-ol (23a)

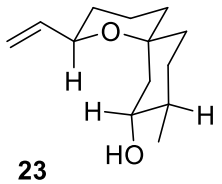

23

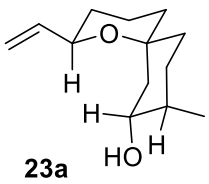

23a

The general procedure for spirocycle synthesis was followed with **22** (15.3 mg, 0.1 mmol) and Re_2O_7 (2.0 mg, 0.004 mmol) in DCM (1.0 mL) at rt for 15 min after which the reaction mixture was purified via flash column chromatography with 0-5% ethyl acetate in hexanes (gradient elution) and concentrated in vacuo to give 11.0 mg (73% yield) of product mixture **23** and **23a** with diastereomeric ratio of 3:1 respectively. **Major (faster-eluting) isomer (23)**: ^{1}H NMR (400 MHz, $CDCl_3$): δ (ppm) 5.82 (ddd, *J* = 17.5, 10.6, 5.1 Hz, 1H), 5.21 (dt, *J* = 17.3, 1.7 Hz, 1H), 5.05 (dt, *J* = 10.6, 1.6 Hz, 1H), 4.04 (ddt, *J* = 12.0, 5.4, 1.6 Hz, 1H), 3.32 (dd, *J* = 11.3, 3.0 Hz, 1H), 2.70 (ddd, *J* = 13.5, 3.7, 2.7 Hz, 1H), 1.70-1.79 (m, 1H), 1.61-1.68 (m, 2H), 1.46-1.57 (m, 2H), 1.36-1.42 (m, 3H), 1.18-1.35 (m, 4H), 1.02 (d, *J* = 6.4 Hz, 3H), 0.92 (dd, *J* = 13.6, 11.0 Hz, 1H); ^{13}C NMR (100 MHz, $CDCl_3$): 140.2, 114.1, 74.3, 72.4, 70.1, 40.6, 39.5, 38.1, 36.1, 31.5, 28.3, 19.4, 18.2; HRMS (ESI) *m/z* calcd for $C_{13}H_{23}O_2$ $[M+H]^+$ 211.1693, found 211.1704; IR (thin film) cm^{-1}: 3401, 3028, 2929, 1442, 1054, 916, 776. **Minor (slower-eluting) isomer (23a):** ^{1}H NMR (400 MHz, $CDCl_3$): δ (ppm) 5.81 (ddd, *J* = 16.6, 10.6, 5.9 Hz, 1H), 5.23 (dt, *J* = 17.2, 5.4 Hz, 1H), 5.08 (dt, *J* = 10.5, 1.3 Hz, 1H), 4.19 (dd, *J* = 11.1, 6.0 Hz, 1H), 3.36 (td, *J* = 7.4, 3.4 Hz, 1H), 2.62 (br, 1H), 1.96-2.05 (m, 1H), 1.88-1.95 (m, 1H), 1.77-1.83 (m, 1H), 1.60-1.76 (m, 5H), 1.22-1.32 (m, 4H), 1.05-1.16 (m, 1H), 0.98 (d, *J* = 6.9 Hz, 3H); ^{13}C NMR (100 MHz, $CDCl_3$): 139.7, 114.9, 74.4, 73.4, 71.3, 31.6, 26.6, 19.1, 17.3 (Note: some peaks did not emerge beyond baseline and hence could not reported); HRMS (ESI) *m/z* calcd for $C_{13}H_{23}O_2$ $[M+H]^+$ 211.1693, found 211.1698; IR (thin film) cm^{-1}: 3371, 2978, 1472, 1050, 946, 718.

Preparation of (E)-12-hydroxy-4-methyldodeca-1,10-dien-6-one (24).

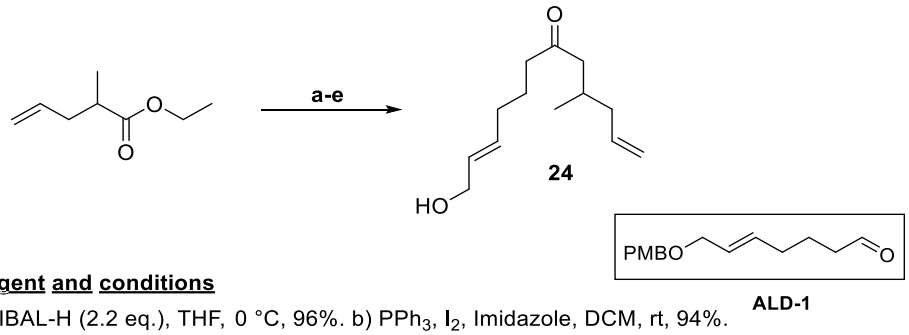

Reagent and conditions

a) DIBAL-H (2.2 eq.), THF, 0 °C, 96%. b) PPh_3, I_2, Imidazole, DCM, rt, 94%.
c) Mg, I_2, **ALD-1,** THF, 76%. d) PCC, Celite, DCM, rt, 89%. e) 10 % TFA in DCM, rt, 81%.

(*E*)-12-hydroxy-4-methyldodeca-1,10-dien-6-one (24)

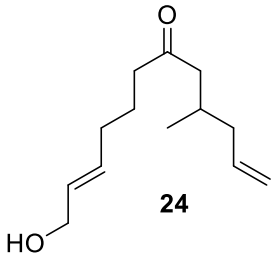

^{1}H NMR (500 MHz, $CDCl_3$): δ (ppm) 5.74 (ddt, *J* = 14.4, 11.2, 7.2 Hz, 1H), 5.61-5.69 (m, 2H), 4.99-5.02 (m, 2H), 4.09 (d, *J* = 3.7 Hz, 2H), 2.41 (dd, *J* = 15.9, 5.4 Hz, 1H), 2.38 (t, *J* = 6.3 Hz, 2H), 2.19 (dd, *J* = 16.0, 7.9 Hz, 1H), 2.11 (oct, *J* = 6.6 Hz, 1H), 2.03-2.07 (m, 3H), 1.95-2.01 (m, 2H), 1.66 (pent, *J* = 7.4 Hz, 2H), 0.90 (d, *J* = 6.9 Hz, 3H); ^{13}C NMR (125 MHz, $CDCl_3$) δ (ppm) 210.6, 136.7, 132.2, 129.8, 116.4, 63.7, 49.4, 42.6, 41.2, 31.6, 28.9, 23.0, 19.8; HRMS (ESI) *m/z* calcd for $C_{13}H_{22}O_2Na$ $[M+Na]^+$ 233.1512, found 233.1507; IR (thin film) cm^{-1}: 3391, 3107, 2927, 1706, 1370, 1088, 998, 703.

(2*R*,6*S*,8*S*,10*R*)-10-methyl-2-vinyl-1-oxaspiro[5.5]undecan-8-ol (25)&

(2*R*,6*S*,8*S*,10*S*)-10-methyl-2-vinyl-1-oxaspiro[5.5]undecan-8-ol (28)

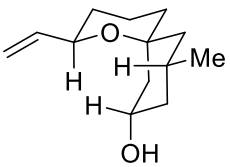

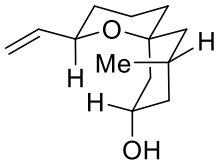

The general procedure for spirocycle synthesis was followed with **24** (30 mg, 0.14 mmol) and Re_2O_7 (2 mg, 0.004 mmol) in DCM (1.0 mL) for 2 h by slowly warming the reaction from 0 °C to rt. The resultant crude mixture was purified via flash column chromatography with 10% ethyl acetate in hexanes as eluent to give a 21 mg (70% yield) of

product mixture **25** and **28** with d.r. of 3.8:1 and **25** as the major diastereomer. **Major (faster-eluting) isomer** (**25**) ^{1}H NMR (500 MHz, $CDCl_3$): δ (ppm) 5.81 (ddd, *J* = 17.3, 10.6, 5.2 Hz, 1H), 5.20 (dt, *J* = 17.3, 1.7 Hz, 1H), 5.05 (dt, *J* = 10.5, 1.5 Hz, 1H), 4.04 (ddt, *J* = 11.4, 3.1, 1.4 Hz, 1H), 3.80 (tt, *J* = 11.3, 4.2 Hz, 1H), 2.71 (ddt, *J* = 13.2, 4.2, 2.2 Hz, 1H), 1.95-2.04 (m, 2H), 1.71-1.78 (m, 1H), 1.63-1.68 (m, 2H), 1.58 (ddt, *J* = 13.4, 4.1, 2.4 Hz, 1H), 1.36-1.41 (m, 3H), 1.24 (qd, *J* = 11.7, 4.2 Hz, 1H), 0.94 (dd, *J* = 13.3, 12.2 Hz, 1H), 0.90 (d, *J* = 6.6 Hz, 3H), 0.86 (t, *J* = 11.2 Hz, 1H), 0.80 (dd, *J* = 13.3, 11.4 Hz, 1H); ^{13}C NMR (125 MHz, $CDCl_3$) δ (ppm) 140.1, 114.2, 74.3, 70.2, 66.9, 47.9, 47.8, 38.0, 36.1, 31.4, 25.7, 21.9, 19.3; HRMS (ESI) *m/z* calcd for $C_{13}H_{23}O_2$ $[M+H]^+$ 211.1693, found 211.1689; IR (thin film) cm^{-1}: 3370, 2930, 2868, 1457, 1366, 1024, 735. **Minor (slower-eluting) isomer** (**28**) ^{1}H NMR (600 MHz, $CDCl_3$): δ (ppm) 5.81 (ddd, *J* = 17.0, 10.4, 5.9 Hz, 1H), 5.20 (d, *J* = 17.3 Hz, 1H), 5.05 (d, *J* = 10.4 Hz, 1H), 4.14 (dd, *J* = 10.9, 5.5 Hz, 1H), 3.61 (tt, *J* = 9.0, 4.4 Hz, 1H), 2.69 (dt, *J* = 11.8, 1.8 Hz, 1H), 1.96 (d, *J* = 12.1 Hz, 1H), 1.67-1.72 (m, 3H), 1.64 (d, *J* = 12.9 Hz, 1H), 1.57 (d, *J* = 12.3 Hz, 1H), 1.50-1.54 (m, 1H), 1.39-1.47 (m, 1H), 1.19-1.31 (m, 4H), 1.07 (t, *J* = 11.7 Hz, 1H), 0.94 (d, *J* = 6.3 Hz, 3H); ^{13}C NMR (150 MHz, $CDCl_3$) δ (ppm) 140.1, 114.8, 74.2, 71.1, 68.4, 49.0, 44.7, 39.9, 32.3, 31.7, 26.4, 22.2, 19.3; HRMS (ESI) *m/z* calcd for $C_{13}H_{23}O_2$ $[M+H]^+$ 211.1693, found 211.1687; IR (thin film) cm^{-1}: 3375, 2927, 2869, 1411, 1365, 1019, 720.

Preparation of (E)-12-hydroxydodec-10-en-1-yn-6-one (29)

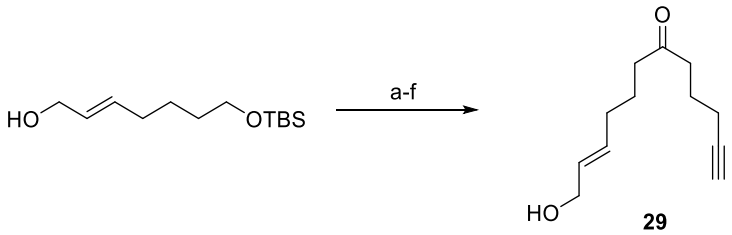

Reagents and conditions

a) TBDPSCl, imidazole, DCM, rt, 98%. b) PPTS, MeOH, 55 °C, 73%.
c) PCC, Celite, DCM, rt, 79%. d) $Me_3SiCCCH_2CH_2CH_2Br$, Mg, I_2, THF, 96%.
e) PCC, Celite, DCM, rt, 77%. f) TBAF, THF, H_2O, rt, 83%.

(*E*)-12-hydroxydodec-10-en-1-yn-6-one (29)

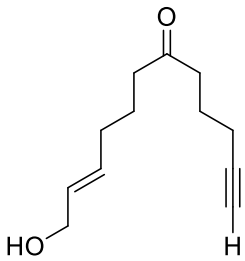

29

^{1}H NMR (500 MHz, $CDCl_3$): δ (ppm) 5.60-5.68 (m, 2H), 4.09 (d, *J* = 0.9 Hz, 2H), 2.54 (t, *J* = 7.2 Hz, 2H), 2.42 (t, *J* = 7.4 Hz, 2H), 2.22 (dt, *J* = 6.8, 2.6 Hz, 2H), 2.04-2.07 (m, 2H), 1.95 (t, *J* = 2.6 Hz, 1H), 1.78 (pent, *J* = 7.1 Hz, 2H), 1.68 (pent, *J* = 7.4 Hz, 2H), 1.49 (s, 1H); ^{13}C NMR (125 MHz, $CDCl_3$) δ (ppm) 210.2, 132.0, 129.9, 83.6, 69.0, 63.6, 42.1, 41.1, 31.5, 23.1, 22.2, 17.8; HRMS (ESI) *m/z* calcd for $C_{12}H_{18}O_2Na$ $[M+Na]^+$ 217.1199, found 217.1192; IR (thin film) cm^{-1}: 3414, 3288, 2934, 1706, 1372, 1091, 973, 639.

(2*R*,6*S*)-2-vinyl-1-oxaspiro[5.5]undecan-8-one (11) and (2*R*,6*R*)-2-vinyl-1-oxaspiro[5.5]undecan-8-one (30)

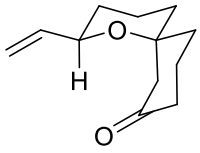

11

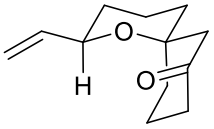

30

The general procedure for spirocycle synthesis was followed with **29** (25 mg, 0.13 mmol) and Re_2O_7 (3 mg, 0.006 mmol) in DCM (0.8 mL) at rt for 10 min. The crude reaction mixture was then quenched with a drop of pyridine and loaded onto 60 Å silica gel to be purified via gradient-elution flash column chromatography with 0-5% ethyl acetate in hexanes as eluent. The eluted fractions were combined and concentrated under reduced pressure to yield 20.2 mg (81%) of product mixture of **11** and **30** in a 1:1 ratio. **Faster-eluting product** (**11**) ^{1}H NMR (500 MHz, $CDCl_3$): δ (ppm) 5.77 (ddd, *J* = 17.5, 10.6, 5.3 Hz, 1H), 5.17 (dt, *J* = 17.3, 1.6 Hz, 1H), 5.04 (dt, *J* = 10.6, 1.5 Hz, 1H), 4.04 (ddt, *J* = 11.2, 2.6, 1.1Hz, 1H), 2.96 (dt, *J* = 13.9, 1.6 Hz, 1H), 2.31-2.38 (m, 2H), 2.25-2.31 (m, 1H), 2.10-2.19 (m, 1H), 1.85-1.89 (m, 1H), 1.75-1.83 (m 2H), 1.63-1.70 (m, 3H), 1.56-1.59 (m, 1H), 1.39-1.45 (m, 1H), 1.20-1.42 (m, 1H); ^{13}C NMR (125 MHz, $CDCl_3$) δ (ppm) 210.0, 139.5, 114.6, 70.6, 46.4, 40.9, 38.9, 34.7, 31.1, 29.7, 20.5, 18.9; HRMS (ESI) *m/z* calcd for $C_{12}H_{19}O_2$ $[M+H]^+$ 195.1380, found 195.1376; IR (thin film) cm^{-1}: 2933, 2870, 1711, 1440, 1227, 1048, 984, 710. **Slower-eluting product** (**30**) ^{1}H NMR (500 MHz, $CDCl_3$): δ (ppm) 5.77 (ddd, *J* = 17.2, 10.6, 5.2 Hz, 1H), 5.16 (dt, *J* = 17.3, 1.4 Hz, 1H), 5.02 (dt, *J* = 10.5, 1.2 Hz, 1H), 3.92 (dd, *J* = 11.6, 3.3 Hz, 1H), 2.37-2.44 (m, 3H), 2.28-2.36 (m, 1H), 2.19-2.26 (m, 1H), 1.74-1.87 (m, 3H), 1.68-1.74 (m, 2H), 1.56-1.67 (m, 2H), 1.48-1.53 (m, 1H), 1.38 (td, *J* = 13.1, 5.8 Hz, 1H); ^{13}C NMR (125 MHz, $CDCl_3$) δ (ppm) 209.9, 139.6, 114.1, 70.6, 55.5, 40.9, 34.6, 30.9, 29.7, 28.4, 20.0, 19.4; HRMS (ESI) *m/z* calcd for $C_{12}H_{19}O_2$ $[M+H]^+$ 195.1380, found 195.1376; IR (thin film) cm^{-1}: 2932, 2850, 1715, 1442, 1225, 1019, 982.

Preparation of (E)-12-hydroxy-2-methyldodeca-1,10-dien-6-one (32)

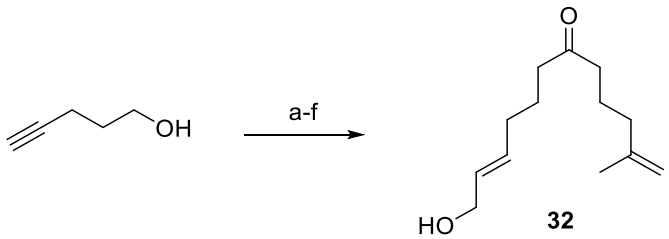

32

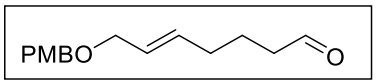

ALD-1

Reagents and conditions *from* ***scheme 6 step (d)***

a) $AlMe_3$ (3.0 equiv), Cp_2ZrCl_2, DCM, rt, 77%. b) MsCl, Et_3N, DCM, 0 °C, 64%.
c) LiBr, Acetone, reflux, 80%. d) Mg, I_2, then **ALD-1**, THF, 71%.
e) PCC Celite, DCM, 98%. f) 10 % TFA in DCM, rt, 48%.

(*E*)-12-hydroxy-2-methyldodeca-1,10-dien-6-one (32)

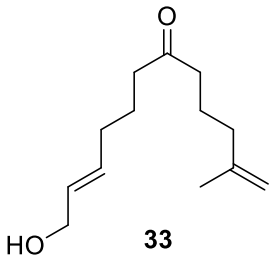

33

^{1}H NMR (400 MHz, $CDCl_3$): δ (ppm) 5.60-5.70 (m, 2H), 4.72 (dt, *J* = 1.3, 0.7 Hz, 1H), 4.66 (dt, *J* = 1.9, 1.0 Hz, 1H), 4.09 (d, *J* = 3.6 Hz, 2H), 2.39 (t, *J* = 7.6 Hz, 2H), 2.38 (t, *J* = 7.6 Hz, 2H), 2.02-2.10 (m, 2H), 2.00 (t, *J* = 7.7 Hz, 2H), 1.71 (pent, *J* = 7.8 Hz, 2H), 1.69 (s, 3H), 1.67 (pent, *J* = 7.4 Hz, 2H), 1.50 (s, 1H); ^{13}C NMR (100 MHz, $CDCl_3$): δ (ppm) 211.0, 145.1, 132.2, 129.8, 110.6, 63.7, 42.1, 42.0, 37.1, 31.6, 23.1, 22.2, 21.4; HRMS (ESI) *m/z* calcd for $C_{13}H_{22}O_2Na$ $[M+Na]^+$ 233.1512, found 233.1504; IR (thin film) cm^{-1}: 3401, 3110, 2932, 1707, 1338, 1065, 921, 703 .

(2*R*,6*S*,8*S*)-8-methyl-2-vinyl-1-oxaspiro[5.5]undecan-8-ol (33) and (2*R*)-8-methyl-2-vinyl-1-oxaspiro[5.5]undec-7-ene (34)

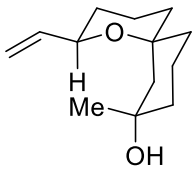

33

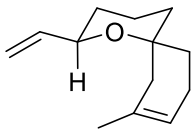

34

The general procedure for spirocycle synthesis was followed with **33** (43.7 mg, 0.21 mmol) and Re_2O_7 (3 mg, 0.006 mmol) in DCM (1.3 mL) at –10 °C. The reaction was slowly warmed up to 0 °C for 2 h after which the crude mixture was purified with gradient-elution flash column chromatography using 0-10% ethyl acetate in hexanes as eluent and eluted fractions concentrated *in vacuo* to give 37.6 mg (86% yield) of product mixture **33** and **34** of ratio of 2.6:1 with **33** as the major product. **Major (slower-eluting) product (33)** ^{1}H NMR (500 MHz, $CDCl_3$): δ (ppm) 5.80 (ddd, *J* = 17.1, 10.6, 5.3 Hz, 1H), 5.20 (d, *J* = 17.2 Hz, 1H), 5.05 (d, *J* = 10.5 Hz, 1H), 4.03 (dd, *J* = 11.3, 4.4 Hz, 1H), 2.26 (d, *J* = 13.9 Hz, 1H), 1.67-1.77 (m, 2H), 1.61-1.67 (m, 3H), 1.53-1.61 (m, 3H), 1.42 (dt, *J* = 12.4, 4.1 Hz, 1H), 1.33-1.38 (m, 3H), 1.32 (s, 3H), 1.22-1.28 (m, 2H); ^{13}C NMR (125 MHz, $CDCl_3$): δ (ppm) 140.0, 114.1, 73.8, 71.2, 70.6, 42.0, 40.9, 40.01, 36.3, 31.6, 28.1, 19.4, 19.3; HRMS (ESI) *m/z* calcd for $C_{13}H_{21}O_2H$ $[M-H]^-$ 209.1536, found 209.1533; IR (thin film) cm^{-1}: 3377, 2927, 2851, 1439, 1022, 916, 776. **Minor (faster-eluting) product** (**34**) ^{1}H NMR (500 MHz, $CDCl_3$): δ (ppm) 5.84 (ddd, *J* = 16.8, 10.5, 5.8 Hz, 1H), 5.35 (s, 1H), 5.21 (d, *J* = 16.8 Hz, 1H), 5.06 (d, *J* = 10.5 Hz, 1H), 4.10 (dd, *J* = 11.2, 5.2 Hz, 1H), 2.30 (d, *J* = 16.7 Hz, 1H), 2.10-2.15 (m, 1H), 2.08 (d, *J* = 17.1 Hz, 1H), 1.96-2.05 (m, 1H), 1.67-1.75 (m, 3H), 1.62-1.67 (m, 4H), 1.52-1.56 (m, 1H), 1.25 (s, 3H); ^{13}C NMR (125 MHz, $CDCl_3$): δ (ppm) 140.4, 131.5, 120.3, 114.4, 72.6, 70.9, 36.6, 36.3, 31.9, 31.7, 23.8, 23.0, 19.3; HRMS (ESI) *m/z* calcd for $C_{13}H_{21}O$ $[M+H]^+$ 193.1587, found 193.1583; IR (thin film) cm^{-1}: 2931, 2844, 1438, 1043, 918,737.

Preparation of (2E,11Z)-1-hydroxytrideca-2,11-dien-7-one (35)

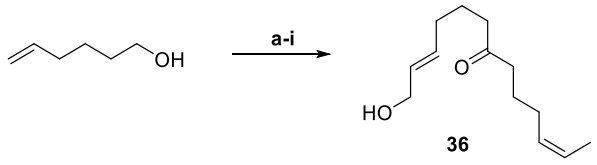

Reagents and conditions

a) TBSCl, imidazole, DCM, rt, 99%. b) Methyl acrylate, Hoveyda-Grubbs II catalyst, DCM, rt, 57%. c) DIBAL-H, DCM, -78 °C, 89%. d) NaH, PMBCl, THF, 0 °C, 77%. e) TBAF, THF, 0 °C, 39%. f) PCC Celite, DCM, rt, 80%. g) Mg, I_2, Z-$CH_3CH{=}CHCH_2CH_2CH_2Br$, THF, 80%. h) PCC Celite, DCM, rt, 94%. i) 10% TFA in DCM, rt, 91%.

(2*E*,11*Z*)-1-hydroxytrideca-2,11-dien-7-one (35)

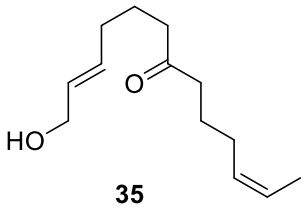

^{1}H NMR (500 MHz, $CDCl_3$): δ (ppm) 5.61-5.69 (m, 2H), 5.47 (dqt, *J* = 12.9, 7.3, 1.7 Hz, 1H), 5.34 (dtq, *J* = 12.4, 7.2, 1.6 Hz, 1H), 4.09 (d, *J* = 3.0 Hz, 2H), 2.40 (t, *J* = 7.2 Hz, 2H), 2.39 (t, *J* = 7.2 Hz, 2H), 2.02-2.10 (m, 4H), 1.67, (pent, *J* = 7.6 Hz, 2H), 1.64 (pent, *J* = 7.5 Hz, 2H), 1.51-1.58 (m, 1H), 1.59 (ddt, *J* = 6.9, 1.76, 0.8 Hz, 3H); ^{13}C NMR (125 MHz, $CDCl_3$): δ (ppm) 210.9, 132.2, 129.8, 129.6, 124.8, 63.7, 42.2, 42.0, 31.6, 26.2, 23.6, 23.1, 12.8; HRMS (ESI) *m/z* calcd for $C_{13}H_{22}O_2Na$ $[M+Na]^+$ 233.1512, found 233.1508; IR (thin film) cm^{-1}: 3404, 3115, 2929, 1707, 1408, 1371, 1266, 1087, 971, 736.

(2*R*,6*R*,7*S*,8*S*)-7-methyl-2-vinyl-1-oxaspiro[5.5]undecan-8-ol (36) and (2*R*,6*R*,7*S*,8*R*)-7-methyl-2-vinyl-1-oxaspiro[5.5]undecan-8-ol (37)

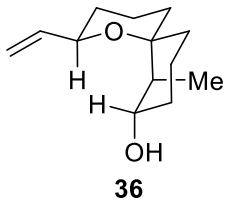

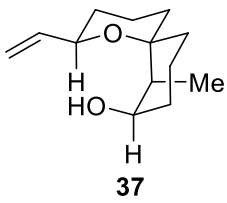

The general procedure for spirocycle synthesis was followed with **36** (10 mg, 0.05 mmol) and Re_2O_7 (3 mg, 0.006 mmol) in DCM (0.6 mL) for 1h at 0 °C. The crude reaction mixture was then purified via gradient-elution flash column chromatography with 0-10% ethyl acetate in hexanes as eluent and the eluted fractions concentrated *in vacuo* to give 8.1 mg (81%) of product mixture **36** and **37** with diastereomeric ratio 4:1 and **36** as the major isomer.

Major (slower-eluting) isomer (**36**) ^{1}H NMR (400 MHz, $CDCl_3$): δ (ppm) 5.83 (ddd, *J* = 16.9, 10.4, 5.8 Hz, 1H), 5.22 (dt, *J* = 16.9, 1.6 Hz, 1H), 5.07 (dt, *J* = 10.5, 1.6 Hz, 1H), 4.00 (dd, *J* = 9.2, 6.2 Hz, 1H), 3.79 (td, *J* = 9.9, 4.4 Hz, 1H), 2.39-2.46 (m, 1H), 1.96 (dt, *J* = 13.7, 4.0 Hz, 1H), 1.68-1.76 (m, 3H), 1.61-1.66 (m, 4H), 1.46-1.54 (m, 1H), 1.28-1.38 (m, 2H), 1.18-1.25 (m, 2H), 0.98 (d, *J* = 7.0 Hz, 3H); ^{13}C NMR (100 MHz, $CDCl_3$): δ (ppm) 139.9, 114.7, 76.1, 70.7, 70.5, 53.4, 36.4, 34.8, 30.8, 29.7, 26.2, 23.6, 18.7; HRMS (ESI) *m/z* calcd for $C_{13}H_{23}O_2$ $[M+H]^+$ 211.1693, found 211.1687; IR (thin film) cm^{-1}: 3402, 2956, 2869, 1467, 1284, 1042, 917, 735. **Minor (faster-eluting) isomer** (**37**) ^{1}H NMR (400 MHz, $CDCl_3$): δ (ppm) 5.82 (ddd, *J* = 17.3, 10.6, 5.9 Hz, 1H), 5.22 (dt, *J* = 17.3, 1.6 Hz, 1H), 5.05 (dt, *J* = 10.6, 1.6 Hz, 1H), 4.16 (dd, *J* = 11.4, 3.4 Hz, 1H), 4.02 (dq, *J* = 11.6, 4.4 Hz, 1H), 3.78 (d, *J* = 11.6 Hz, 1H), 2.63 (pent, *J* = 6.8 Hz, 1H), 2.34-2.43 (m, 1H), 2.00-2.08 (m, 1H), 1.79 (dt, *J* = 11.4, 4.5 Hz, 1H), 1.71 (ddt, *J* = 13.5, 3.4, 1.5 Hz, 1H), 1.62-1.65 (m, 2H), 1.47-1.52 (m, 2H), 1,37-1.45 (m, 2H), 1.27-1.30 (m, 2H), 0.86 (d, *J* = 6.9 Hz, 3H); ^{13}C NMR (100 MHz, $CDCl_3$): δ (ppm) 140.4, 113.9, 70.6, 69.1, 68.5, 53.4, 34.3, 33.4, 33.0, 31.4, 28.8, 19.2, 18.4; HRMS (ESI) *m/z* calcd for $C_{13}H_{23}O_2$ $[M+H]^+$ 211.1693, found 211.1687; IR (thin film) cm^{-1}: 3403, 2981, 2876, 1414, 1254, 1012, 937, 731.

2.0 SYNTHESIS AND H_2O_2-MEDIATED TARGETED CELLULAR RELEASE OF A PEDERIN ANALOGUE

2.1 Introduction

Reactive oxygen species (ROS) are well-known for playing a dual role as destructive and constructive species in cells. Indeed, ROS are engaged in many redox-governing activities of the cells for the preservation of cellular homeostasis.[43] However, its overproduction, despite the enormous antioxidant and repair mechanisms that developed in biological systems, has been reported to result in oxidative stress[44] which is considered a deleterious process and is involved in the damage of cell structures, causing various diseased states including neurodegenerative disorders, cancer, diabetes, reperfusion injuries, aging and arthitis.[45] The unique chemical environment in tissues that are impacted by oxidative stress creates opportunities for localized biological effector activation or release, providing the potential for targeted therapy. This has resulted in the development of new prodrugs with better therapeutic profiles than their corresponding parent drugs, and it is believed that the use of the targeted prodrug approach will be facilitated in the coming few years with the percentage of prodrugs in the medicines market expected to exceed 20%.[46.]

Hydrogen peroxide (H_2O_2) is the most persistent of the reactive oxygen species formed through oxidative stress[47] and is a highly attractive agent for initiating effector release because, in addition to its localized production, it is small and can diffuse into sterically crowded sites while exhibiting a unique reactivity profile. The concentration of H_2O_2 in cancer cells has been determined to be several orders of magnitude higher than in normal cells[48] thereby providing an

opportunity for selective release. This dissertation describes the development of a new small molecule agent that uses endogenous H_2O_2 to release biological effectors, thereby creating opportunities to activate therapeutically beneficial cellular pathways.

2.2 The Role of Boron in Drug Design

Boron has unique chemical properties which make it a special element in drug discovery. It is in the same period as carbon and nitrogen which form the basis of life, as well as being strongly Lewis acidic and having empty p-orbitals that allow for dative bonding with biological nucleophiles like hydroxyl and amine groups present in enzyme pockets.[77] Nevertheless medicinal chemists have overlooked the element, holding largely unfounded beliefs that boron is toxic. These beliefs have been disproven by the plethora of studies which found boron not to be inherently toxic and however can be considered in drug discovery.[78]

The involvement of boron compounds in drug design have gained notoriety over the past decade with the approval of boron-containing drugs by the FDA including bortezomib (Velcade®), a dipeptide boronic acid for treatment of multiple myeloma (the first in-class proteasome inhibitor as well as the first boron-containing drug on the market), tavaborole (Kerydin) for the treatment of onychomicosis and crisaborole (Eucrisa) for the treatment of mild to moderate atopic dermatitis (Figure 2.1).[79-81] Several other boron-containing compounds are being evaluated for different therapeutic applications.[77]

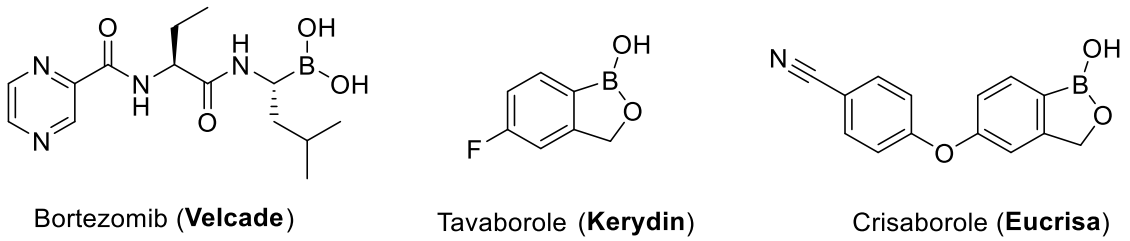

Figure 2.1 Boron-containing drugs approved by FDA

2.2.1 Boronate-based small molecules for H_2O_2-mediated molecular release

Boronic acid (and ester-containing) prodrugs targeting the overexpressed level of reactive oxygen species within tumor microenvironment represent a promising area for the discovery of new selective anticancer chemotherapy.[49] This strategy that emerged only ten years ago[50] is exponentially growing and could become clinically useful in future.[51]

The use of H_2O_2 to release compounds through boronate oxidation was significantly advanced by the Chang group,[52] who showed (among other developments) that the oxidative conversion of aryl boronates such as compound **2.1** to their corresponding phenols **2.2** promotes ionization of benzylic carbamates or carbonates (1,6-elimination), ultimately leading to fluorophore **2.3** and quinone methide (**2.4**) release (Scheme 2.1).

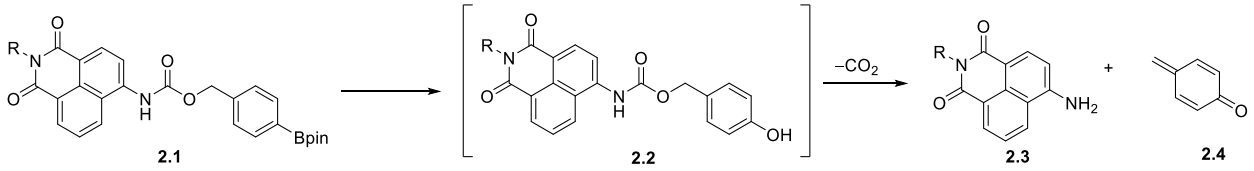

Scheme 2.1 Fluorophore release through aryl boronate oxidation and 1,6-elimination

Similarly, Lo's employment of the conversion of boronate **2.5** to phenol, to effect benzylic leaving group departure, (Scheme 2.2)[53] also played a part in the development of numerous fluorophore-releasing compounds and other diagnostic tools in oxidatively stressed cells.[54]

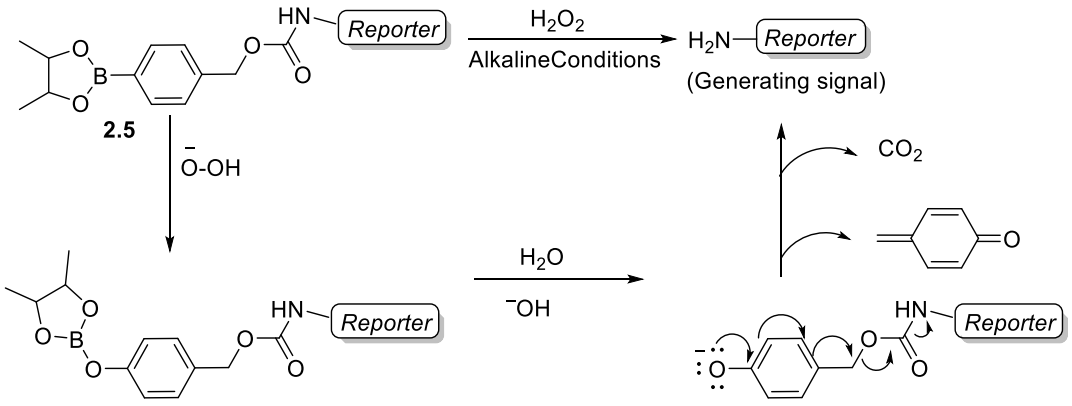

Scheme 2.2 Boronate probe in H_2O_2-mediated reporter signal release

Fréchet and co-workers described the modification of Dextran, a water-soluble biocompatible polymer of glucose, at its hydroxyl functionalities with arylboronic esters in the preparation of oxygen-sensitive dextran (Oxi-DEX), a carrier biopolymer that selectively releases its payload in the presence of biologically relevant concentrations of H_2O_2 (Scheme 2.3).[55] When used in a model vaccine application, Oxi-DEX particles loaded with ovalbumin (OVA) increased the presentation to $CD8^+$ T-cells 27-fold relative to OVA encapsulated in a classical vehicle not sensitive to oxidation. No presentation was observed from cells incubated with unencapsulated OVA.

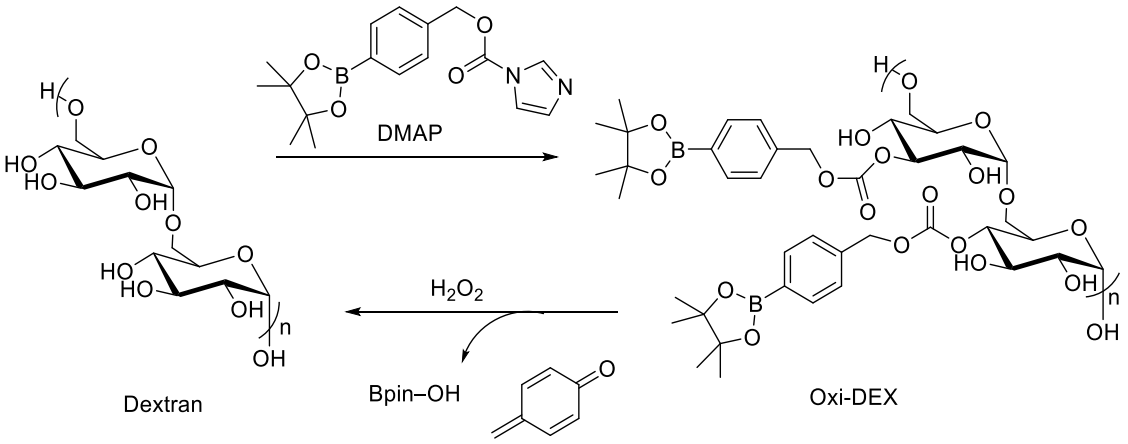

Scheme 2.3 Synthesis and degradation of Oxi-DEX

Subsequently, Mosey and co-workers reported the preparation of structurally diverse α-alkoxy carbamates via the multicomponent sequence of nitrile hydrozirconation, acylation and alcohol addition.[56] They demonstrated that these carbamates release their alcohol component in response to precise chemical stimuli, and that the rate of alcohol release is controlled by the rate of quinone methide formation rather than boronate oxidation or the collapse of the tetrahedral intermediate. This study thus provides an entry into the development of drug delivery vehicles (Scheme 2.4).

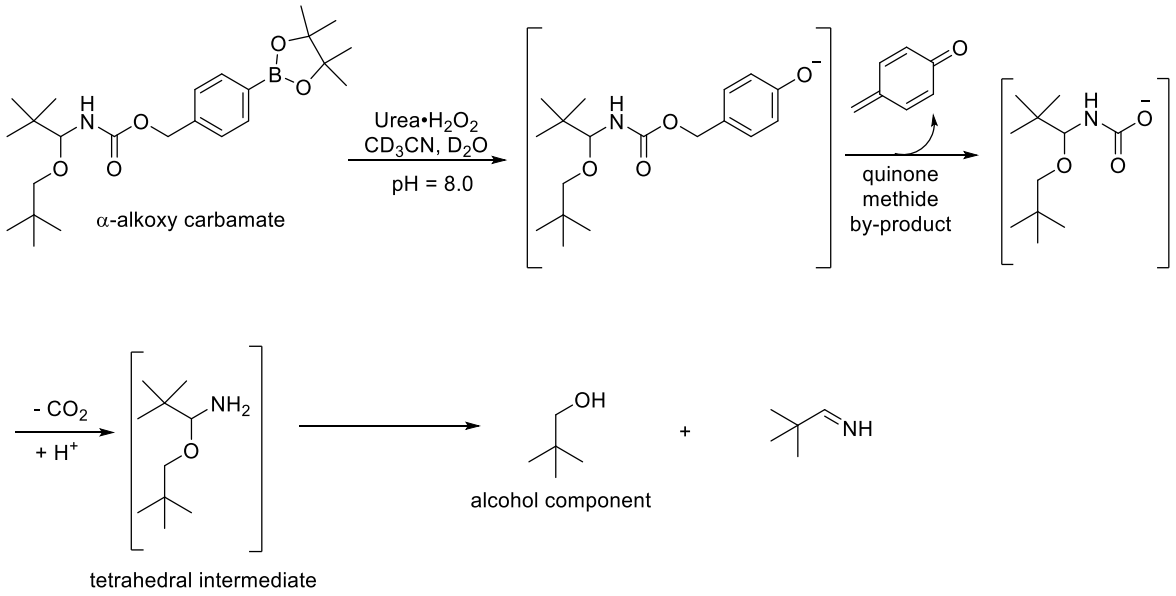

Scheme 2.4 Peroxide-mediated alcohol release from α-alkoxy carbamate

The accompanying release of quinone methide alkylating agents in these and other release methods however, limits applications of these approaches to processes in which cytotoxicity is the end result and precludes applications in which cellular function is promoted.[57] Our group has embarked on a project to develop new boronate-based motifs for peroxide-mediated molecular release without the accompanying release of toxic by-products.

Hanna and coworkers have described the liberation of alcohols, aldehydes and ketones and the intracellular fluorophore release through peroxide mediated fragmentation of α-boryl ethers that can be accessed through operationally facile ketone or aldehyde borylation reactions (Scheme 2.5).[58] They observed that α-boryl ethers release alcohols extremely rapidly in the presence of H_2O_2, while α-boryl carbonates decompose somewhat more slowly, providing a predictable mechanism for controlling the rate of alcohol release.

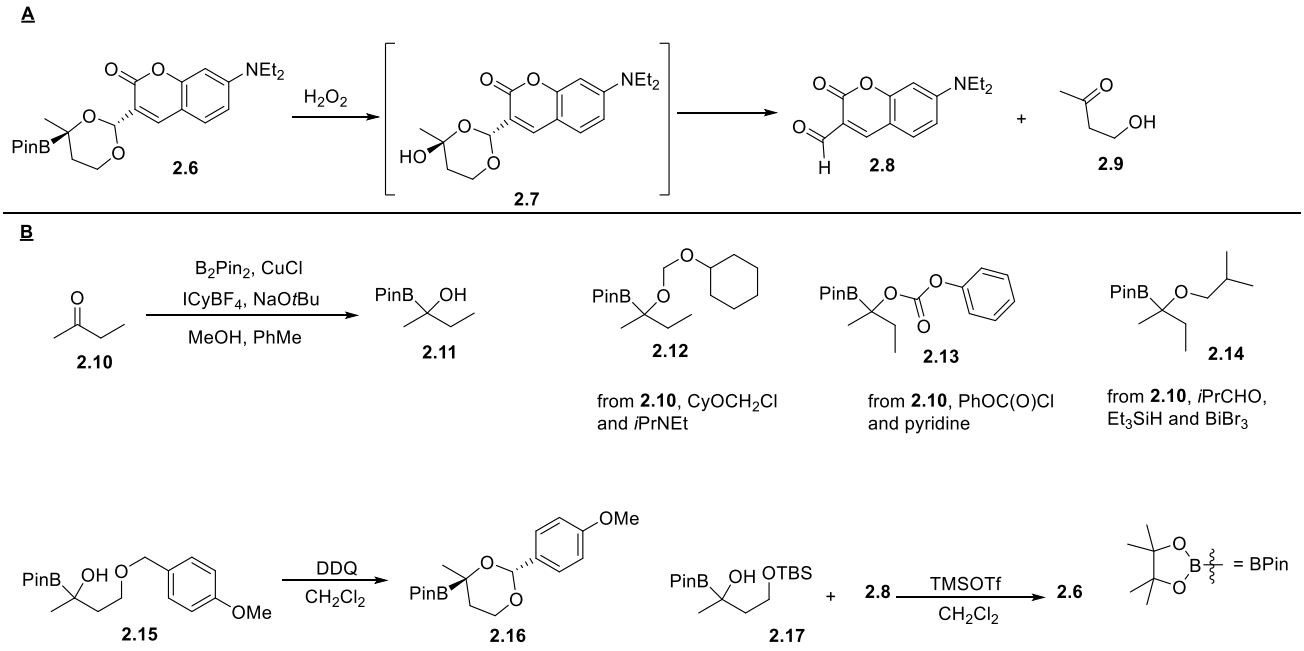

Scheme 2.5 A) Molecular release in the presence of H_2O_2. B) Synthesis of α-boryl ethers and related structures

2.2.2 Research objectives

Based on the findings by Hanna and co-workers, we have set out to develop a boronate-based small molecule agent for H_2O_2-mediated targeted release of its payload in malignant tumor cells. Our objective is to synthesize a potent cytotoxin that can be functionalized into a boronate-based biological agent to be activated in cells under oxidative stress.

Our group previously described the total synthesis of pederin (Figure 2.2)[59] (a natural product isolated from the beetles of the *Paederis* family and the causative agent of the inflammatory condition known as *Paederis* dermatitis)[60] and analogues. This potent cytotoxin[61] is known to target the 60S subunit of the ribosome[62] with protein synthesis inhibition being its mode of biological activity.[63]

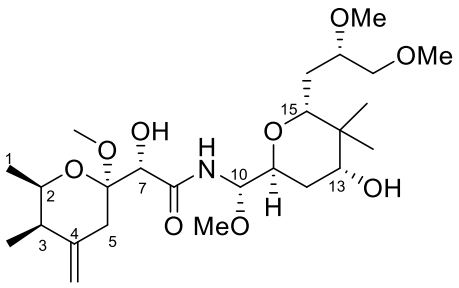

Figure 2.2 Structure of pederin

The potency of pederin and its analogues was measured in cell viability studies against the HCT-116 colon cancer cell line[64], and it was determined that pederin has a 0.6 ±0.1 nM GI_{50} value which amounts to potent cytotoxity. The absence of the C10 methoxy group in pederin results in the reduction of potency by about 6 nM, contrary to reports that related compounds that lack oxygenation at C10 show significantly diminished activity.[65] In the pederin/ribosome complex studied, the lack of hydrogen-bonding contacts involving the C13 hydroxyl group suggests that it serves no role in ribosome binding. This is consistent with results by Siedel-Dugan and co-workers[66] showing that deoxygenation at the corresponding position of a related natural product, psymberin, rather increased activity. Replacement of the C13 hydroxyl group in pederin with a methyl ether, results in an analogue with significantly higher cytotoxicity, which suggests that enhanced hydrophobicity at C13 could be a general strategy to enhance potency in these family of natural products.

Based on the structure-activity relationship (SAR) studies conducted with pederin and its analogues[59], we chose to synthesize another pederin analogue **2.18** (Figure 2.3A), which would be the cytotoxic biological effector to be used in this research. This analogue bears the methyl ether at C13 and lacks the C10 methoxy substituent. We assumed that this compound would possess a significant level of potency towards similar cell lines that are affected by pederin.

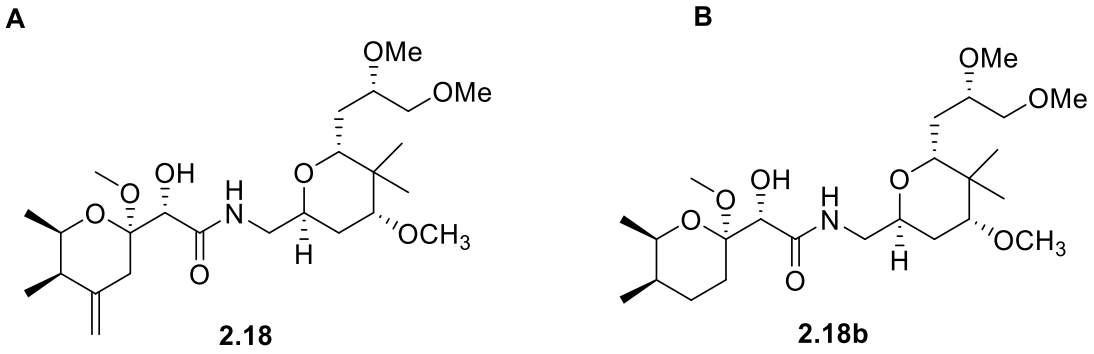

Figure 2.3 A) Proposed pederin analogue as biological effector B) Similar less potent analogue

This assumption of potency of the proposed analogue was informed by the fact that a similar analogue **2.18b** (Figure 2.3B) that was studied[59] as part of the SAR studies highlights the importance of the exocyclic alkene. Removing two functional groups from pederin resulted in more than a hundred-fold reduction in potency of the analogue. In the pederin/ribosome model, the exocyclic alkene of the pederic acid fragment (left-hand fragment) of pederin intercalates between adjacent adenine and guanine residues in the binding pocket and it was proposed that this interaction acts as an anchor that organizes other functional groups of the acyl fragment into a suitable binding orientation. Deletion of the exocyclic alkene in **2.18b** causes a disruption in the structural organization of the compound by the removal of ring conformational restraints, and this reduces the binding contribution of the adjacent acyl fragment thereby reducing activity. Hence, we envision that in the absence of the C10 ether substituent, restoring the exocyclic alkene as well as etherifying the C13 hydroxy substituent will generate a significantly potent cytotoxin.

The synthesis of the proposed analogue **2.18** is envisaged to follow the synthetic route for the preparation of the left- and right-hand components of pederin and analogues[59,64] (Scheme 2.6).

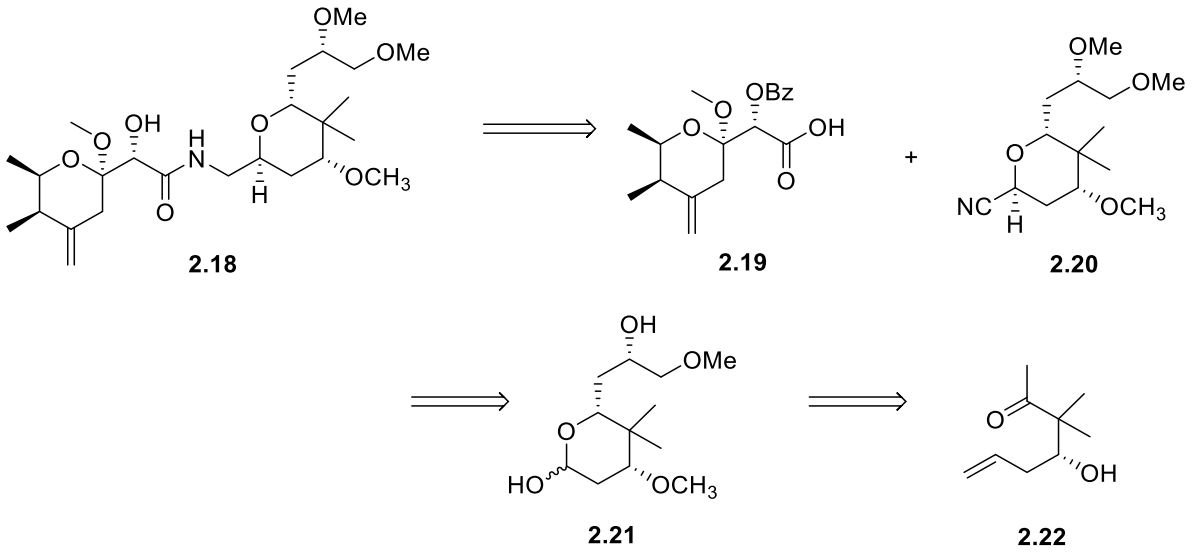

Scheme 2.6 Retrosynthetic analysis of pederin analogue

Compound **2.18** can be accessed by coupling the C7-benzoylated pederic acid **2.19** with the amine from the hydrogenation of nitrile **2.20** to form the amide bond, followed by benzoyl ester cleavage. As earlier reported, the nitrile **2.20** can be prepared from the corresponding lactol **2.21** which can be accessed from the known keto alcohol **2.22**.[67] The pederic acid fragment **2.19** can also be accessed via the reported route by Green and co-workers in the total synthesis of theopederin.[68]

2.3 Results and Discussion

2.3.1 Total synthesis of a pederin analogue

We began the synthesis of the cytotoxic pederin analogue with the preparation of compound **2.20** from the keto alcohol **2.22** (Scheme 2.7)**.**

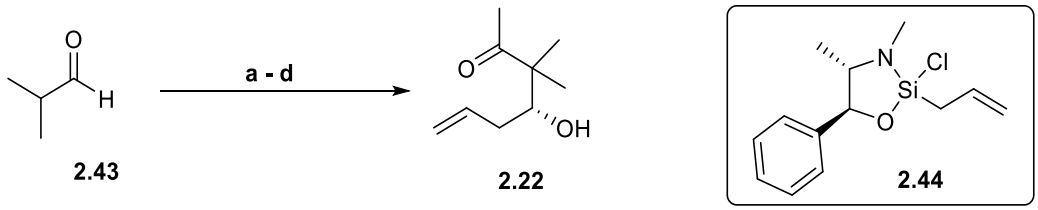

2.43 2.22 2.44

Scheme 2.7 Synthesis of keto alcohol 22

Reagents and conditions*: a) Morpholine, reflux, 98% crude yield. b) acetyl chloride, THF, reflux, 73%. c) H_2O, $NaHCO_3$, rt, 68%. d) Leighton's Silane (**44**)*[26]*, toluene, -15 °C, 98%, 94% ee.*

Compound **2.43** was refluxed with morpholine in toluene with the removal of water under Dean-Stark experimental setup to yield the enamine product, which was subsequently reacted with acetyl chloride to form a keto iminium salt. Hydrolysis of the iminium salt and subsequent Leighton allylation[69] with **2.44** afforded keto alcohol **2.22** in excellent yield and enantiomeric excess.

Methylation of keto alcohol **2.22** with 2,6-di-*tert*-butylpyridine and methyl triflate afforded compound **2.23** in 80% yield (Scheme 2.8).

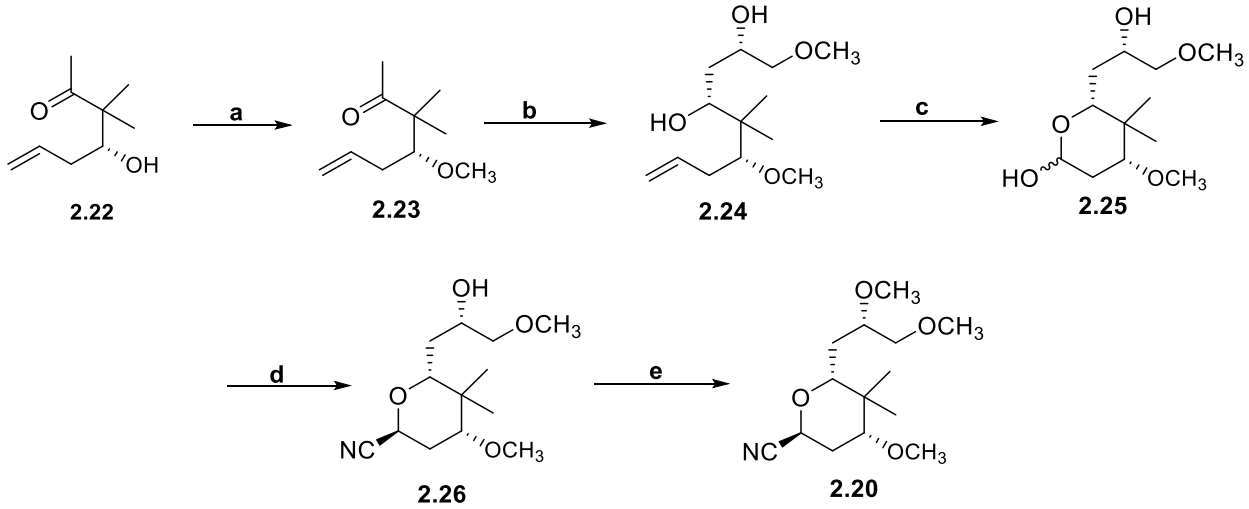

2.22 2.23 2.24 2.25 2.26 2.20

Scheme 2.8 Synthesis of nitrile 2.20 from keto alcohol 2.22

Reagents and conditions*: a) Methyl triflate, 2,6-di-tert-butylpyridine, CH_2Cl_2, 0 °C to rt, 80%. b) (+)-DIP-Cl, $MeOCH_2CHO$, Et_3N, Et_2O, –78 °C, then $LiBH_4$, Et_2O, –40 °C. 72%. c) O_3, PPh_3, CH_2Cl_2, –78 °C, 95%. d)TMSCN, $BiBr_3$, CH_3CN, 0 °C, then $BF_3 \cdot OEt_2$, –40 °C, 69%. e) NaH, MeI, DMF, 0 °C, 97%.*

From compound **2.23**, a one-pot Paterson boron aldol reaction[70] with α-methoxy acetaldehyde followed by ketone reduction with $LiBH_4$ afforded the diol **2.24** after peroxide quenching and work-up. Ozonolysis of **2.24** afforded the lactol **2.25** which underwent cyanation at the C2 position to obtain the nitrile **2.26**. Williamson etherification of the secondary alcohol of **2.26** with methyl iodide completed synthesis of nitrile **2.20** in excellent yield.

As indicated earlier, preparation of the left-hand component (the pederic acid fragment) of the natural product analogue follows the protocol used by Green and co-workers. Synthesis of compound **2.19** began with the three-step preparation of the dithiolane-protected δ-lactone **2.27** (Scheme 2.9).

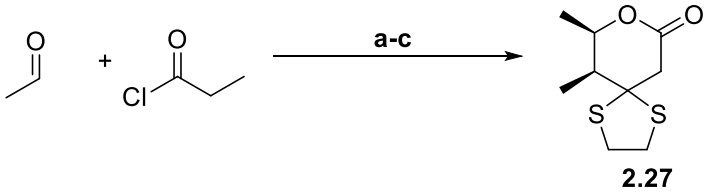

2.27

Scheme 2.9 Preparation of 2.27

Reagents and conditions*: a) $LiClO_4$, TMS-QD, DIPEA, Et_2O, DCM, –78 °C, (crude). b) LDA, THF, –78 °C, t-butyl acetate, 56%. c) $BF_3 \bullet OEt_2$, ethanedithiol, DCM, –45 °C - rt, 81%.*

Reaction of acetyl chloride and acetaldehyde in the presence of $LiClO_4$ and TMS-quinidine, followed by Claisen condensation with *tert*-butyl acetate, and a two-component dithiolane protection of the β-ketoester and lactonization afforded compound **2.27** as a single diastereomer after recrystallization.

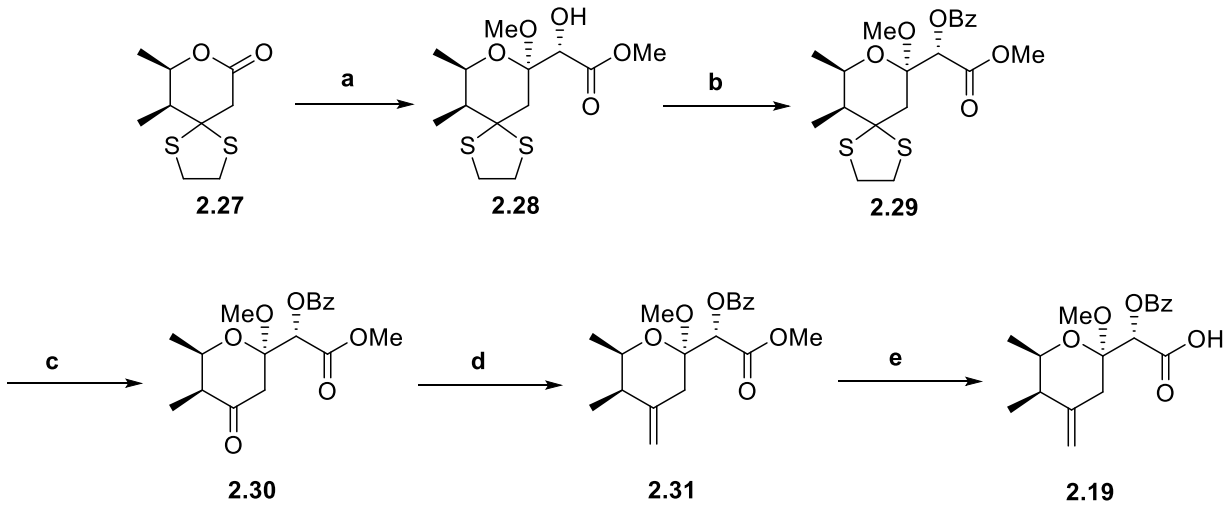

Scheme 2.10 Synthesis of pederic acid fragment 2.19

Reagents and conditions*: a) LDA, THF, –78 °C, $CH_3OC(O)CH_2OC(CH_3)_2OCH_3$, $ZnCl_2$, HMPA, then 10-CSA, $(MeO)_3CH$, MeOH/DCM (1:1), rt, 94%. b) BzCl, DMAP, pyridine, 86%. c) PIFA, CH_3CN/H_2O (8:1), –15 °C to rt, 92%. d) $TiCl_4$–Zn–CH_2I_2, THF, rt, 80%. e) Me3SnOH, DCE, 80 °C, 56%.*

Claisen condensation between lactone **2.27** and the glycolate followed by reaction with camphorsulfonic acid and trimethyl orthoformate afforded compound **2.28**, which was benzoylated at C7-hydroxy to afford **2.29**. Dithiolane cleavage and subsequent methylenation of the resultant ketone with the Takai variant of the Lombardo methylenation reagent[71] gave compound **2.31**. The Nicolaou protocol for mild methyl ester hydrolysis[72] was employed for the

hydrolysis of the methyl ester **2.31** to obtain the benzoyl-protected pederic acid fragment **2.19** in moderate yield (Scheme 2.10).

To put the analogue together, nitrile **2.20** was first reduced to the corresponding amine **2.32** under hydrogen atmosphere with catalytic amounts of palladium on carbon and platinum (IV) oxide. The crude amine **2.32** was then used in the coupling reaction with the pederic acid component **2.19** in the presence of EDC•HCl and *N*-hydroxybenzotriazole to obtain the C7-benzoylated pederin analogue **2.33**. Benzoyl ester removal with 0.55 equivalents of potassium carbonate afforded the pederin analogue **2.18** in 88% yield (Scheme 2.11).

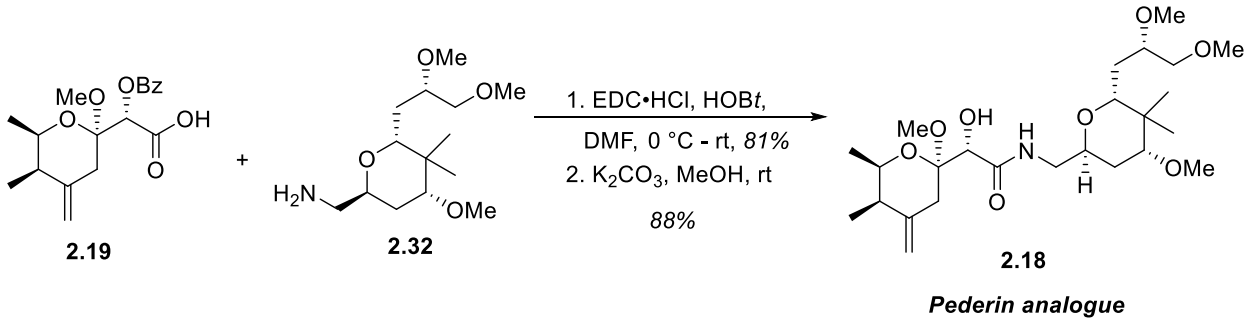

Scheme 2.11 Completion of the synthesis of analogue 2.18

2.3.2 Borylation of pederin analogue

After the synthesis of the pederin analogue **2.18**, we focused on finding an effective borylation strategy for the conversion of the C7 hydroxy substituent to an α-boryl ether, as previously shown in the work by Hanna and co-workers. We attempted to synthesize compound **2.39** as our borylated analogue from the **2.18** and chloride **2.38** (Scheme 2.12). However, the synthesis of the chloride **2.38** proved unsuccessful as strategies to incorporate the pinacol borane (BPin) group in the molecule failed.

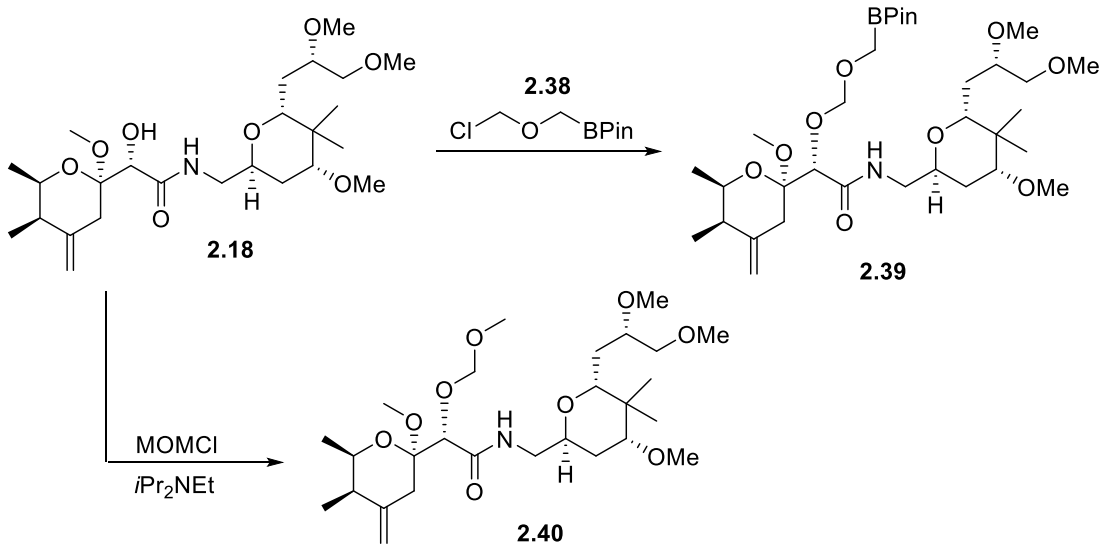

Scheme 2.12 Unsuccessful initial attempt at borylation

Owing to significant purity challenges, we were not quite successful as well in our initial attempts to prepare compound **2.40** which would be the negative control for the borylated analogue in the targeted release study.

Our attention was shifted to the previously reported borylation strategy Mosey and co-workers[56] in the versatile approach to α-alkoxy carbamate synthesis and stimulus-responsive alcohol release. In this study they prepared the carbamate **2.42** from chloroformate **2.35** in a multi-component reaction involving the hydrozirconation of *tert*-butyl nitrile, nucleophilic acyl substitution with the chloroformate **2.35** followed by the addition of alcohol nucleophile into the acylimine intermediate (Scheme 2.13).

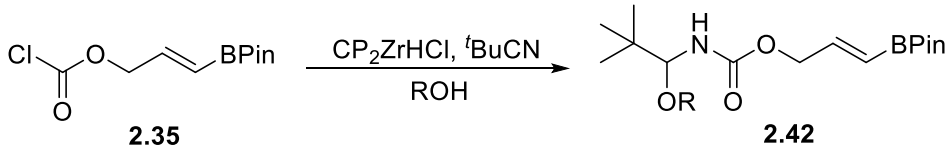

Scheme 2.13 α-alkoxy carbamate synthesis

Addition of alcohol to chloroformate **2.35** would generate the carbonate, which we envision would be an effective linker for molecular release under H_2O_2 conditions akin to what was observed with carbamate **2.42** in Mosey's work. Hence, we successfully prepared compound **2.36** from **2.35** and the pederin analogue **2.18,** and the corresponding negative control substrate **2.34** in excellent yields with tetramethyl ethylenediamine (TMEDA) as base in THF. (Scheme 2.14).

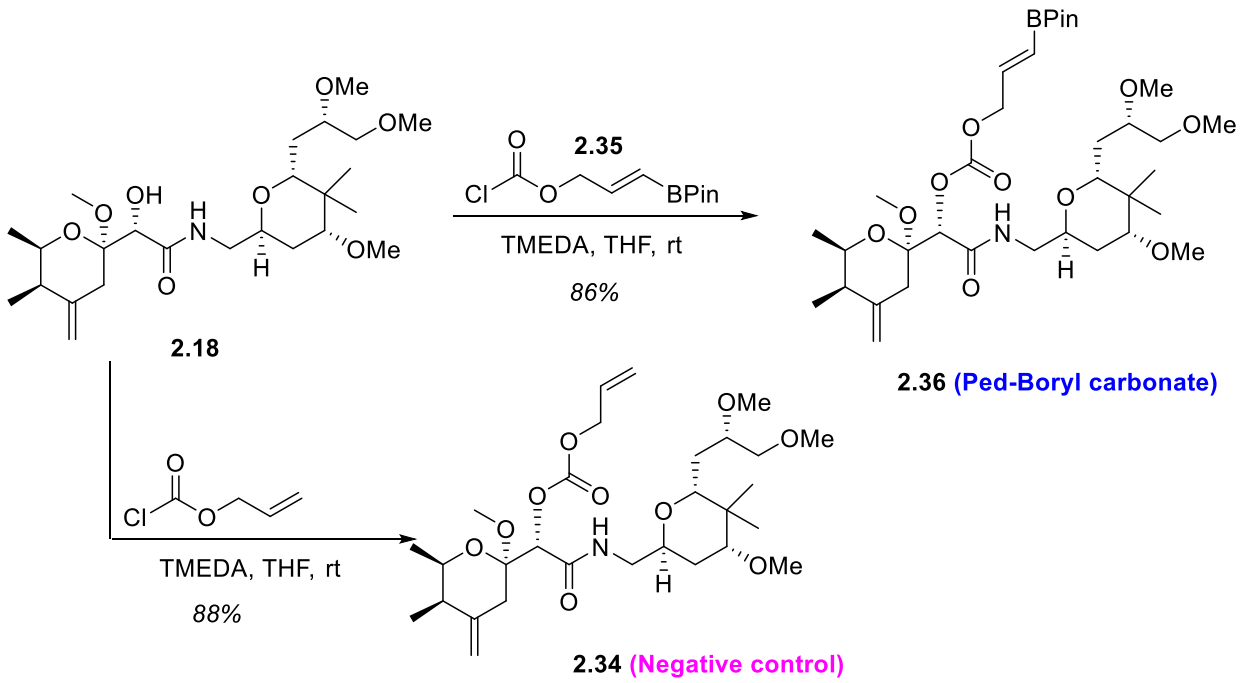

Scheme 2.14 Preparation of borylated pederin analogue 2.36 and negative 2.34 control from 2.18

2.3.3 Pederin analogue release and cell viability studies

Through our collaboration with Prof. Alex Deiters' lab, initial biological evaluation of the synthesized pederin analogue and negative control was performed[73] in comparison with the cytotoxic anti-cancer chemotherapy drug doxorubicin. Cell viability studies were carried out specifically by Amy Ryan of the Deiters' research group, in which GI_{50} values were obtained for

the various cell lines after incubation for 48 hours (Figure 2.4).[73] The synthesized pederin analogue **2.18** has demonstrated superior potency over doxorubicin and compound **2.34** in HeLa (cervical cancer), HCT116 (human colorectal carcinoma), HEK293T (transfectable derivative of the human embryonic kidney cells) and MCF7 (breast cancer) cell lines. Although diminished to a sub-micromolar activity in the HuH7 (liver carcinoma) cells, the pederin analogue is still slightly more potent than doxorubicin and the negative control.

Cell line	Doxorubicin (nM)	Pederin Analogue (nM)	Pederin (-) (nM)
HeLa	322	50.8	924
HCT116	365	50.9	681
Huh7	874	201	956
HEK293T	347	28.1	861
MCF7	178	21.0	NA

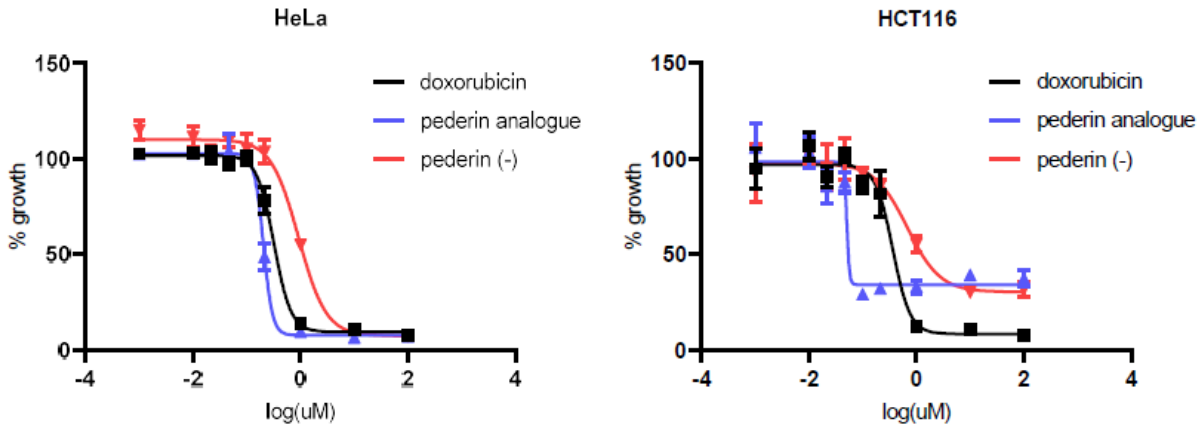

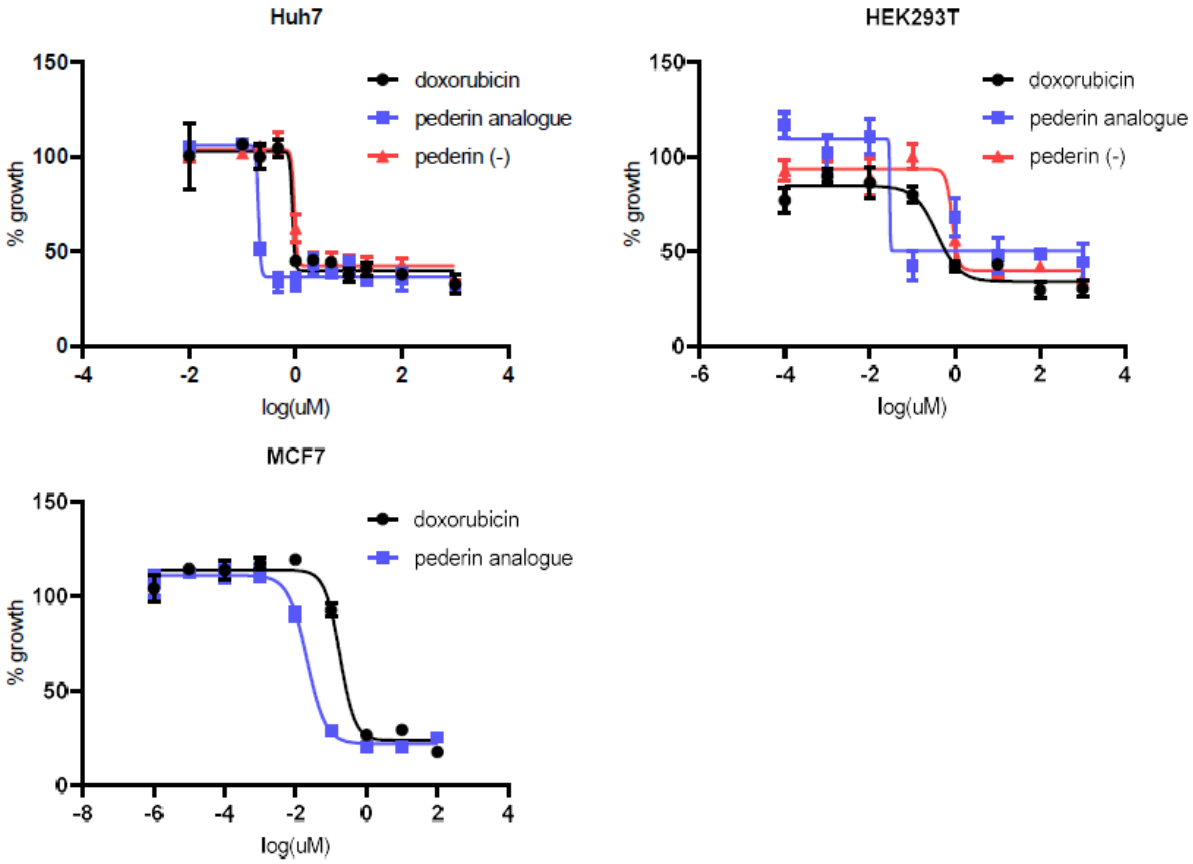

Figure 2.4 Evaluation of cytotoxicity of pederin analogues and doxorubicin

We performed NMR experiments to study the breakdown pattern of the pederin boronate analogue **2.36,** as an entry into the actual targeted release study in cells. The reaction conditions were selected to mimic physiological pH and temperature[74], and the molecular breakdown with and without H_2O_2 was evaluated (Figure 2.5). In the presence of peroxide, **2.36** breaks down to release the analogue **2.18**, CO_2 and acrolein (Scheme 2.15).

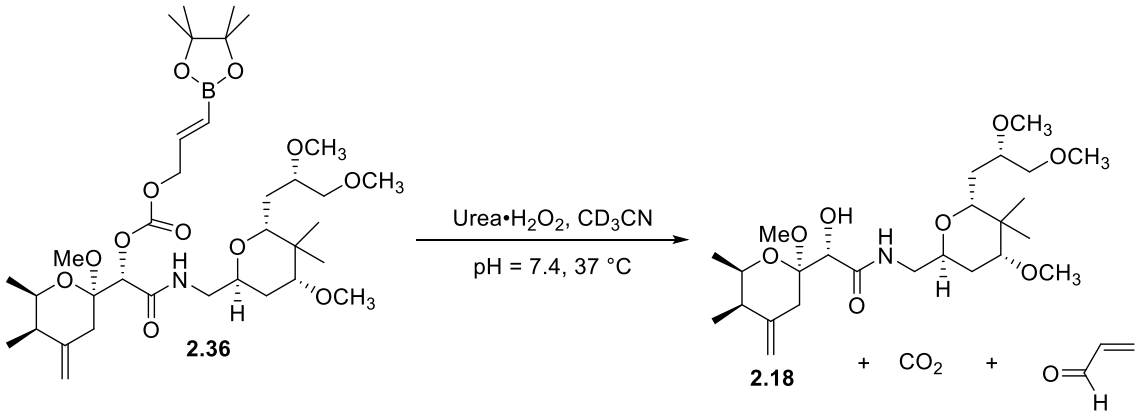

Scheme 2.15 Boronate linker cleavage from compound 2.36

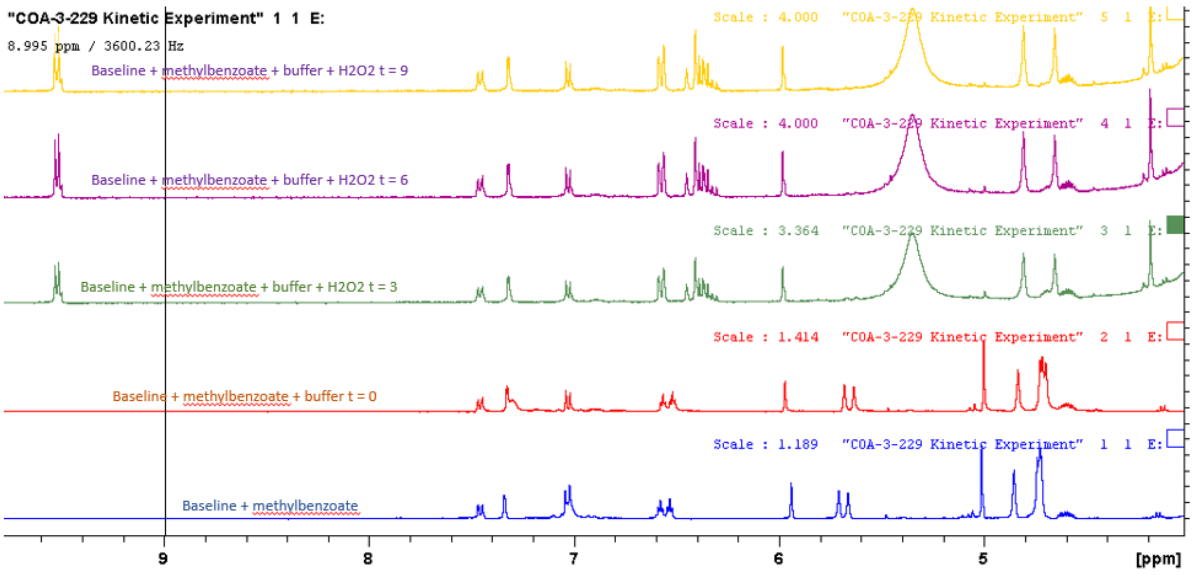

Figure 2.5 1H NMR analysis of pederin boronate breakdown

The analogue **2.36** was found to be quite stable to pH 7.4 and 37 °C in deuterated acetonitrile prior to the addition of H_2O_2. The addition of peroxide leads to the breakdown as expected with the release of acrolein and pederin analogue **2.18**. The NMR signal around 9.6 ppm represents acrolein release whereas the upfield shift of the singlet peak at 5 ppm to 4.2 ppm represents the release of compound **2.18**. The half-life of the compound **2.36** in the presence of peroxide was also evaluated in the NMR study (Figure 2.6). We found that the half-life of **2.36** in

the presence of 11 equivalents of peroxide was approximately 4 minutes whereas it is about 2 minutes in the presence of 15 equivalents of H_2O_2.

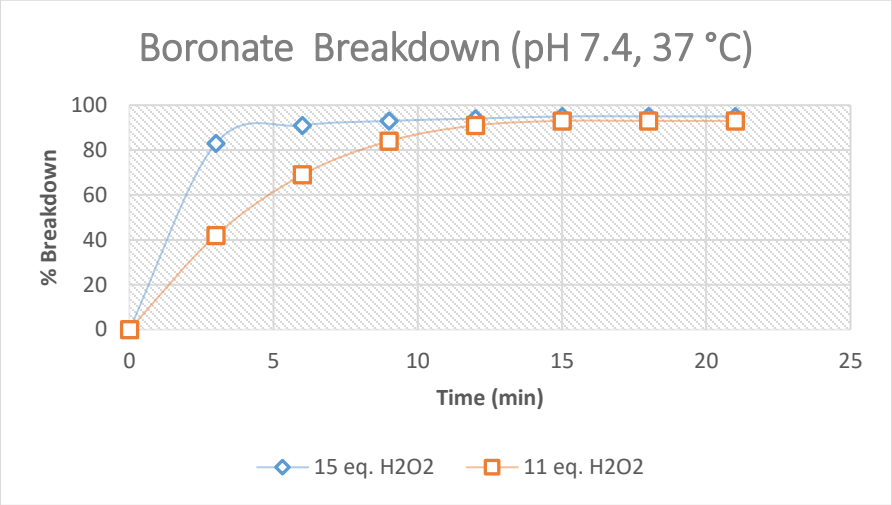

Figure 2.6 Breakdown of pederin boronate 2.36 over time

Ryan also carried out a biological evaluation of the pederin-boronate **2.36** in comparison with the pederin analogue **2.18**, the negative control **2.34** and doxorubicin when incubated with RAW 264.7 cell lines (Figure 2.7).[73] No significant difference was observed between the negative control and the boronate.

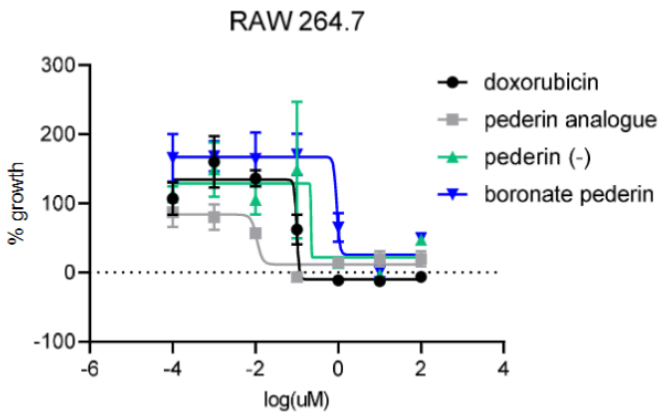

	GI50 (nM)
doxorubicin	100
pederin	10.8
pederin (-)	220
boronate pederin	922

Figure 2.7 Biological evaluation of pederin-boronate 2.36

HeLa cells stimulated with paraquat (to enhance peroxide production in the cells) were incubated with the pederin analogues and cytotoxity was evaluated by SRB assay. Significant change in GI_{50} values was observed for cells incubated with paraquat and those without paraquat, indicating considerable release of pederin analogue **2.18** from **2.36** in cells having high levels of peroxide (Figure 2.8).[73]

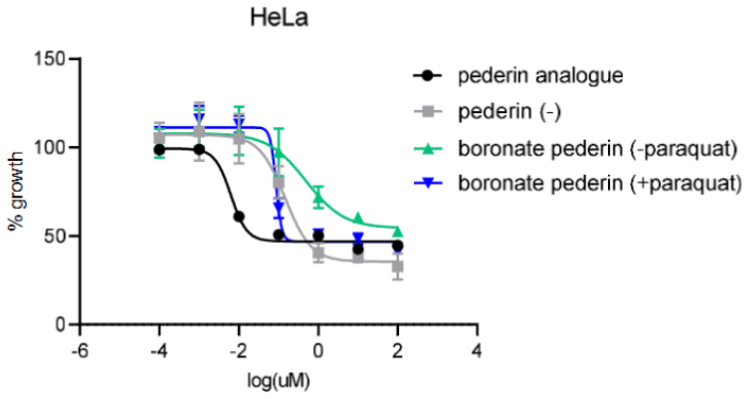

	GI50 (nM)
pederin analogue	6.29
pederin (-)	98.3
boronate pederin (-paraquat)	486
boronate pederin (+paraquat)	86.4

Figure 2.8 Evaluation of boronate release in HeLa cells stimulated with paraquat

Further cell studies are currently on-going in the Deiters' group to unravel the viability of the targeted release strategy in the activation of cellular pathways, with the overall aim of providing a fundamental basis for designing uniquely selective probes and potential prodrugs for disease states that are characterized by oxidative stress.

2.4 Conclusion

In conclusion, we have synthesized a new pederin analogue with nanomolar toxicity towards a variety of cells under oxidative stress. We have also developed a new boronate-based small molecule probe which effectively releases the pederin analogue under peroxide conditions to cancer cells. This release strategy, having shown promise in cell viability studies, provides future opportunities into the development of potential anti-cancer prodrugs and other therapeutics.

2.5 Experimental

2.5.1 General information

All reactions were performed in dry solvents under argon atmosphere using oven dried glassware unless otherwise specified. Dichloromethane was distilled over CaH_2 whereas diethyl ether and tetrahydrofuran solvents were distilled over sodium and benzophenone before use. Flash column chromatography with 60 Å silica gel and reagent grade solvents i.e., ethyl acetate, hexanes, diethyl ether or pentanes as eluent was performed to purify all compounds made. In the case of boron-based compounds, the silica gel used was pretreated with 5% boric acid and dried under

vacuum before used for the purification of the said compounds. Analytical TLC was performed on E. Merck pre-coated (25 mm) silica gel 60 F_{-254} plates and visualized under UV (254 nm). High resolution and low-resolution mass spectra were collected on a VG 7070 spectrometer. IR spectra were obtained on a PerkinElmer FT-IR UATR spectrometer. ^{1}H NMR, ^{11}B and ^{13}C NMR spectra were obtained on a Bruker Avance 300 spectrometer at 300 MHz and 75 MHz respectively, a Bruker Avance 400 spectrometer at 400 MHz and 100 MHz, or a Bruker Avance 500 spectrometer at 500 MHz and 125 MHz and a Bruker Avance 600 MHz and 150 MHz as specified. The chemical shifts are reported in parts per million (ppm) on the delta (δ) scale. The solvent peak was used as a reference value, for ^{1}H NMR: $CDCl_3$ = 7.26 ppm, CD_2Cl_2 = 5.31 ppm, C_6D_6 = 7.16 ppm, CD_3CN = 1.93 ppm, for ^{13}C NMR: $CDCl_3$ = 77.2 ppm. Data are reported as follows: m = multiplet, s = singlet, d = doublet, t = triplet, q = quartet, pent = pentet, dd = doublet of doublets, dt = doublet of triplets, sext = sextet, sept = septet, oct = octet, dq = doublet of quartet, dp = doublet of pentet, ddd = doublet of doublet of doublets, ddt = doublet of doublet of triplets, tt = triplet of triplet, br = broad.

2.5.2 Pederin analogue synthesis

Preparation of (R)-4-methoxy-3,3-dimethylhept-6-en-2-one (2.23)

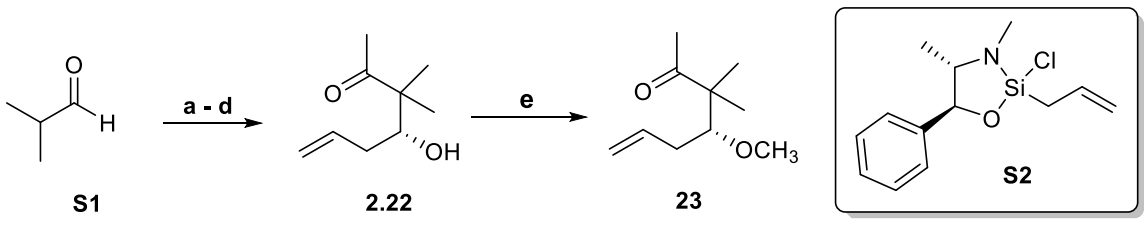

Reactions and Conditions

a) Morpholine, toluene, reflux, 98%. b) acetyl chloride, THF, reflux, 73%. c) H_2O, $NaHCO_3$ rt, 68%. d) Leighton's Silane **(S2)**, toluene, -15 °C, 98%. e) 2,6-*t*Bu_2py, MeOTf, DCM, 0 °C - rt, 82%.[67,69]

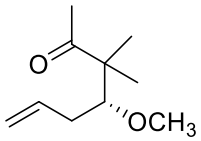

2.23

(*R*)-4-methoxy-3,3-dimethylhept-6-en-2-one (2.23)

To a solution of keto alcohol **2.22**[67] (611 mg, 3.91 mmol) in dichloromethane (15 mL) at 0 °C under argon atmosphere was added 2,6-di-*tert*-butyl pyridine (1.35 g, 7.04 mmol) and stirred for 10 min whereupon methyl triflate (962 mg, 5.37 mmol) was added dropwise and the reaction mixture stirred at 0 °C for another 10 min. The reaction was then warmed slowly to rt and stirred for 38 h after which water (30 mL) was added to the mixture and the organic layer separated. The aqueous layer was extracted with dichloromethane (3 x 30 mL) and the combined organic phase washed with saturated $NaHCO_3$(aq) (20 mL) and brine (30 mL). The organic mixture was dried with Na_2SO_4, filtered and concentrated under reduced pressure to give crude product. The crude product was purified with flash column chromatography (20% ethyl acetate in hexanes) to obtain the desired product (550 mg, 82%). ^{1}H NMR (300 MHz, $CDCl_3$): δ (ppm) 5.88 (ddt, *J* = 17.2, 10.0, 7.2 Hz, 1H,), 5.10 (ddt, *J* = 17.0, 3.1, 1.5 Hz, 1H), 5.04 (ddt, *J* = 10.1, 2.0, 1.1 Hz, 1H), 3,42 (dd, *J* = 6.4, 5.3 Hz, 1H), 3.38 (s, 3H), 2.20 (ddd, *J* = 5.4, 1.4, 1.4 Hz, 1H), 2.18 (ddd, *J* = 5.7, 1.5, 1.5 Hz, 1H), 2.16 (s, 3H), 1.15 (s, 3H), 1.08 (s, 3H)); ^{13}C NMR (75 MHz, $CDCl_3$): δ (ppm) 213.4, 136.2, 116.7, 86.1, 60.1, 52.5, 35.8, 26.7, 21.1, 20.4; HRMS (ESI) *m/z* calcd for $C_{10}H_{19}O_2$ $(M+H)^+$ 171.1380, found 171.1388; IR (thin film) cm^{-1}: 2968, 1732, 1638, 1421, 1176, 845, 780.

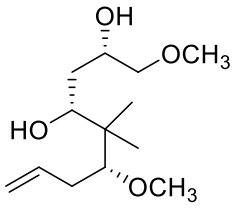

2.24

(2*S*,4*R*,6*R*)-1,6-dimethoxy-5,5-dimethylnon-8-ene-2,4-diol (2.24)

To a solution of (+)-B-chlorodiisopinocamphenylborane ((+)-DIP-Cl) (1.50 g, 4.68 mmol) in Et_2O (3.0 mL) at 0 ºC was added Et_3N (497 mg, 4.91 mmol), followed by a solution of **2.23** (530 mg, 3.11 mmol) in Et_2O (2.0 mL). The reaction mixture was stirred at 0 ºC for 30 min, then was cooled to –78 ºC, whereupon 2-methoxy acetaldehyde[67] (800 mg, 10.8 mmol) was added slowly dropwise.

The resulting mixture was stirred at –78 ºC overnight. $LiBH_4$ (2 M in THF, 6.0 mL, 12.0 mmol) was added dropwise at –78 ºC and the reaction was stirred for 22 h. The reaction was slowly warmed up to –40 ºC and stirred for 3 h, then was quenched with MeOH (10 mL), H_2O_2 (30% aq., 10 mL) and stirred overnight. The organic layer and aqueous layer were separated, and the aqueous phase was extracted with EtOAc (3x30 mL). The combined organic layer was washed with brine (30 mL) and ice-cold satd. $Na_2S_2O_3$ (aq.) (30 mL), dried with Na_2SO_4, filtered, and concentrated under reduced pressure. The resulting crude product was purified by flash chromatography (40% EtOAc in hexanes) to provide the desired product **2.24** as a viscous oil (dr = 15:1, 552 mg, 72%): ^{1}H NMR (300 MHz, $CDCl_3$) Major diasteromer: δ (ppm) 5.91 (ddt, *J* = 17.1, 10.1, 7.1 Hz, 1H), 5.11 (dq, *J* = 17.3, 1.7 Hz, 1H), 5.06 (d, *J* = 10.1 Hz, 1H), 4.40 (d, J = 1.7 Hz, 1H), 4.17 (s, 1H), 4.06-3.98 (m, 1H), 3.82 (d, *J* = 11.0 Hz), 3.44 (s, 3H), 3.42-31 (m, 2H), 3.39 (s, 3H), 3.18 (dd, *J* = 7.9, 3.8 Hz), 2.41-2.25 (m, 2H), 1.65-1.43 (m, 3H), 1.61 (dt, *J* = 14.0, 2.5 Hz, 1H), 1.51-1.44 (m, 1H), 0.97 (s, 3H), 0.85 (s, 3H);); ^{13}C NMR (75 MHz, $CDCl_3$): δ (ppm) 136.5, 116.7, 90.3, 78.0, 76.9, 71.4, 60.3, 59.2, 41.4, 35.1, 34.3, 21.8, 20.8; *m/z* calcd for $C_{13}H_{27}O_4$ $(M+H)^+$ 247.1903, found 247.1917; IR (thin film) cm^{-1}: 3548, 2959, 1628, 1407, 1206, 822, 793.

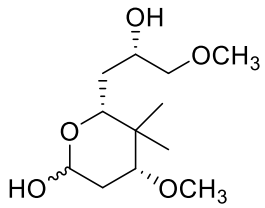

2.25

(4*R*,6*R*)-6-((*S*)-2-hydroxy-3-methoxypropyl)-4-methoxy-5,5-dimethyltetrahydro-2*H*-pyran-2-ol (2.25)

Ozone was gently bubbled through a solution of **2.24** (371 mg, 1.51 mmol) in CH_2Cl_2 (50 mL) at –78 ºC until the reaction mixture sustained a deep blue color. Ph_3P (1.18 g, 4.52 mmol) was added and the reaction mixture was warmed to rt and stirred for 4 h. The reaction mixture was concentrated under reduced pressure and purified by flash chromatography (CH_2Cl_2: EtOAc = 2:1 then EtOAc: MeOH = 10:1) to provide the desired product **2.25** as an impure mixture with traces of triphenylphosphine oxide

(approx. 352 mg, 95% crude yield); HRMS (ESI) *m/z* calcd for $C_{13}H_{24}O_5Na$ $(M+Na)^+$ 271.1516, found 271.1531; IR (thin film) cm^{-1}: 3609, 2967, 1414 1375, 1206, 1124, 1085, 822, 793.

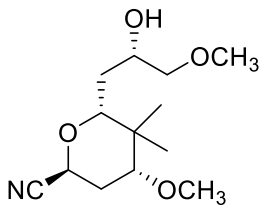

2.26

(2*S*,4*R*,6*R*)-6-((*S*)-2-hydroxy-3-methoxypropyl)-4-methoxy-5,5-dimethyltetrahydro-2*H*-pyran-2-carbonitrile (2.26)

To a solution of **2.25** (111 mg, 0.45 mmol) in anhydrous CH_3CN (5 mL) was added TMSCN (600 µL, 4.5 mmol) at 0 ºC. After stirring at 0 ºC for 20 min, $BiBr_3$ (101 mg, 0.22 mmol) was added to the reaction as powder in one portion. The reaction mixture was stirred at 0 ºC for 1 h, then cooled to –35 ºC, whereupon freshly distilled BF_3•OEt_2 (24 µL, 0.2 mmol) was added dropwise. The reaction was monitored by TLC closely and more BF_3•OEt_2 (24 µL, 0.2 mmol) was added to complete the cyanation. The reaction mixture was added to ice-cold sat. $NaHSO_4$ (0.25M, aq., 20 mL). The aqueous layer was extracted with EtOAc (3 x 15 mL). The organic layers were combined and washed with saturated $NaHCO_3$ (aq., 20 mL), dried with Na_2SO_4, filtered, and concentrated under reduced pressure. The resulting crude product was purified by flash chromatography (30% EtOAc in hexanes) to provide the desired product **2.26** as a viscous oil (80 mg, 69% yield): ^{1}H NMR (500 MHz, $CDCl_3$): δ (ppm) 4.96 (dd, *J* = 6.1, 0.9 Hz, 1H), 3.96 (pent, *J* = 5.4 Hz, 1H), 3.62 (dd, *J* = 10.5, 2.0 Hz, 1H), 3.42-3.35 (m, 2H), 3.40 (s, 3H), 3.38 (s, 3H) 3.17 (dd, *J* = 11.8, 4.4 Hz, 1H), 2.70 (d, *J* = 1.0 Hz), 2.08 (ddd, *J* = 13.6, 4.5, 1.2 Hz, 1H), 1.86 (ddd, *J* = 13.5, 11.8, 6.1 Hz, 1H), 1.77 (ddd, *J* = 14.6, 5.4, 2.2 Hz, 1H), 1.66 (ddd, *J* = 14.6, 10.5, 6.7 Hz, 1H), 0.98 (s, 3H), 0.86 (s, 3H); ^{13}C NMR (125 MHz, $CDCl_3$): δ (ppm) 117.4, 81.1, 80.9, 75.9, 69.2, 64.0, 59.2, 57.7, 39.2, 32.2, 29.0, 22.2, 12.7; HRMS (ESI) *m/z* calcd for $C_{13}H_{23}NO_4Na$ $(M+Na)^+$ 280.1519, found 280.1531; IR (thin film) cm^{-1}: 3458, 2848, 2231, 1460, 1365, 1160, 841.

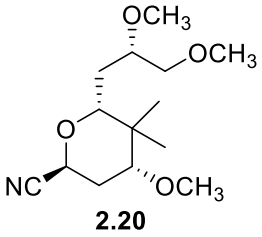

2.20

(2*S*,4*R*,6*R*)-6-((*S*)-2,3-dimethoxypropyl)-4-methoxy-5,5-dimethyltetrahydro-2*H*-pyran-2-carbonitrile (2.20)

To a solution of **2.26** (77 mg, 0.3 mmol) in DMF (1.5 mL) was added NaH (60% in mineral oil, 18 mg, 0.45 mmol) at 0 ºC. After stirring for 10 min, MeI (85 mg, 0.6 mmol) was added, and the reaction was stirred for 30 min at 0 ºC. TLC showed the starting material was fully consumed after 4 hrs. The reaction was quenched with saturated 3 mL of saturated NH_4Cl (aq.) and the mixture was separated. The organic layer was extracted with EtOAc (3 x 3 mL). The organic layers were combined, washed with brine (3 x 3 mL), dried with Na_2SO_4, filtered, and concentrated under reduced pressure. The resulting crude product was purified by flash chromatography (20% EtOAc in hexanes) to provide the desired product **2.20** as an oil (80 mg, 97%): ^{1}H NMR (500 MHz, $CDCl_3$): δ (ppm) 4.93 (dd, *J* = 6.0, 1.1 Hz, 1H), 3.54-3.51 (m, 1H), 3.49 (dd, *J* = 10.3, 1.8 Hz, 1H), 3.47-3.45 (m, 1H), 3.44-3.41 (m, 1H), 3.39 (s, 3H), 3.38 (s, 3H), 3.38 (s, 3H), 3.16 (dd, *J* = 11.8, 4.5 Hz, 1H), 2.07 (ddd, *J* = 13.5, 4.5, 1.4 Hz, 1H), 1.88-1.78 (m, 2H), 1.71-1.63 (m, 1H), 0.97 (s, 3H), 0.85 (s, 3H); ^{13}C NMR (125 MHz, $CDCl_3$): δ (ppm) 117.6, 81.1, 79.0, 77.6, 72.9, 64.0, 59.2, 57.7, 57.1, 39.1, 29.6, 29.1, 22.1, 12.6; HRMS (ESI) *m/z* calcd for $C_{14}H_{26}NO_4$ $(M+H)^+$ 272.1856, found 272.1871; IR (thin film) cm^{-1}: 2852, 2204, 1447, 1363, 1206, 1104, 841, 710.

Preparation of (9R,10S)-9,10-dimethyl-8-oxa-1,4-dithiaspiro[4.5]decan-7-one (2.27)

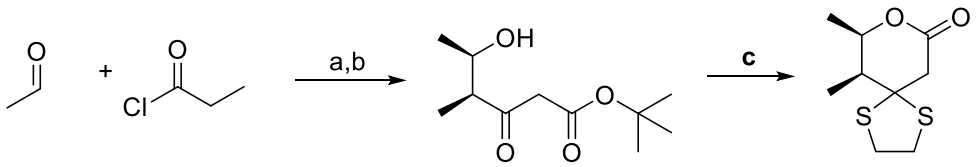

Reactions and conditions

a) $LiClO_4$, TMS-QD, DIPEA, Et_2O, DCM, -78 °C, (crude)
b) LDA, THF, -78 °C, *t*-butyl acetate, 56%.[68]
c) BF_3•OEt_2, ethanedithiol, DCM, -45 °C - rt, 81%

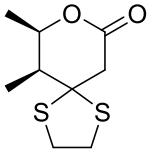

2.27

(9*R*,10*S*)-9,10-dimethyl-8-oxa-1,4-dithiaspiro[4.5]decan-7-one (2.27)

To a solution of **S4**[68] (2.50 g, 11.6 mmol) in CH_2Cl_2 (69.0 mL) at –40 °C were sequentially added 1,2-ethanedithiol (3.00 mL, 34.7 mmol) and $BF_3 \cdot Et_2O$ (7.30 mL, 57.8 mmol). The reaction was warmed to room temperature. After 48 hours, the reaction mixture was carefully poured into a 0 °C solution of saturated aqueous $NaHCO_3$ (100 mL). The reaction mixture was extracted with CH_2Cl_2 (3 x 50 mL), and the combined organic layers were washed with saturated aqueous $NaHCO_3$ (20 mL) and brine (20 mL), then dried (Na_2SO_4), filtered, and concentrated under reduced pressure to afford a crude orange residue. The material was purified via flash column chromatography (hexanes to 20% EtOAc in hexanes) to afford the desire product and its C_2 diastereomer (~12.3:1) as a yellow solid. The solid was recrystallized from 20% ethyl acetate in hexanes to obtain the desired product (2.05 g, 81%). ^{1}H NMR (500 MHz, $CDCl_3$): δ (ppm) 4.88 (dq, *J* = 6.5, 2.7 Hz, 1H), 3.43-3.28 (m, 4H), 3.12 (dd, *J* = 18.5, 0.9 Hz, 1H), 3.06 (d, *J* = 18.4 Hz, 1H), 2.16 (ddq, *J* = 7.1, 2.6, 0.8 Hz, 1H), 1.37 (d, *J* = 6.5 Hz, 3H), 1.18 (d, *J* = 7.1 Hz, 3H); ^{13}C NMR (125 MHz, $CDCl_3$): δ (ppm) 168.1, 78.5, 68.1, 44.1, 43.6, 39.5, 39.4, 18.8, 11.4; HRMS (ESI) *m/z* calcd for $C_9H_{15}O_2S_2$ $(M+H)^+$ 219.0508, found 219.0519; IR (thin film) cm^{-1}: 3108, 2841, 1742, 1421, 1375, 1163, 861, 727.

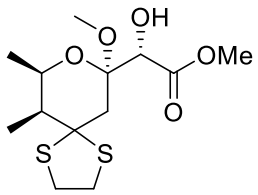

2.28

methyl (*S*)-2-hydroxy-2-((7*R*,9*R*,10*S*)-7-methoxy-9,10-dimethyl-8-oxa-1,4-dithiaspiro[4.5]decan-7-yl)acetate (2.28)

To a solution of LDA in THF (0.5M, 23.2 mmol, 46.6 mL) was added a solution of freshly prepared methyl 2-((2-methoxypropan-2-yl)oxy)acetate[75] (3.76 g, 23.2 mmol) in THF (23.2 mL) slowly dropwise over 10 min at –78 °C and the mixture stirred for an hour. Freshly distilled HMPA (6.20 g, 34.6 mmol) was added slowly dropwise over 8 min and the reaction was stirred for 15 min, whereupon $ZnCl_2$ (1.0 M, 23.2 mmol, 23.2 mL) was added slowly over 15 mins and the reaction stirred for 2 h. A solution of **2.27** (460 mg, 2.1 mmol) in THF (12.4 mL) was then added added over 4 mins and the reaction stirred at –78 °C for 2 h and slowly warmed to –40 °C and stirred for 17 h. The reaction was quenched with saturated NH_4Cl (aq.) (40 mL) and the aqueous layer was extracted with with ethyl acetate (3 x 30 mL). The combined organic layer was washed with brine, dried over $MgSO_4$ and concentrated under reduced pressure to give an orange oil as crude product. The crude product was diluted with a 1:1 mixture of MeOH and DCM (60 mL) followed by the addition of $CH(OMe)_3$ (10.92 g, 102.9 mmol) whereupon 10-camphorsulfonic acid (0.65 g 2.8 mmol) was added. The mixture was stirred at rt for 2 h and then poured into ice-cold saturated $NaHCO_3$ (aq.) (40 mL) in a separatory funnel. The aqueous layer was extracted with Et_2O (3 x 30 mL) and the combined organic layers was washed with saturated $NaHCO_3$ (aq.) (40 mL), brine (50 mL), dried with Na_2SO_4 and concentrated under reduced pressure. The crude product was then purified with flash column chromatography (30% ethyl acetate in hexanes) to provide the desired product as an oil (637 mg, 94% over 2 steps): ^{1}H NMR (500 MHz, $CDCl_3$): δ (ppm) 4.36 (dq, *J* =6.5, 1.9 Hz, 1H), 4.27 (d, *J* = 5.6 Hz, 1H), 3.81 (s, 3H), 3.32 (s, 3H), 3.30-3.10 (m, 4H), 2.81 (d, *J* = 5.6 Hz, 1H), 2.32 (d, *J* = 14.5 Hz, 1H), 2.26 (dd, *J* = 14.5, 1.0 Hz, 1H), 1.67 (tq, *J* = 7.1, 1.2 Hz, 1H), 1.19 (d, *J* = 6.6 Hz, 3H), 0.99 (d, *J* = 6.9

Hz, 3H); ^{13}C NMR (125 MHz, $CDCl_3$): δ (ppm) 172.2, 99.0, 72.8, 69.4, 68.4, 52.6, 48.2, 45.8, 39.4, 37.9, 18.7, 9.8; HRMS (ESI) *m/z* calcd for $C_{13}H_{22}O_5S_2$ $(M-H)^-$ 321.0909 found 321.1724; IR (thin film) cm^{-1}: 3325, 2852, 1741, 1468, 1377, 1342, 1210, 848, 769.

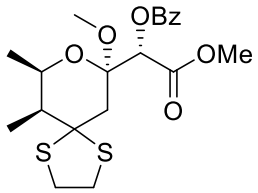

2.29

(*S*)-2-methoxy-1-((7*R*,9*R*,10*S*)-7-methoxy-9,10-dimethyl-8-oxa-1,4-dithiaspiro[4.5]decan-7-yl)-2-oxoethyl benzoate (2.29)

To a solution of **2.28** (630 mg, 1.95 mmol) in dry pyridine (21.0 mL) at 0 °C was added benzoyl chloride (1.98 g, 14.1 mmol) followed by DMAP (50 mg, 0.4 mmol) and the mixture was stirred at 0 °C for 10 min and warmed to rt. Stirring was continued at rt for 17 h and then cooled to 0 °C whereupon tartaric acid (10% w/v, 50 mL) was added and stirred for 10 min. The aqueous and organic layers were separated, and the aqueous layer was extracted with ethyl acetate (3 x 40 mL). The combined organic layers was washed with tartaric acid (10% w/v, 30 mL), $NaHCO_3$ (30 mL), brine (30 mL), dried over $MgSO_4$ and concentrated under reduced pressure. The crude product was purified with flash column chromatography to obtain the desired product (720 mg, 86%): ^{1}H NMR (300 MHz, $CDCl_3$): δ (ppm) 8.08-8.05 (m, 2H), 7.61-7.55 (m, 1H), 7.47-7.42 (m, 2H), 5.37 (s, 1H), 4.40 (dq, *J* = 6.5, 1.8 Hz, 1H), 3.78 (s, 3H), 3.35-3.11 (m, 4H), 3.30 (s, 3H), 2.84 (d, *J* = 14.6 Hz, 1H), 2.40 (dd, *J* = 14.6, 1.1 Hz, 1H), 1.69 (tq, *J* = 6.9, 1.4 Hz, 1H), 1.19 (d, *J* = 6.5 Hz, 3H), 1.00 (d, *J* = 7.0 Hz, 3H); ^{13}C NMR (75 MHz, $CDCl_3$): δ (ppm) 168.4, 165.6, 133.6, 130.1(2C), 128.9, 128.4(2C), 98.6, 71.9, 69.5, 68.2, 52.4, 47.8, 45.8, 39.4, 38.0, 37.4, 18.7, 9.8; HRMS (ESI) *m/z* calcd for $C_{20}H_{26}O_6S_2Na$ $(M+Na)^+$ 449.1063 found 449.1078**;** IR (thin film) cm^{-1}: 3082, 2882, 1780, 1707, 1455, 1329, 1242, 1110, 870, 749.

(*S*)-2-methoxy-1-((2*R*,5*S*,6*R*)-2-methoxy-5,6-dimethyl-4-oxotetrahydro-2*H*-pyran-2-yl)-2-oxoethyl benzoate (2.30)

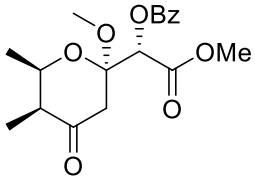

2.30

To a 50 mL round bottom flask wrapped in aluminum foil was added a solution of **2.29** (669 mg, 1.57 mmol) in MeCN/H_2O (8:1 v/v, 20 mL). The solution was stirred at –15 °C for 20 min whereupon (Bis(trifluoroacetoxy)iodo)benzene (2.06 g, 4.80 mmol) was added and stirring continued at –15 °C for 30 min. The mixture was poured into saturated $NaHCO_3$(aq.) (50 mL) and extracted with ethyl acetate (3 x 50 mL). The organic phase was dried with Na_2SO_4 and concentrated under reduced pressure and the purified with flash column chromatography (30% ethyl acetate in hexanes) to obtain the desired product (507 mg, 92%): ^{1}H NMR (400 MHz, $CDCl_3$): δ (ppm) 8.06-8.04 (m, 2H), 7.63-7.58 (m, 1H), 7.48-7.44 (m, 2H), 5.48 (s, 1H), 4.19 (dq, *J* = 6.5, 2.8 Hz, 1H), 3.83 (s, 3H), 3.28 (s, 3H), 3.26 (d, *J* = 15.7 Hz, 1H), 2.65 (dd, *J* = 15.7, 1.0 Hz, 1H), 2.35 (dq, *J* = 7.2, 2.6 Hz, 1H), 1.25 (d, *J* = 6.6 Hz, 3H), 1.07 (d, *J* = 7.2 Hz, 3H); ^{13}C NMR (100 MHz, $CDCl_3$): δ (ppm) 208.8, 168.5, 165.3, 133.8, 130.0(2C), 128.5(2C), 100.9, 77.2, 70.9, 68.1, 52.6, 48.8, 48.6, 41.8, 16.9, 9.8; HRMS (ESI) *m/z* calcd for $C_{18}H_{22}O_7Na$ $(M+Na)^+$ 373.1263 found 373.1272**;** IR (thin film) cm^{-1}: 3079, 2868, 1740, 1712, 1699, 1446, 1319, 1240, 1115, 859, 763.

(*S*)-2-methoxy-1-((2*R*,5*R*,6*R*)-2-methoxy-5,6-dimethyl-4-methylenetetrahydro-2*H*-pyran-2-yl)-2-oxoethyl benzoate (2.31)

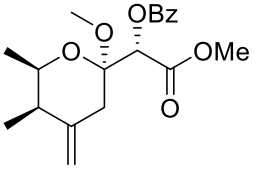

2.31

To a solution of **2.30** (500 mg, 1.42 mmol) in THF (10 mL) under nitrogen atmosphere was added freshly prepared Takai-Lombardo methylenation reagent[71] (0.2 M, 1.6 mmol, 8 mL) slowly dropwise. The reaction was monitored until starting material was fully consumed whereupon the mixture was poured into ice-cold

saturated $NaHCO_3$(aq.) (30 mL) and extracted with ethyl acetate (3 x 20 mL). The organic phase was washed with $NaHCO_3$(aq.) (30 mL), brine, dried with $MgSO_4$ and concentgrated under reduced pressure. The crude product was purified with flash column chromatography (20% ethyl acetate in hexanes) to obtain the desired product (390 mg, 80 %): ^{1}H NMR (400 MHz, $CDCl_3$): δ (ppm) 8.10-8.08 (m, 2H), 7.62-7.58 (m, 1H), 7.48-7.45 (m, 2H), 5,42 (s, 1H), 4.87 (dd, *J* = 1.9, 1.9 Hz, 1H), 4.80 (dd, *J* = 1.9, 1.9 Hz, 1H), 3.91 (dq, *J* = 6.5, 2.5 Hz, 1H), 3.81 (s, 3H), 3.26 (s, 3H), 2.92 (dt, *J* = 14.5, 2.1 Hz, 1H), 2.46 (d, *J* = 14.5 Hz, 1H), 2.23 (dq, *J* = 6.8, 2.3 Hz, 1H), 1.15 (d, *J* = 6.5 Hz, 3H), 0.95 (d, *J* = 7.0 Hz, 3H); ^{13}C NMR (100 MHz, $CDCl_3$): δ (ppm) 168.6, 165.6, 146.2, 133.6, 130.0(2C), 128.5(2C), 110.0, 99.3, 77.2, 72.1, 69.4, 52.4, 48.4, 41.5, 33.7, 17.7, 11.6; HRMS (ESI) *m/z* calcd for $C_{19}H_{24}O_6Na$ $(M+Na)^+$ 371.1465 found 371.1482**;** IR (thin film) cm^{-1}: 3090, 2874, 1748, 1689, 1451, 1327, 1252, 1105, 979, 830, 773.

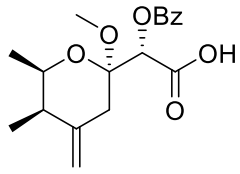

2.19

(*S*)-2-(benzoyloxy)-2-((2*R*,5*R*,6*R*)-2-methoxy-5,6-dimethyl-4-methylenetetrahydro-2*H*-pyran-2-yl)acetic acid (2.19)

To a solution of **2.31** (400 mg, 1.15 mmol) in dichloroethane (64 mL) was added Me_3SnOH (1.04 g, 5.75 mmol) and the mixture stirred at 80 °C for 8 h. The reaction mixture was cooled to rt whereupon $NaHSO_4$(aq.) (0.01 M, 50 mL) was added and the aqueous and organic layers separated. The aqueous layer was extracted with ethyl acetate (3 x 30 mL) and the combined organic layer was dried with MgSO4 and concentrated under reduced pressure. The crude product was purified with flash column chromatography (30-80% ethyl acetate in hexanes, 100% ethyl acetate then 5% methanol in ethyl acetate) to obtain the desired product (214 mg, 56%): ^{1}H NMR (300 MHz, $CDCl_3$): δ (ppm) 8.11-8.09 (m, 2H), 7.63-7.58 (m, 1H), 7.49-7.44 (m, 2H), 5.67 (s, 1H), 4.93 (dd, *J* = 1.9, 1.9 Hz, 1H), 4.84 (dd, *J* = 1.9, 1.9 Hz, 1H), 4.09 (dq, *J* = 6.5, 2.5 Hz, 1H), 3.26 (s, 3H), 2.67-2.53 (m, 2H), 2.32 (dq, *J* = 6.6, 2.4 Hz,

1H), 1.26 (d, *J* = 6.3 Hz, 3H), 1.12 (d, *J* = 7.2 Hz, 3H); HRMS (ESI) *m/z* calcd for $C_{18}H_{21}O_6$ $(M-H)^-$ 333.1333 found 333.1334**;** IR (thin film) cm^{-1}: 3205, 3063, 2887, 1760, 1737, 1453, 1338, 1241, 1085, 955, 867, 710.

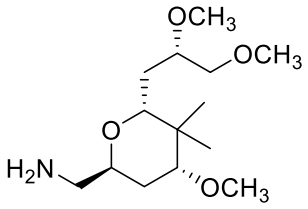

2.32

((2*S*,4*R*,6*R*)-6-((*S*)-2,3-dimethoxypropyl)-4-methoxy-5,5-dimethyltetrahydro-2*H*-pyran-2-yl) methanamine (2.32)

To a solution of **2.20** (36 mg, 0.13 mmol) in glacial acetic acid (2 mL) in a 5 mL round bottom flask purged with hydrogen gas was added Pd/C (10% w/w, 7 mg, 0.006 mmol) and PtO_2 (7 mg, 0.03 mmol) whereupon a balloon filled with hydrogen gas was mounted over the mixture and stirred at rt until complete consumption of nitrile. The reaction mixture was filtered through a plug of celite and the filtrate azeotroped with toluene under reduced pressure. The crude product was diluted with saturated $NaHCO_3$(aq.) (30 mL) and extracted with dichloromethane. The organic phase was dried over Na_2SO_4 and concentrated under reduced pressure. The crude product (34 mg) was used directly in the subsequent amide coupling reaction.

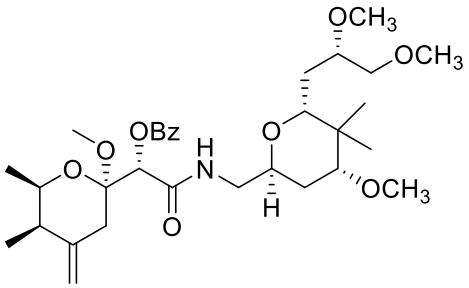

2.33

Benzoylated Pederin Analogue (2.33)

To a solution of **2.19** (34 mg, 0.101 mmol) and **2.32** (28 mg, 0.101 mmol**)** in DMF (5 mL) at 0 °C was added a solution of *N*-(3-Dimethylaminopropyl)-N′-ethylcarbodiimide hydrochloride (21.3 mg, 0.111 mmol) and HOBt (15 mg, 0.111 mmol) in DMF (3 mL). The mixture was stirred at 0 °C for 5 min whereupon Hunig's base (7.8 mg, 0.061 mmol) was added. The reaction proceeded at 0 °C for 10 min and the mixture was slowly warmed to rt and stirred overnight. The mixture was diluted with water (30 mL) and extracted with ethyl acetate (3 x 10 mL). the organic phase was washed with

water (30 mL), brine (20 mL), dried over $MgSO_4$ and concentrated under reduced pressure. The crude product was purified with flash column chromatography (30% ethyl acetate in hexanes) to obtain the desired product (49 mg, 81%): ^{1}H NMR (400 MHz, $CDCl_3$): δ (ppm) 8.13-8.09 (m, 2H), 7.60-7.56 (m, 1H), 7.47-7.43 (m, 2H), 6.97 (dd, *J* = 7.8, 3.1 Hz, 1H), 5.42 (s, 1H), 4.87 (dd, *J* = 1.8, 1.8 Hz, 1H), 4.80 (dd, *J* = 1.8, 1.8 Hz, 1H), 4.04-3.96 (m, 2H), 3.80 (ddd, *J* = 13.9, 8.6, 5.6 Hz, 1H), 3.53-3.31 (m, 4H), 3.40 (s, 3H), 3.33 (s, 3H), 3.28 (s, 3H), 3.22 (s, 3H), 3.12 (ddd, *J* = 13.0, 8.5, 3.8 Hz, 1H), 3.04 (dd, *J* = 8.1, 3.2 Hz, 1H), 2.80 (dt, *J* = 14.5, 2.0 Hz, 1H), 2.48 (d, *J* = 14.5 Hz, 1H), 2.25 (dq, *J* = 4.5, 2.5 Hz, 1H), 1.78-1.64 (m, 4H), 1.19 (d, *J* = 6.6 Hz, 3H), 1.00 (d, *J* = 7.0 Hz, 3H), 0.96 (s, 3H), 0.88 (s, 3H); ^{13}C NMR (100 MHz, $CDCl_3$): δ (ppm) 166.8, 145.9, 133.3, 130.0 (2C), 129.5, 128.4 (2C), 110.2, 99.3, 81.6, 78.1, 77.2, 74.8, 72.5, 69.6, 59.0, 57.4, 56.9, 48.3, 41.5, 38.1, 33.9, 29.5, 27.0, 18.0, 11.8 (*three signals are buried with the baseline due to low concentration*); HRMS (ESI) *m/z* calcd for $C_{32}H_{48}NO_9$ $(M-H)^-$ 590.3324 found 590.3317**;** IR (thin film) cm^{-1}: 3425, 3016, 2897, 1720, 1692, 1453, 1329, 1271, 1079, 961, 880, 754.

Pederin Analogue (2.18)

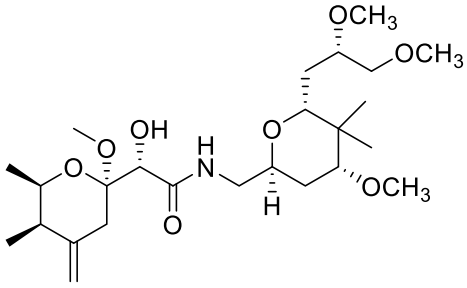

2.18

To a solution of **2.33** (40 mg, 0.07 mmol) in methanol (1.5 mL) was added K_2CO_3 (5 mg, 0.04 mmol) and the mixture stirred at rt for 4 h. A solution of brine (3 mL) and HCl(aq.) (1*N*, 3 mL) was added to the reaction mixture and extracted with ethyl acetate (3 x 10 mL) the combined organic phase was washed with $NaHCO_3$(aq.) (3mL), dried over $MgSO_4$ and concentrated under reduced pressure. The crude product was purified with flash column chromatography (30-80% ethyl acetate in hexanes) to obtain the desired product (30 mg, 88%): ^{1}H NMR (400 MHz, $CDCl_3$): δ (ppm) 7.13 (dd, *J* = 7.0, 3.8 Hz, 1H), 4.85 (dd, *J* = 1.7, 1.7 Hz, 1H), 4.73 (dd, *J* = 1.7, 1.7 Hz, 1H), 4.20 (d, *J* = 3.8 Hz, 1H), 4.03-3.97 (m, 2H), 3.95 (d, *J* =

3.8 Hz, 1H), 3.75 (ddd, *J* = 13.3, 7.9, 4.6 Hz, 1H), 3.45-3.34 (m, 4H), 3.38 (s, 3H), 3.37 (m, 3H), 3.32 (s, 3H), 3.31 (s, 3H), 3.15 (ddd, *J* = 13.1, 8.9, 4.2 Hz, 1H), 3.04 (dd, *J* = 6.3, 4.3 Hz, 1H), 2.33 (d, *J* = 14.3 Hz, 1H), 2.24 (dq, *J* = 7.1, 4.7 Hz, 1H), 2.14 (d, *J* = 14.3 Hz, 1H), 1.72-1.62 (m, 4H), 1.19 (d, *J* = 6.6 Hz, 3H), 1.00 (s, 3H), 0.96 (d, *J* = 7.0 Hz, 3H), 0.90 (s, 3H); ^{13}C NMR (100 MHz, $CDCl_3$): δ (ppm) 171.2, 145.5, 110.6, 100.0, 81.7, 78.3, 77.2, 76.4, 74.3, 70.9, 69.4, 67.1, 59.2, 57.6, 57.1, 48.4, 42.6, 41.4, 37.9, 33.0, 29.2, 27.4, 25.1, 18.0, 11.9; HRMS (ESI) *m/z* calcd for $C_{25}H_{45}NO_8Na$ $(M+Na)^+$ 510.3037 found 510.3062**;** IR (thin film) cm^{-1}: 3437, 3310, 3026, 2906, 1723, 1689, 1455, 1322, 1238, 1088, 977, 868, 795.

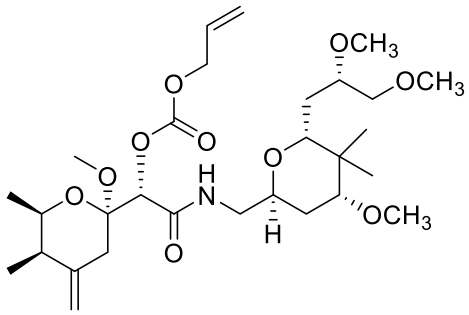

2.34

Pederin Analogue – (Allyl Carbonate (2.34)) To a solution of **2.18** (5.4 mg, 0.011 mmol) in THF (0.2 mL) was added TMEDA (3.8 mg, 0.033 mmol) and allyl chloroformate (4.0 mg, 0.033 mmol) and stirred at rt. The mixture was concentrated under reduced pressure and purified with flash column chromatography (10-20% ethyl acetate in hexanes) to obtain the desired product (6.1mg, 97%): ^{1}H NMR (400 MHz, $CDCl_3$): δ (ppm) 6.95 (dd, *J* = 7.8, 3.2 Hz, 1H), 5.93 (ddt, *J* = 17.4, 10.6, 5.7 Hz, 1H), 5.40-5.34 (m, 1H), 5.29-5.25 (m, 1H), 5.09 (s, 1H), 4.84 (dd, *J* = 1.8, 1.8 Hz, 1H), 4.73 (dd, *J* = 1.8, 1.8 Hz, 1H), 4.68-4.64 (m, 2H), 4.01-3.93 (m, 2H), 3.78 (ddd, *J* = 13.4, 8.2, 5.1 Hz, 1H)**,** 3.54-3.41 (m, 4H), 3.39 (s, 3H), 3.37 (s, 3H), 3.30 (s, 3H), 3.22 (s, 3H), 3,12 (ddd, *J* = 13.2, 8.8, 3.7 Hz, 1H), 3.04 (dd, *J* = 7.7, 4.3 Hz, 1H), 2.58 (dt, *J* = 14.6, 2.4 Hz, 1H), 2.38 (d, *J* = 14.6 Hz, 1H), 2.22 (dq, *J* = 7.3, 4.9 Hz, 1H), 1.73-1.63 (m, 4H), 1.17 (d, *J* = 6.6 Hz, 3H), 0.98 (s, 3H), 0.96 (d, *J* = 7.0 Hz, 3H), 0.89 (s, 3H); HRMS (ESI) *m/z* calcd for $C_{29}H_{49}NO_{10}Na$ $(M+Na)^+$ 594.3249 found 594.3273**;** IR (thin film) cm^{-1}: 3422, 3062, 2927, 1770, 1659, 1468, 1347, 1251, 1138, 938, 818, 725.

Preparation of Chloroformate (2.35)

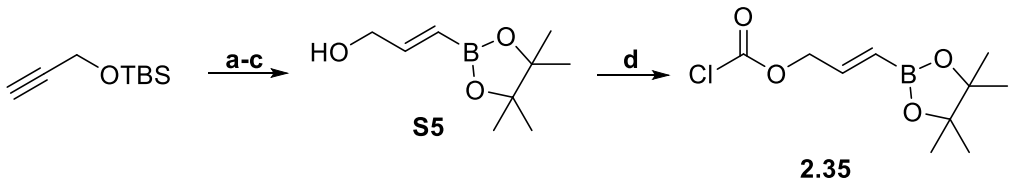

Reactions & Conditions

a) TBSCl, DMAP, DCM, 90%. b) Cp_2ZrHCl, H-Bpin, Et_3N, 60 °C, 83%.
c) 10-CSA, MeOH, rt, 91%. d) $C(O)Cl_2$, 1,4-dioxane, rt, 97% crude yield.

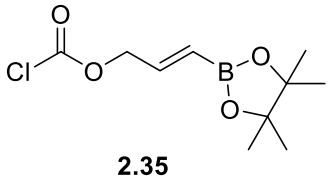

Chloroformate (2.35)

A previously reported protocol[56] for the preparation of **2.35** was followed with alcohol **S5** (70 mg, 0.38 mmol) and phosgene (15% wt, 500 µL, 0.76 mmol) to afford product (90 mg, 97% crude yield) upon evaporation of all volatiles in the reaction mixture. Crude ^{1}H NMR (400 MHz, $CDCl_3$): δ (ppm) 6.49 (dt, *J* = 18.0, 5.1 Hz, 1H), 5.72 (dt, *J* = 18.0, 1.4 Hz, 1H), 4.18 (dd, *J* = 5.1, 1.6 Hz, 2H), 1.02 (s, 12H).

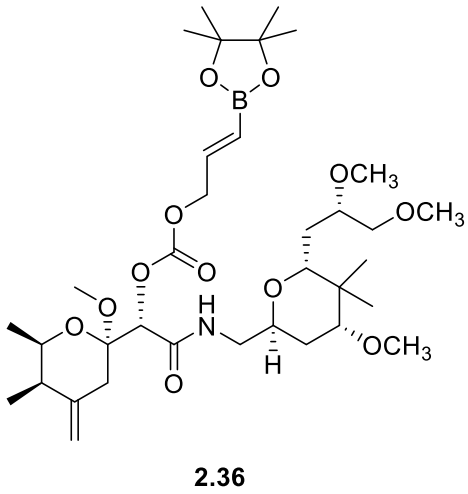

Boronate-Pederin Analogue (2.36)

The procedure for the synthesis of **2.34** was followed with **2.18** (7.6 mg, 0.015 mmol) and **2.35** (5.5 mg, 0.023 mmol) to obtain the desired product **2.36** (9.6 mg, 89%): ^{1}H NMR (400 MHz, C_6D_6): δ (ppm) 6.94 (dd, *J* = 7.7, 4.5 Hz, 1H), 6.60 (dt, *J* = 18.1, 4.9 Hz, 1H), 5.73 (dt, *J* = 18.2, 1.5 Hz, 1H), 5.09 (s, 1H), 4.83 (dd, *J* = 1.6, 1.6 Hz, 1H), 4.79-4.66 (m, 2H), 4.74 (dd, *J* = 1.6, 1.6 Hz, 1H), 4.00-3.94 (m, 2H), 3.82-3.74 (m, 1H), 3.54-3.41 (m, 4H). 3.39 (s, 3H), 3.37 (s, 3H), 3.30 (s, 3H), 3.23 (s, 3H), 3.13 (ddd, *J* = 13.0, 8.9, 3.5 Hz, 1H), 3.04 (dd, *J* = 7.8, 4.2 Hz, 1H), 2.58 (d, *J* = 14.6 Hz, 1H), 2.38

(d, *J* = 14.6 Hz, 1H), 1.76-1.64 (m, 4H), 1.26 (s, 12H), 1,17 (d, *J* = 6.8 Hz, 3H), 0.98 (s, 3H), 0.96 (d, *J* = 7.2 Hz, 3H), 0.88 (s, 3H); ^{11}B NMR (400 MHz, C_6D_6): δ (ppm) 30.49; ^{13}C NMR (100 MHz, C_6D_6): 165.3, 151.7, 145.2, 144.6, 127.4, 126.3, 109.1, 98.5, 82.0, 81.9, 80.4, 77.6, 75.1, 75.0, 68.4, 68.1, 63.2, 57.7, 55.9, 55.7, 47.0, 40.8, 37.2, 33.1, 29.2, 26.1, 23.7 (4C) 23.6 (2C), 16.8, 10.6; HRMS (ESI) *m/z* calcd for $C_{35}H_{60}NO_{12}BNa$ $(M+Na)^+$ 720.4101 found 720.4098**;** IR (thin film) cm^{-1}: 3442, 3100, 2947, 1769, 1692, 1448, 1351, 1235, 1121, 915, 847, 775.

2.5.3 Boronate breakdown – ^{1}H NMR study

2.5.3.1 ^{1}H NMR sample preparation

Compound **2.36** (8.4 mg, 0.012 mmol) was dissolved in CD_3CN (475 μL) and D_2O (50 μL) was added followed by pH 7.4 phosphate buffer (25 μL, 0.1 M, D_2O) and methylbenzoate (internal standard, 25 μL, 1.5 M, CD_3CN). The resulting solution was transferred to an NMR tube. This sample preparation is modeled after Phillips' protocol.[76]

2.5.3.2 Procedure for monitoring pederin breakdown of pederin analogue 2.36

The release of pederin analogue **2.18** from the breakdown of **2.36** was monitored via ^{1}H NMR spectroscopy at 300 K. An initial ^{1}H NMR scan of compound **2.36** in CD_3CN and phosphate buffer (pH 7.4) was taken to obtain baseline integration values relative to the internal standard (methylbenzoate). The NMR sample was treated with a solution of H_2O_2•Urea (3.0 M, 60 μL, 15 equivalents), and mixing was achieved by inverting the NMR tube three times. The release of pederin analogue **2.18** was directly measured by integration of the C7 methine proton adjacent the alcohol functional group.

APPENDIX A (SPECTROSCOPIC DATA FOR CHAPTER 1)

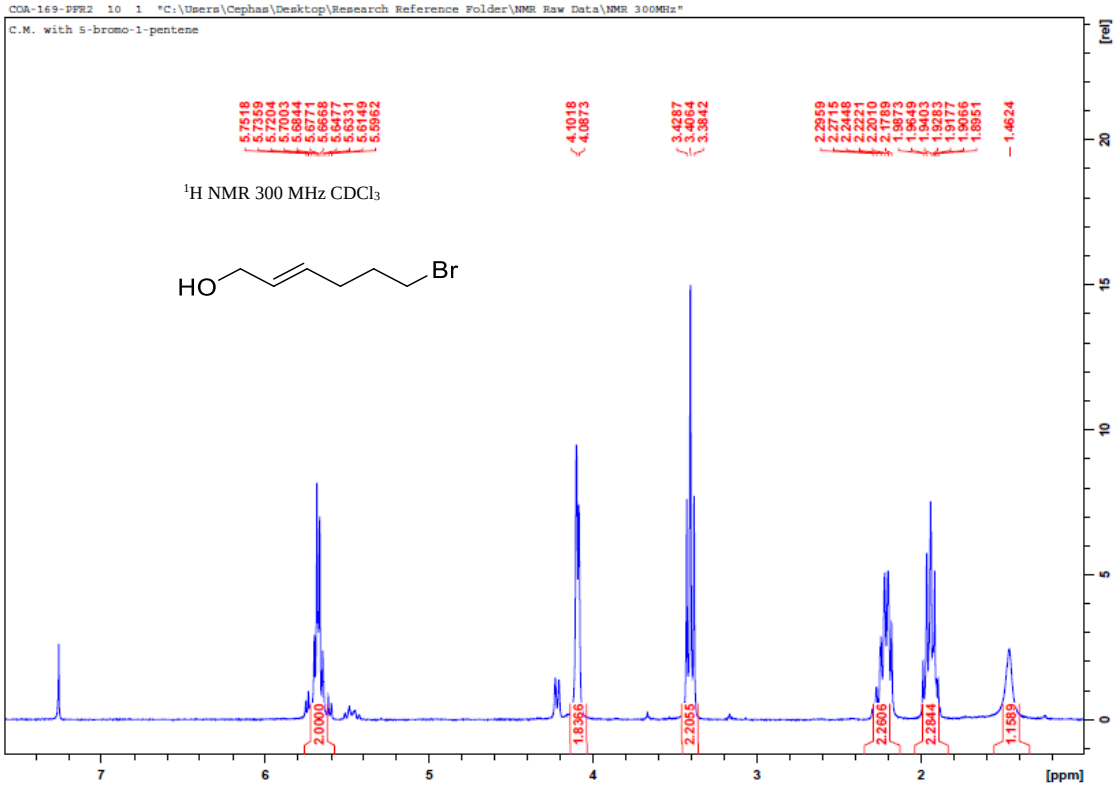

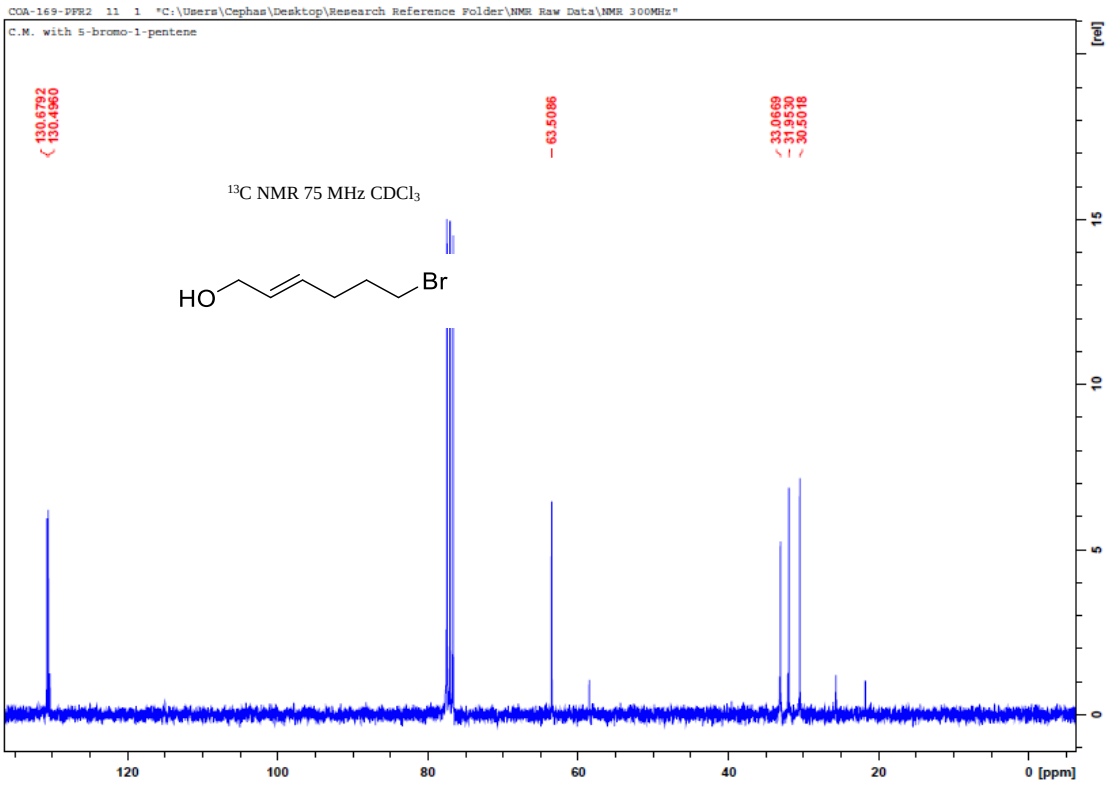
COA-169-PFR2 11 1 "C:\Users\Cephas\Desktop\Research Reference Folder\NMR Raw Data\NMR 300MHz"
C.M. with 5-bromo-1-pentene
130.6792
130.4960
63.5086
33.0669
31.9530
30.5018
^{13}C NMR 75 MHz $CDCl_3$
HO
Br
[rel]
120
100
80
60
40
20
0 [ppm]

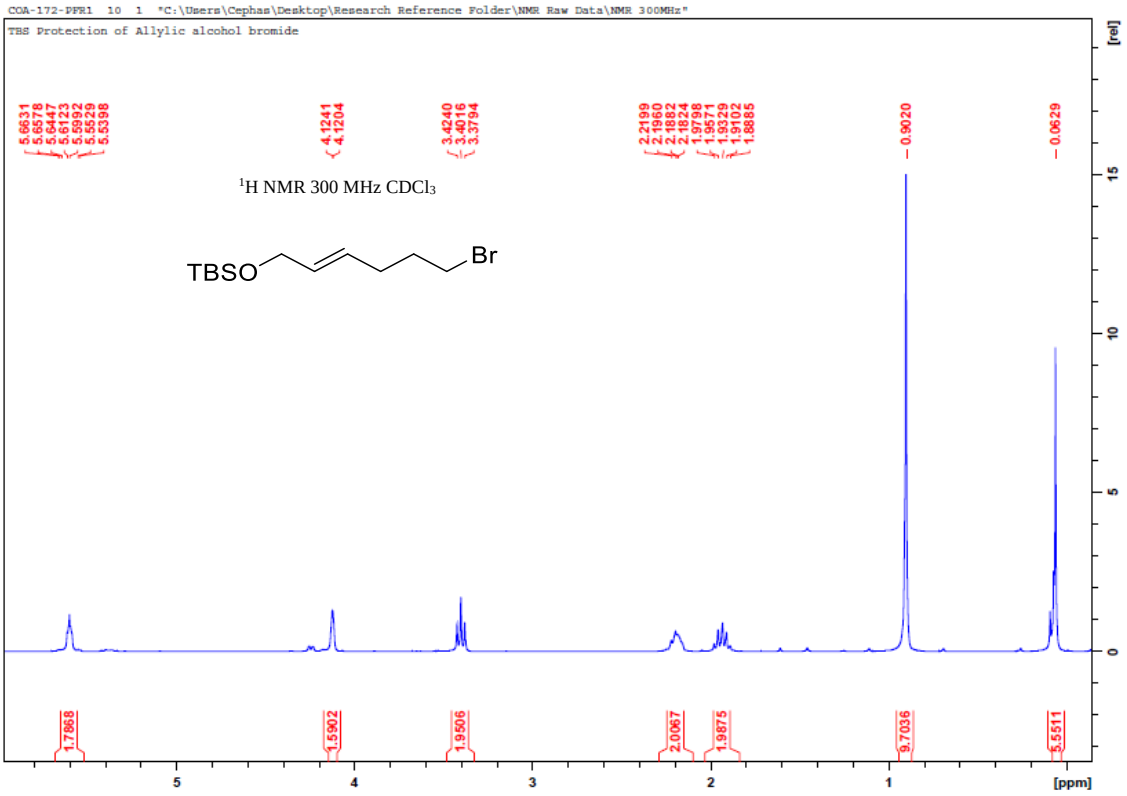
COA-172-PFR1 10 1 "C:\Users\Cephas\Desktop\Research Reference Folder\NMR Raw Data\NMR 300MHz"
TBS Protection of Allylic alcohol bromide
5.6631
5.6578
5.6447
5.6123
5.5922
5.5828
5.5398
4.1241
4.1204
3.4240
3.4016
3.3794
2.2199
2.1960
2.1882
2.1824
1.9798
1.9571
1.9329
1.9102
1.8885
0.9020
0.0629
^{1}H NMR 300 MHz $CDCl_3$
TBSO
Br
1.7868
1.5902
1.9506
2.0067
1.9875
9.7036
5.5511
[rel]
[ppm]

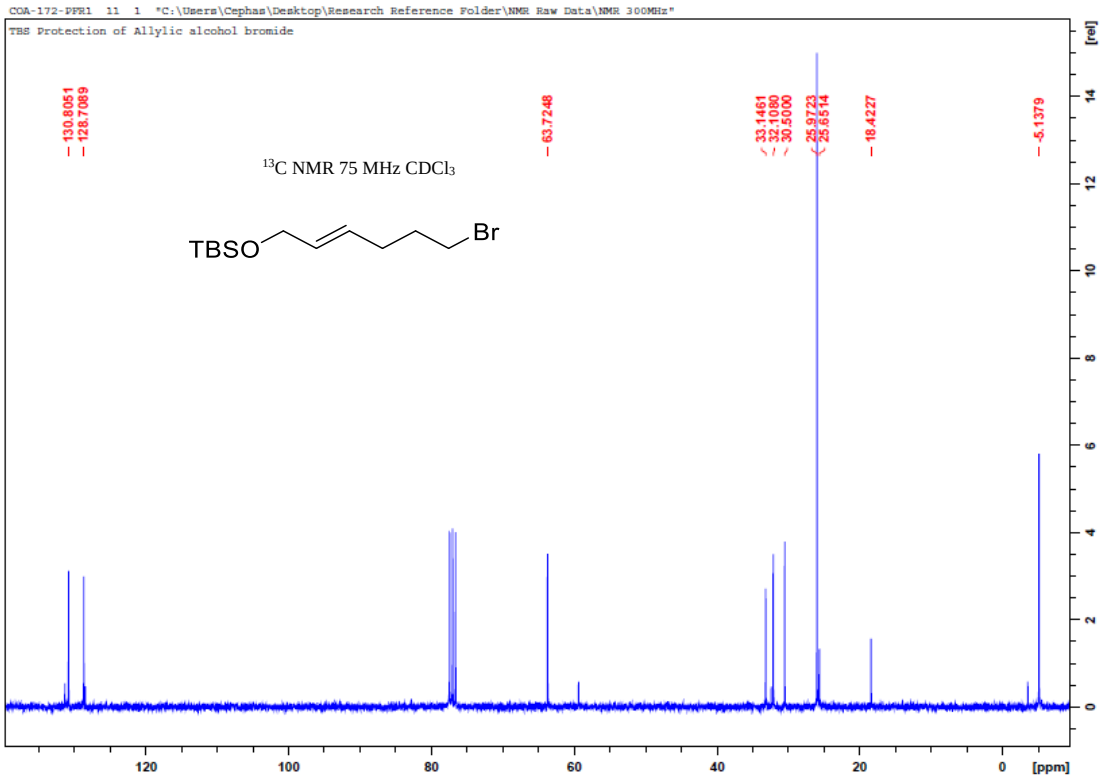
COA-172-PFR1 11 1 "C:\Users\Cephas\Desktop\Research Reference Folder\NMR Raw Data\NMR 300MHz"
TBS Protection of Allylic alcohol bromide
130.8051
128.7089
63.7248
33.1461
32.1080
30.5000
25.9723
25.8514
18.4227
-5.1379
[rel]
[ppm]
13C NMR 75 MHz CDCl3
TBSO
Br

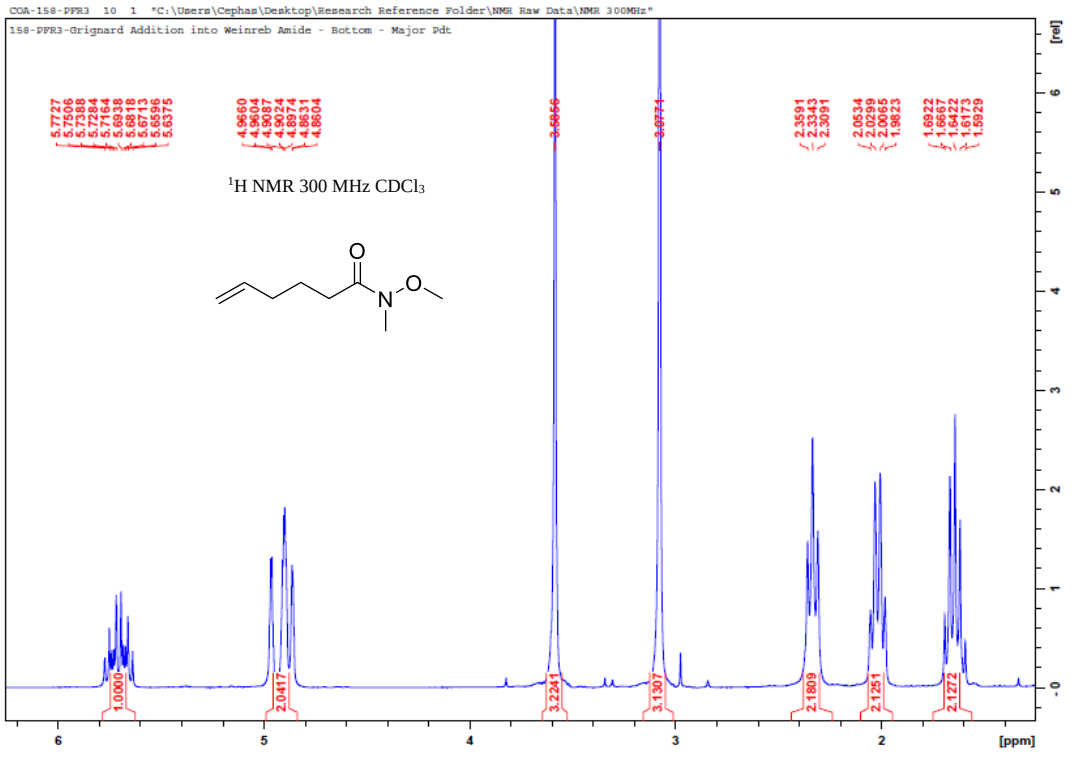
COA-158-PFR3 10 1 "C:\Users\Cephas\Desktop\Research Reference Folder\NMR Raw Data\NMR 300MHz"
158-PFR3-Grignard Addition into Weinreb Amide - Bottom - Major Pdt
5.7727
5.7506
5.7388
5.7284
5.7164
5.6938
5.6818
5.6713
5.6596
5.6375
4.9660
4.9604
4.9087
4.9024
4.8974
4.8831
4.8804
3.5866
3.5771
2.3591
2.3343
2.3091
2.0534
2.0299
2.0065
1.9823
1.6922
1.6667
1.6422
1.6173
1.5929
1.0000
2.0417
3.2241
3.1307
2.1809
2.1251
2.1272
[rel]
[ppm]
1H NMR 300 MHz CDCl3
O
N
O

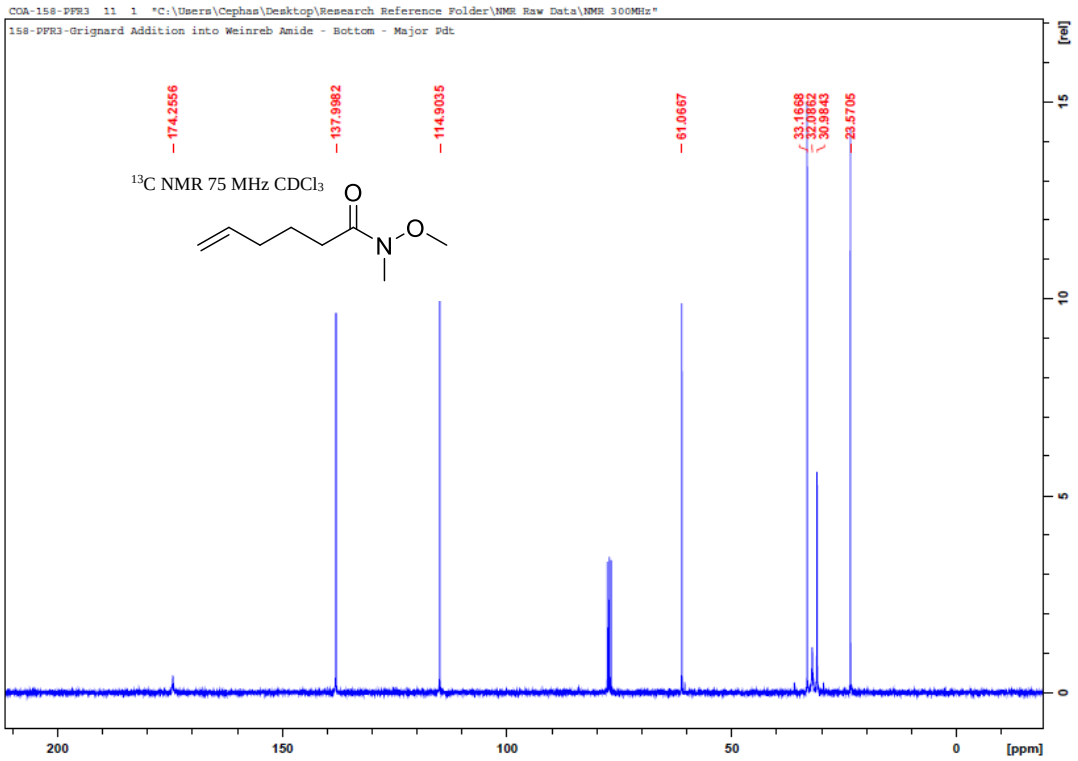

^{13}C NMR 75 MHz $CDCl_3$

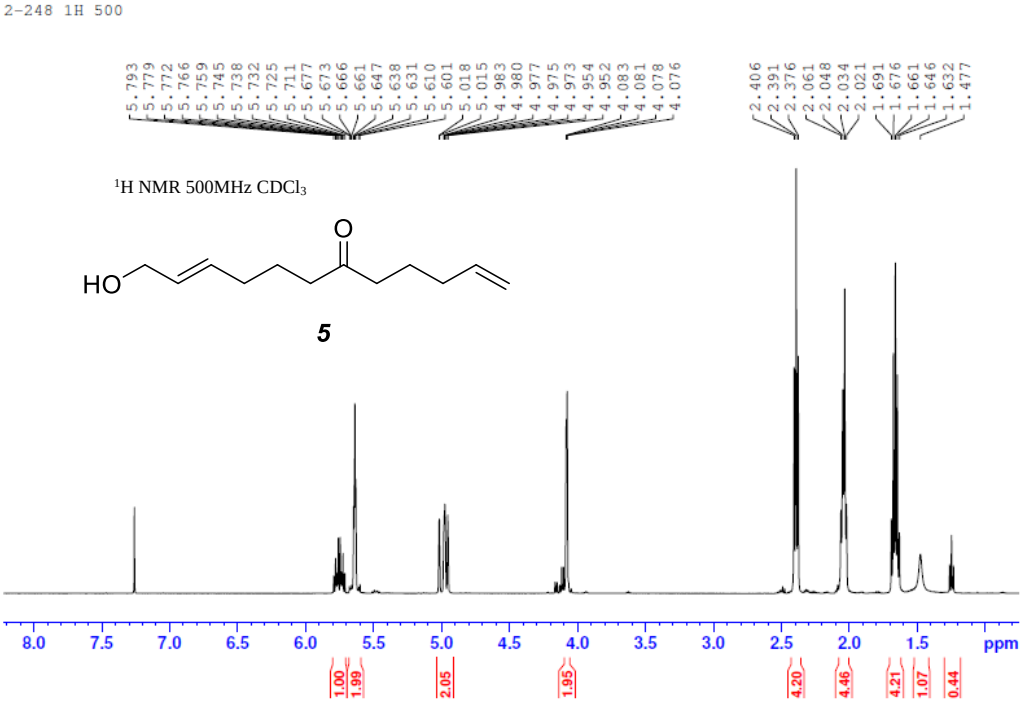

^{1}H NMR 500MHz $CDCl_3$

5

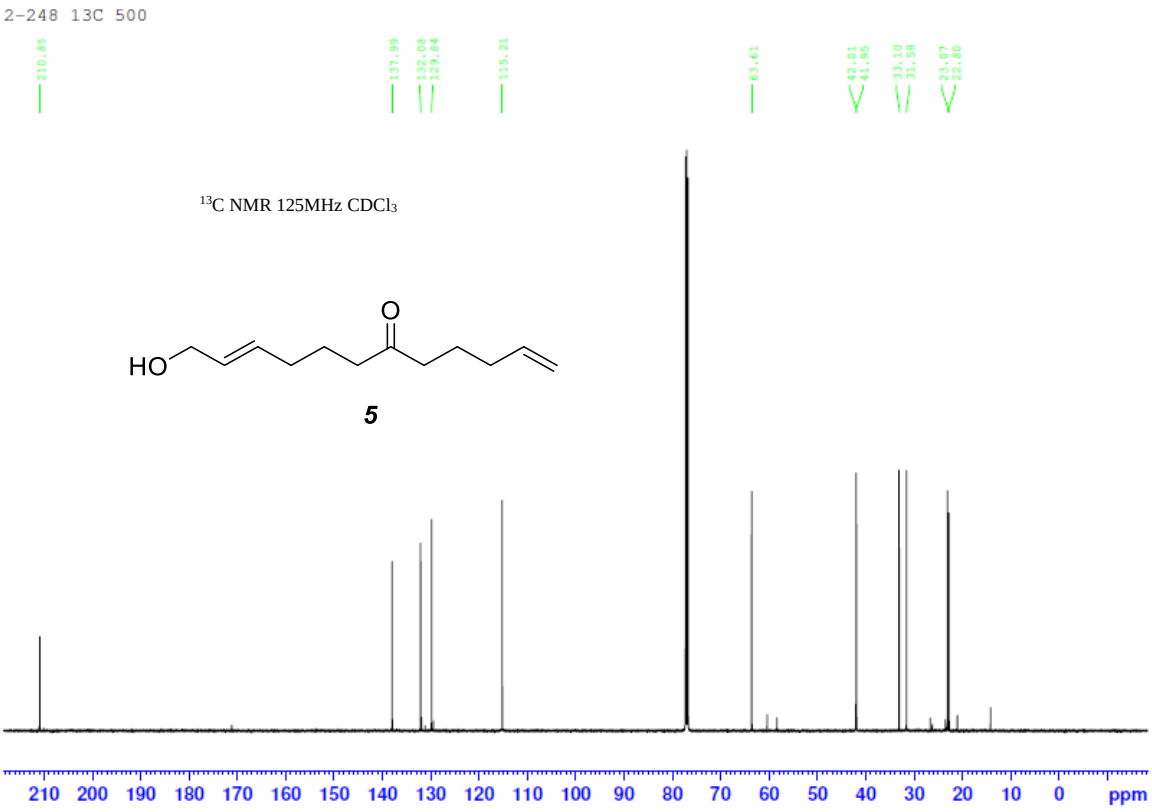
2-248 13C 500
210.85
137.99
132.08
129.84
115.21
63.61
42.01
41.95
33.10
31.58
23.07
22.80
^{13}C NMR 125MHz $CDCl_3$
HO
O
5
210 200 190 180 170 160 150 140 130 120 110 100 90 80 70 60 50 40 30 20 10 0 ppm

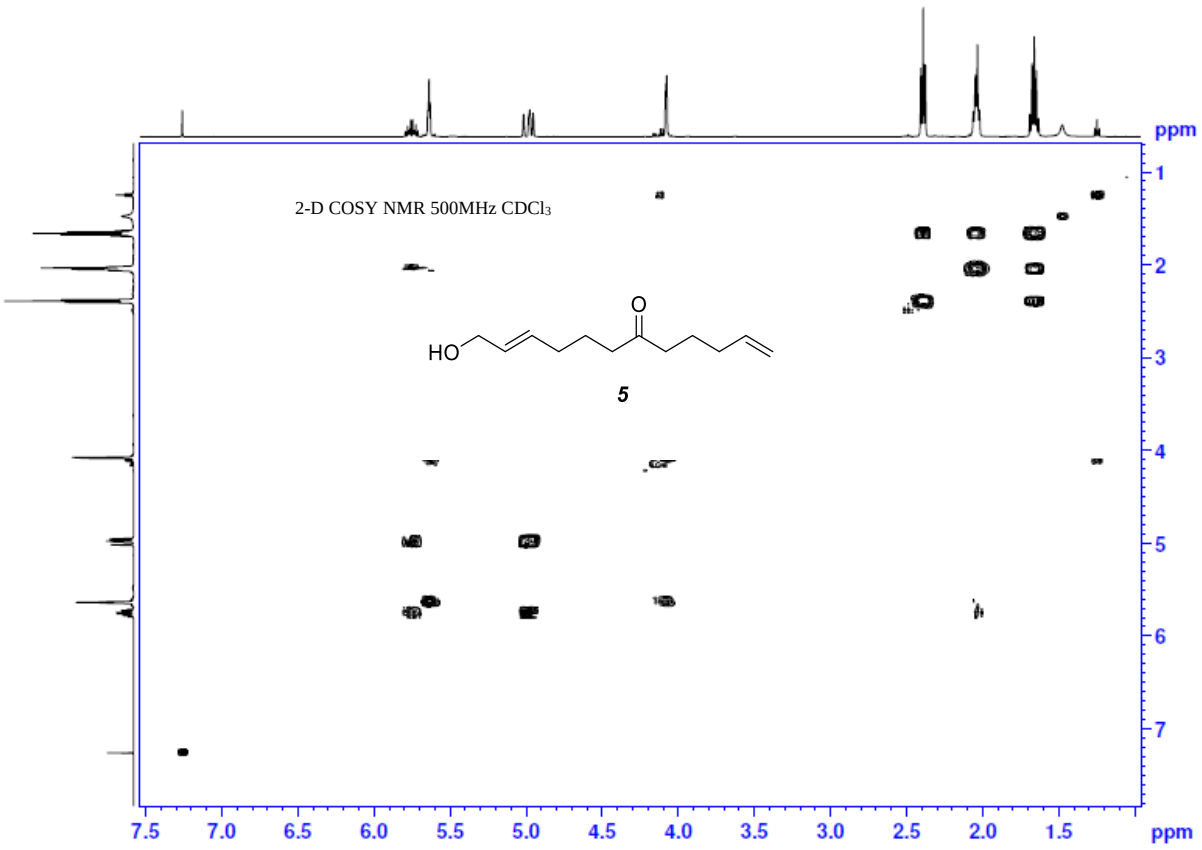

2-D COSY NMR 500MHz $CDCl_3$

5

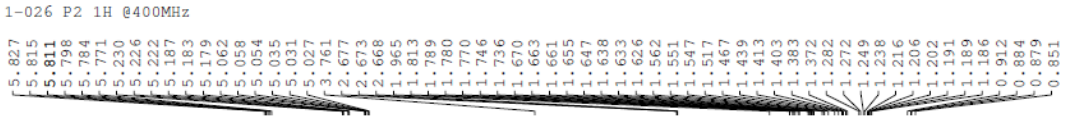

^1H NMR 400MHz $CDCl_3$

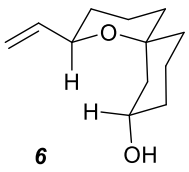

6

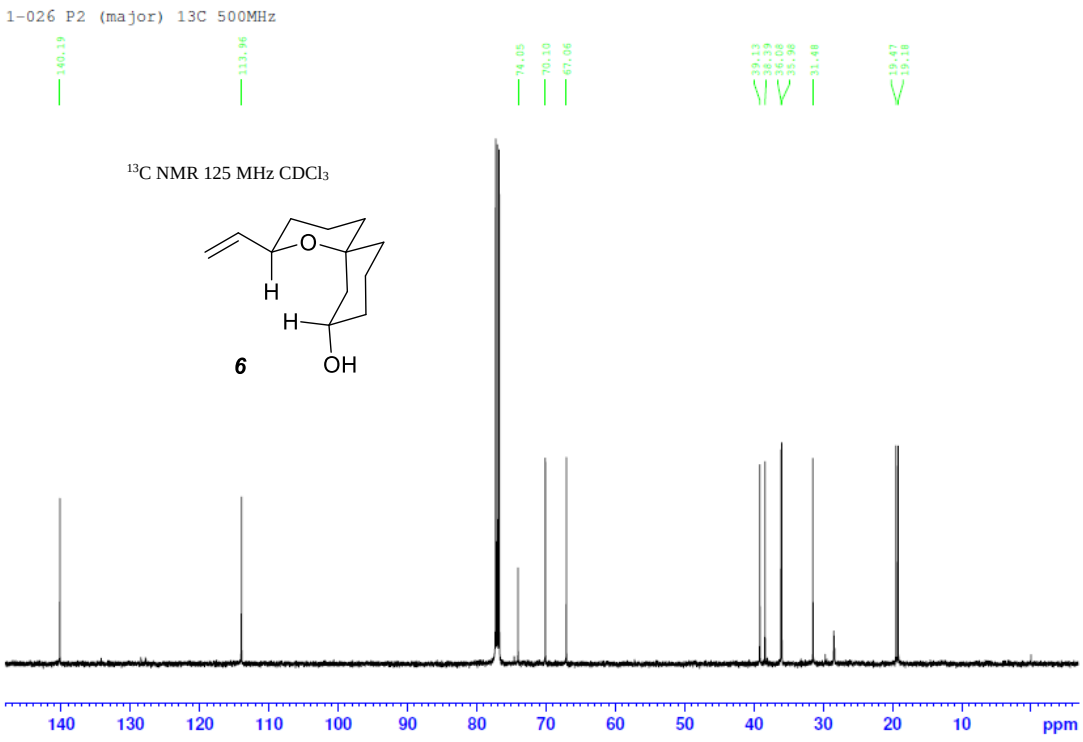
1-026 P2 (major) 13C 500MHz
140.19
113.96
74.05
70.10
67.06
39.13
38.39
36.08
35.98
31.48
19.47
19.18
13C NMR 125 MHz CDCl3
O
H
H
OH
6
140
130
120
110
100
90
80
70
60
50
40
30
20
10
ppm

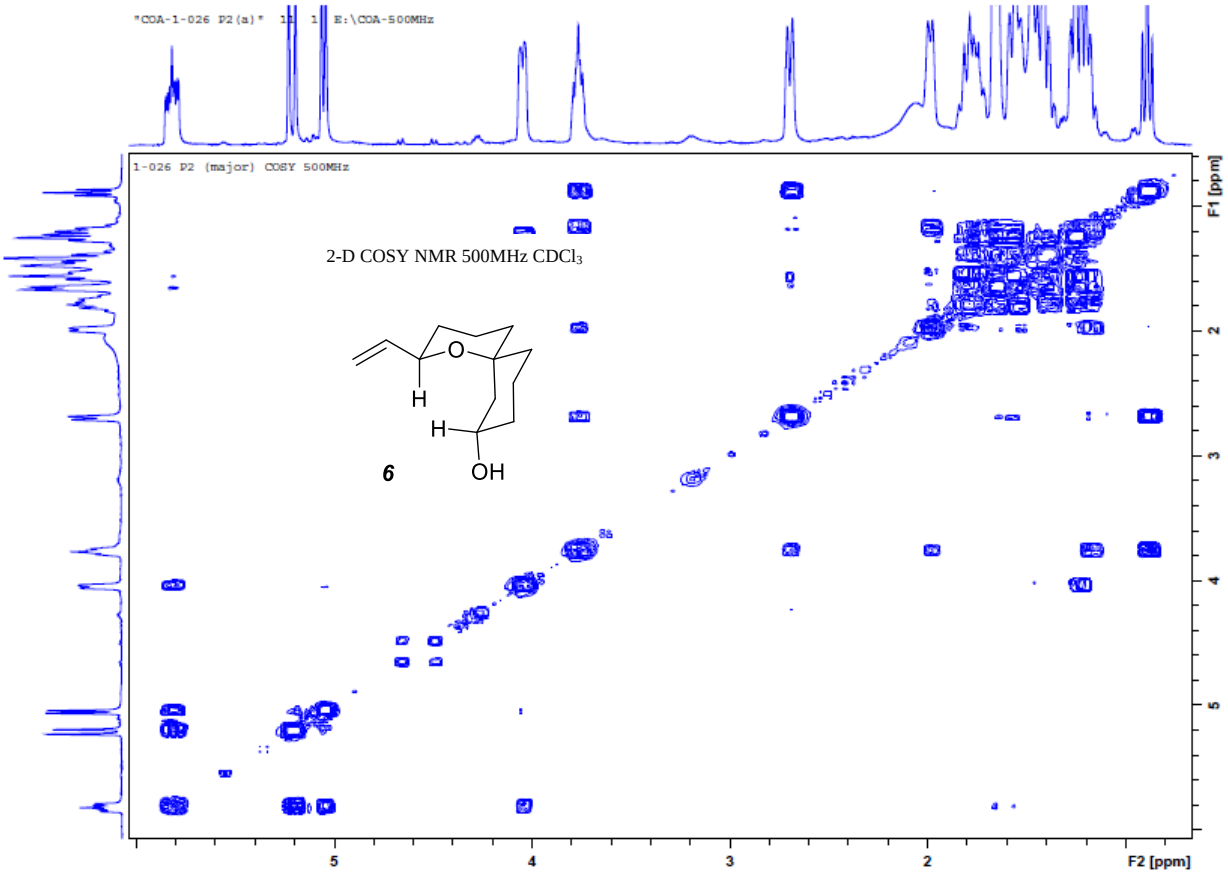

2-D COSY NMR 500MHz $CDCl_3$

6

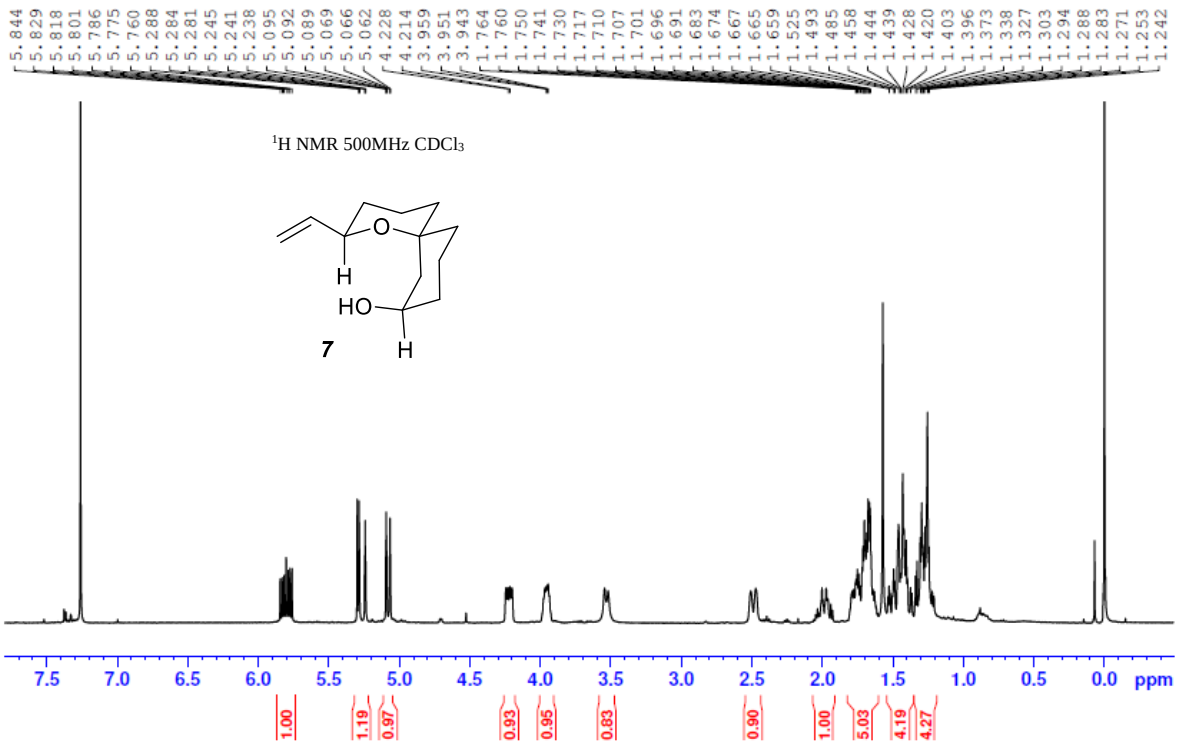

^{1}H NMR 500MHz $CDCl_3$

7

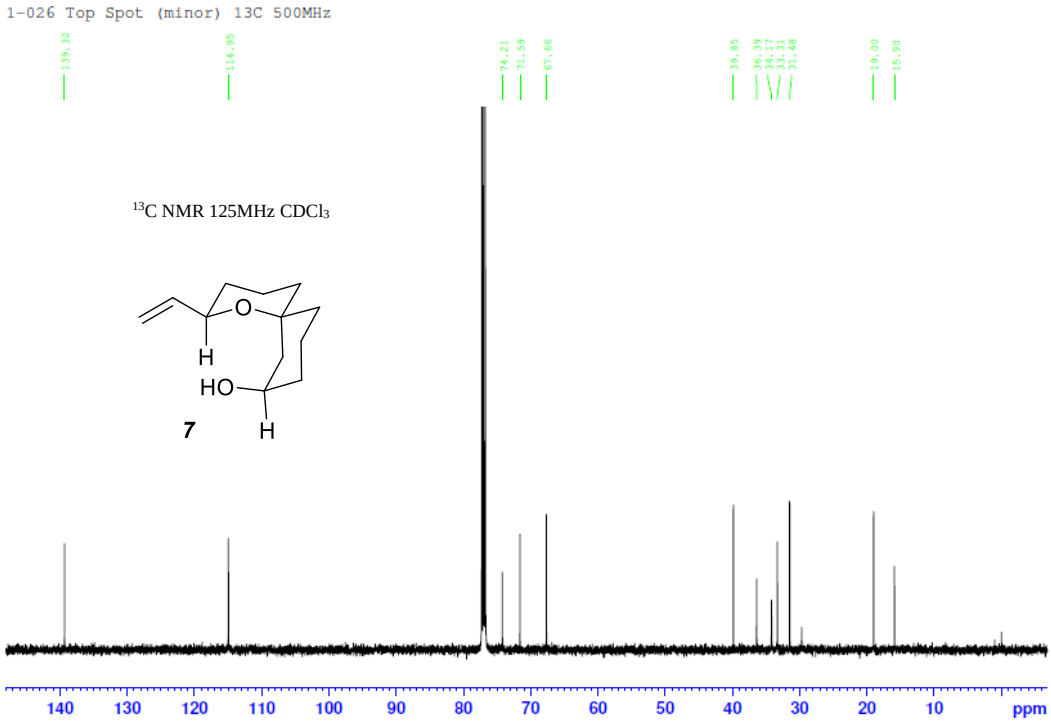

^{13}C NMR 125MHz $CDCl_3$

7

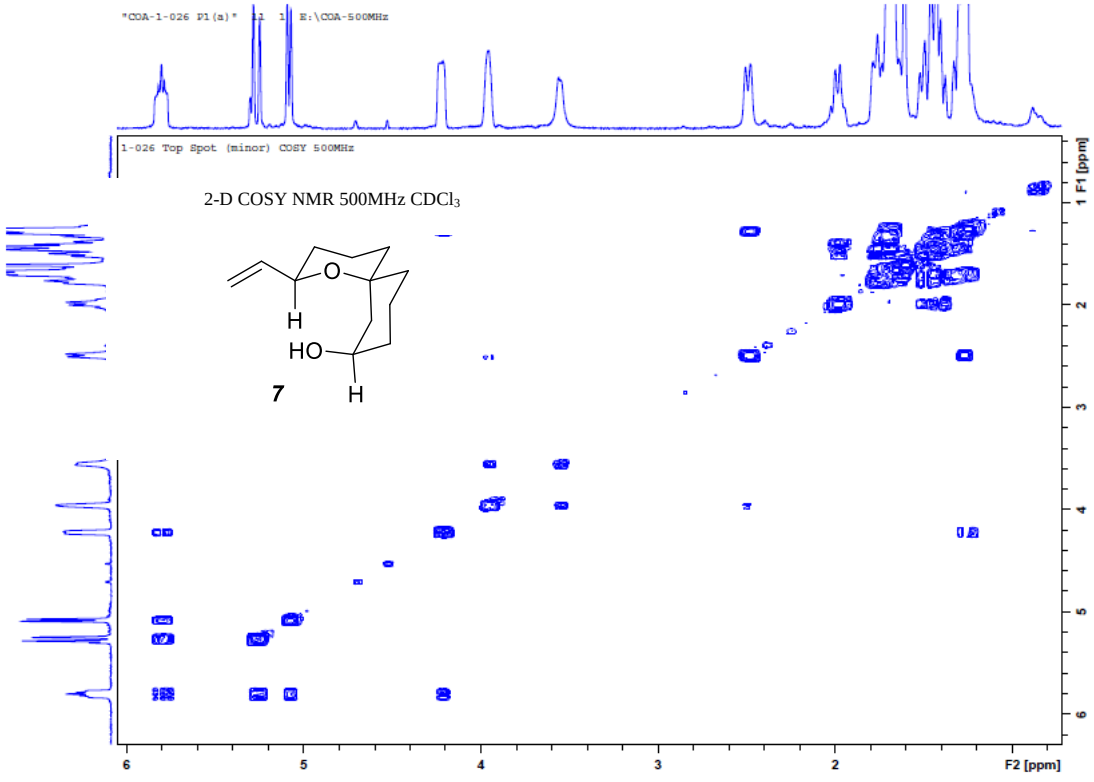

2-D COSY NMR 500MHz $CDCl_3$

7

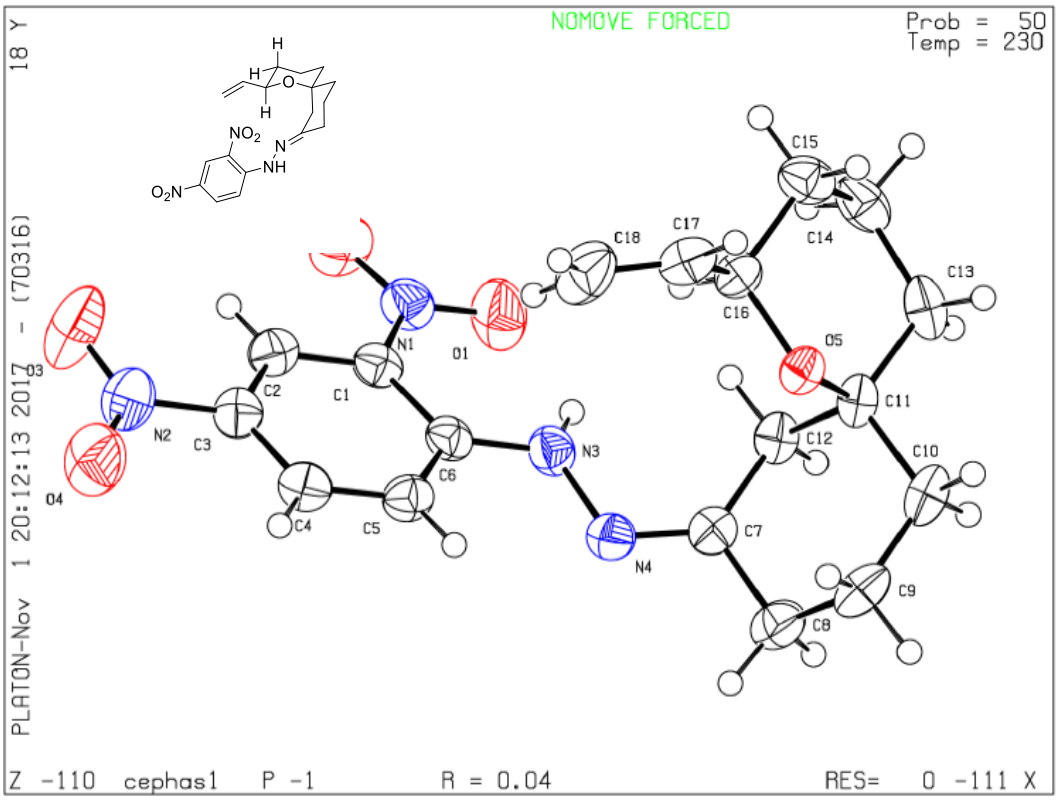

Bond precision: C-C = 0.0019 A Wavelength=1.54178

Cell: a=8.9124(3) b=9.5638(3) c=11.5721(4)
alpha=78.2389(17) beta=76.9753(19) gamma=72.7914(19)
Temperature: 230 K

	Calculated	Reported
Volume	907.95(5)	907.94(5)
Space group	P -1	P -1
Hall group	-P 1	-P 1
Moiety formula	C18 H22 N4 O5	?
Sum formula	C18 H22 N4 O5	C18 H22 N4 O5
Mr	374.40	374.39
Dx,g cm-3	1.370	1.369
Z	2	2
Mu (mm-1)	0.847	0.847
F000	396.0	396.0
F000'	397.31	
h,k,lmax	10,11,13	10,11,13
Nref	3335	3244
Tmin,Tmax	0.850,0.903	0.750,0.910
Tmin'	0.844	

Correction method= # Reported T Limits: Tmin=0.750 Tmax=0.910
AbsCorr = MULTI-SCAN

Data completeness= 0.973 Theta(max)= 68.440

R(reflections)= 0.0355(2931) wR2(reflections)= 0.1248(3244)

S = 1.488 Npar= 332

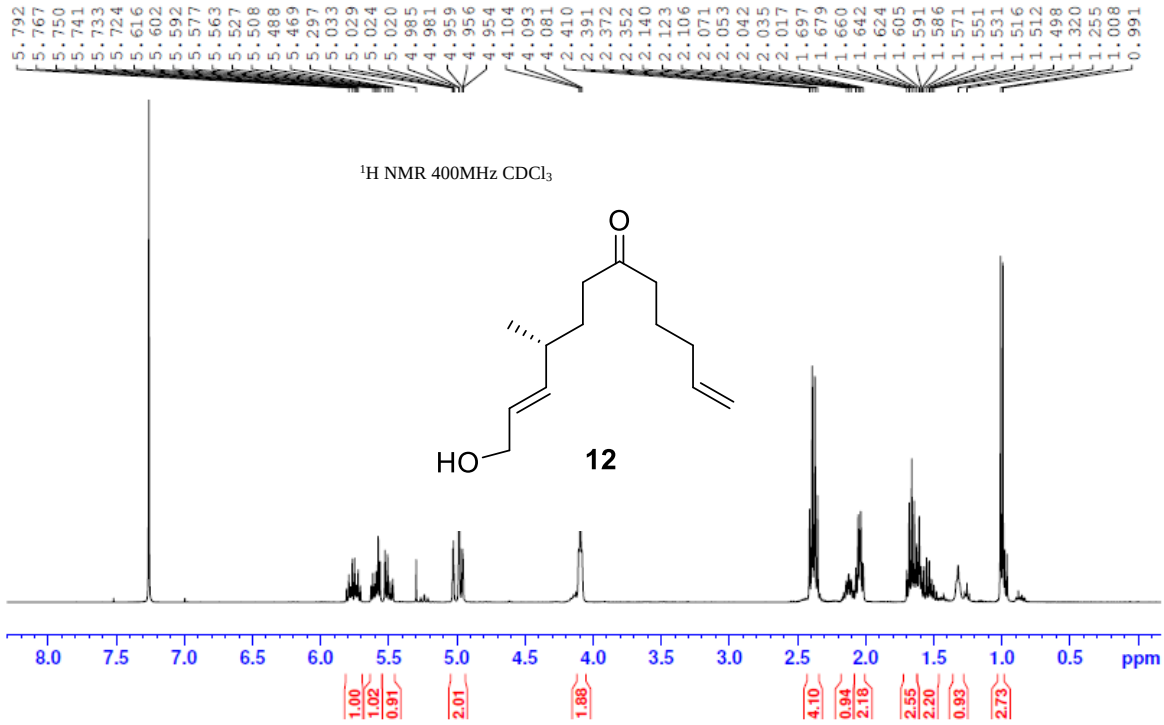
5.792
5.767
5.750
5.741
5.733
5.724
5.616
5.602
5.592
5.577
5.563
5.527
5.508
5.488
5.469
5.297
5.033
5.029
5.024
5.020
4.985
4.981
4.959
4.956
4.954
4.104
4.093
4.081
2.410
2.391
2.372
2.352
2.140
2.123
2.106
2.071
2.053
2.042
2.035
2.017
1.697
1.679
1.660
1.642
1.624
1.605
1.591
1.586
1.571
1.551
1.531
1.516
1.512
1.498
1.320
1.255
1.008
0.991
1H NMR 400MHz CDCl3
O
HO
12
8.0
7.5
7.0
6.5
6.0
5.5
5.0
4.5
4.0
3.5
3.0
2.5
2.0
1.5
1.0
0.5
ppm
1.00
1.02
0.91
2.01
1.88
4.10
0.94
2.18
2.55
2.20
0.93
2.73

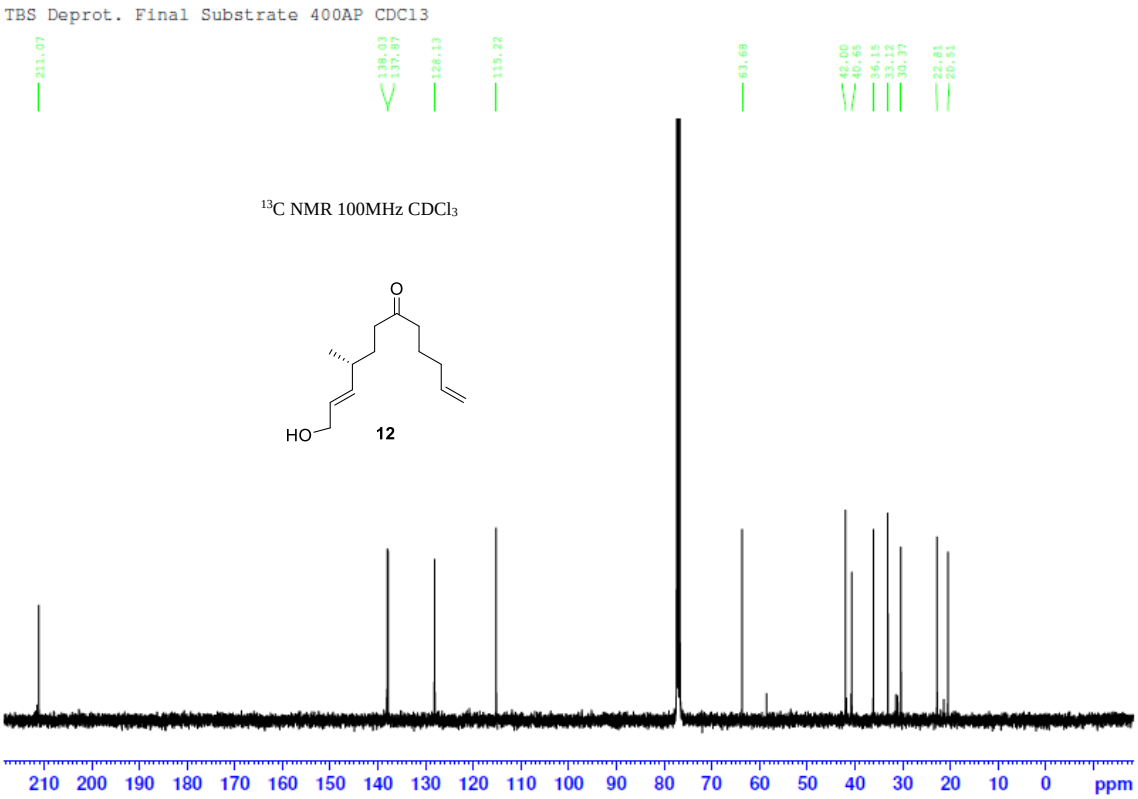
TBS Deprot. Final Substrate 400AP CDCl3
211.07
138.03
137.87
128.13
115.22
63.69
42.00
40.65
36.15
33.12
30.37
22.61
20.51
13C NMR 100MHz CDCl3
O
HO
12
210 200 190 180 170 160 150 140 130 120 110 100 90 80 70 60 50 40 30 20 10 0 ppm

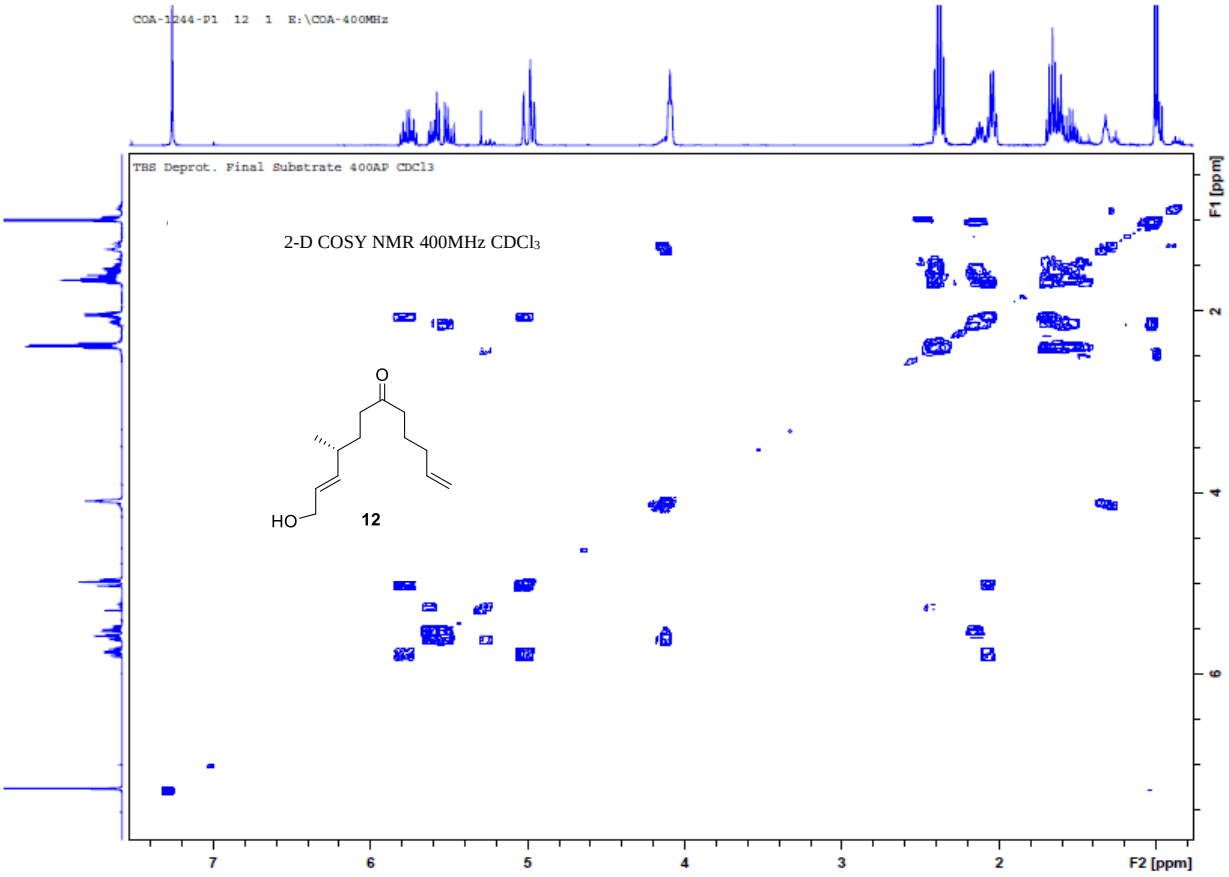
COA-1244-P1 12 1 E:\COA-400MHz
TBS Deprot. Final Substrate 400AP CDCl3
2-D COSY NMR 400MHz CDCl3
O
HO
12
F1 [ppm]
F2 [ppm]
2
4
6
7
5
4
3
2

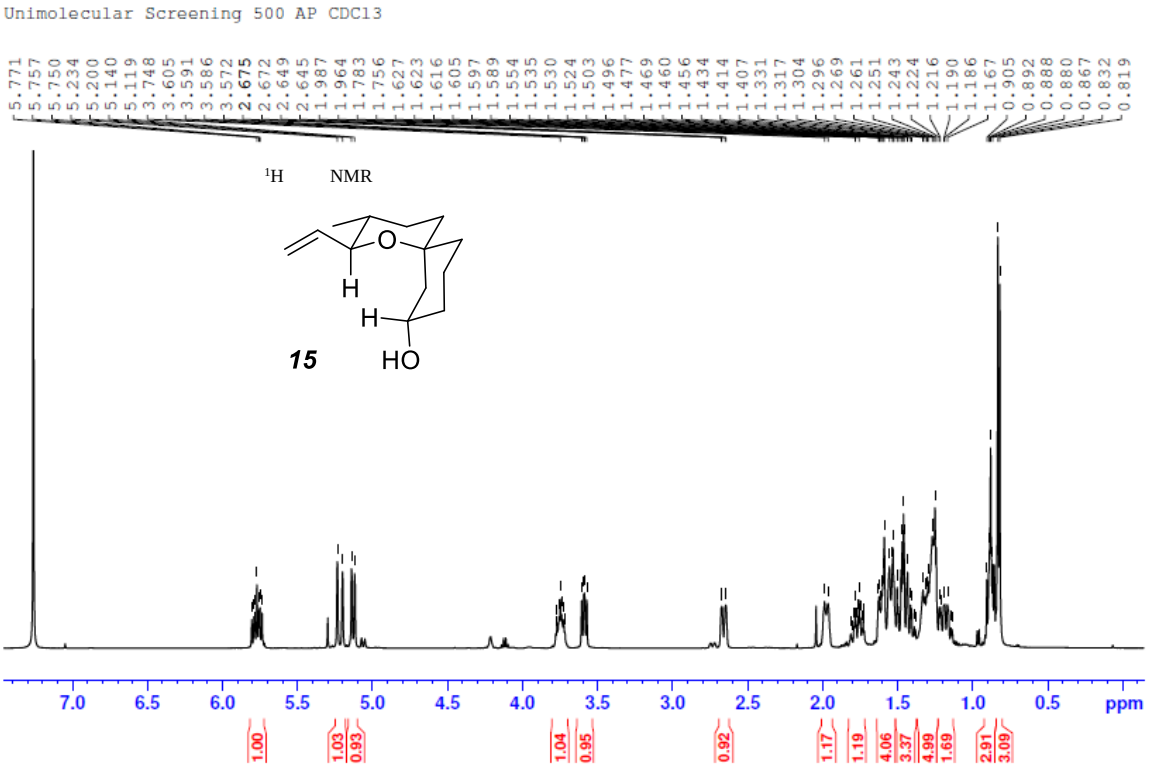
Unimolecular Screening 500 AP CDCl3
5.771 5.757 5.750 5.234 5.200 5.140 5.119 3.748 3.605 3.591 3.586 3.572 2.675 2.672 2.649 2.645 1.987 1.964 1.783 1.756 1.627 1.623 1.616 1.605 1.597 1.589 1.554 1.535 1.530 1.524 1.503 1.496 1.477 1.469 1.460 1.456 1.434 1.414 1.407 1.331 1.317 1.304 1.296 1.269 1.261 1.251 1.243 1.224 1.216 1.190 1.186 1.167 0.905 0.892 0.888 0.880 0.867 0.832 0.819
1H NMR
O
H
H
15
HO
7.0 6.5 6.0 5.5 5.0 4.5 4.0 3.5 3.0 2.5 2.0 1.5 1.0 0.5 ppm
1.00 1.03 0.93 1.04 0.95 0.92 1.17 1.19 4.06 3.37 4.99 1.69 2.91 3.09

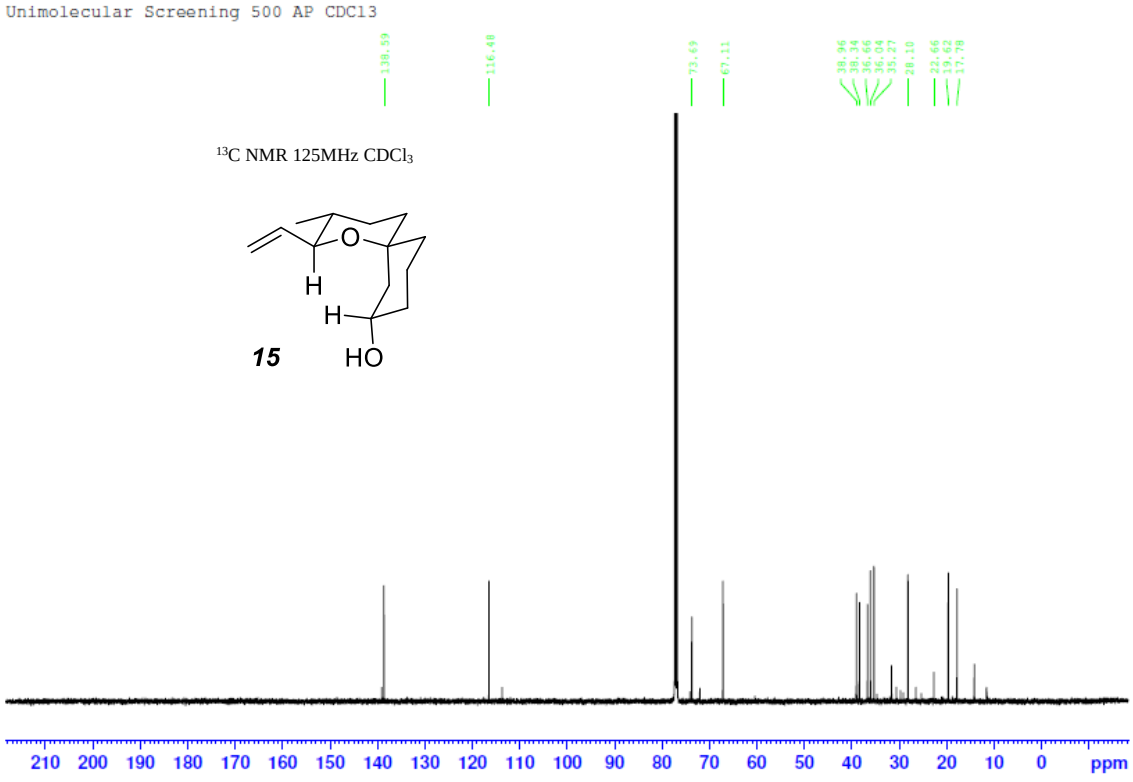
Unimolecular Screening 500 AP CDCl3
138.59 116.48 73.69 67.11 38.96 38.34 36.66 36.04 35.27 28.10 22.66 19.62 17.78
13C NMR 125MHz CDCl3
O
H
H
15
HO
210 200 190 180 170 160 150 140 130 120 110 100 90 80 70 60 50 40 30 20 10 0 ppm

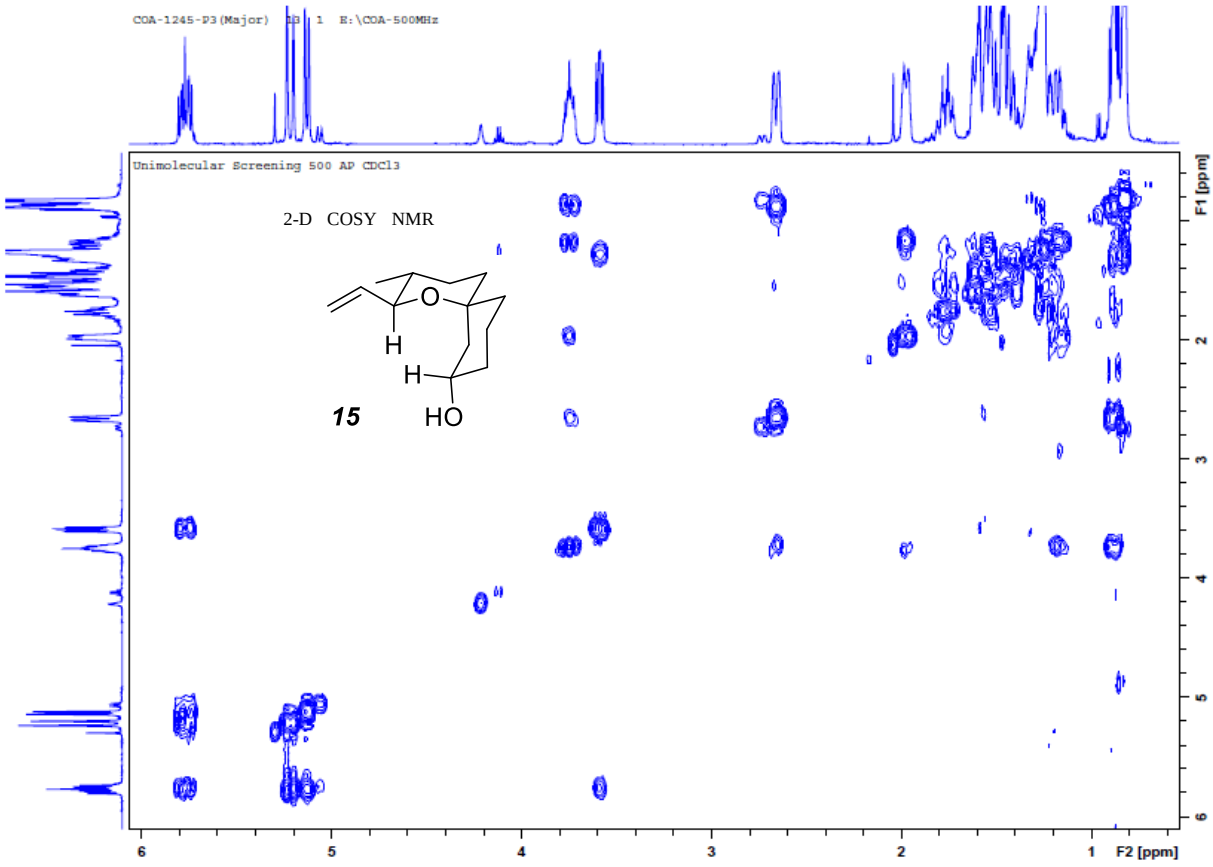
COA-1245-P3(Major) 2D 1 E:\COA-500MHz
Unimolecular Screening 500 AP CDCl3
2-D COSY NMR
O
H
H
15
HO
F1 [ppm]
F2 [ppm]
1
2
3
4
5
6

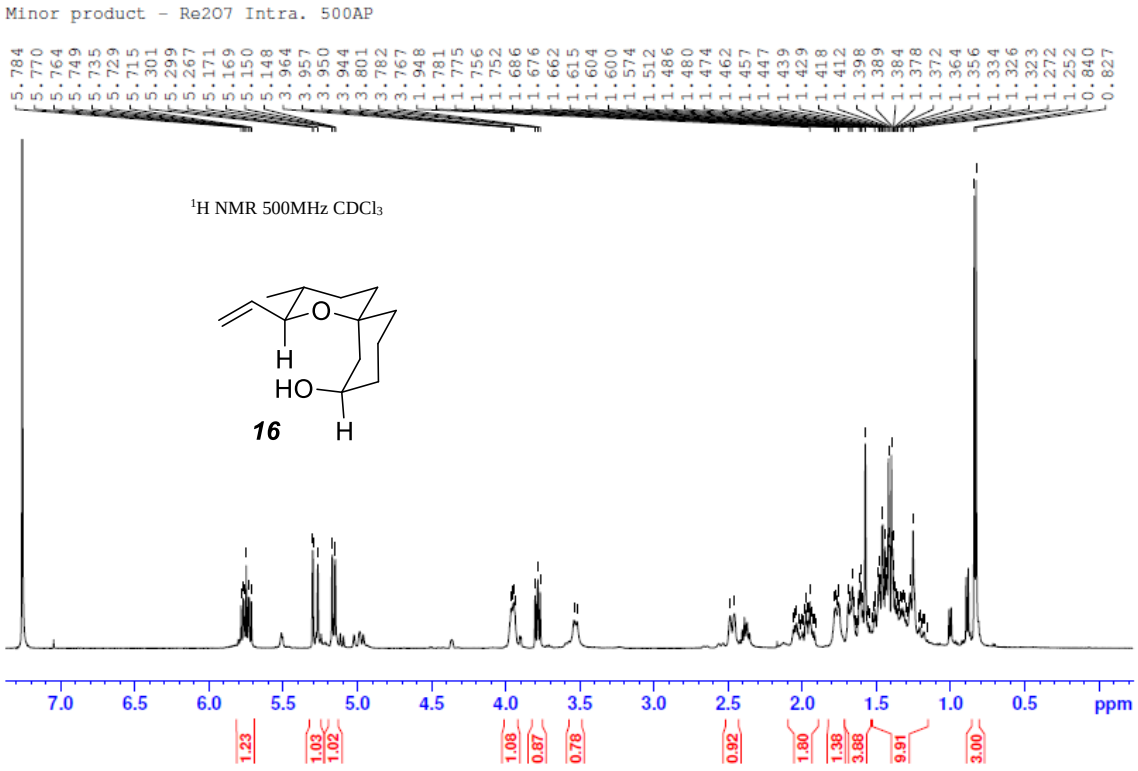
Minor product - Re207 Intra. 500AP
5.784 5.770 5.764 5.749 5.735 5.729 5.715 5.301 5.299 5.267 5.171 5.169 5.150 5.148 3.964 3.957 3.950 3.944 3.801 3.782 3.767 1.948 1.781 1.775 1.756 1.752 1.686 1.676 1.662 1.615 1.604 1.600 1.574 1.512 1.486 1.480 1.474 1.462 1.457 1.447 1.439 1.429 1.418 1.412 1.398 1.389 1.384 1.378 1.372 1.364 1.356 1.334 1.326 1.323 1.272 1.252 0.840 0.827
1H NMR 500MHz CDCl3
O
H
HO
16
H
7.0 6.5 6.0 5.5 5.0 4.5 4.0 3.5 3.0 2.5 2.0 1.5 1.0 0.5 ppm
1.23 1.03 1.02 1.08 0.87 0.78 0.92 1.80 1.38 3.88 9.91 3.00

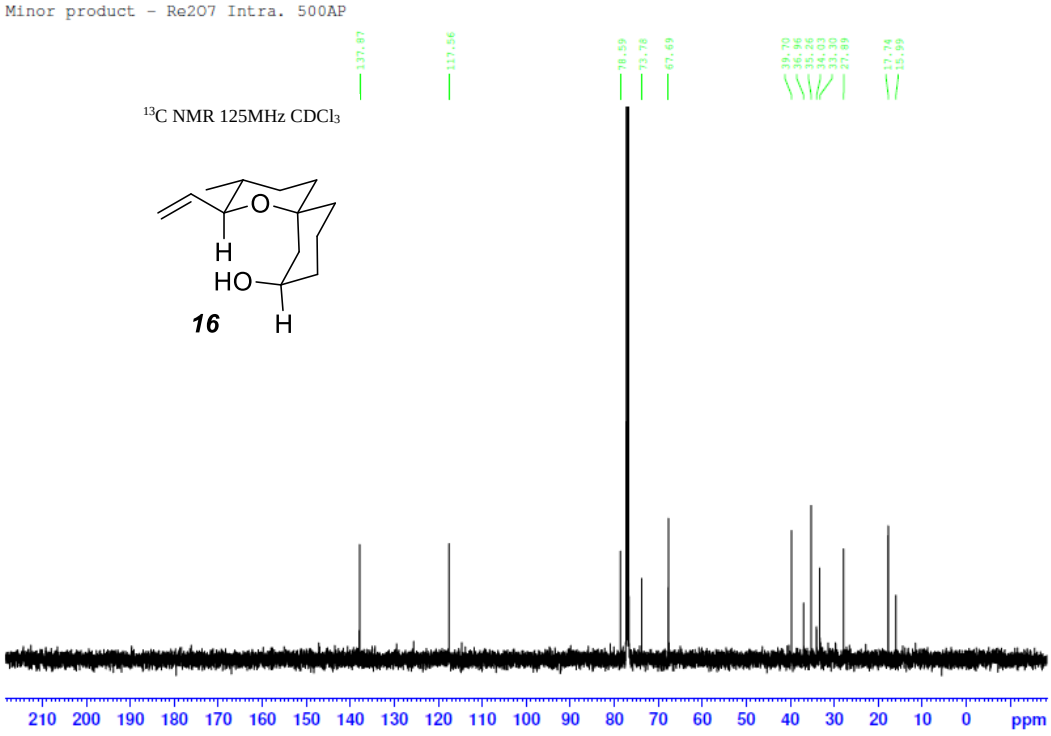
Minor product - Re207 Intra. 500AP
137.87 117.56 78.59 73.78 67.69 39.70 36.96 35.26 34.03 33.30 31.89 27.89 17.74 15.99
13C NMR 125MHz CDCl3
O
H
HO
16
H
210 200 190 180 170 160 150 140 130 120 110 100 90 80 70 60 50 40 30 20 10 0 ppm

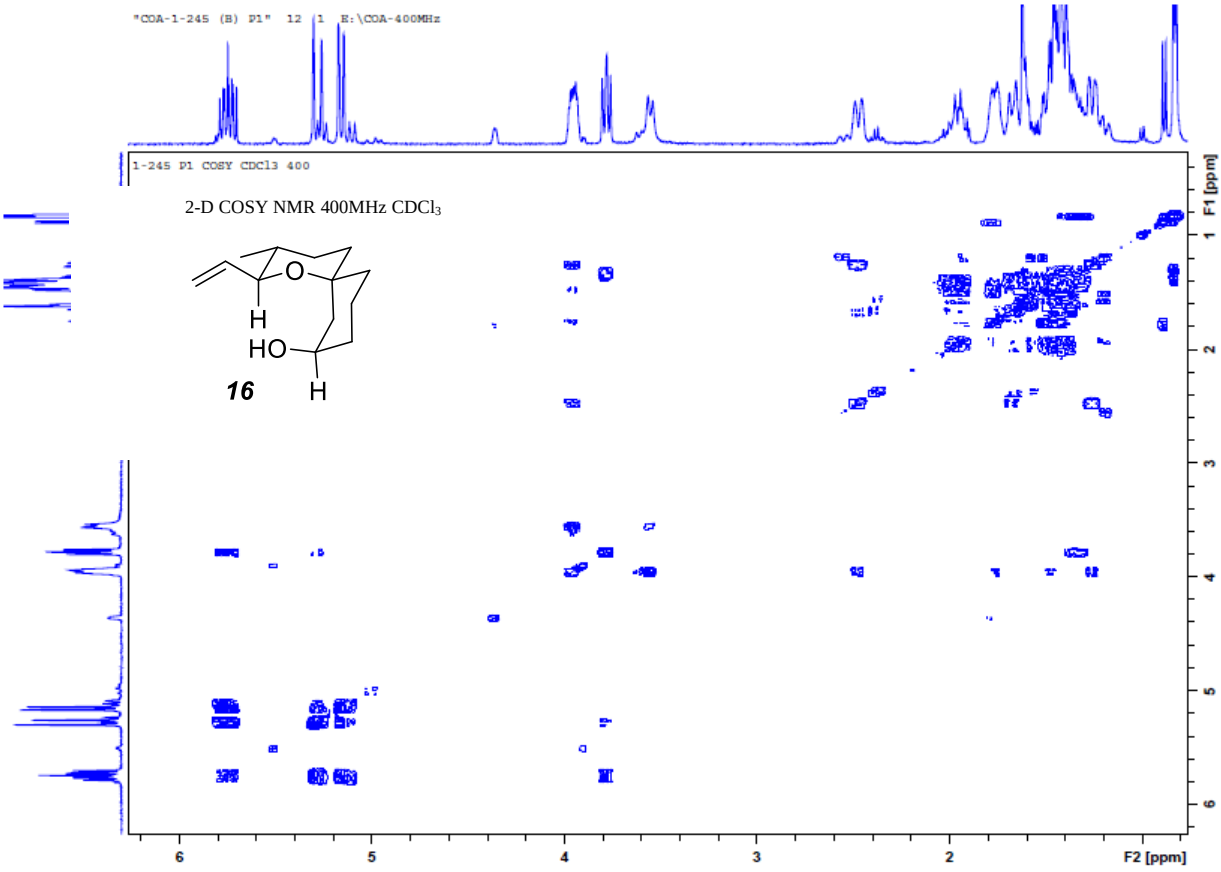
"COA-1-245 (B) P1" 12 1 E:\COA-400MHz
1-245 P1 COSY CDCl3 400
2-D COSY NMR 400MHz $CDCl_3$
O
H
HO
16
H
F1 [ppm]
F2 [ppm]
1
2
3
4
5
6

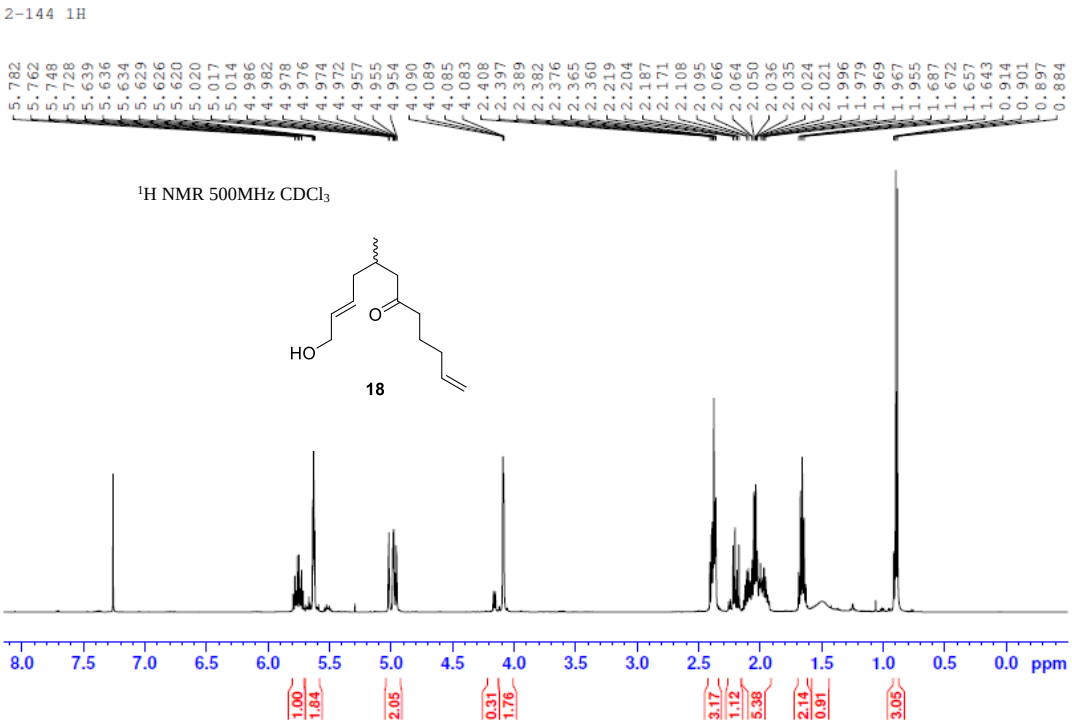
2-144 1H
5.782
5.762
5.748
5.728
5.639
5.636
5.634
5.629
5.626
5.620
5.020
5.017
5.014
4.986
4.982
4.978
4.976
4.974
4.972
4.957
4.955
4.954
4.090
4.089
4.085
4.083
2.408
2.397
2.389
2.382
2.376
2.365
2.360
2.219
2.204
2.187
2.171
2.108
2.095
2.066
2.064
2.050
2.036
2.035
2.024
2.021
1.996
1.979
1.969
1.967
1.955
1.687
1.672
1.657
1.643
0.914
0.901
0.897
0.884
1H NMR 500MHz CDCl3
HO
O
18
8.0
7.5
7.0
6.5
6.0
5.5
5.0
4.5
4.0
3.5
3.0
2.5
2.0
1.5
1.0
0.5
0.0
ppm
1.00
1.84
2.05
0.31
1.76
3.17
1.12
5.38
2.14
0.91
3.05

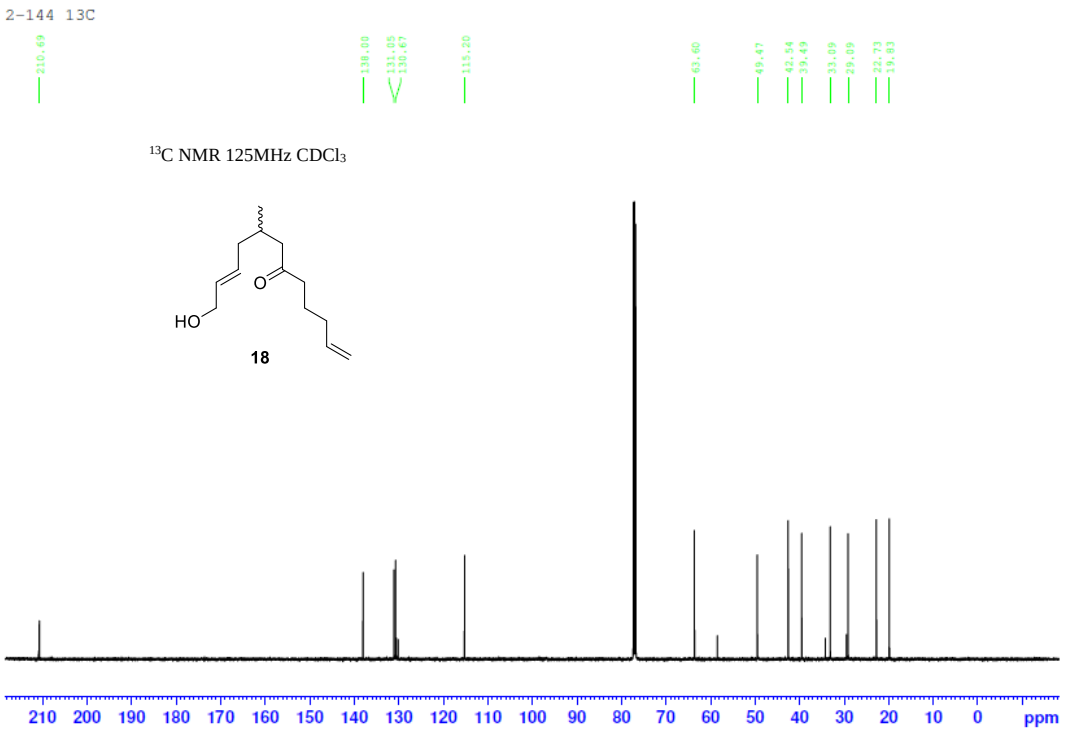

^{13}C NMR 125MHz $CDCl_3$

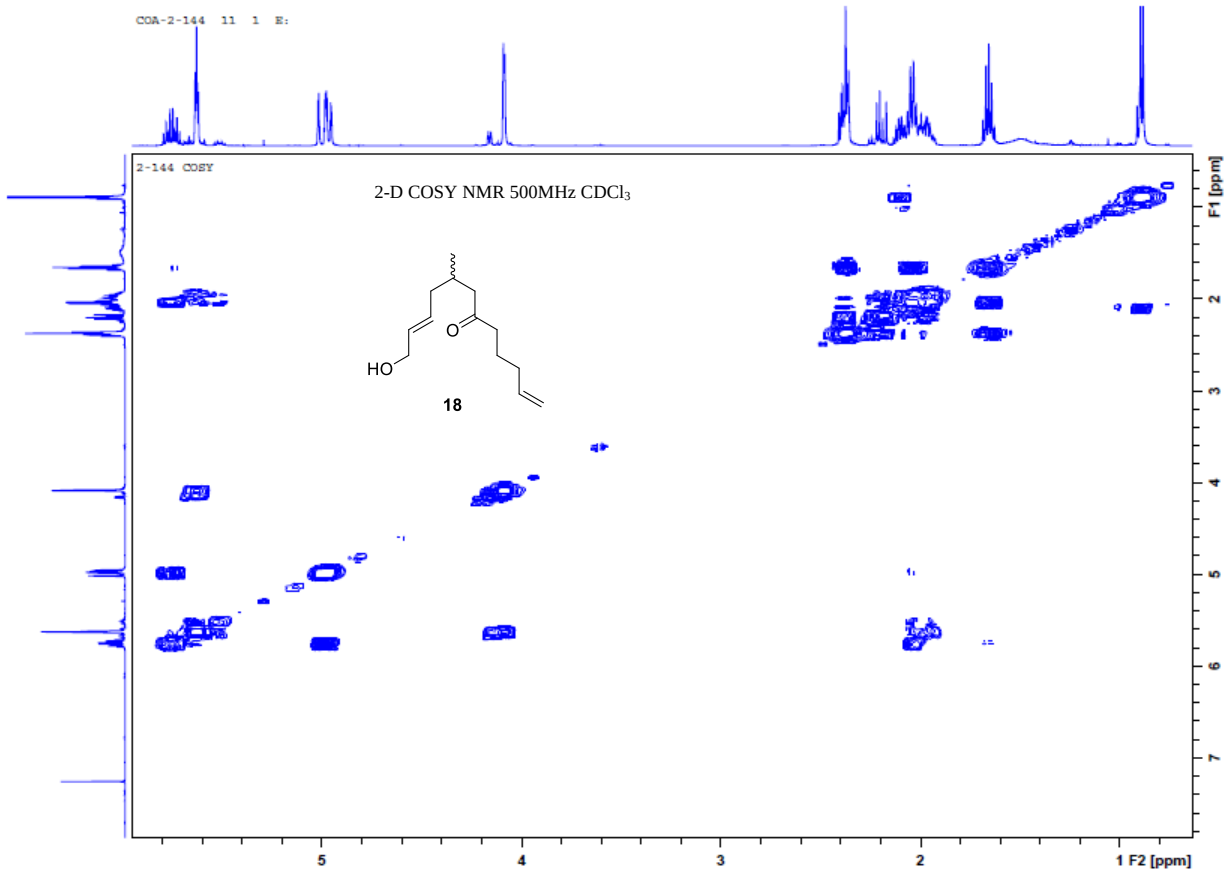
COA-2-144 11 1 E:
2-144 COSY
2-D COSY NMR 500MHz $CDCl_3$
HO
O
18
F1 [ppm]
1 F2 [ppm]

2-145 P2 1H

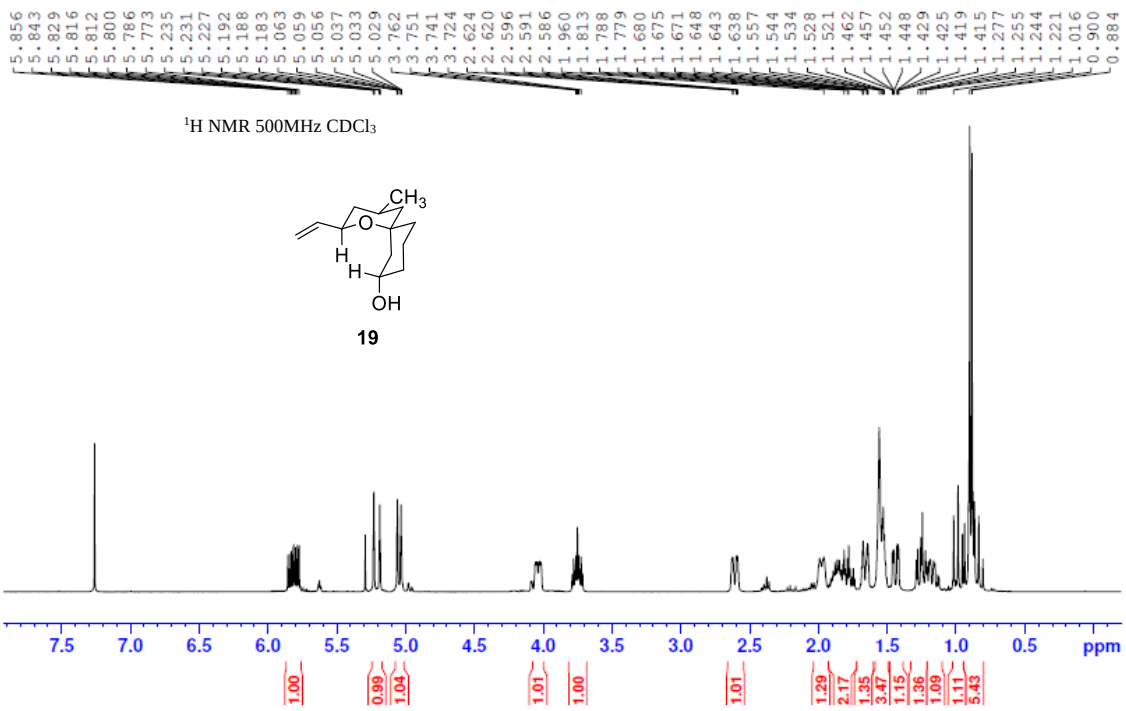

^{1}H NMR 500MHz $CDCl_3$

19

2-145 P2 13C

^{13}C NMR 125MHz $CDCl_3$

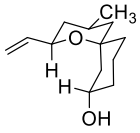

19

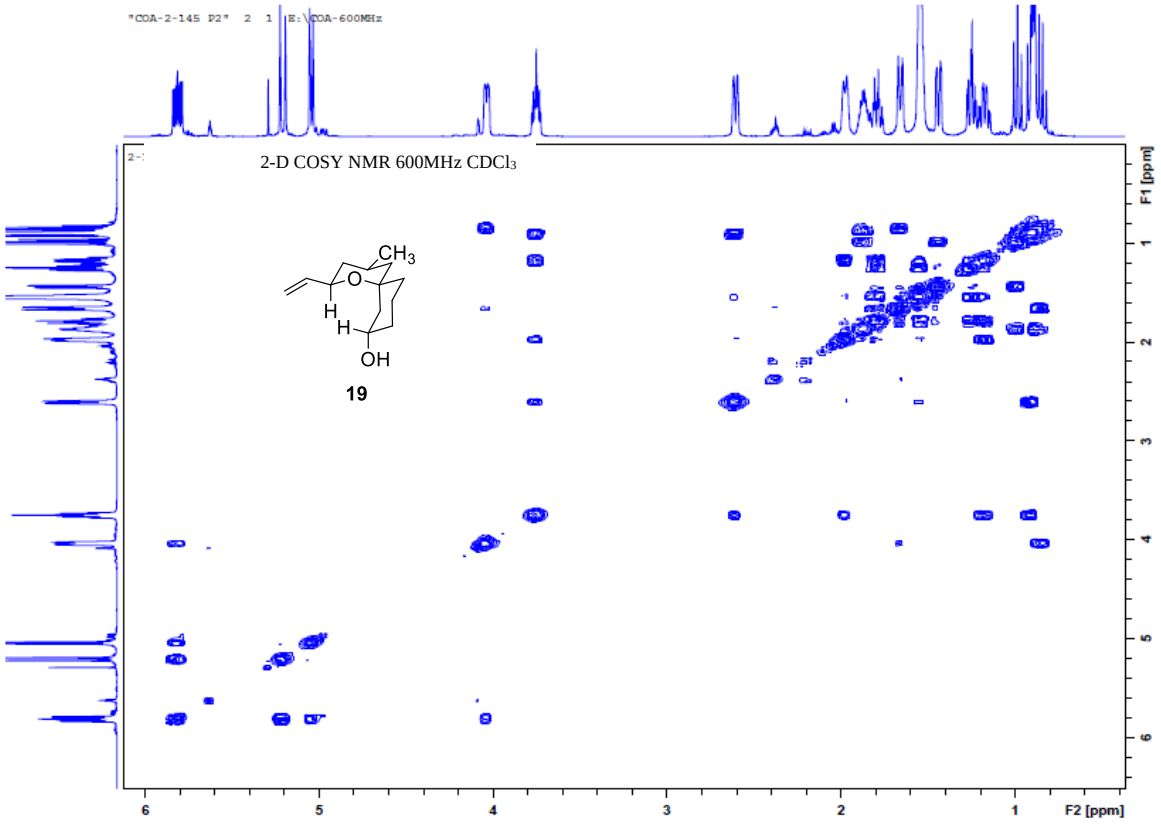
"COA-2-145 P2" 2 1 E:\COA-600MHz
2-D COSY NMR 600MHz CDCl3
CH3
O
H
H
OH
19
F1 [ppm]
F2 [ppm]
6
5
4
3
2
1

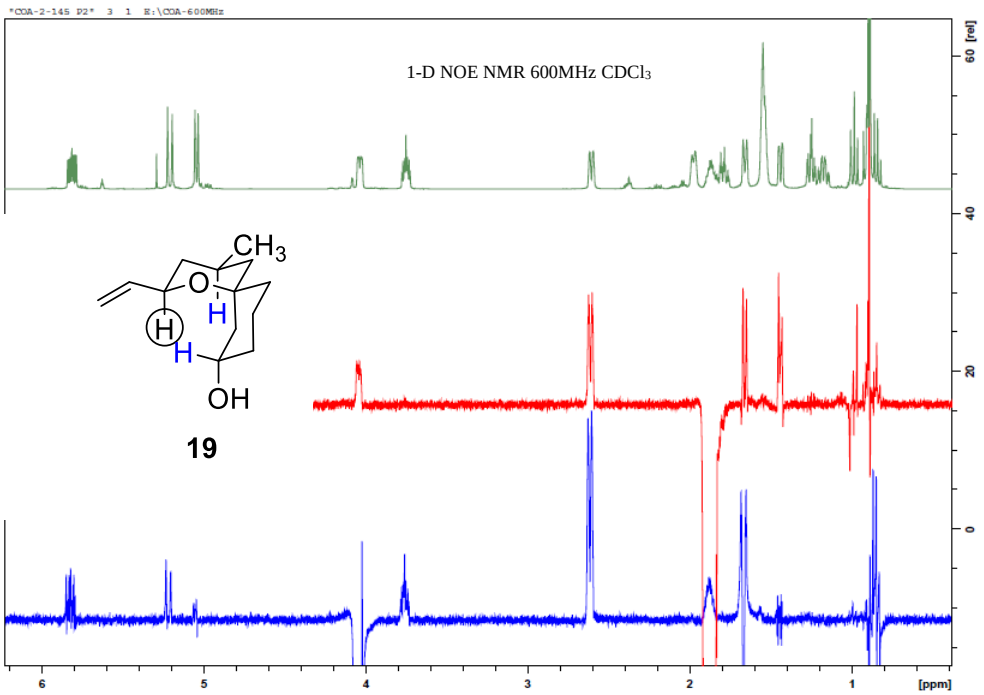
1-D NOE NMR 600MHz CDCl3
CH3
O
H
H
OH
19
[ppm]

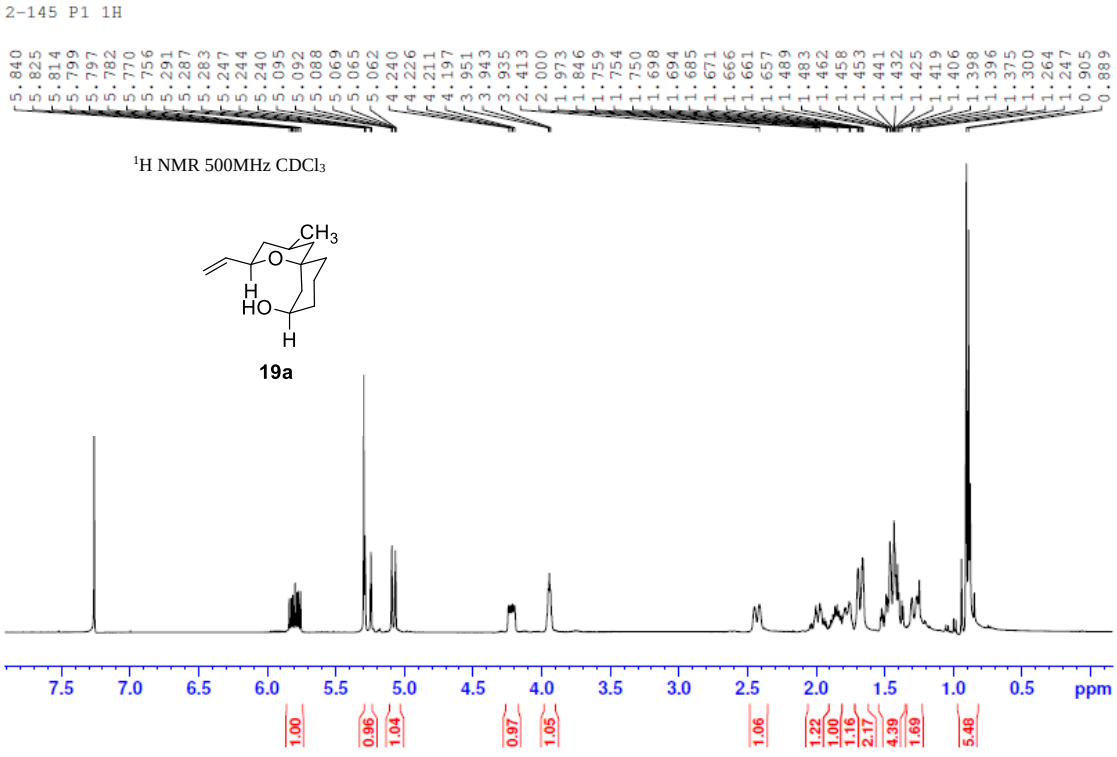
2-145 P1 1H
1H NMR 500MHz CDCl3
CH3
O
H
HO
H
19a
ppm

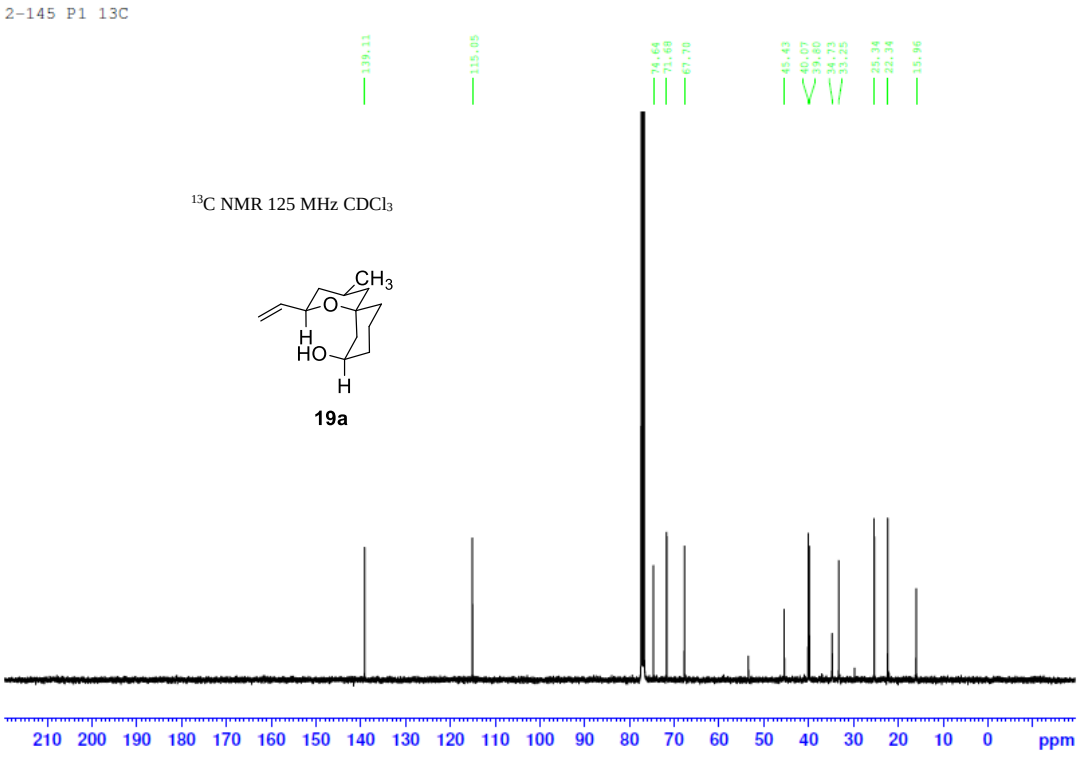

^{13}C NMR 125 MHz $CDCl_3$

19a

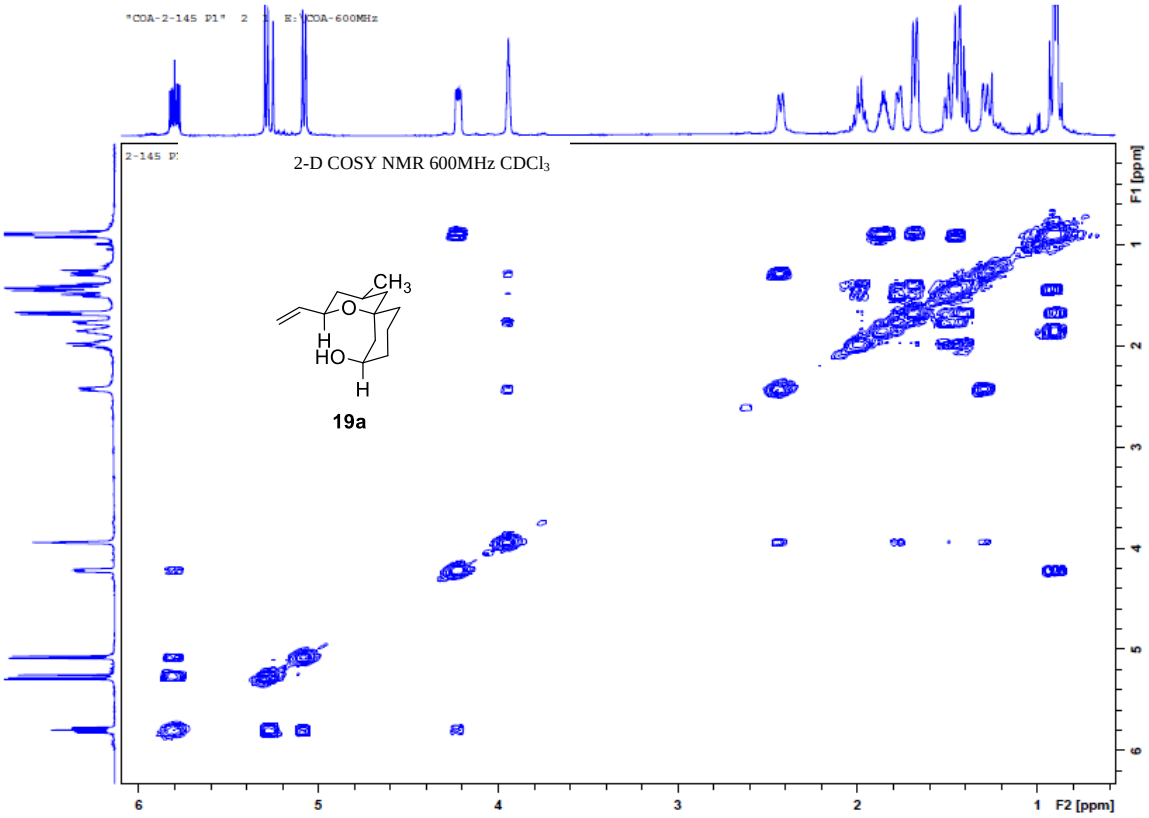

2-D COSY NMR 600MHz $CDCl_3$

19a

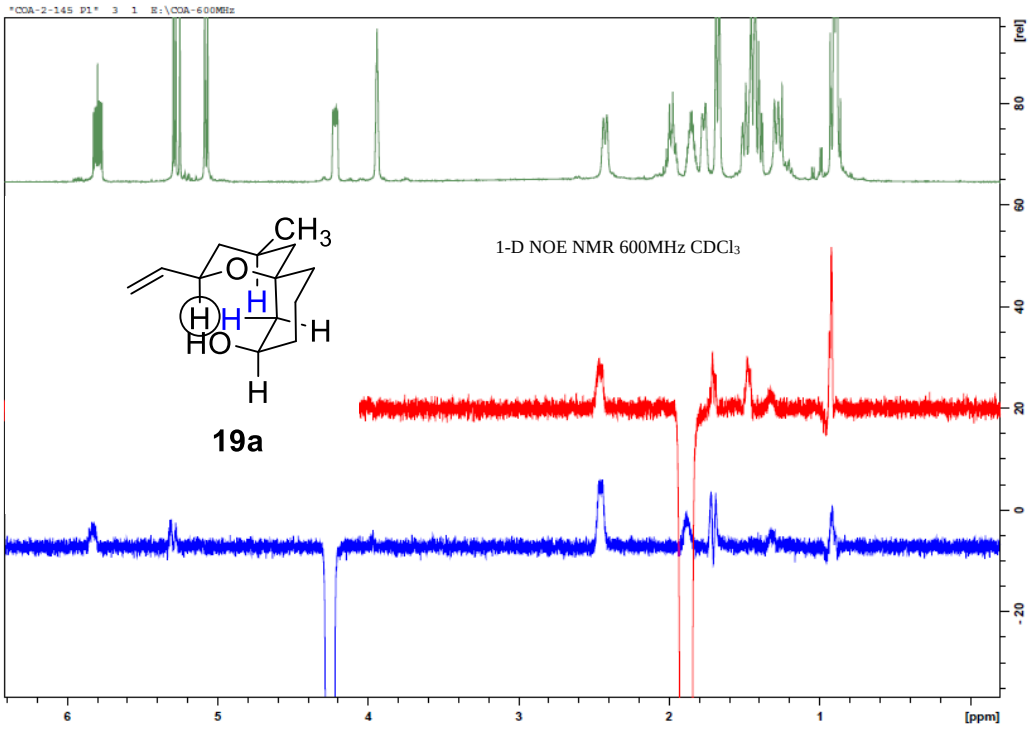
COA-2-145 P1 3 1 E:\COA-600MHz
[rel]
80
60
40
20
0
-20
CH3
O
H
H
H
HO
H
19a
1-D NOE NMR 600MHz CDCl3
6
5
4
3
2
1
[ppm]

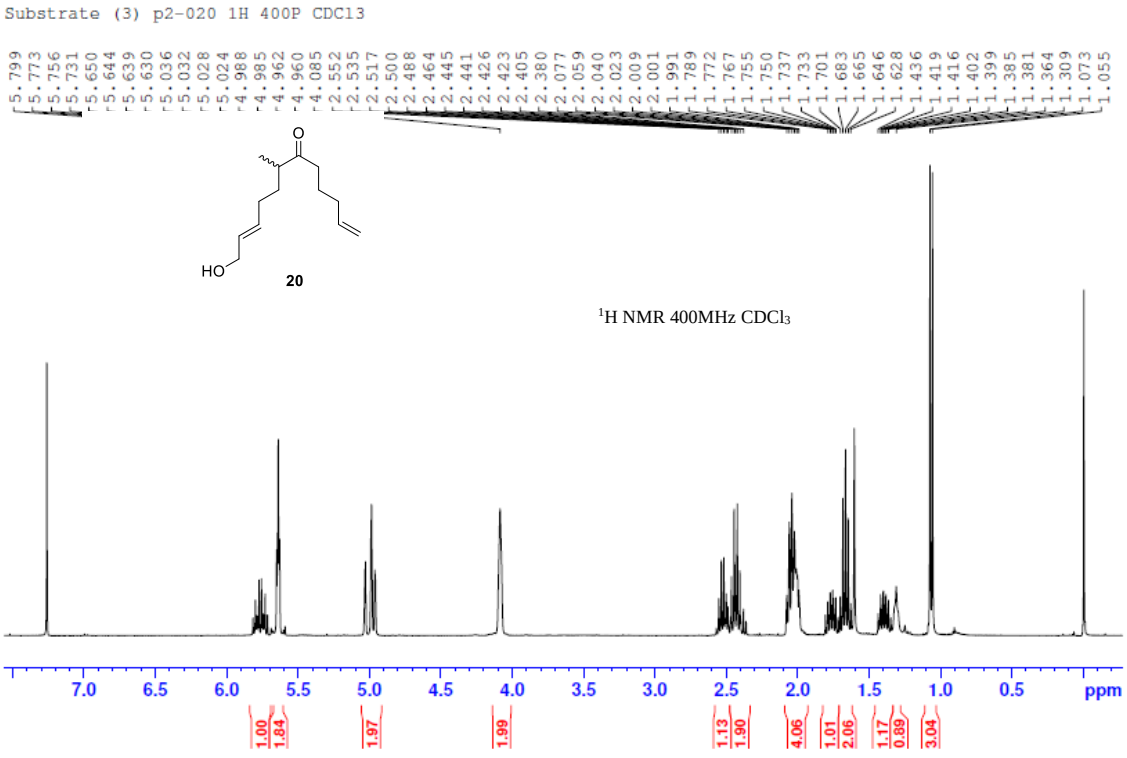
Substrate (3) p2-020 1H 400P CDC13
5.799
5.773
5.756
5.731
5.650
5.644
5.639
5.630
5.036
5.032
5.028
5.024
4.988
4.985
4.962
4.960
4.085
2.552
2.535
2.517
2.500
2.488
2.464
2.445
2.441
2.426
2.423
2.405
2.380
2.077
2.059
2.040
2.023
2.009
2.001
1.991
1.789
1.772
1.767
1.755
1.750
1.737
1.733
1.701
1.683
1.665
1.646
1.628
1.436
1.419
1.416
1.402
1.399
1.385
1.381
1.364
1.309
1.073
1.055
O
HO
20
1H NMR 400MHz CDCl3
7.0
6.5
6.0
5.5
5.0
4.5
4.0
3.5
3.0
2.5
2.0
1.5
1.0
0.5
ppm
1.00
1.84
1.97
1.99
1.13
1.90
4.06
1.01
2.06
1.17
0.89
3.04

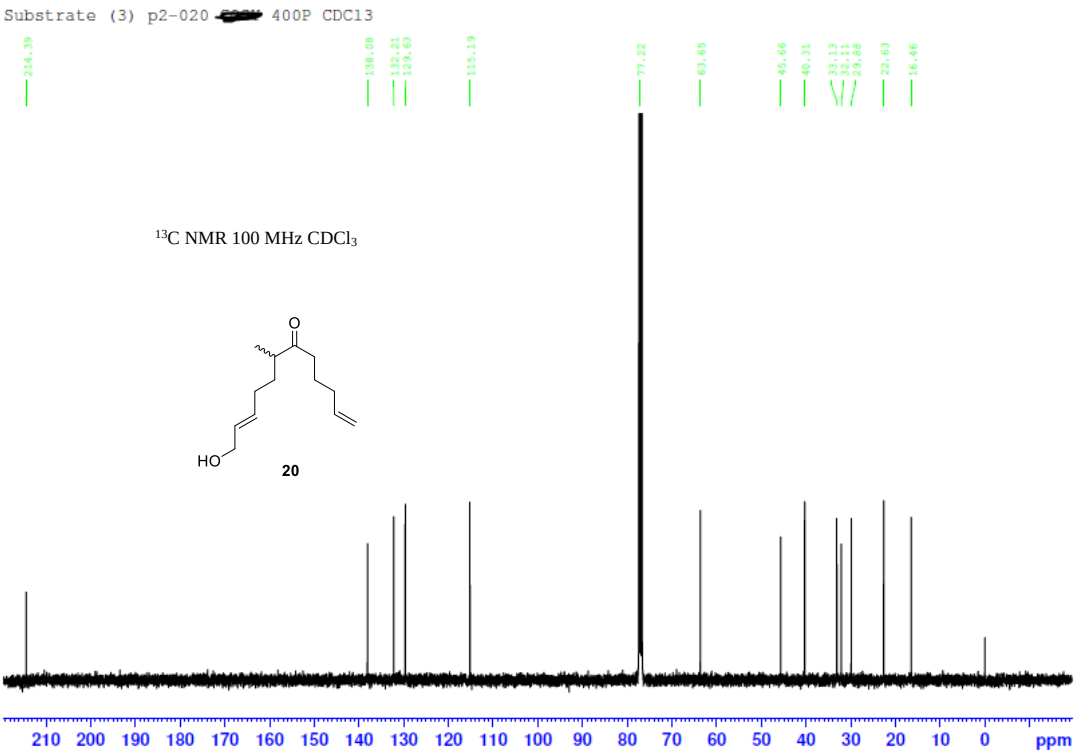
Substrate (3) p2-020 [redacted] 400P CDCl3
214.39
138.08
132.21
129.63
115.19
77.22
63.65
45.66
40.31
33.13
32.11
29.88
22.63
16.46
^{13}C NMR 100 MHz $CDCl_3$
O
HO
20
210 200 190 180 170 160 150 140 130 120 110 100 90 80 70 60 50 40 30 20 10 0 ppm

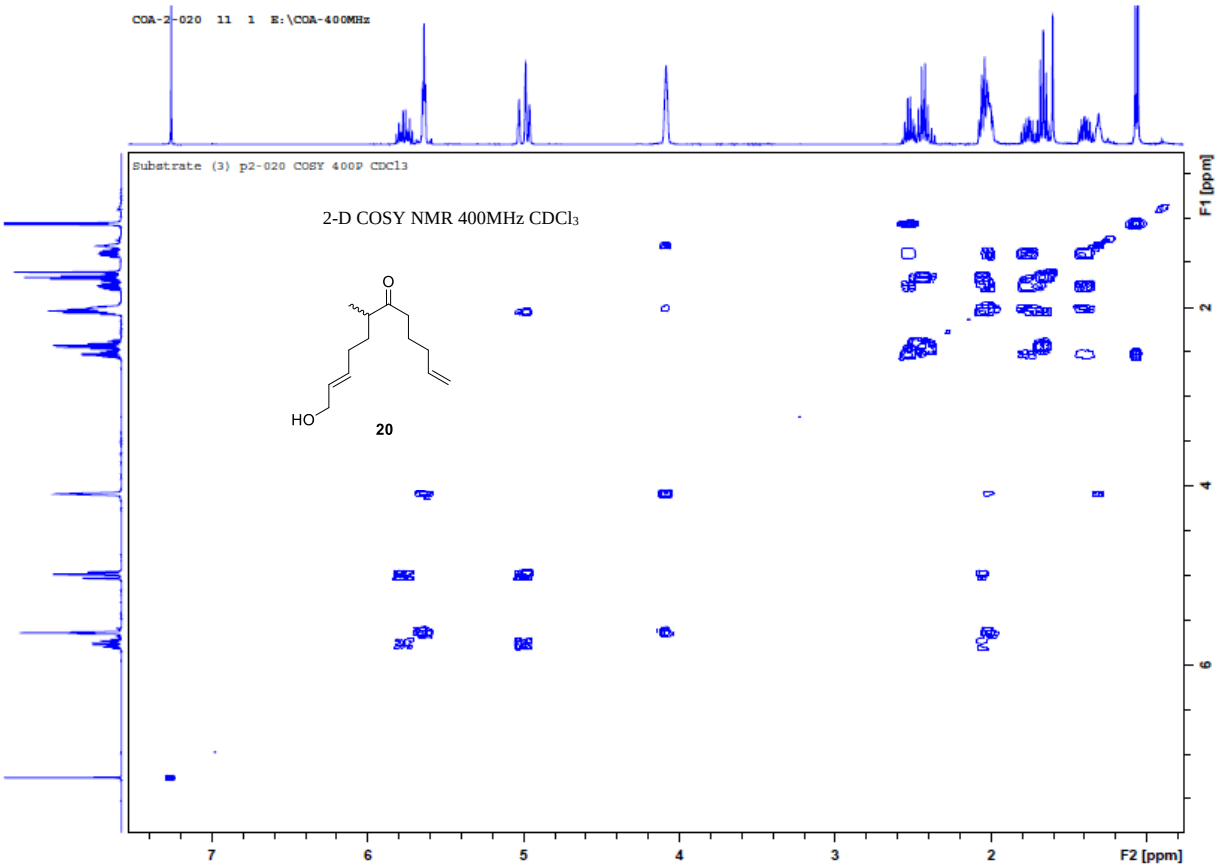
COA-2-020 11 1 E:\COA-400MHz
Substrate (3) p2-020 COSY 400P CDCl3
2-D COSY NMR 400MHz CDCl3
O
HO
20
F1 [ppm]
F2 [ppm]
2
4
6
7
5
3

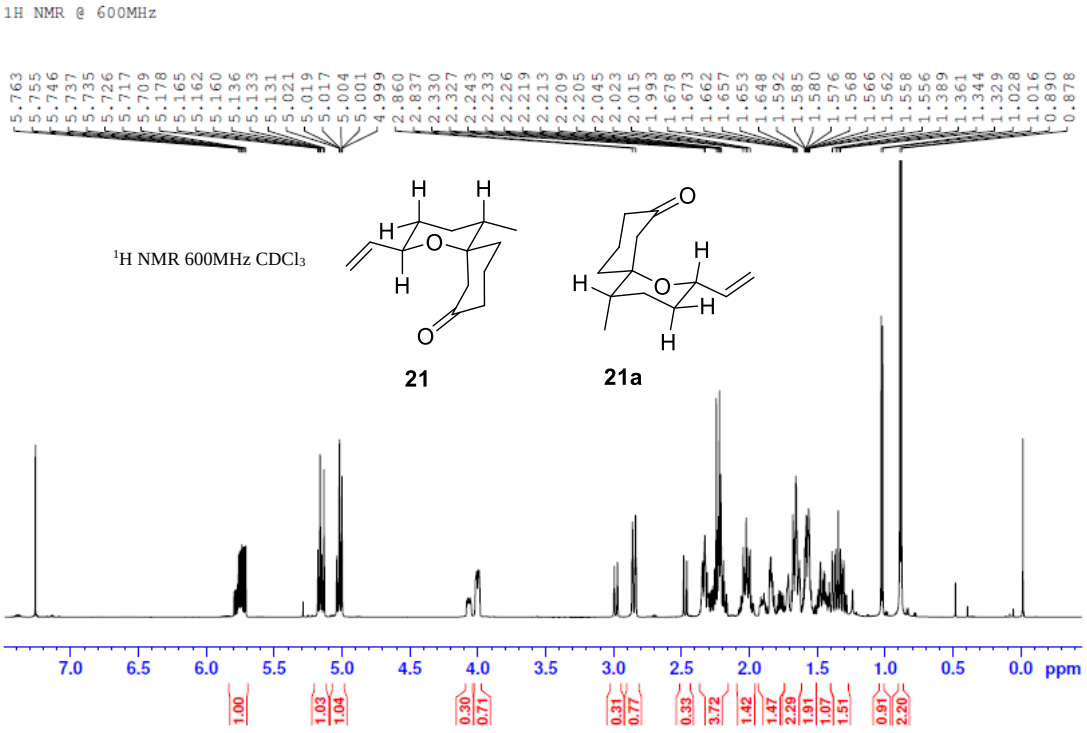
1H NMR @ 600MHz
5.763 5.755 5.746 5.737 5.735 5.726 5.717 5.709 5.178 5.165 5.162 5.160 5.136 5.133 5.131 5.021 5.019 5.017 5.004 5.001 4.999 2.860 2.837 2.330 2.327 2.243 2.233 2.226 2.219 2.213 2.209 2.205 2.045 2.023 2.015 1.993 1.678 1.673 1.662 1.657 1.653 1.648 1.592 1.585 1.580 1.576 1.568 1.566 1.562 1.558 1.556 1.389 1.361 1.344 1.329 1.028 1.016 0.890 0.878
1H NMR 600MHz CDCl3
21
21a
7.0 6.5 6.0 5.5 5.0 4.5 4.0 3.5 3.0 2.5 2.0 1.5 1.0 0.5 0.0 ppm
1.00 1.03 1.04 0.30 0.71 0.31 0.77 0.33 3.72 1.42 1.47 2.29 1.91 1.07 1.51 0.91 2.20

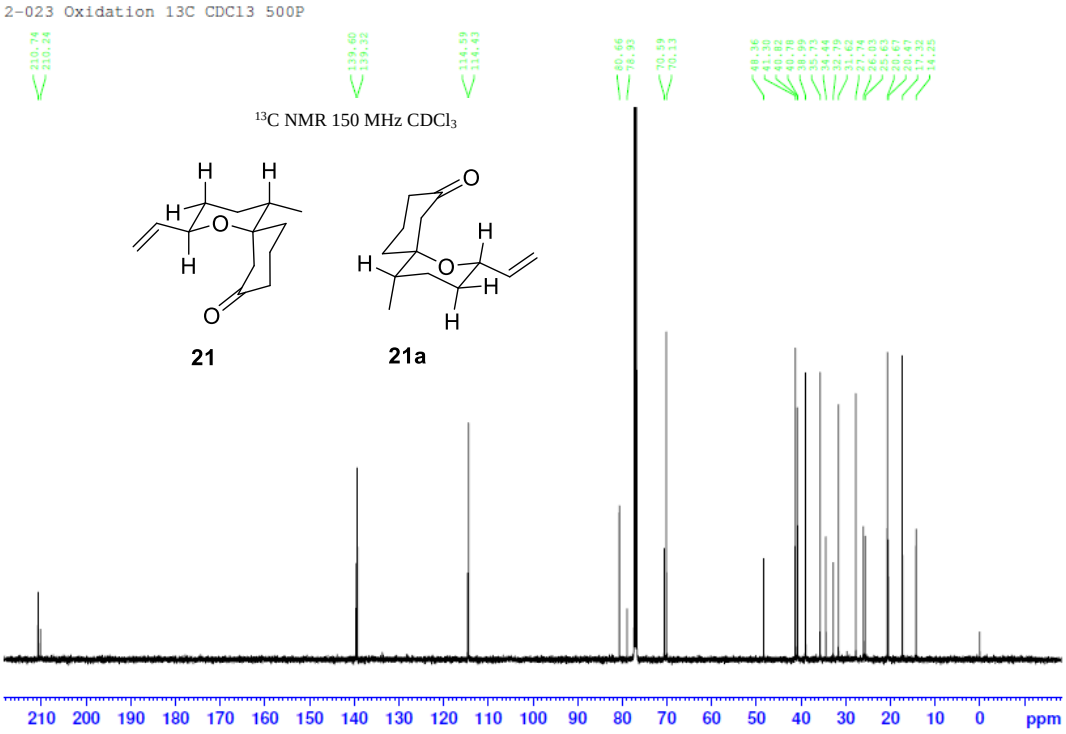
2-023 Oxidation 13C CDCl3 500P
210.74 210.24 139.60 139.32 114.59 114.43 80.66 78.93 70.59 70.13 48.36 41.30 40.82 40.78 38.99 35.73 34.44 32.79 32.62 27.74 26.03 25.63 20.67 20.47 17.32 14.26
13C NMR 150 MHz CDCl3
21
21a
210 200 190 180 170 160 150 140 130 120 110 100 90 80 70 60 50 40 30 20 10 0 ppm

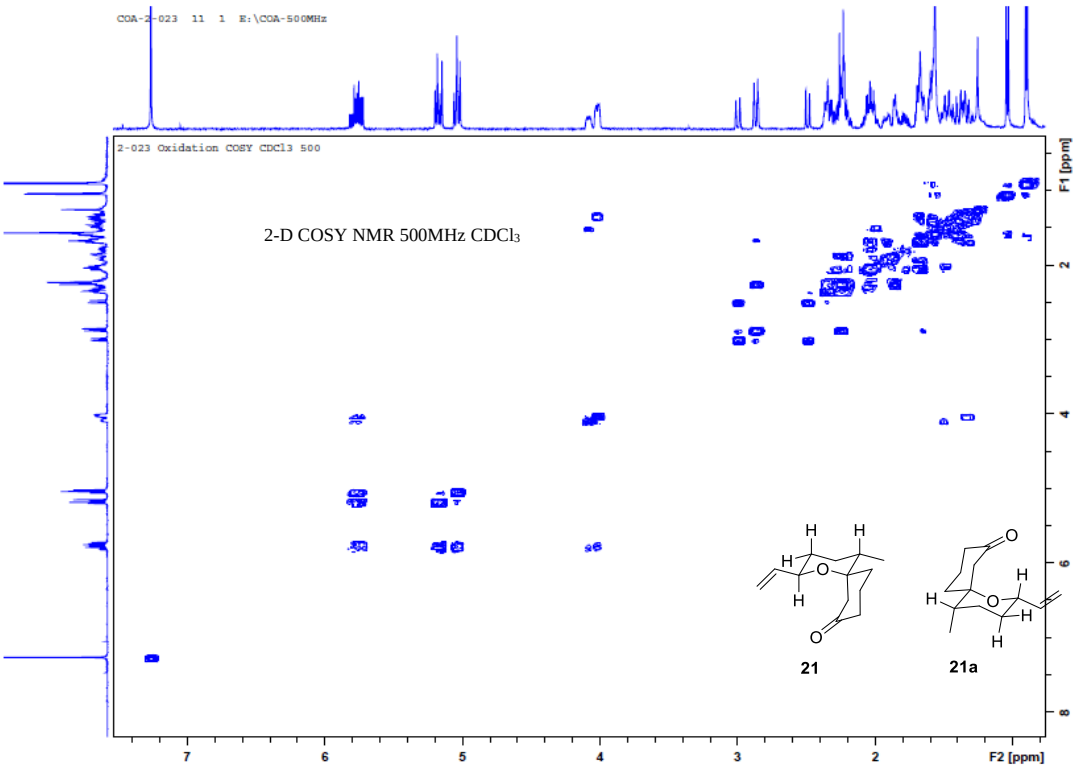

2-D COSY NMR 500MHz $CDCl_3$

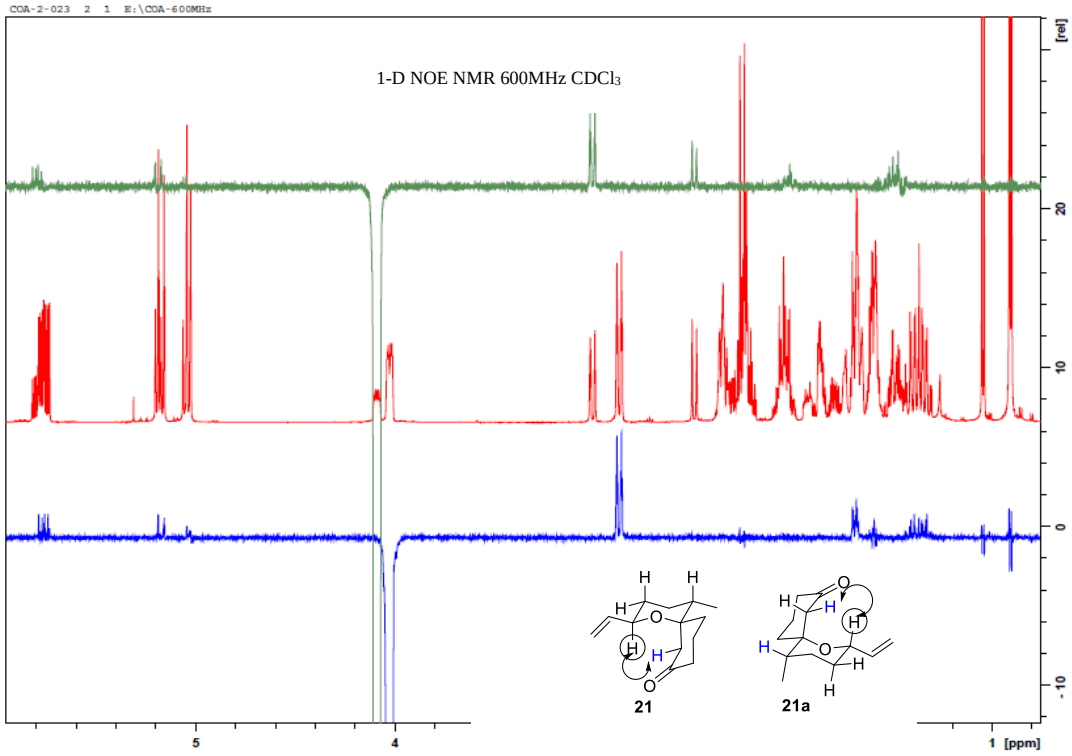

1-D NOE NMR 600MHz $CDCl_3$

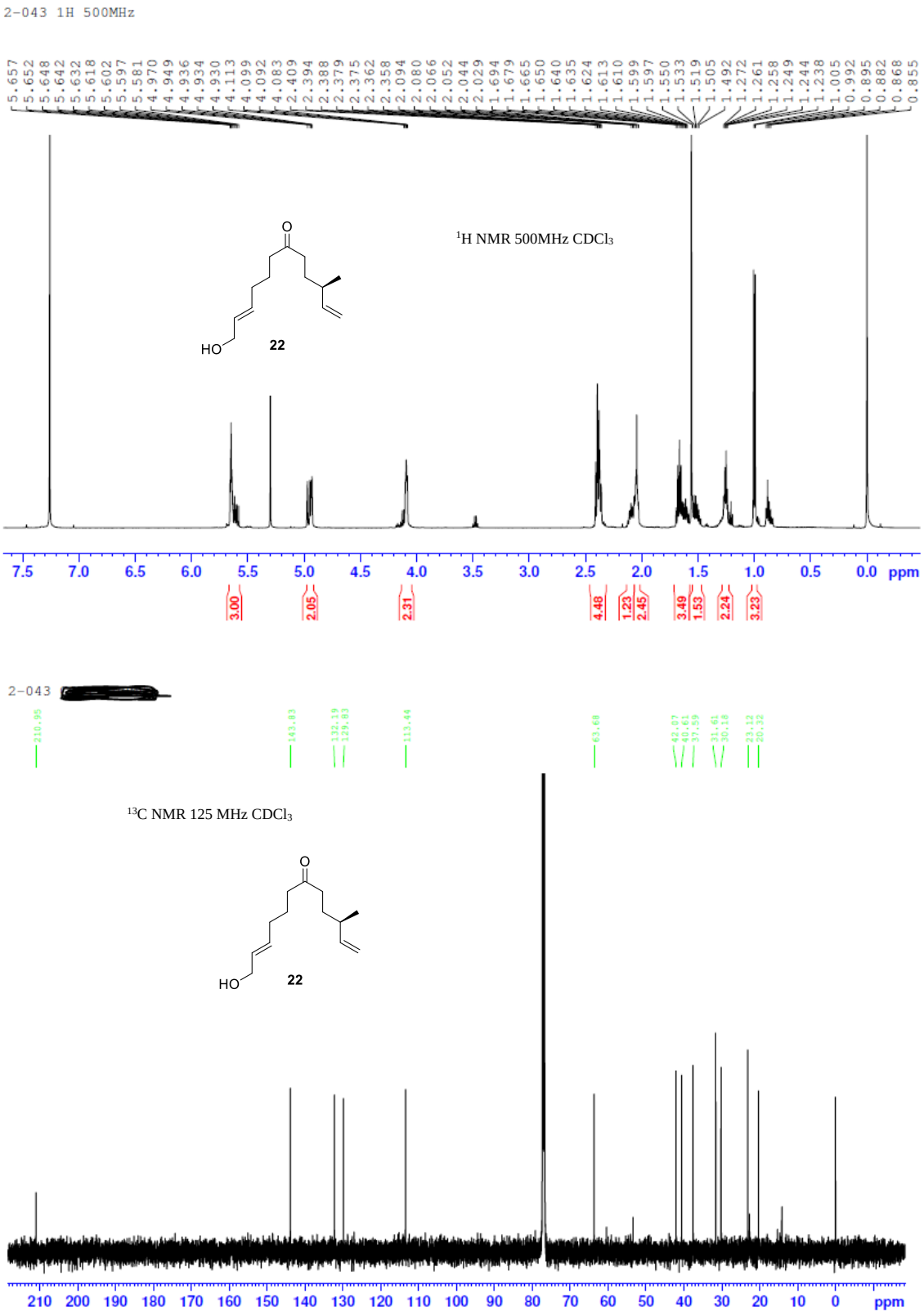
2-043 1H 500MHz
5.657
5.652
5.648
5.642
5.632
5.618
5.602
5.597
5.581
4.970
4.949
4.936
4.934
4.930
4.113
4.099
4.092
4.083
2.409
2.394
2.388
2.379
2.375
2.362
2.358
2.094
2.080
2.066
2.052
2.044
2.029
1.694
1.679
1.665
1.650
1.640
1.635
1.624
1.613
1.610
1.599
1.597
1.550
1.533
1.519
1.505
1.492
1.272
1.261
1.258
1.249
1.244
1.238
1.005
0.992
0.895
0.882
0.868
0.855
O
HO
22
1H NMR 500MHz CDCl3
7.5
7.0
6.5
6.0
5.5
5.0
4.5
4.0
3.5
3.0
2.5
2.0
1.5
1.0
0.5
0.0
ppm
3.00
2.05
2.31
4.48
1.23
2.45
3.49
1.53
2.24
3.23
2-043
210.95
143.83
132.19
129.83
113.44
63.68
42.07
40.61
37.99
31.61
30.18
23.12
20.32
13C NMR 125 MHz CDCl3
O
HO
22
210
200
190
180
170
160
150
140
130
120
110
100
90
80
70
60
50
40
30
20
10
0
ppm

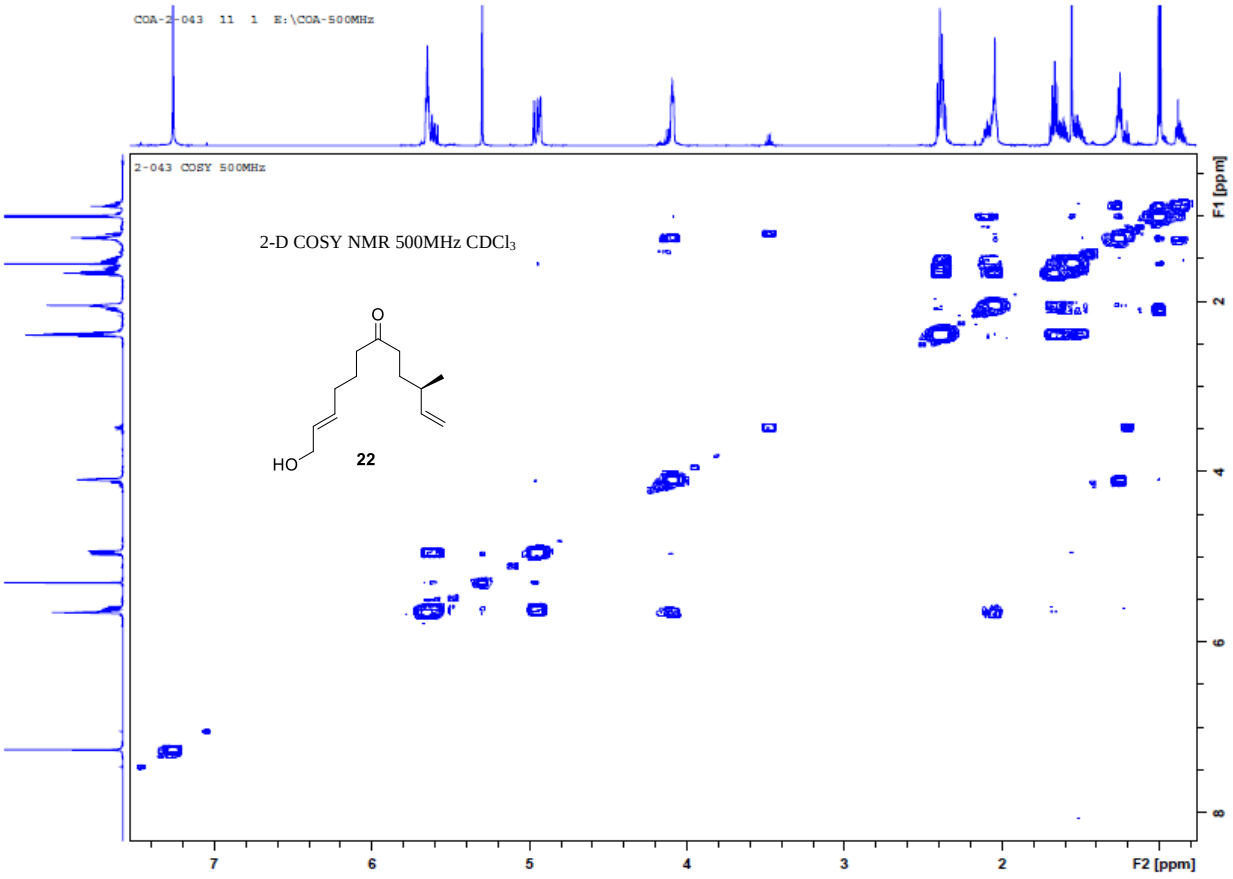
COA-2-043 11 1 E:\COA-500MHz
2-043 COSY 500MHz
2-D COSY NMR 500MHz CDCl3
O
HO
22
F1 [ppm]
F2 [ppm]
2
4
6
8
7
6
5
4
3
2

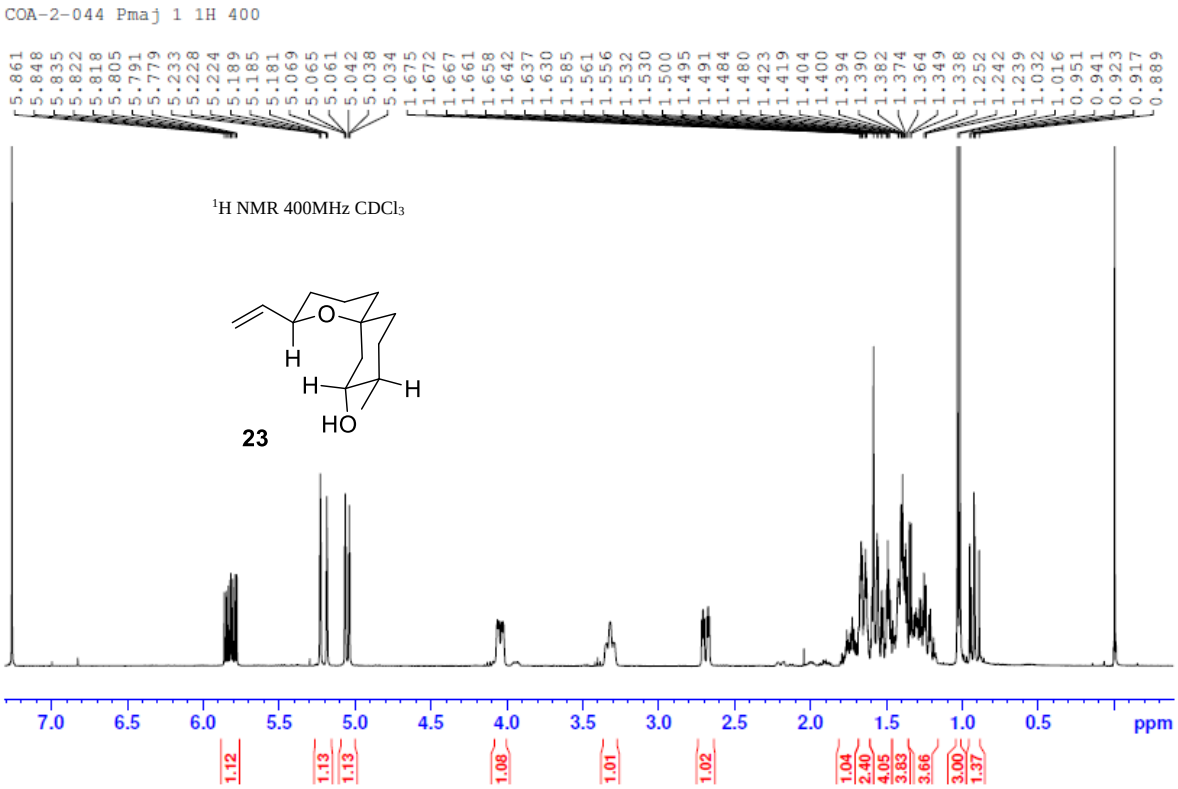
COA-2-044 Pmaj 1 1H 400
5.861
5.848
5.835
5.822
5.818
5.805
5.791
5.779
5.233
5.228
5.224
5.189
5.185
5.181
5.069
5.065
5.061
5.042
5.038
5.034
1.675
1.672
1.667
1.661
1.658
1.642
1.637
1.630
1.585
1.561
1.556
1.532
1.530
1.500
1.495
1.491
1.484
1.480
1.423
1.419
1.404
1.400
1.394
1.390
1.382
1.374
1.364
1.349
1.338
1.252
1.242
1.239
1.032
1.016
0.951
0.941
0.923
0.917
0.889
^{1}H NMR 400MHz $CDCl_3$
O
H
H
H
HO
23
7.0
6.5
6.0
5.5
5.0
4.5
4.0
3.5
3.0
2.5
2.0
1.5
1.0
0.5
ppm
1.12
1.13
1.13
1.08
1.01
1.02
1.04
2.40
4.05
3.83
3.66
3.00
1.37

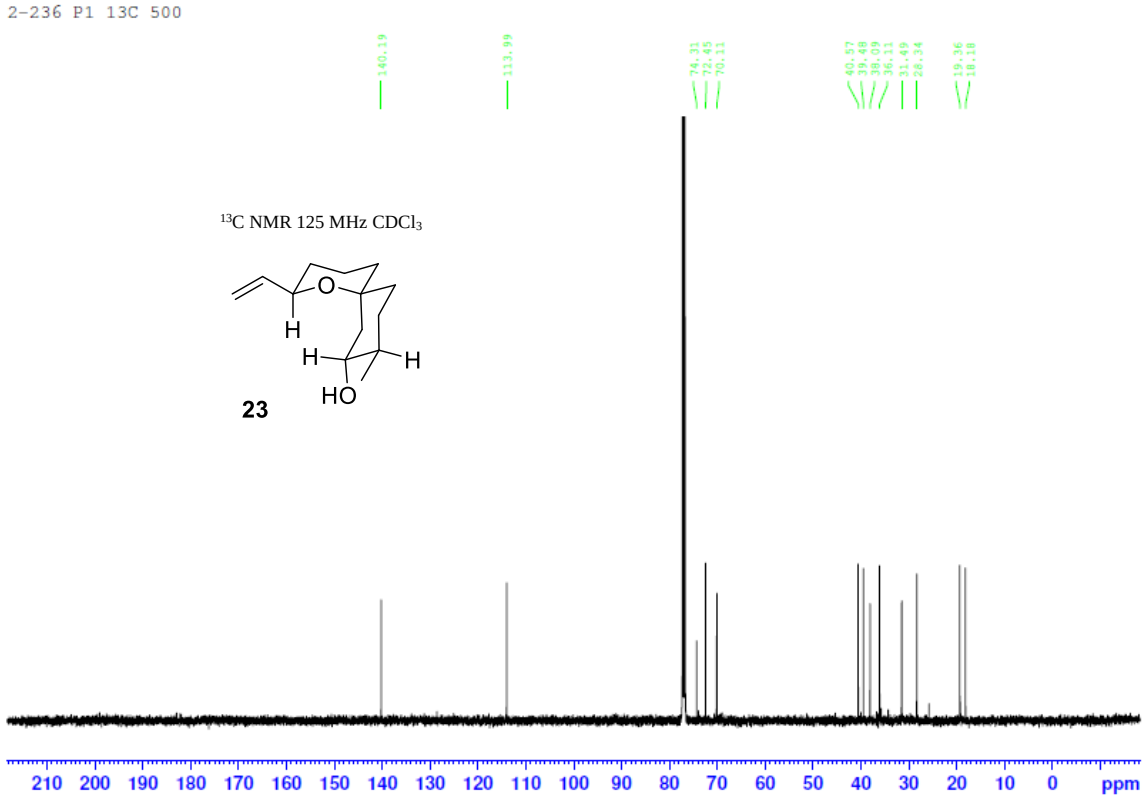
2-236 P1 13C 500
140.19
113.99
74.31
72.45
70.11
40.57
39.68
39.09
36.11
31.49
28.34
19.36
18.18
^{13}C NMR 125 MHz $CDCl_3$
O
H
H
H
HO
23
210
200
190
180
170
160
150
140
130
120
110
100
90
80
70
60
50
40
30
20
10
0
ppm

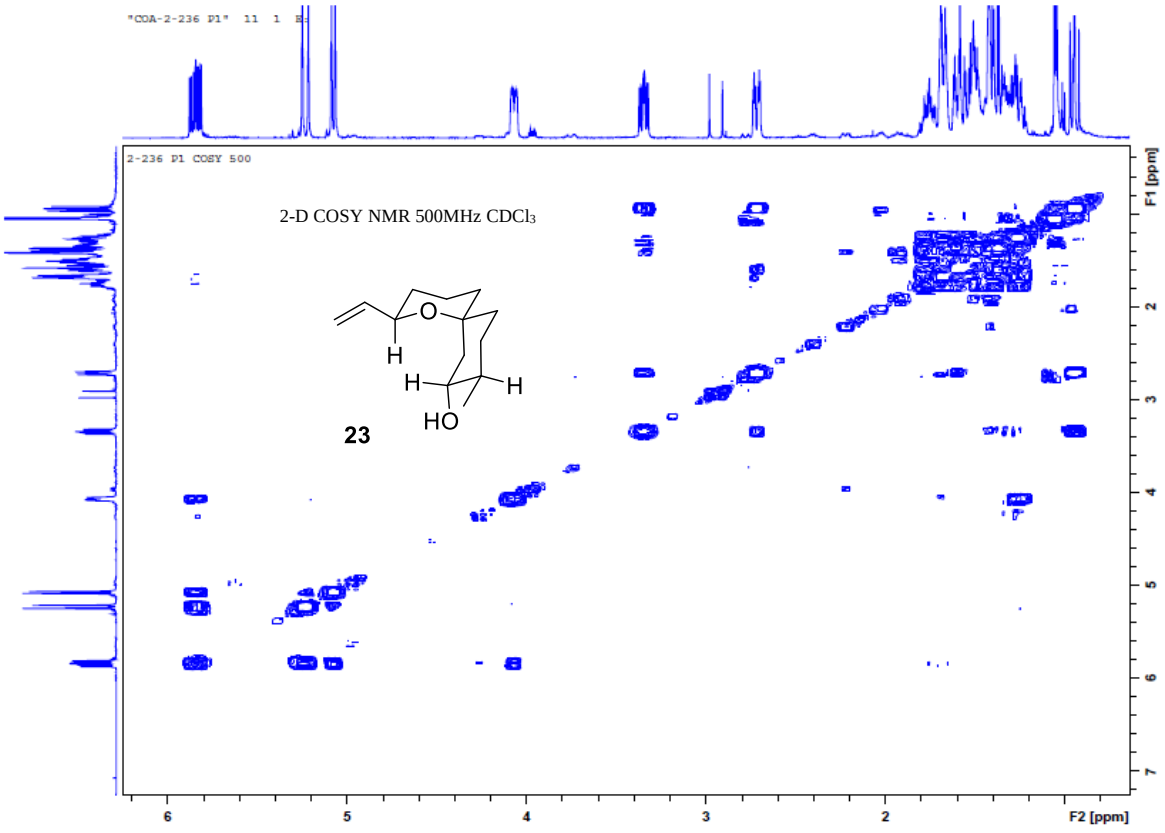
"COA-2-236 P1" 11 1
2-236 P1 COSY 500
2-D COSY NMR 500MHz $CDCl_3$
O
H
H
H
HO
23
F1 [ppm]
F2 [ppm]
6
5
4
3
2

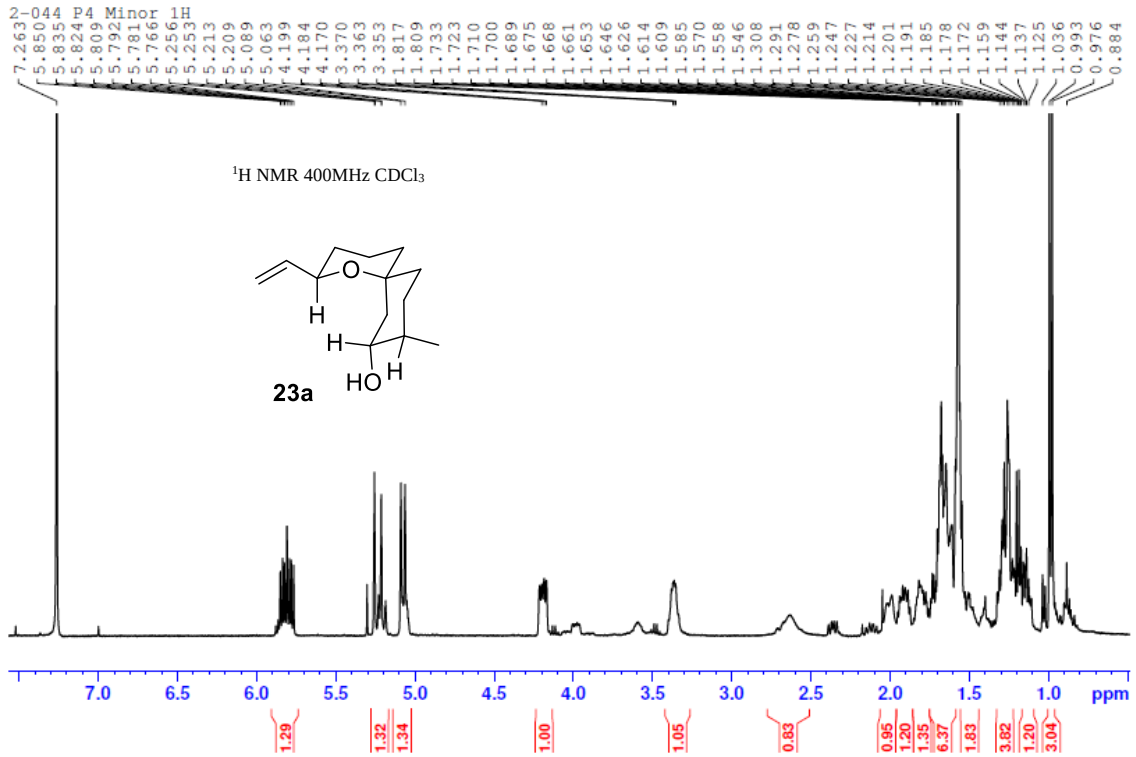
2-044 P4 Minor 1H
^{1}H NMR 400MHz $CDCl_3$
23a
ppm

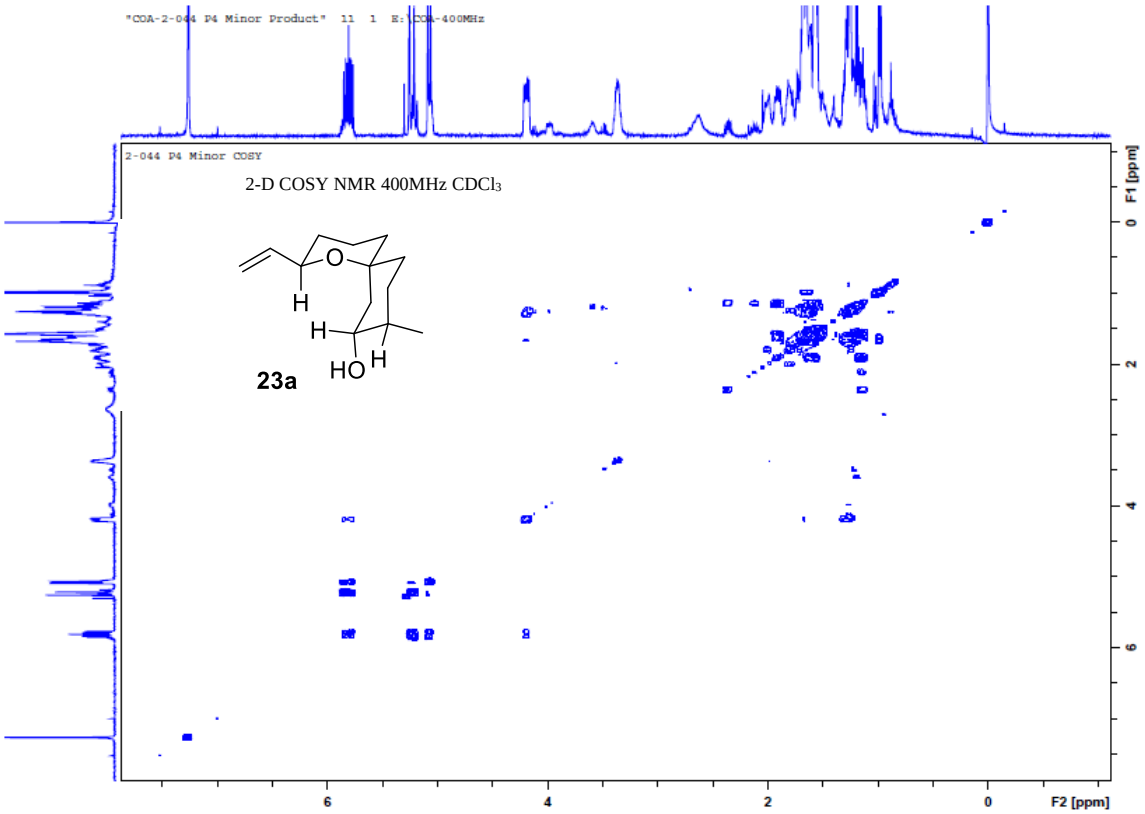
2-044 P4 Minor COSY
2-D COSY NMR 400MHz $CDCl_3$
23a
F1 [ppm]
F2 [ppm]

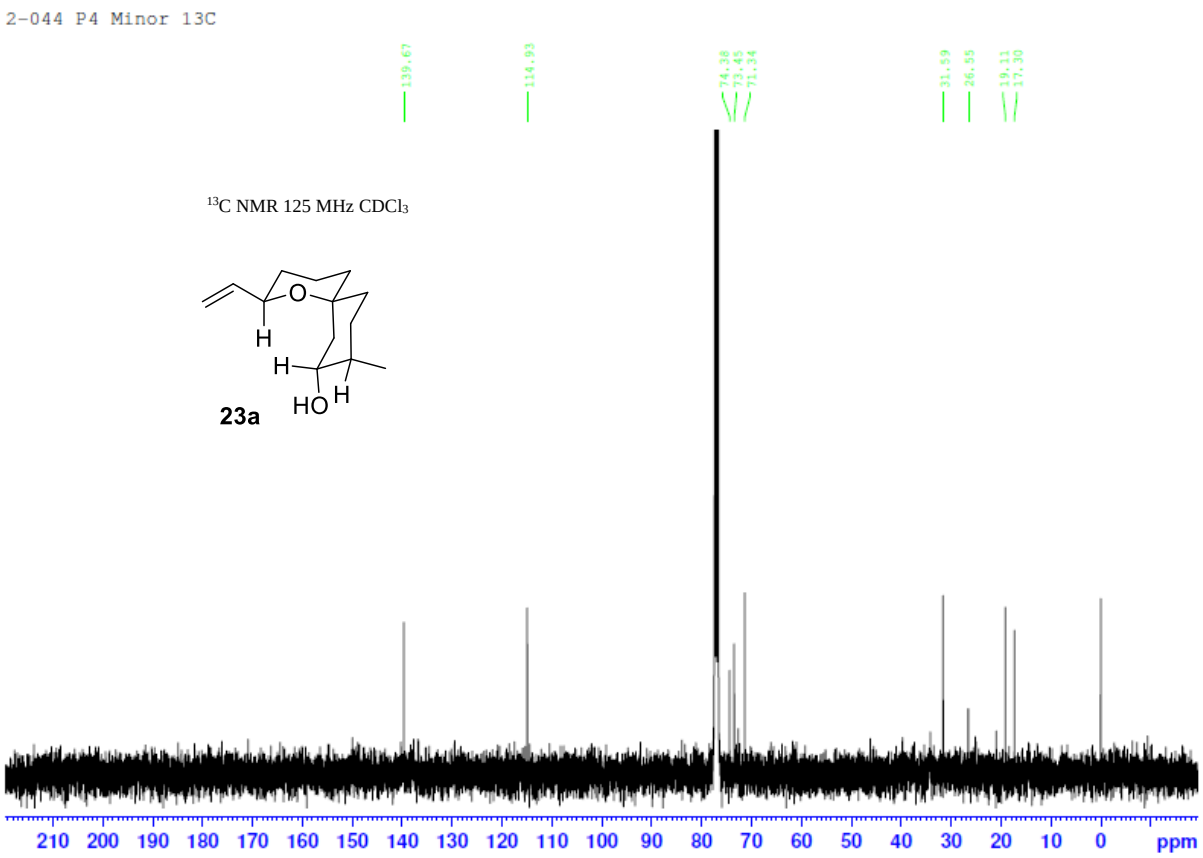
2-044 P4 Minor 13C
139.67
114.93
74.38
73.45
71.34
31.59
26.55
19.11
17.30
^{13}C NMR 125 MHz $CDCl_3$
O
H
H
HO
H
23a
210 200 190 180 170 160 150 140 130 120 110 100 90 80 70 60 50 40 30 20 10 0 ppm

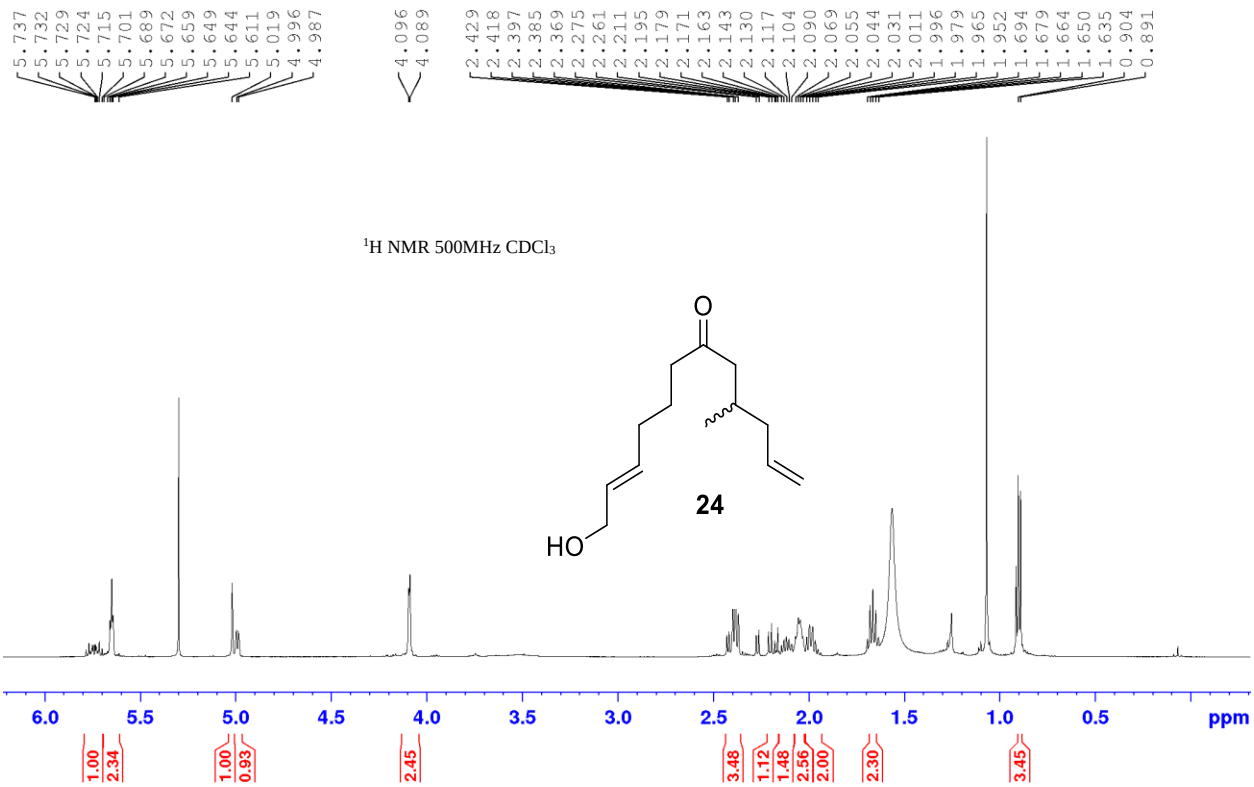
5.737
5.732
5.729
5.724
5.715
5.701
5.689
5.672
5.659
5.649
5.644
5.611
5.019
4.996
4.987
4.096
4.089
2.429
2.418
2.397
2.385
2.369
2.275
2.261
2.211
2.195
2.179
2.171
2.163
2.143
2.130
2.117
2.104
2.090
2.069
2.055
2.044
2.031
2.011
1.996
1.979
1.965
1.952
1.694
1.679
1.664
1.650
1.635
0.904
0.891
1H NMR 500MHz CDCl3
O
HO
24
6.0
5.5
5.0
4.5
4.0
3.5
3.0
2.5
2.0
1.5
1.0
0.5
ppm
1.00
2.34
1.00
0.93
2.45
3.48
1.12
1.48
2.56
2.00
2.30
3.45

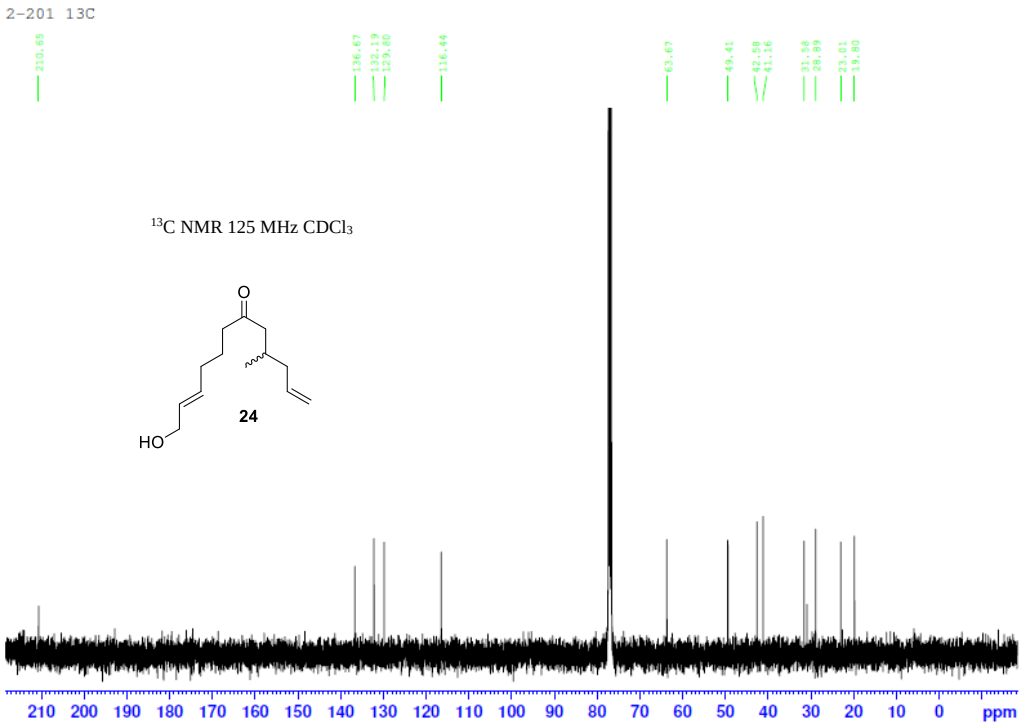
2-201 13C
210.65
136.67
132.19
129.80
116.44
63.67
49.41
42.58
41.16
31.58
28.89
23.01
19.80
^{13}C NMR 125 MHz $CDCl_3$
O
HO
24
210 200 190 180 170 160 150 140 130 120 110 100 90 80 70 60 50 40 30 20 10 0 ppm

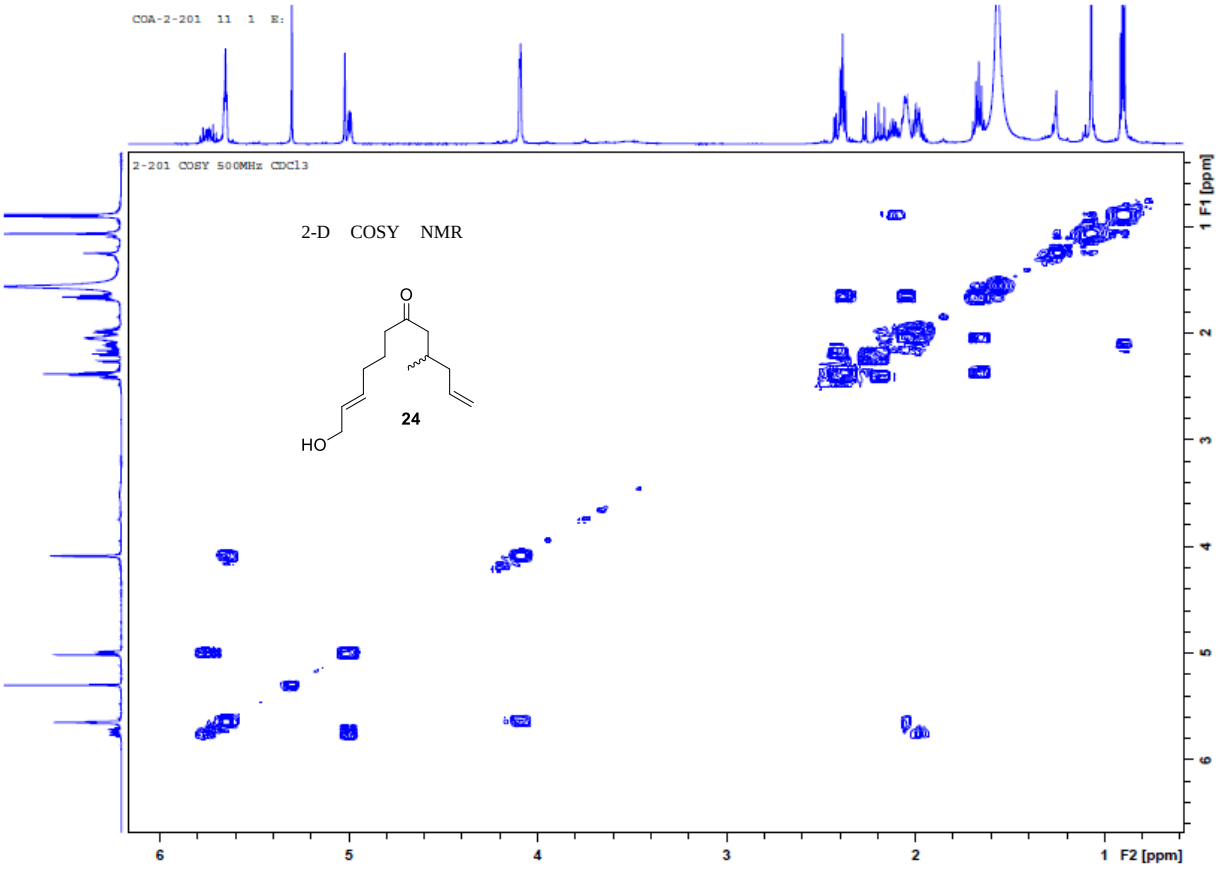
COA-2-201 11 1 E:
2-201 COSY 500MHz CDCl3
2-D COSY NMR
O
HO
24
F1 [ppm]
F2 [ppm]

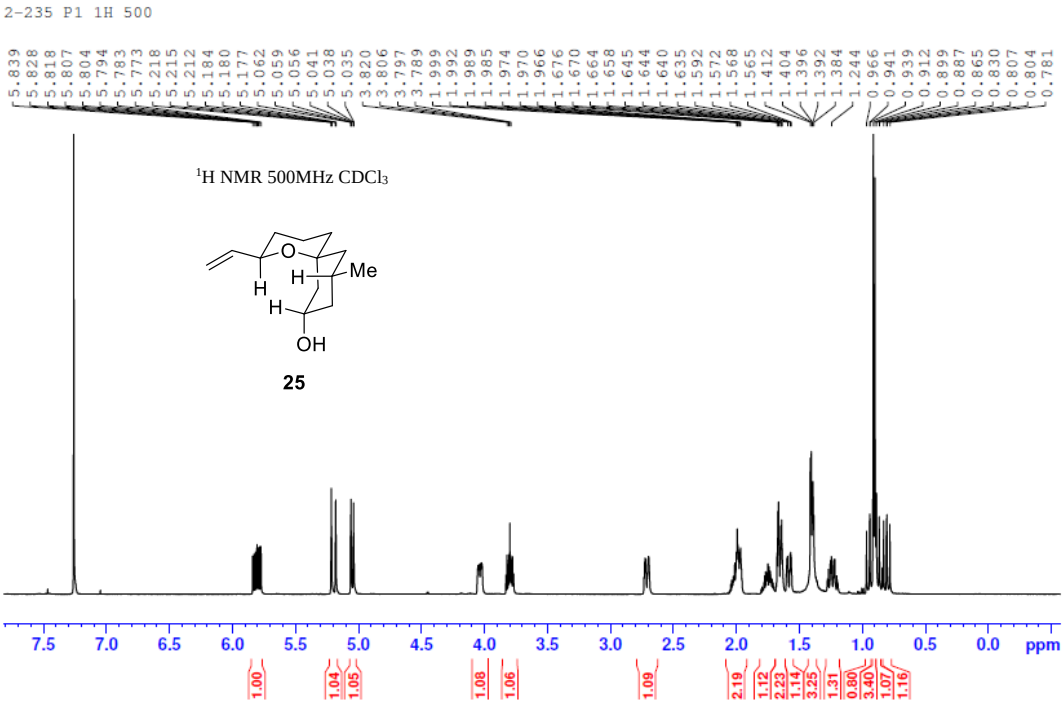

^{1}H NMR 500MHz $CDCl_3$

25

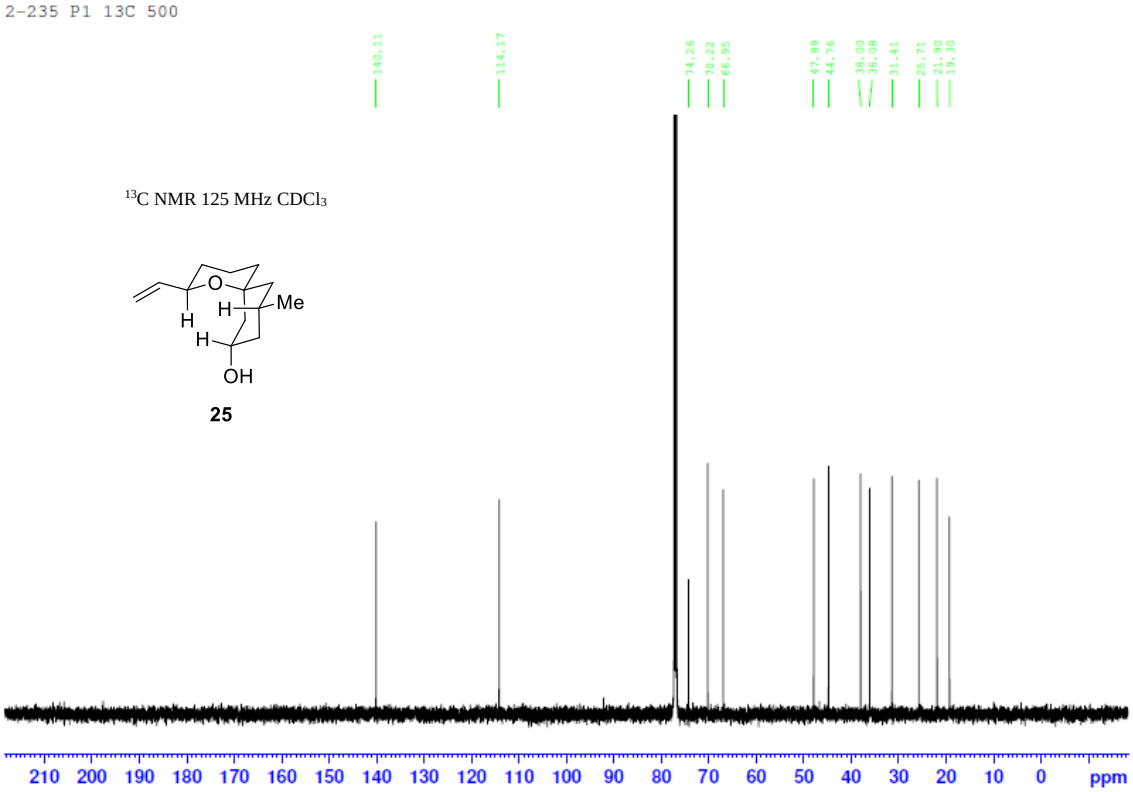

^{13}C NMR 125 MHz $CDCl_3$

25

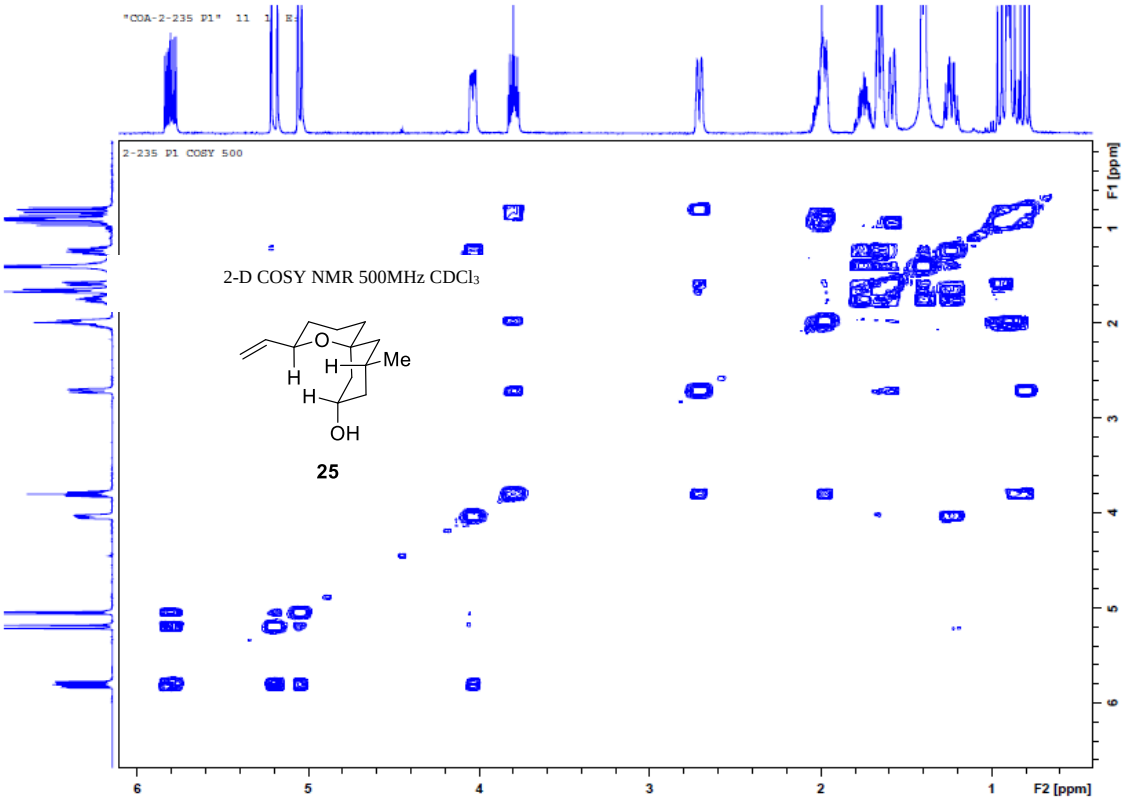

2-D COSY NMR 500MHz $CDCl_3$

25

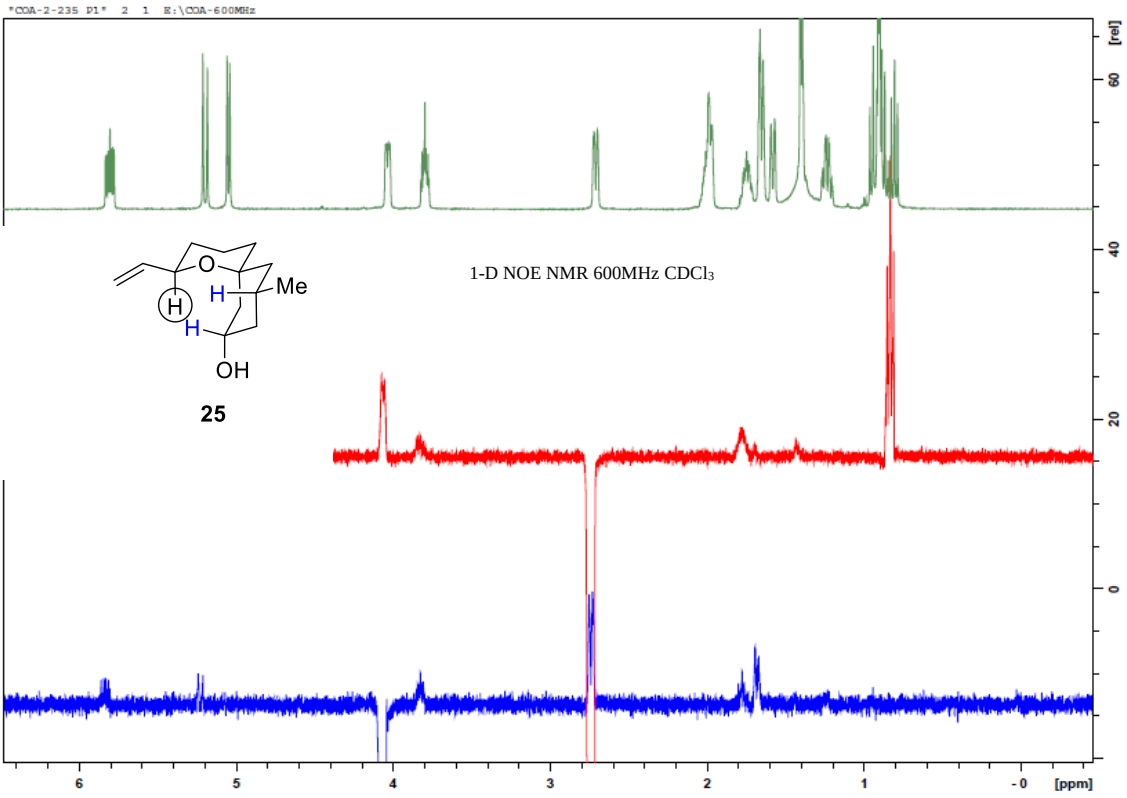

25

1-D NOE NMR 600MHz $CDCl_3$

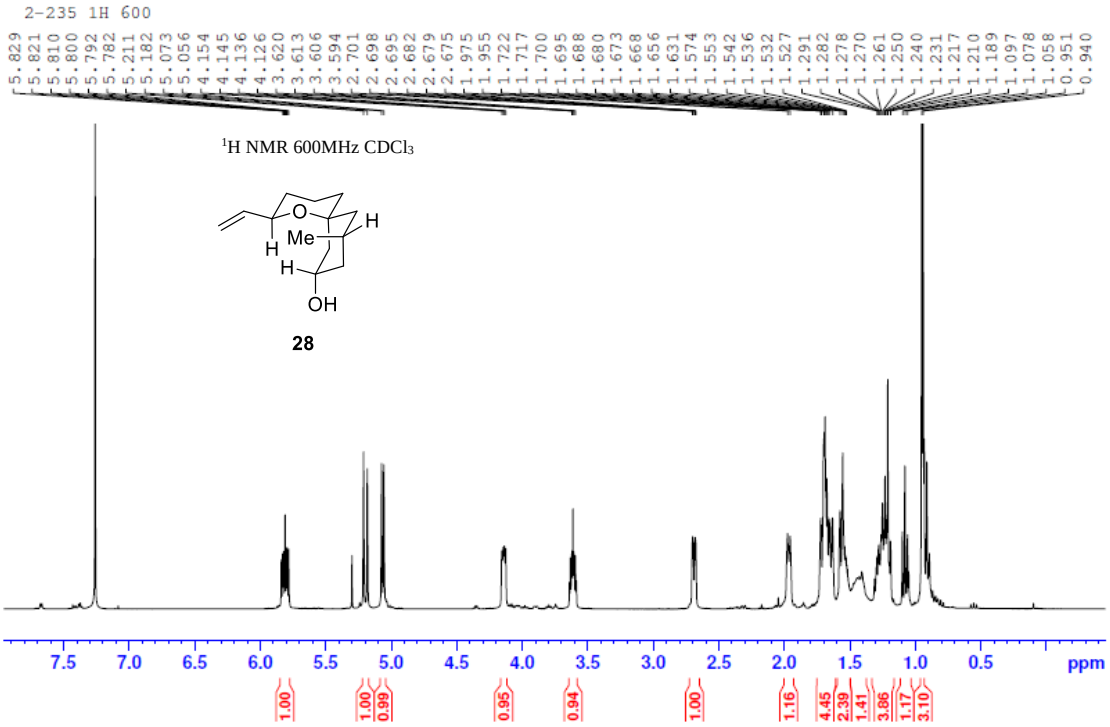
2-235 1H 600
5.829 5.821 5.810 5.800 5.792 5.782 5.211 5.182 5.073 5.056 4.154 4.145 4.136 4.126 3.620 3.613 3.606 3.594 2.701 2.698 2.695 2.682 2.679 2.675 1.975 1.955 1.722 1.717 1.700 1.695 1.688 1.680 1.673 1.668 1.656 1.631 1.574 1.553 1.542 1.536 1.532 1.527 1.291 1.282 1.278 1.270 1.261 1.250 1.240 1.231 1.217 1.210 1.189 1.097 1.078 1.058 0.951 0.940
1H NMR 600MHz CDCl3
O
H
Me
H
H
OH
28
7.5 7.0 6.5 6.0 5.5 5.0 4.5 4.0 3.5 3.0 2.5 2.0 1.5 1.0 0.5 ppm
1.00 1.00 0.99 0.95 0.94 1.00 1.16 4.45 2.39 1.41 3.86 1.17 3.10

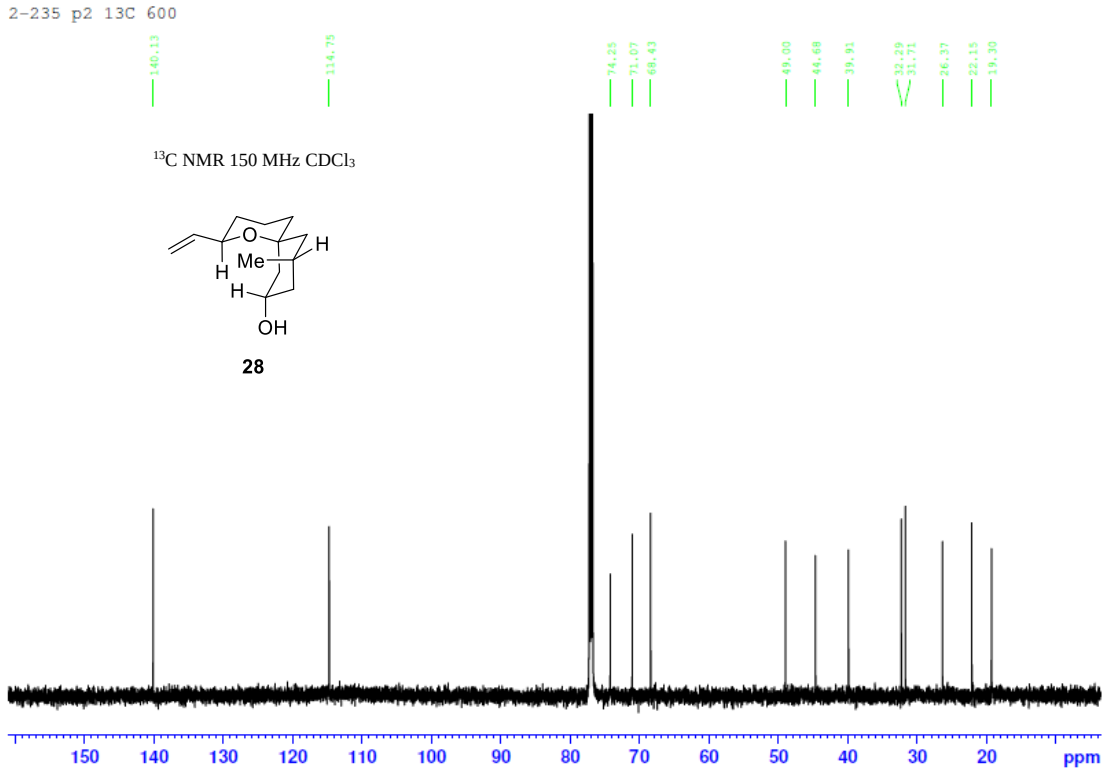
2-235 p2 13C 600
140.13 114.75 74.25 71.07 68.43 49.00 44.68 39.91 32.29 31.71 26.37 22.15 19.30
13C NMR 150 MHz CDCl3
O
H
Me
H
H
OH
28
150 140 130 120 110 100 90 80 70 60 50 40 30 20 ppm

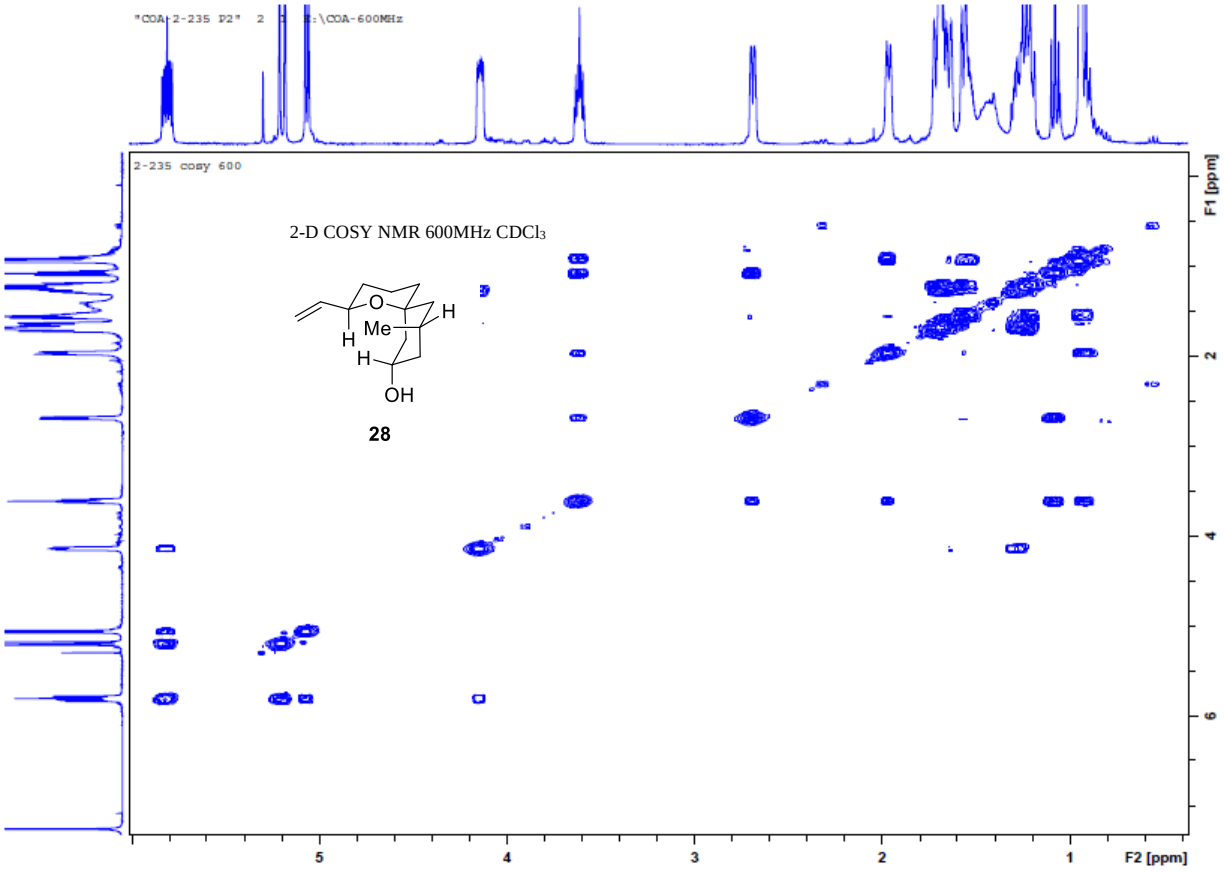
"COA-2-235 P2" 2 E:\COA-600MHz
2-235 cosy 600
2-D COSY NMR 600MHz CDCl3
O
H
Me
H
H
OH
28
F1 [ppm]
F2 [ppm]
2
4
6
5
4
3
2
1

2-192 1H 500

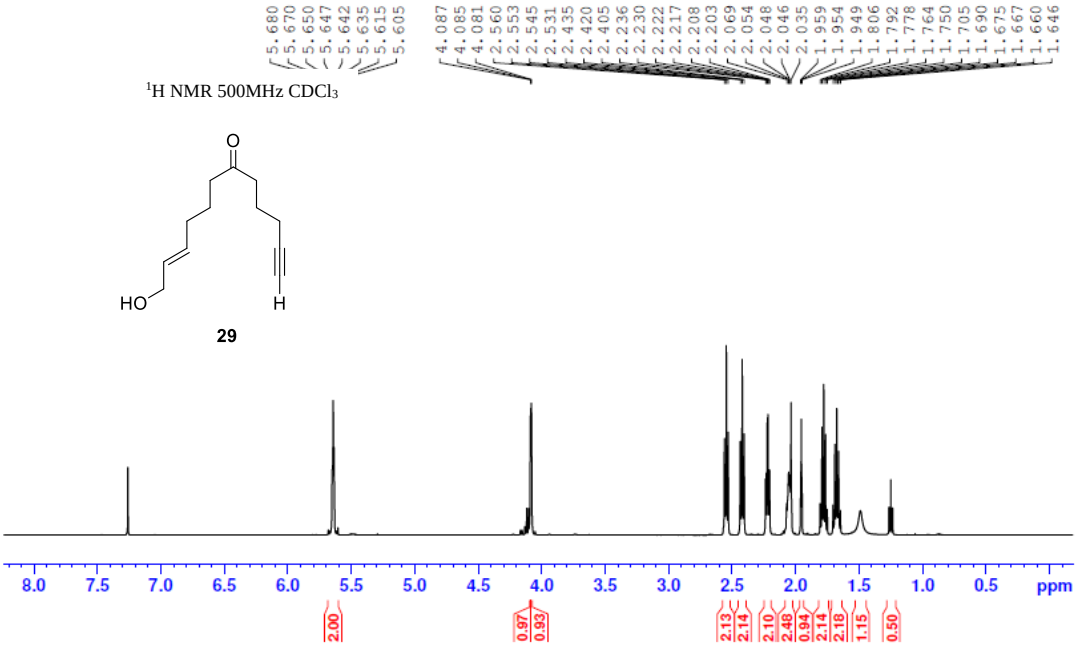

^{1}H NMR 500MHz $CDCl_3$

29

2-192 13C 500

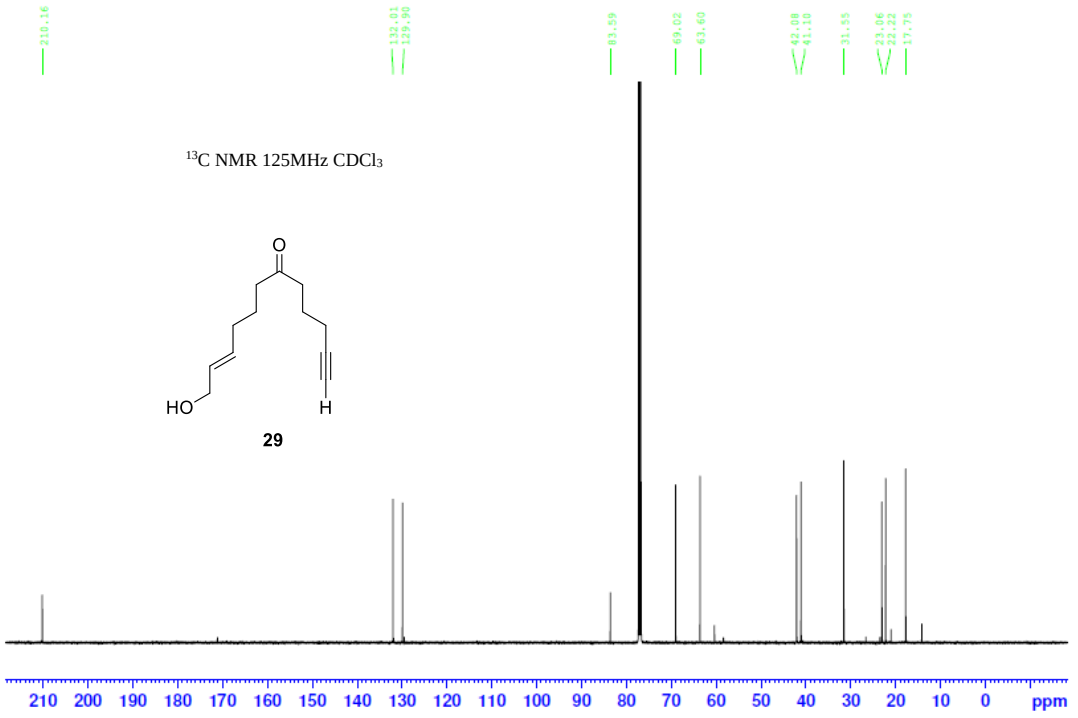

^{13}C NMR 125MHz $CDCl_3$

29

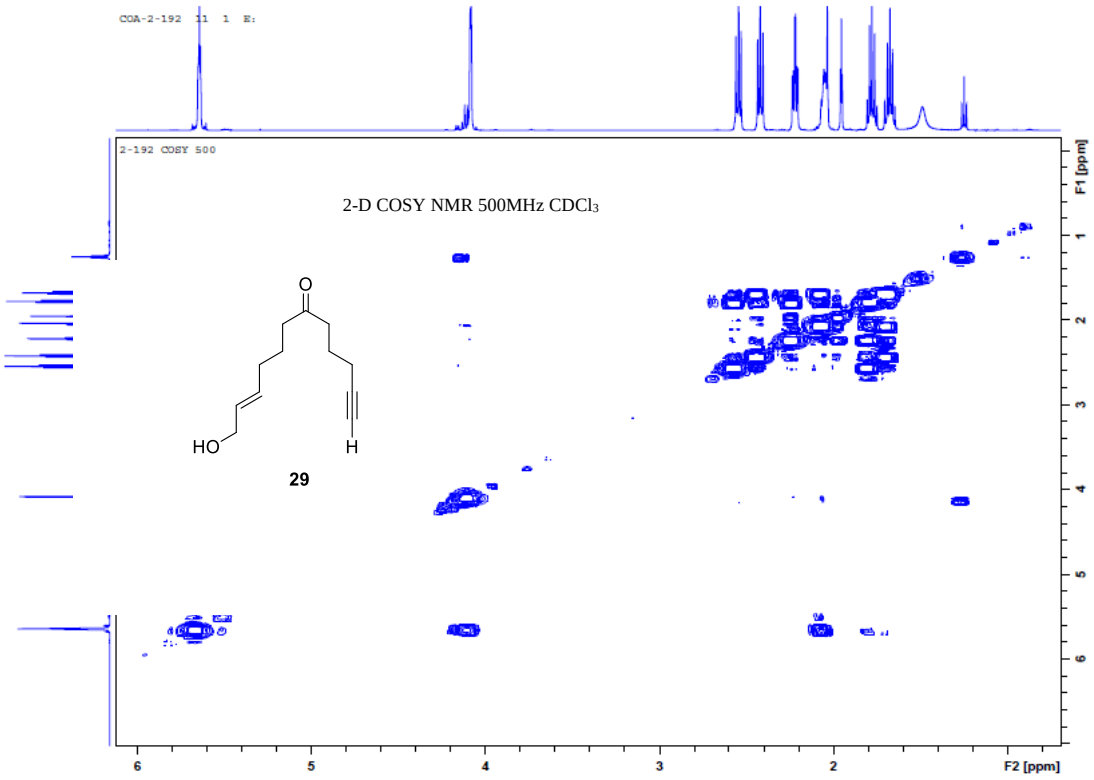
COA-2-192 11 1 E:
2-192 COSY 500
2-D COSY NMR 500MHz CDCl3
O
HO
H
29
F1 [ppm]
F2 [ppm]
6
5
4
3
2
1

2-193 P1 500 1H

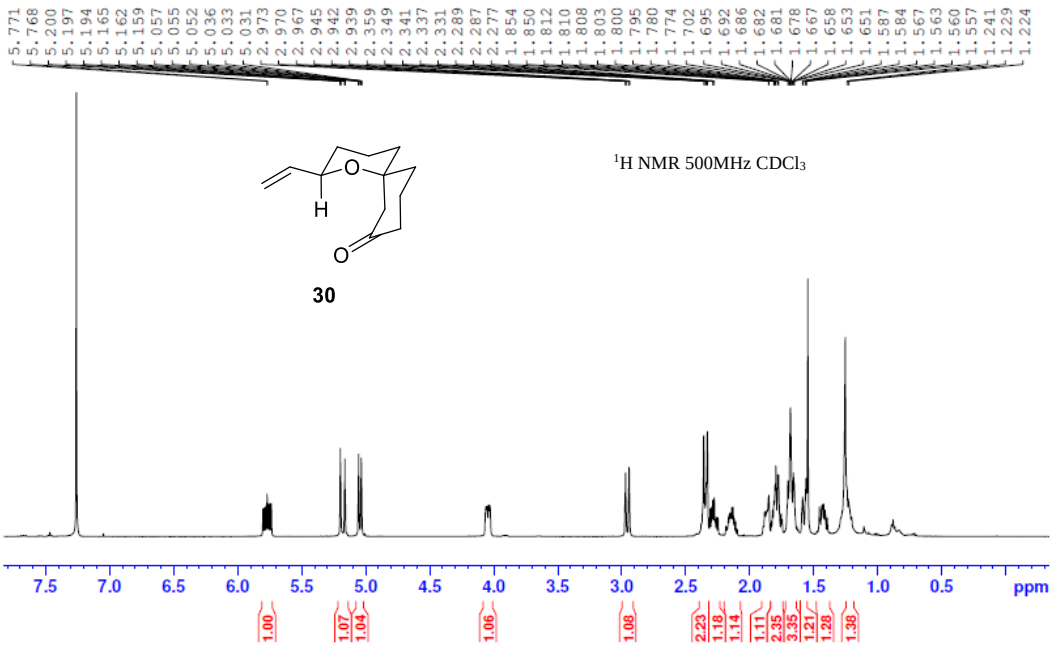

2-193 P1 500 13C

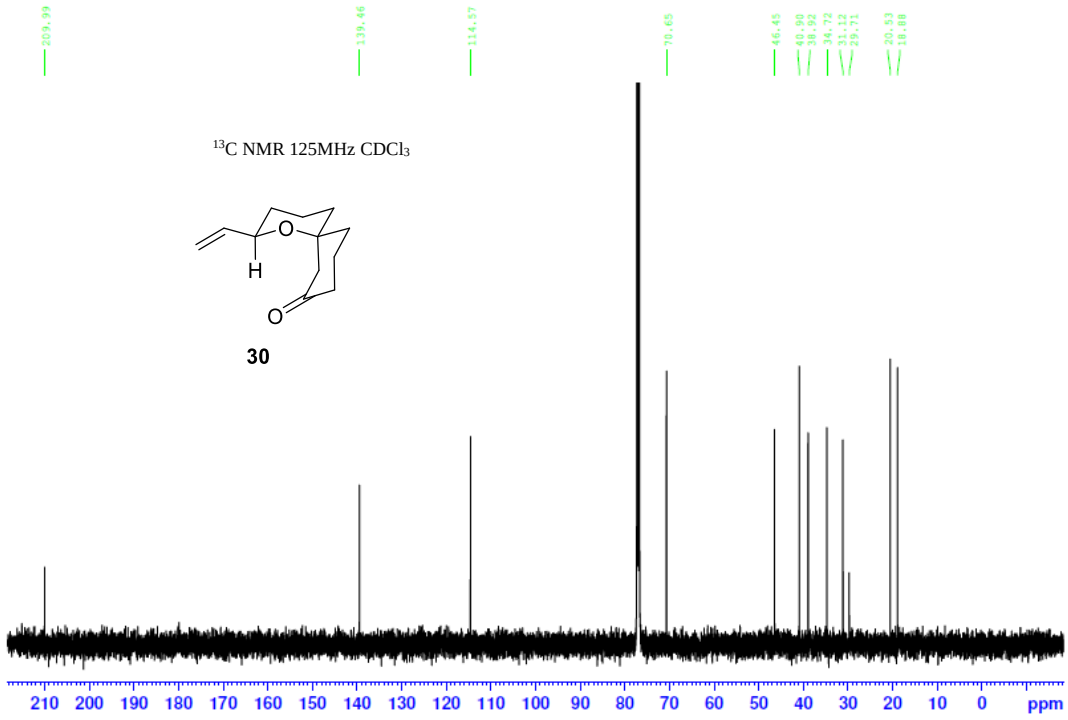

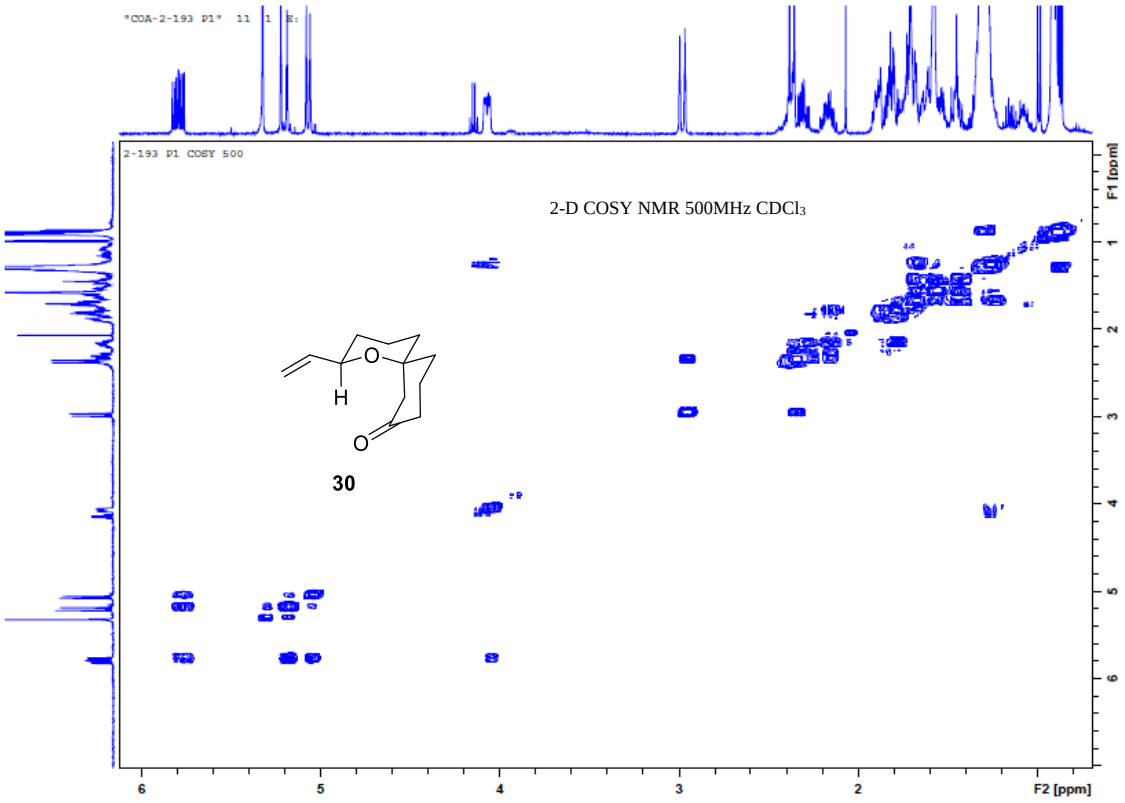
"COA-2-193 P1" 11 1 H:
2-193 P1 COSY 500
2-D COSY NMR 500MHz $CDCl_3$
O
H
O
30
F1 [ppm]
F2 [ppm]
6
5
4
3
2
1
2
3
4
5
6

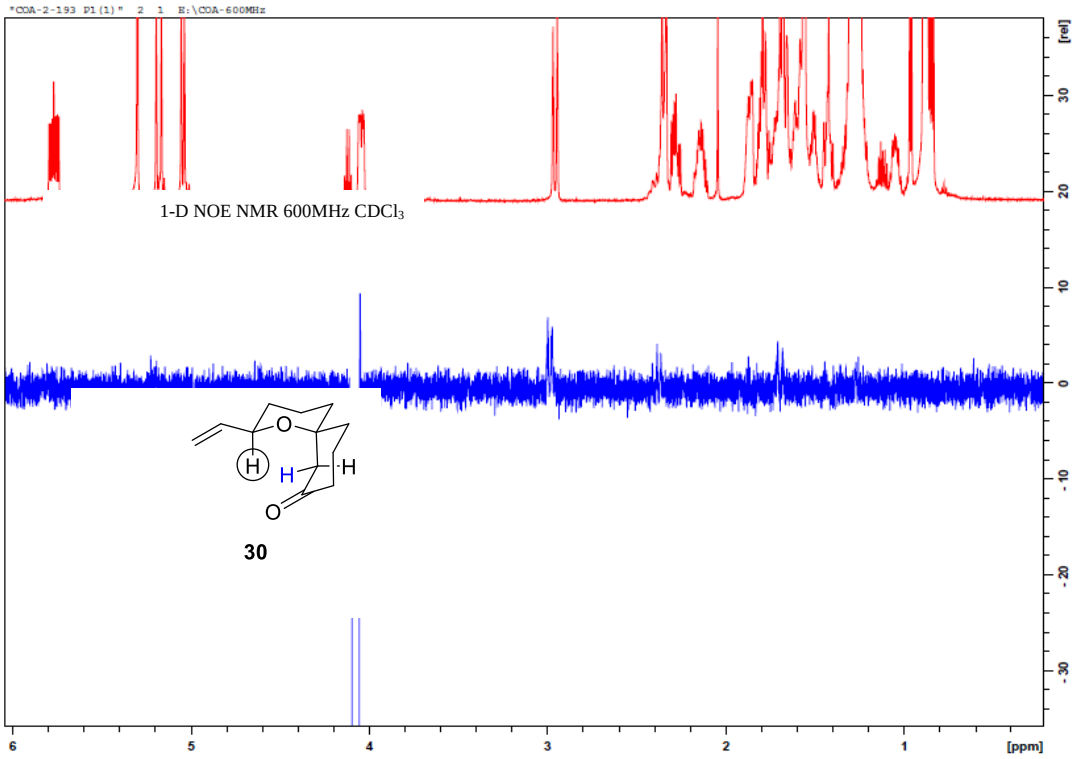

1-D NOE NMR 600MHz $CDCl_3$

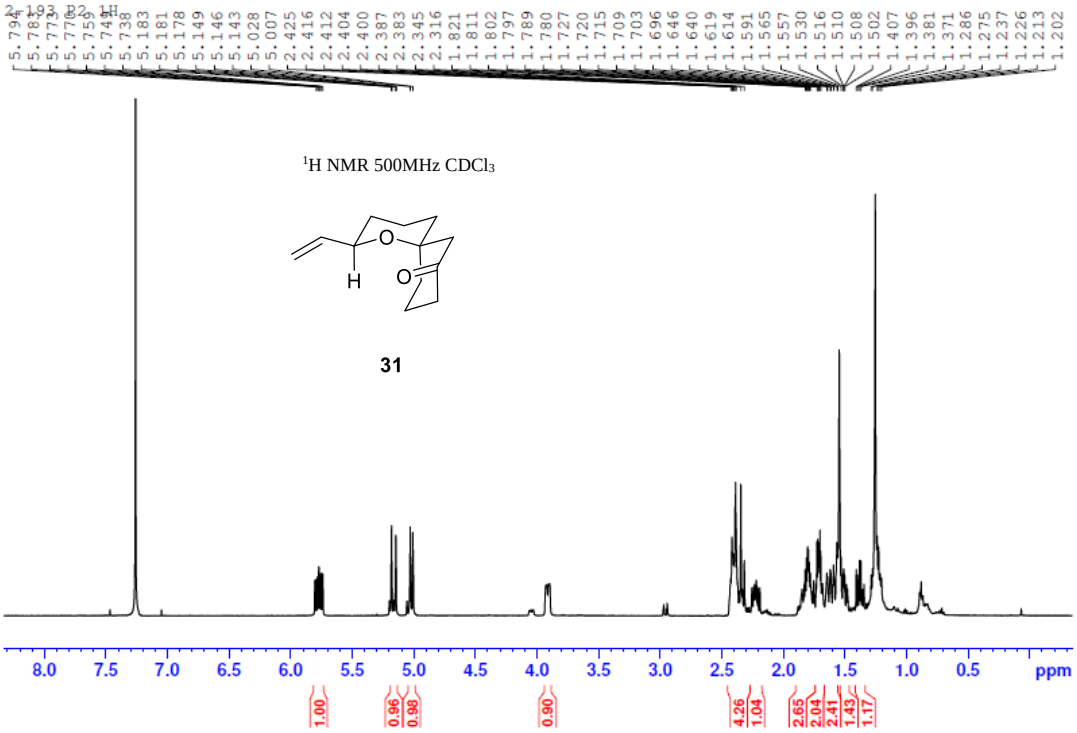

^{1}H NMR 500MHz $CDCl_3$

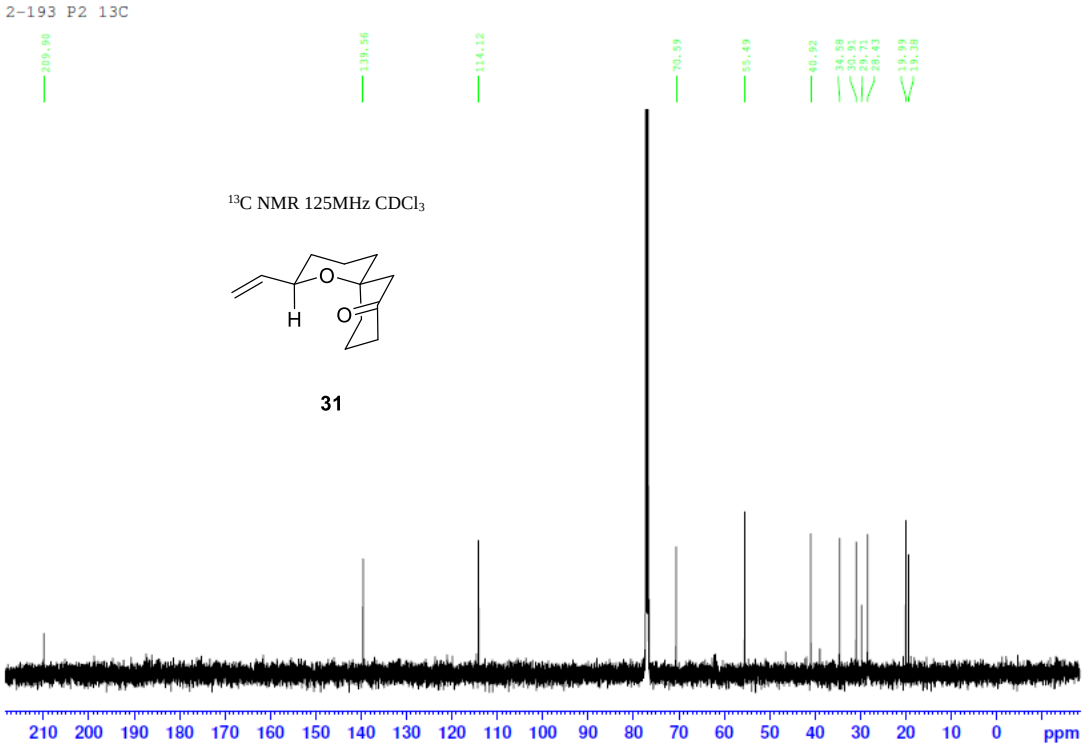

^{13}C NMR 125MHz $CDCl_3$

31

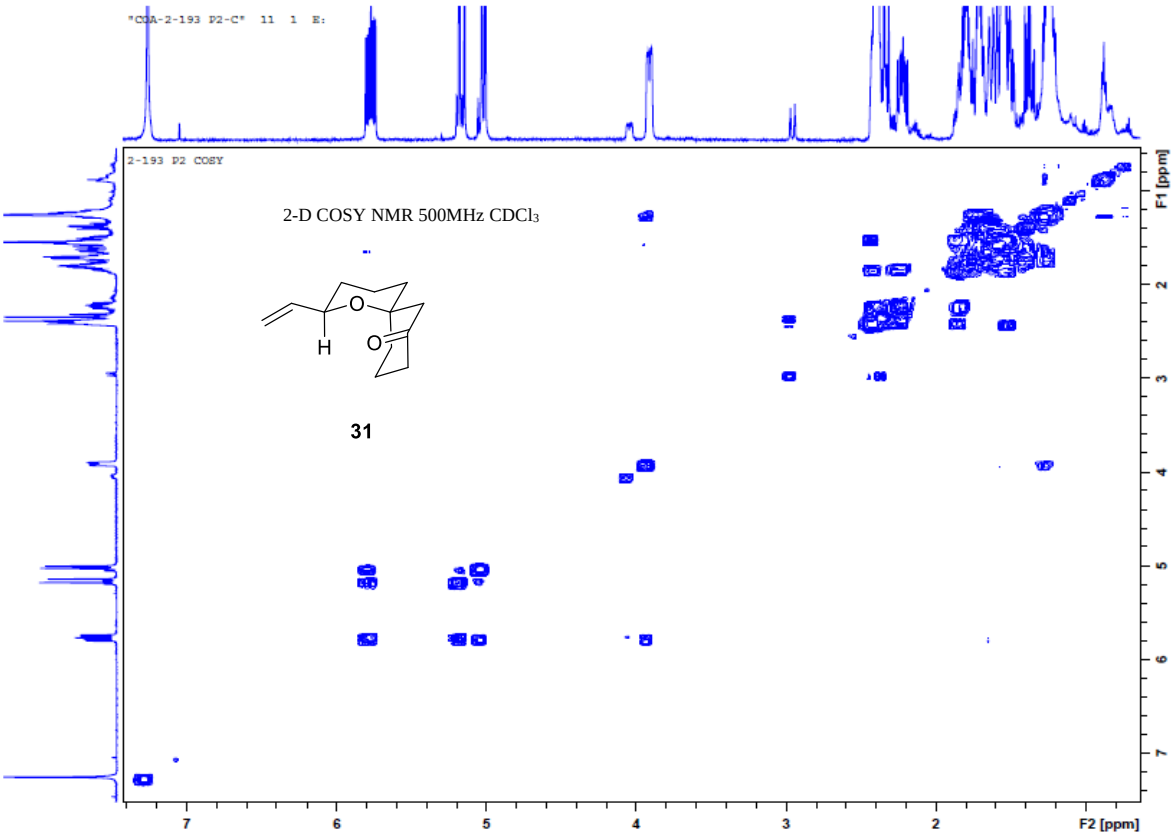
"CDA-2-193 P2-C" 11 1 E:
2-193 P2 COSY
2-D COSY NMR 500MHz $CDCl_3$
O
H
O
31
F1 [ppm]
F2 [ppm]
7
6
5
4
3
2

2-177 Product 1H 400

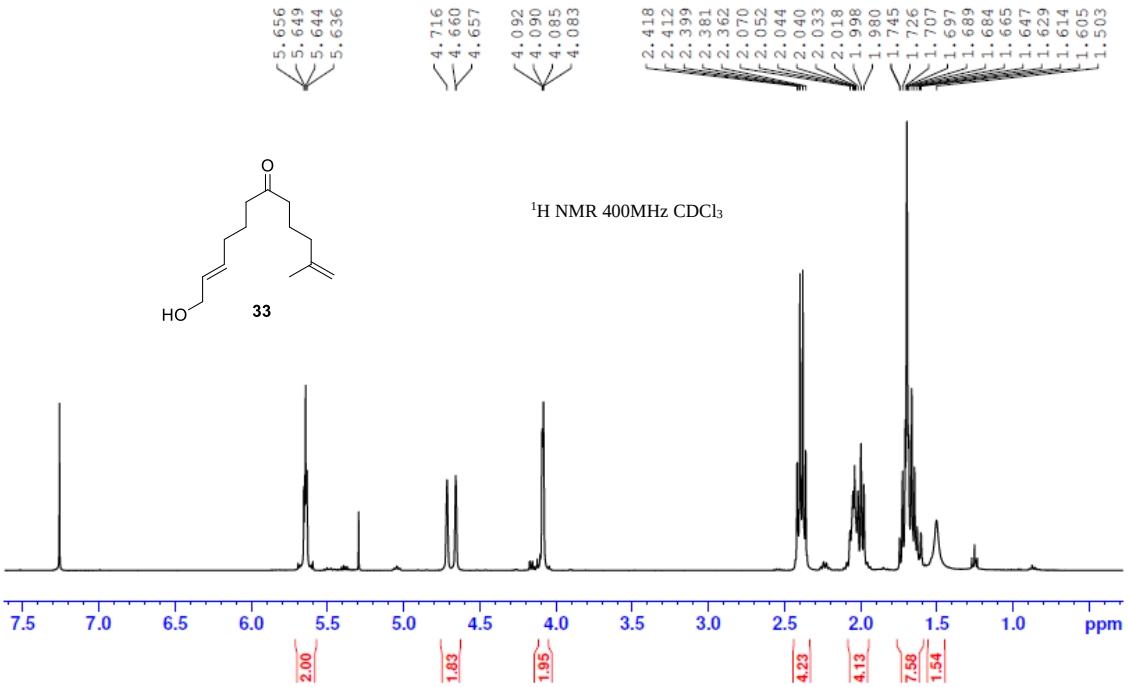

2-177 Product COSY 400

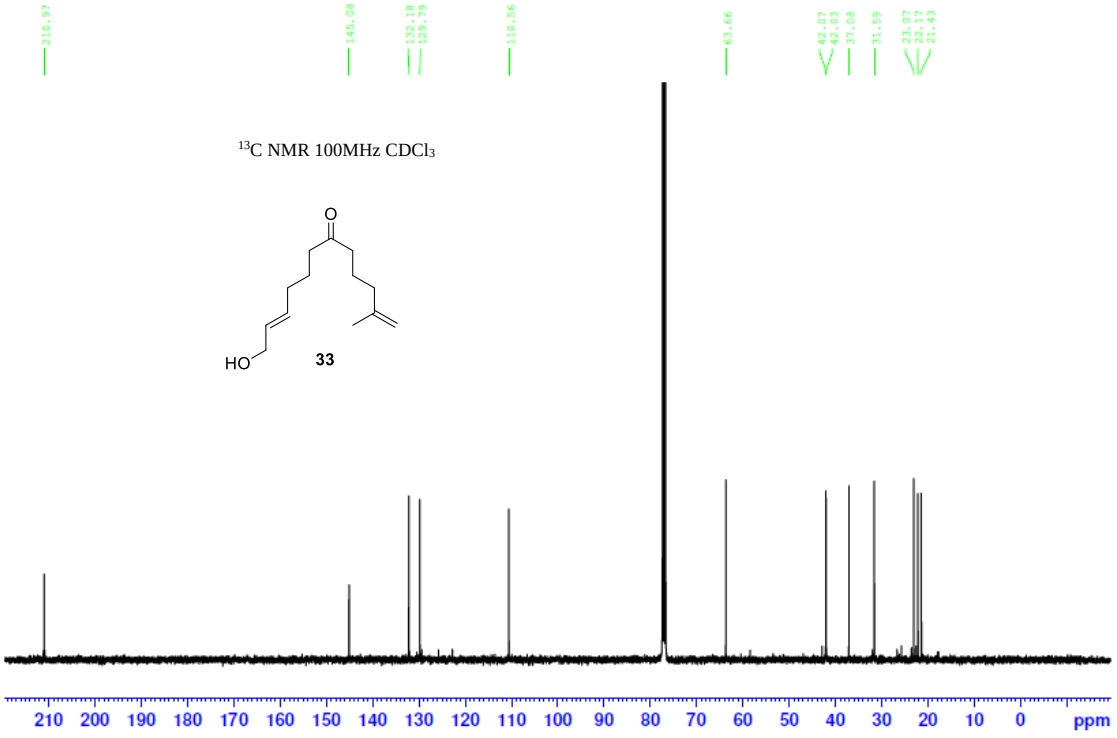

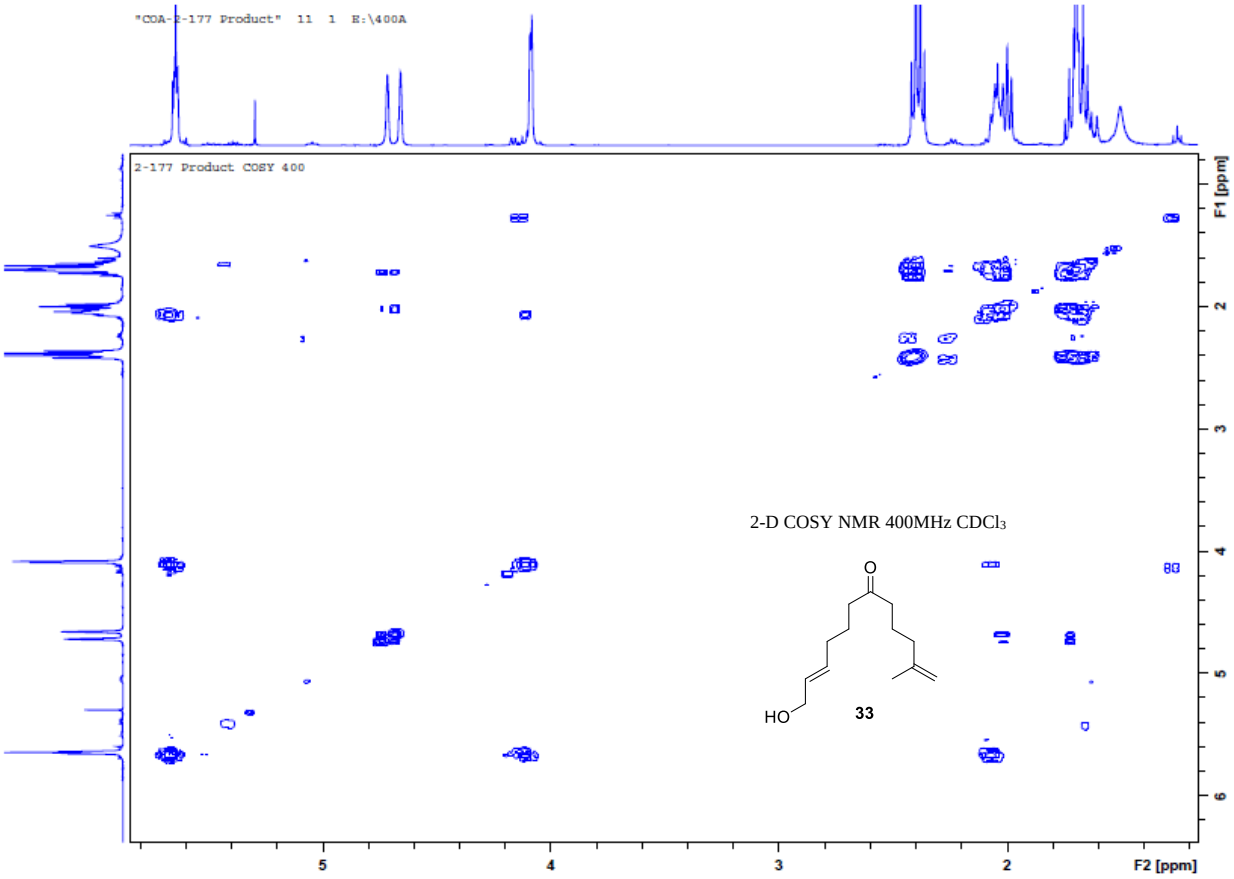
"COA-2-177 Product" 11 1 E:\400A
2-177 Product COSY 400
F1 [ppm]
F2 [ppm]
2-D COSY NMR 400MHz $CDCl_3$
HO
O
33

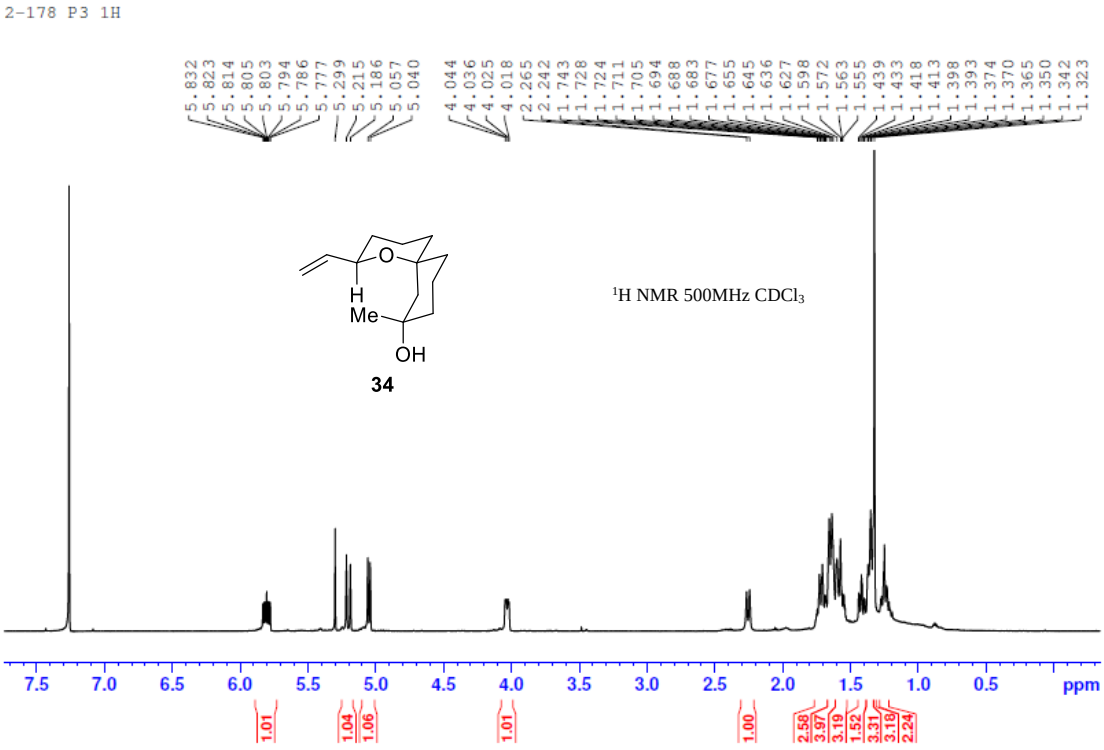
2-178 P3 1H
5.832
5.823
5.814
5.805
5.803
5.794
5.786
5.777
5.299
5.215
5.186
5.057
5.040
4.044
4.036
4.025
4.018
2.265
2.242
1.743
1.728
1.724
1.711
1.705
1.694
1.688
1.683
1.677
1.655
1.645
1.636
1.627
1.598
1.572
1.563
1.555
1.439
1.433
1.418
1.413
1.398
1.393
1.374
1.370
1.365
1.350
1.342
1.323
O
H
Me
OH
34
1H NMR 500MHz CDCl3
7.5
7.0
6.5
6.0
5.5
5.0
4.5
4.0
3.5
3.0
2.5
2.0
1.5
1.0
0.5
ppm
1.01
1.04
1.06
1.01
1.00
2.58
3.97
3.19
1.52
3.31
3.18
2.24

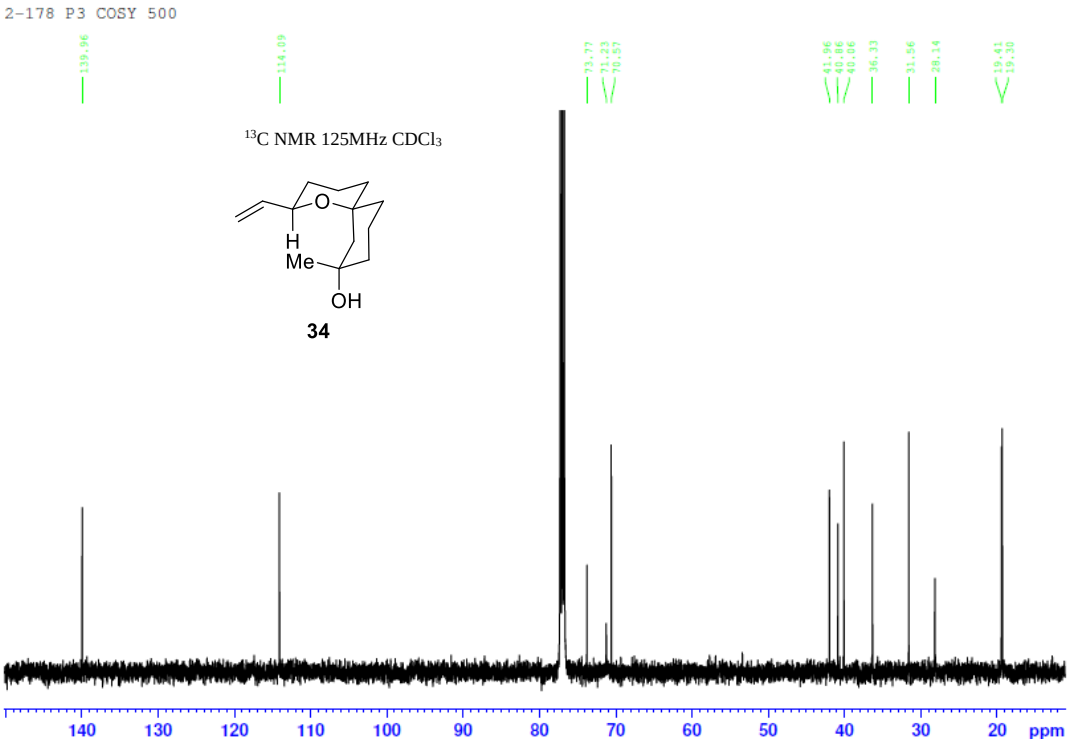
2-178 P3 COSY 500
139.96
114.09
73.77
71.23
70.57
41.96
40.86
40.06
36.33
31.56
29.14
19.41
19.30
13C NMR 125MHz CDCl3
O
H
Me
OH
34
140
130
120
110
100
90
80
70
60
50
40
30
20
ppm

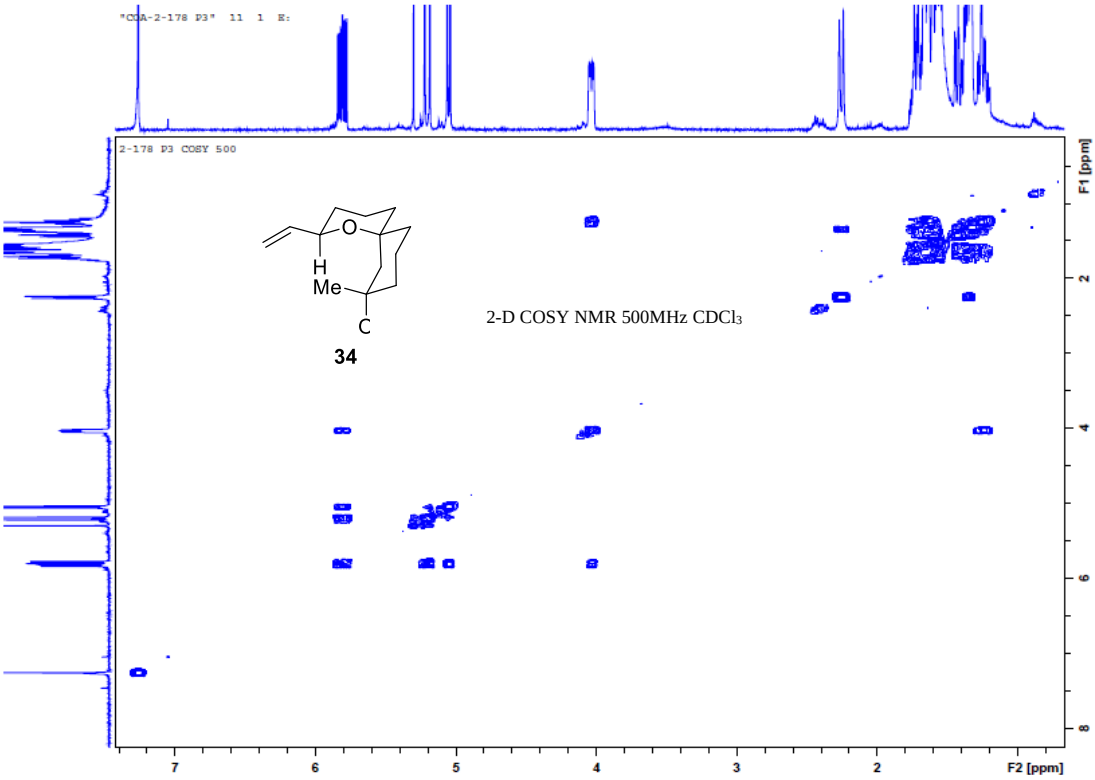

34

2-D COSY NMR 500MHz $CDCl_3$

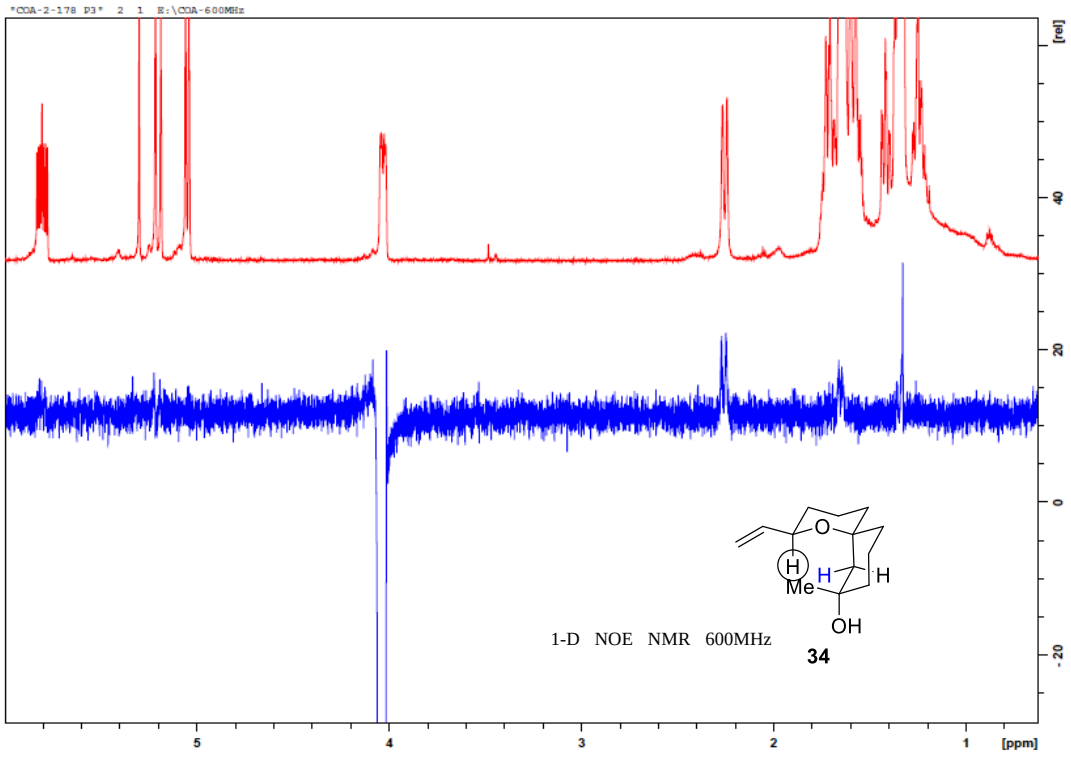

1-D NOE NMR 600MHz

34

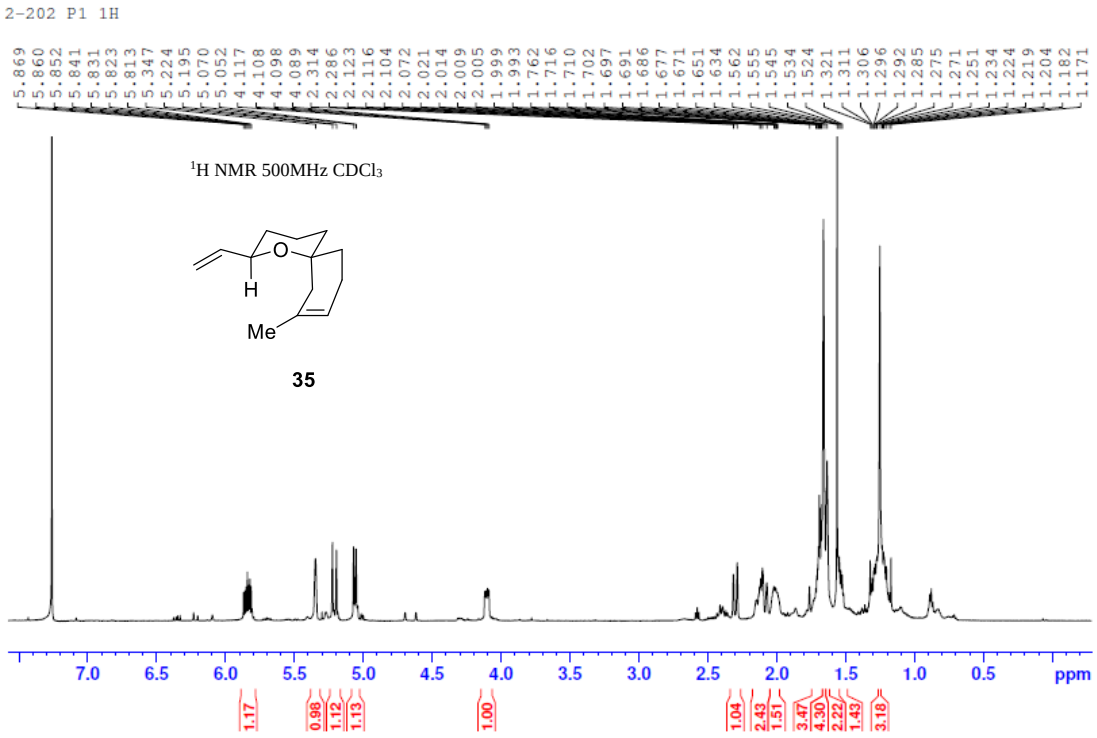
2-202 P1 1H
5.869 5.860 5.852 5.841 5.831 5.823 5.813 5.347 5.224 5.195 5.070 5.052 4.117 4.108 4.098 4.089 2.314 2.286 2.123 2.116 2.104 2.072 2.021 2.014 2.009 2.005 1.999 1.993 1.762 1.716 1.710 1.702 1.697 1.691 1.686 1.677 1.671 1.651 1.634 1.562 1.555 1.545 1.534 1.524 1.321 1.311 1.306 1.296 1.292 1.285 1.275 1.271 1.251 1.234 1.224 1.219 1.204 1.182 1.171
1H NMR 500MHz CDCl3
O
H
Me
35
7.0 6.5 6.0 5.5 5.0 4.5 4.0 3.5 3.0 2.5 2.0 1.5 1.0 0.5 ppm
1.17 0.98 1.12 1.13 1.00 1.04 2.43 1.51 3.47 4.30 2.22 1.43 3.18

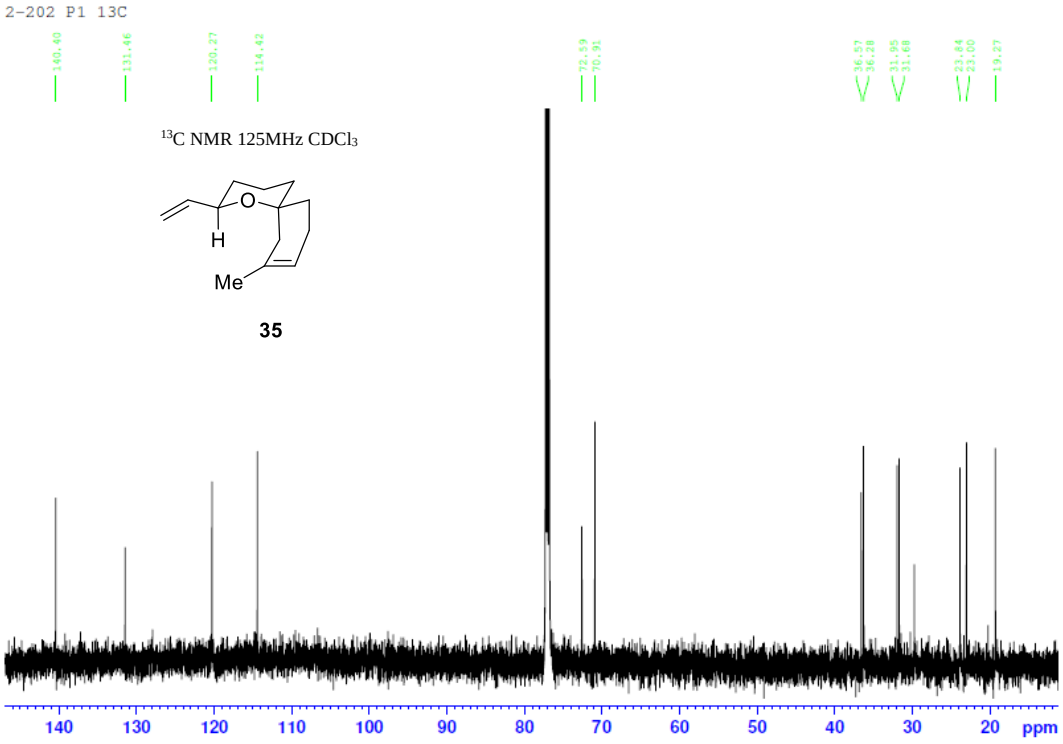
2-202 P1 13C
140.40 131.46 120.27 114.42 72.59 70.91 36.57 36.28 31.95 31.68 23.84 23.00 19.27
13C NMR 125MHz CDCl3
O
H
Me
35
140 130 120 110 100 90 80 70 60 50 40 30 20 ppm

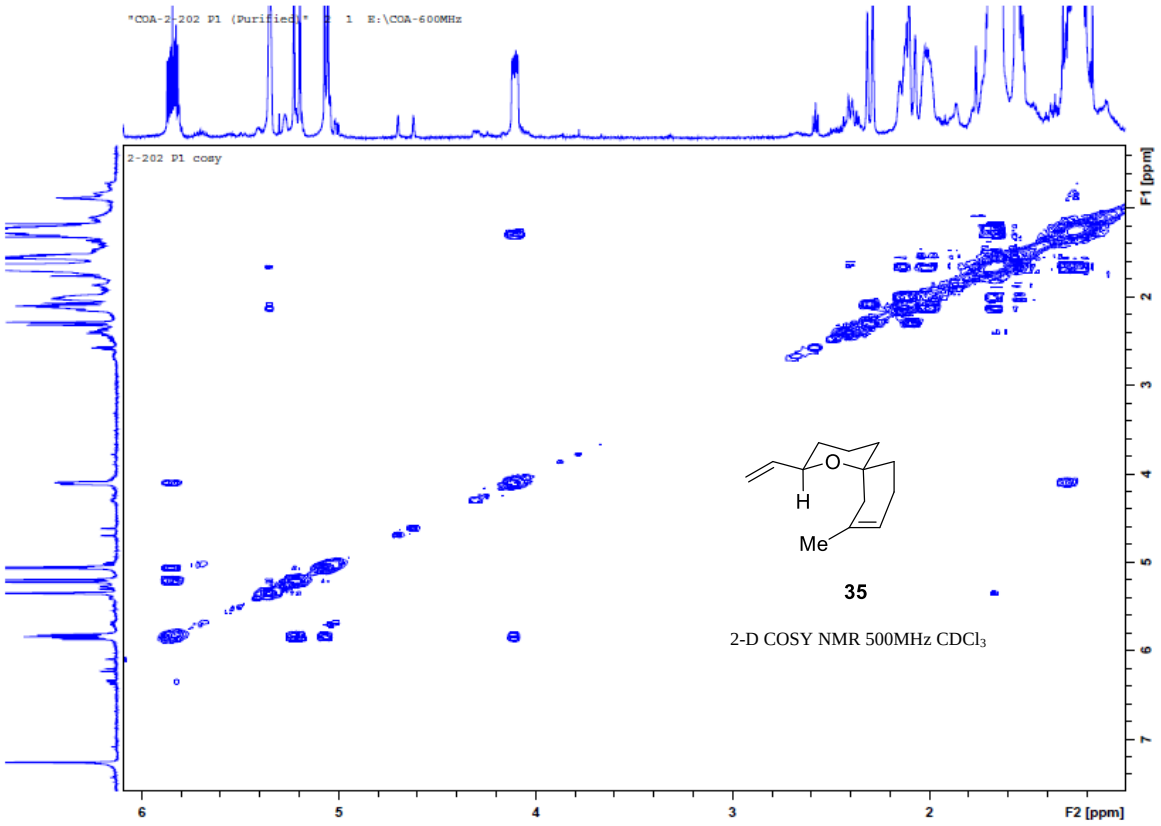

35

2-D COSY NMR 500MHz $CDCl_3$

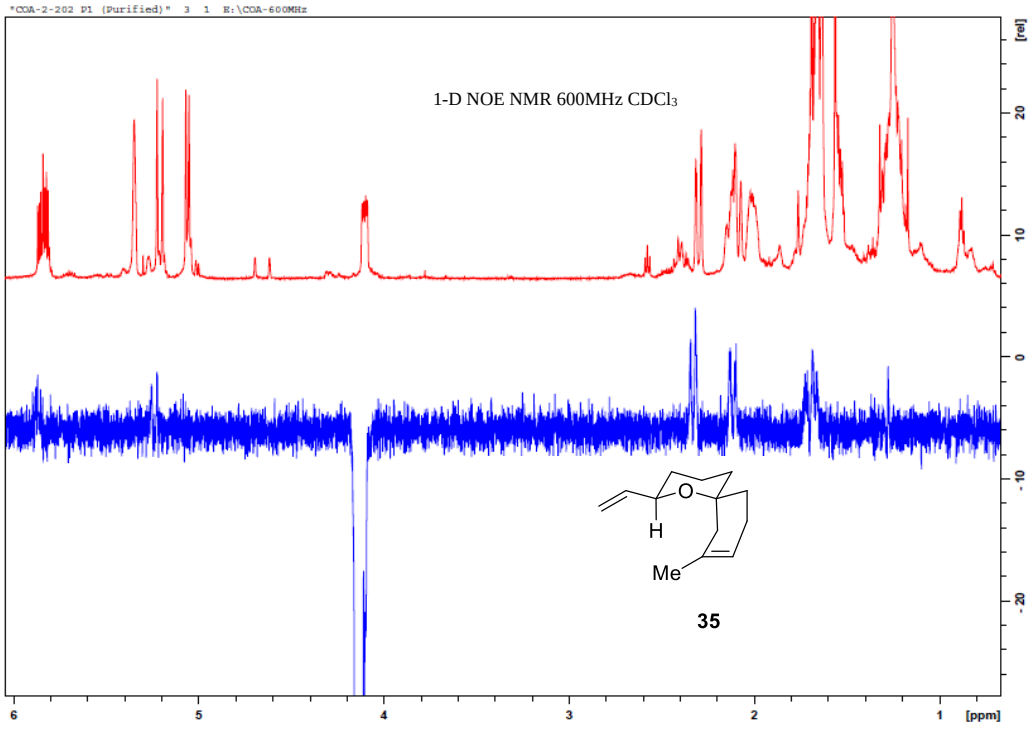
"COA-2-202 P1 (Purified)" 3 1 E:\COA-600MHz
1-D NOE NMR 600MHz CDCl3
[rel]
20
10
0
-10
-20
O
H
Me
35
6
5
4
3
2
1
[ppm]

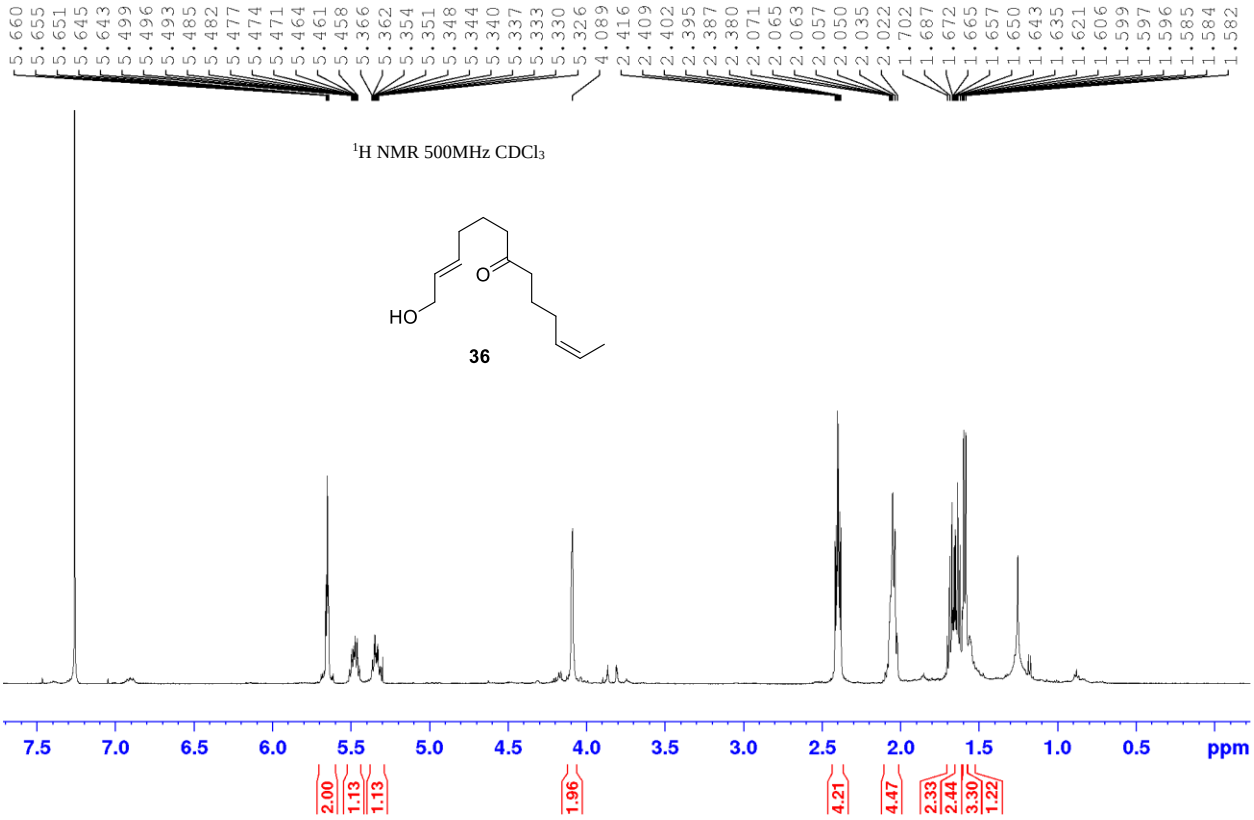
5.660 5.555 5.651 5.645 5.643 5.499 5.496 5.493 5.485 5.482 5.477 5.474 5.471 5.464 5.461 5.458 5.366 5.362 5.354 5.351 5.348 5.344 5.340 5.337 5.333 5.330 5.326 4.089 2.416 2.409 2.402 2.395 2.387 2.380 2.071 2.065 2.063 2.057 2.050 2.035 2.022 1.702 1.687 1.672 1.665 1.657 1.650 1.643 1.635 1.621 1.606 1.599 1.597 1.596 1.585 1.584 1.582
1H NMR 500MHz CDCl3
O
HO
36
7.5 7.0 6.5 6.0 5.5 5.0 4.5 4.0 3.5 3.0 2.5 2.0 1.5 1.0 0.5 ppm
2.00 1.13 1.13 1.96 4.21 4.47 2.33 2.44 3.30 1.22

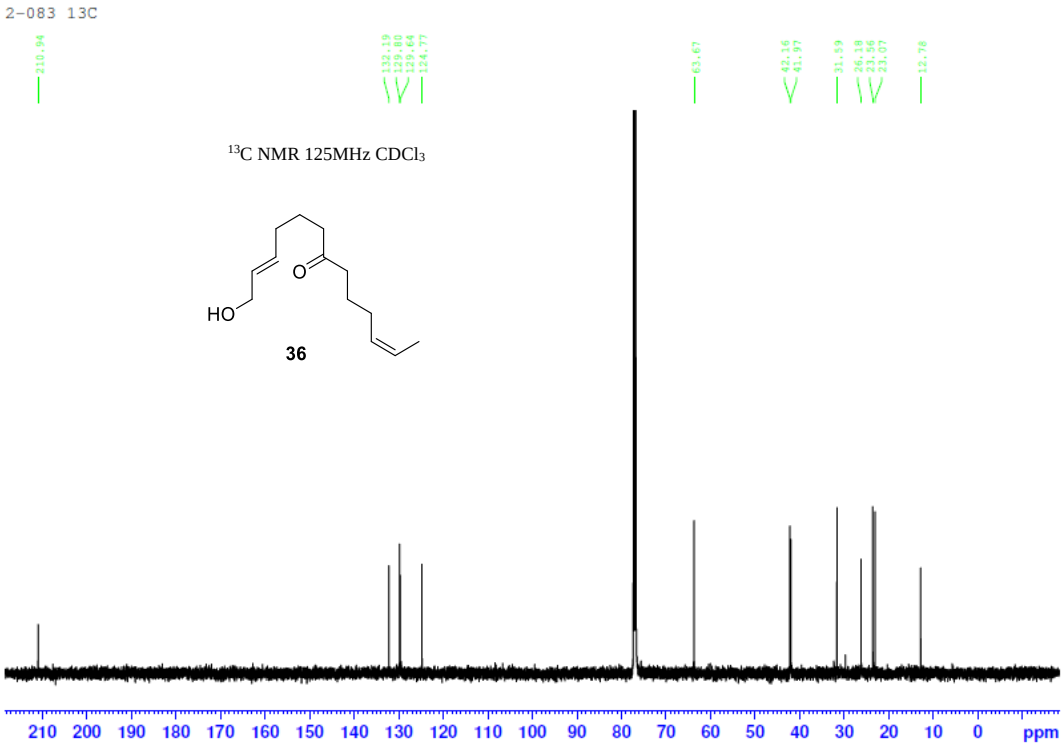
2-083 13C
210.94
132.19
130.80
129.64
124.77
63.67
42.16
41.97
31.59
26.18
23.56
23.07
12.78
^{13}C NMR 125MHz $CDCl_3$
HO
O
36
210 200 190 180 170 160 150 140 130 120 110 100 90 80 70 60 50 40 30 20 10 0 ppm

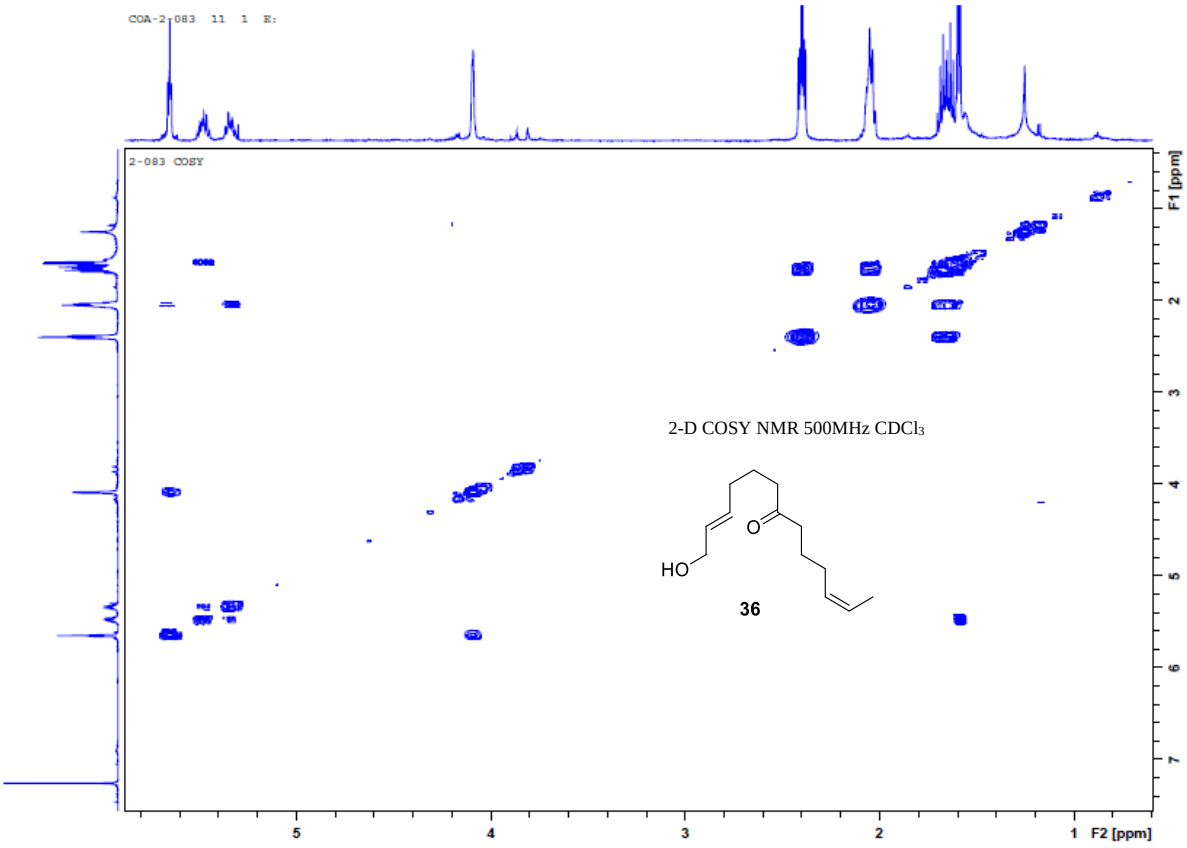
COA-2-083 11 1 E:
2-083 COSY
F1 [ppm]
F2 [ppm]
2-D COSY NMR 500MHz $CDCl_3$
HO
O
36

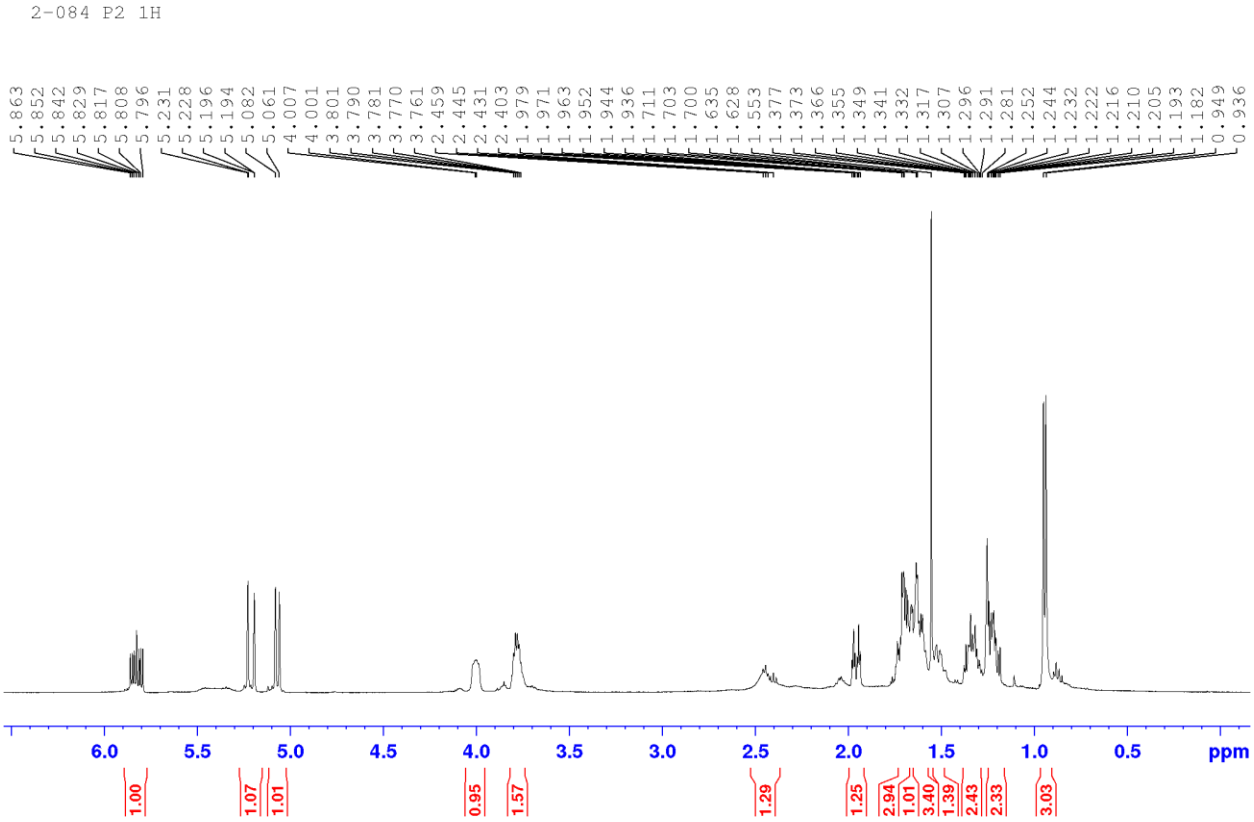

.

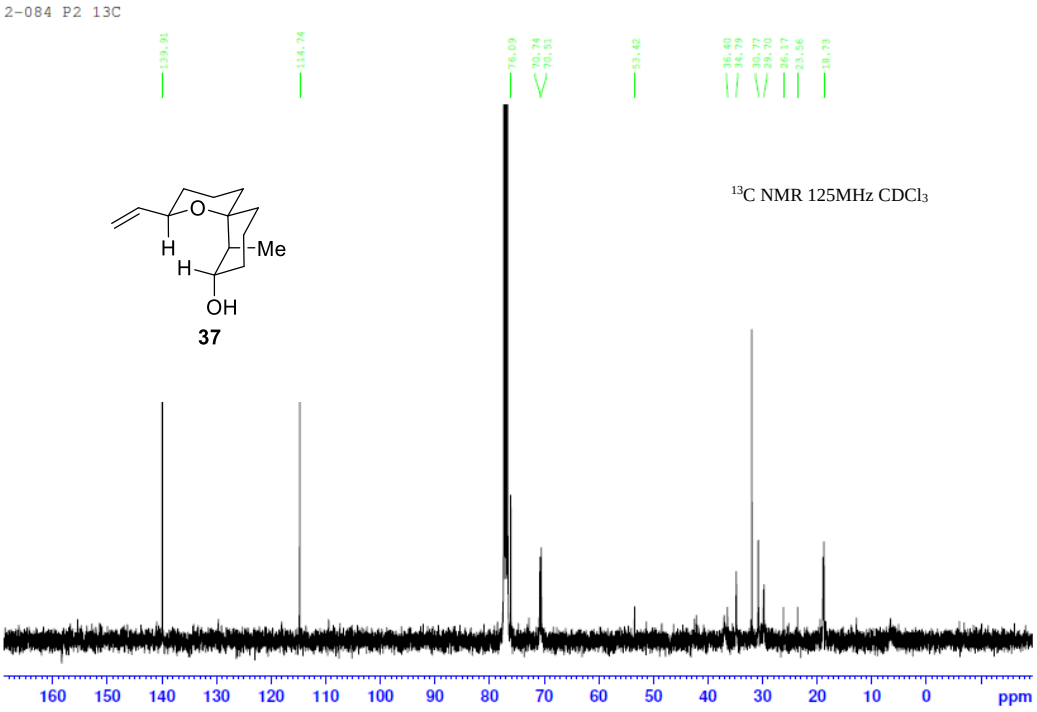

37

^{13}C NMR 125MHz $CDCl_3$

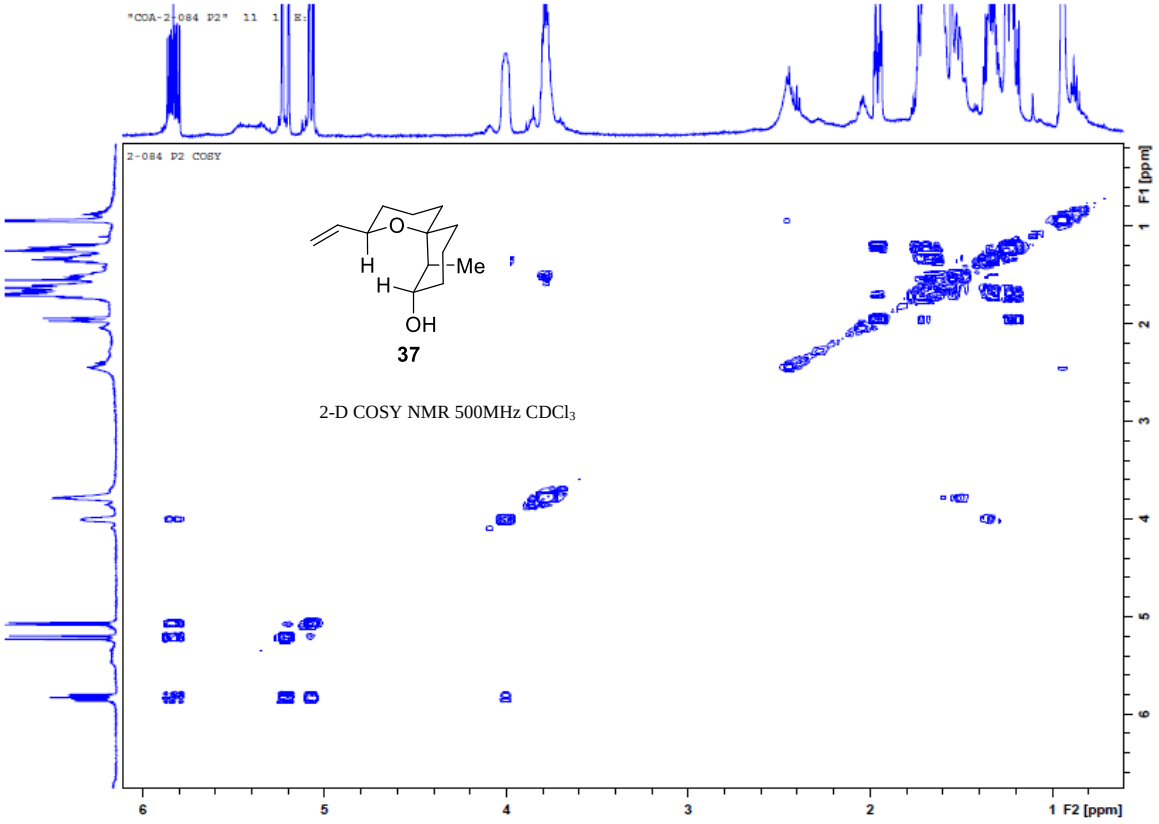

37

2-D COSY NMR 500MHz $CDCl_3$

2-084 P1 1H

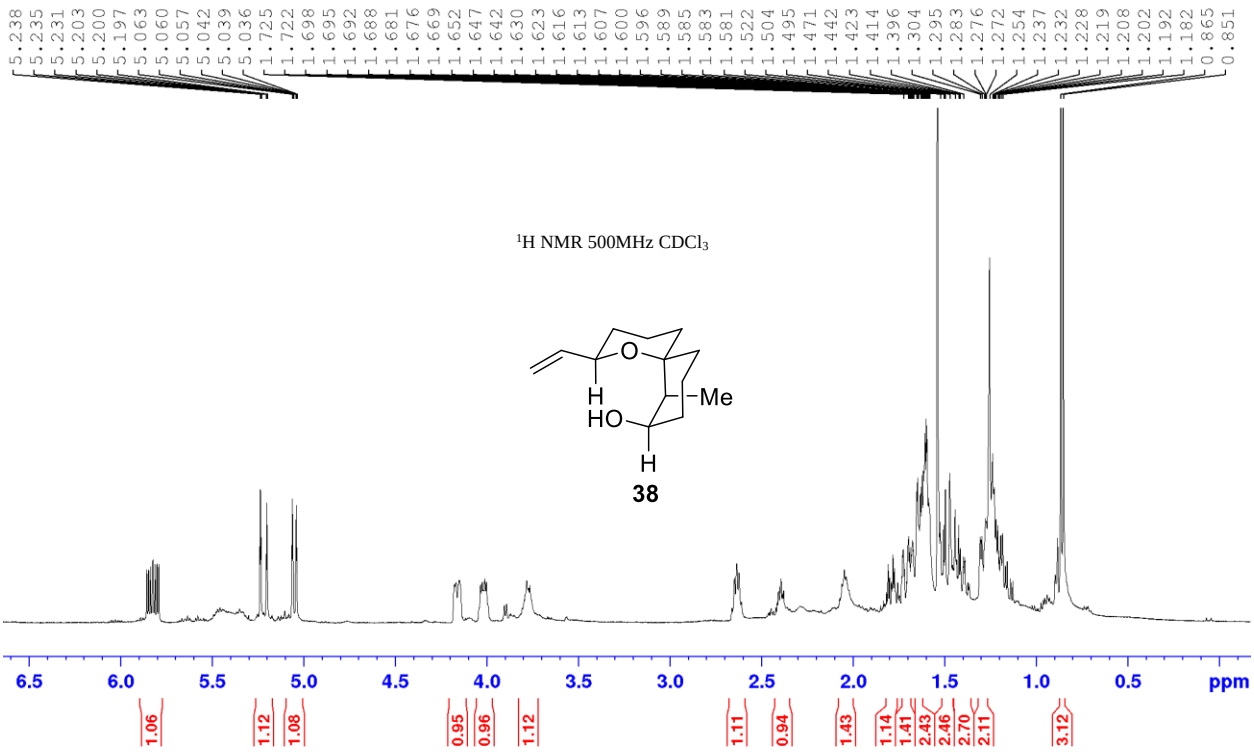

^{1}H NMR 500MHz $CDCl_3$

38

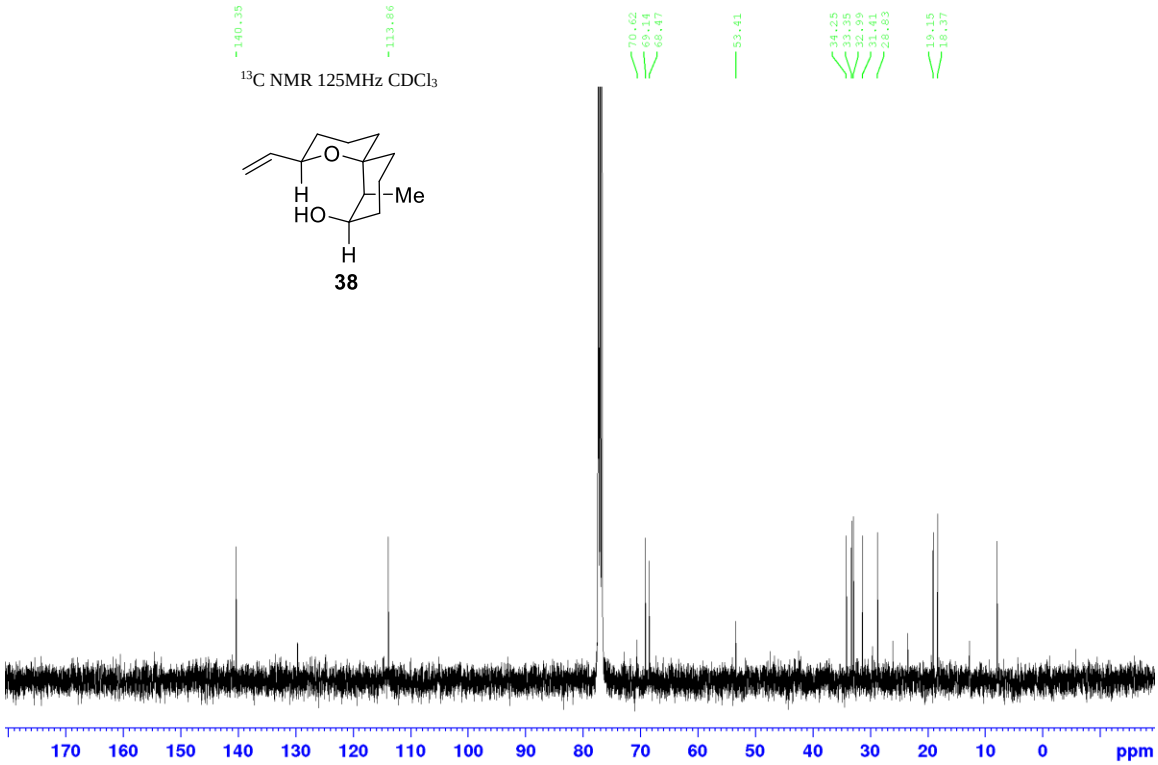

^{13}C NMR 125MHz $CDCl_3$

38

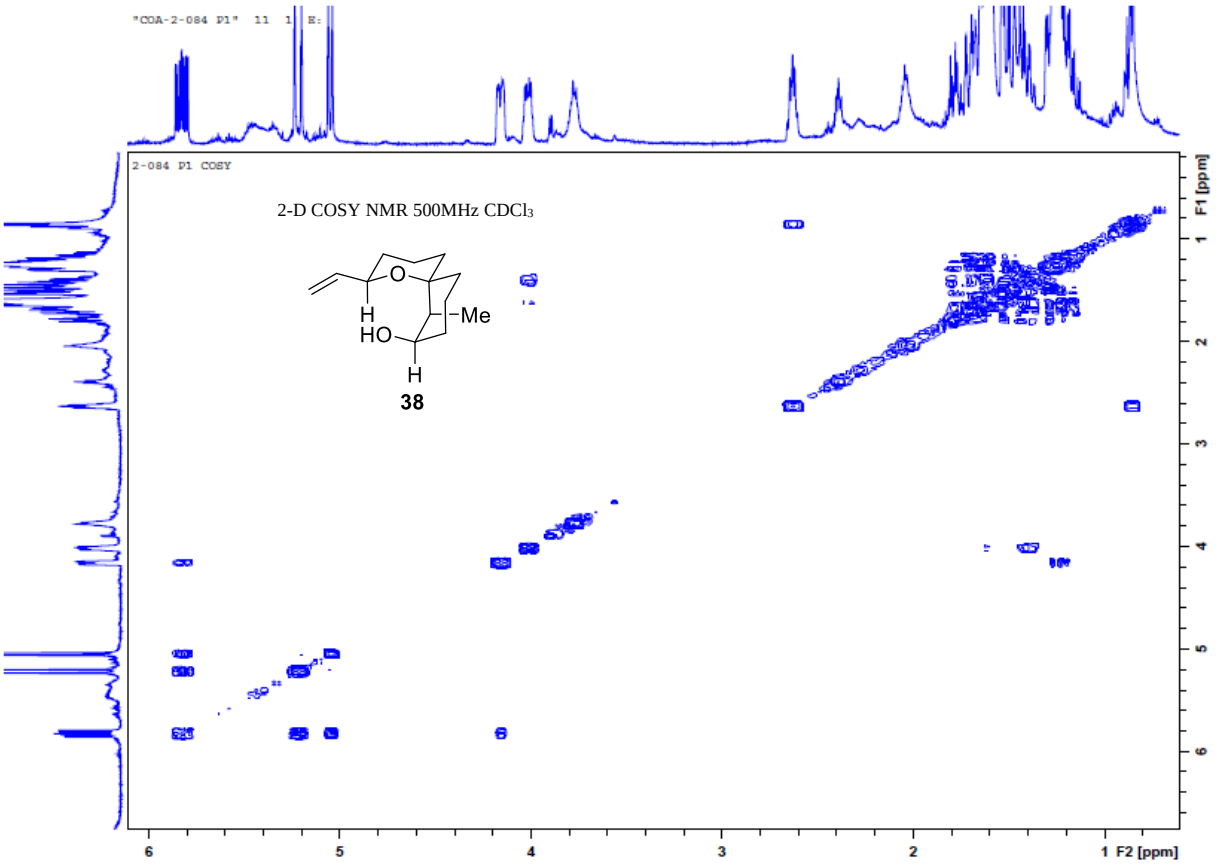
"COA-2-084 P1" 11 1 E:
2-084 P1 COSY
2-D COSY NMR 500MHz CDCl3
O
H
HO
H
Me
38
F1 [ppm]
F2 [ppm]
1
2
3
4
5
6

APPENDIX B (SPECTROSCOPIC DATA FOR CHAPTER 2)

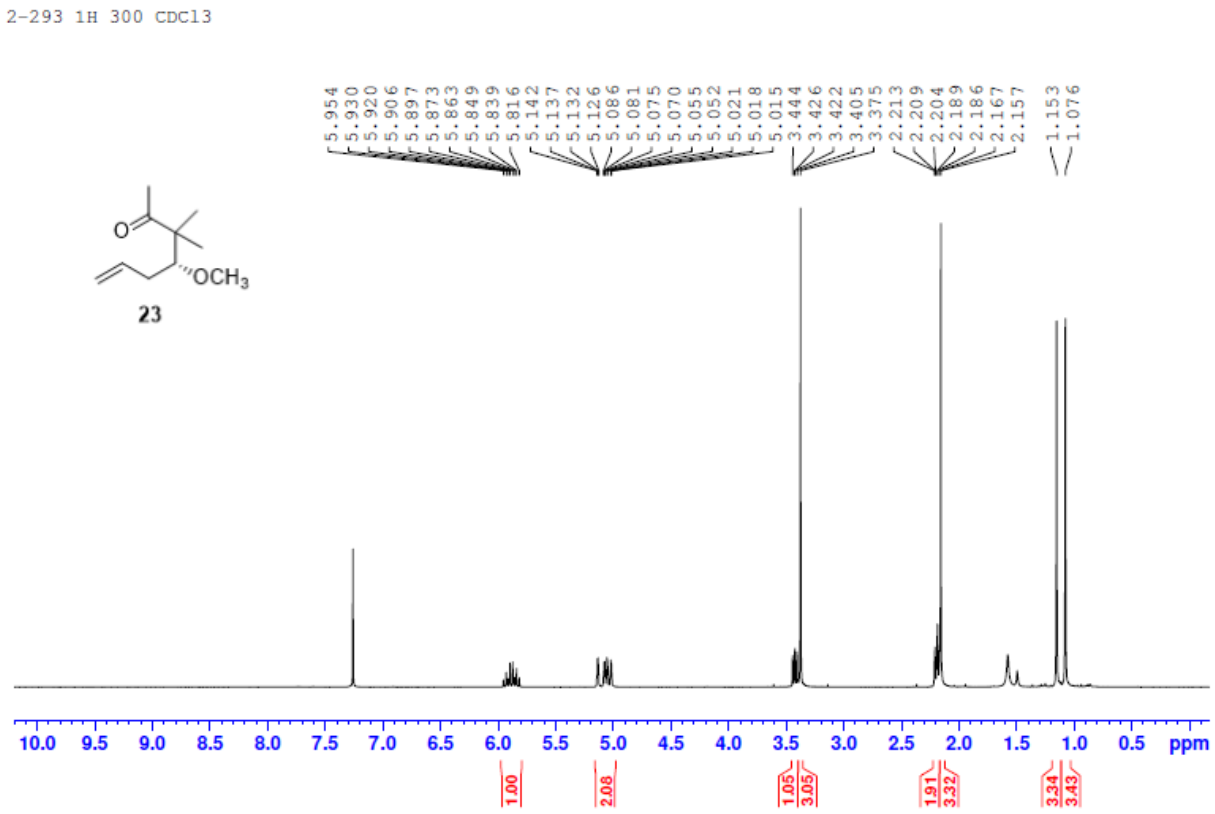

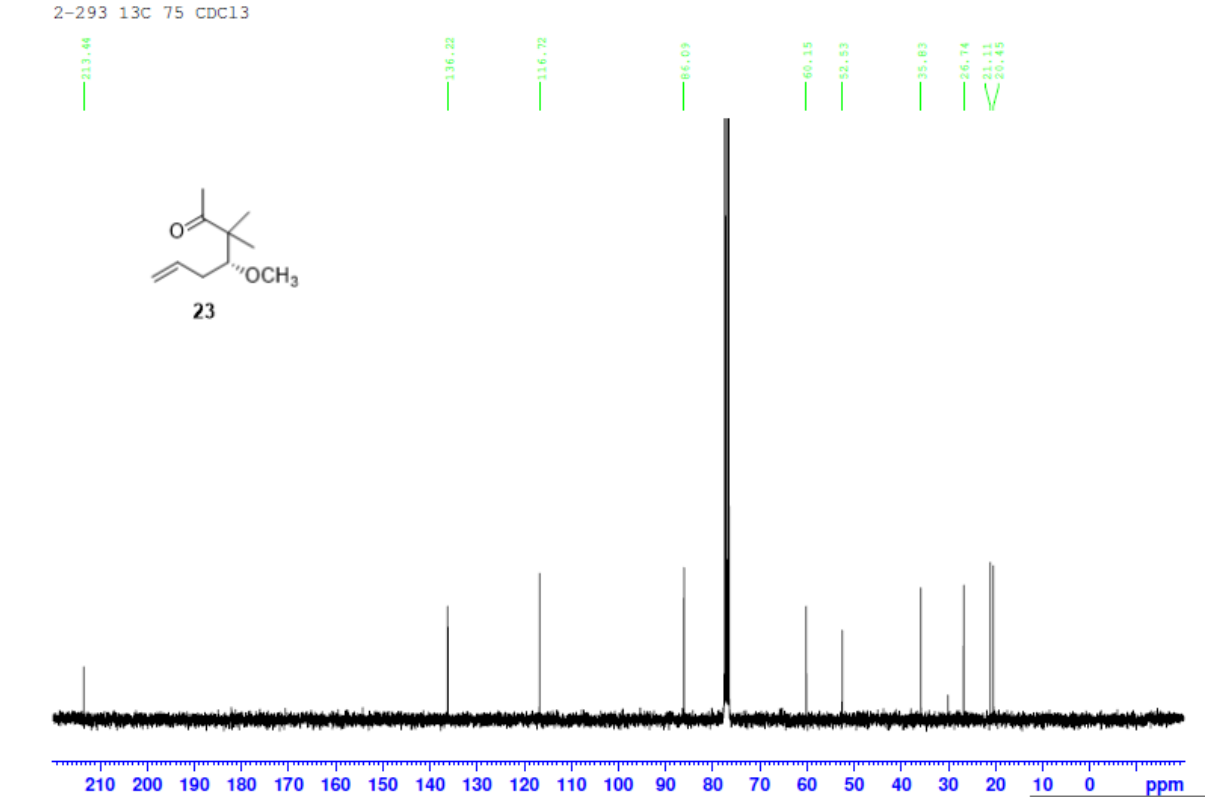
2-293 13C 75 CDCl3
213.44
136.22
116.72
86.09
60.15
52.53
35.83
26.74
21.11
20.45
O
OCH3
23
210 200 190 180 170 160 150 140 130 120 110 100 90 80 70 60 50 40 30 20 10 0 ppm

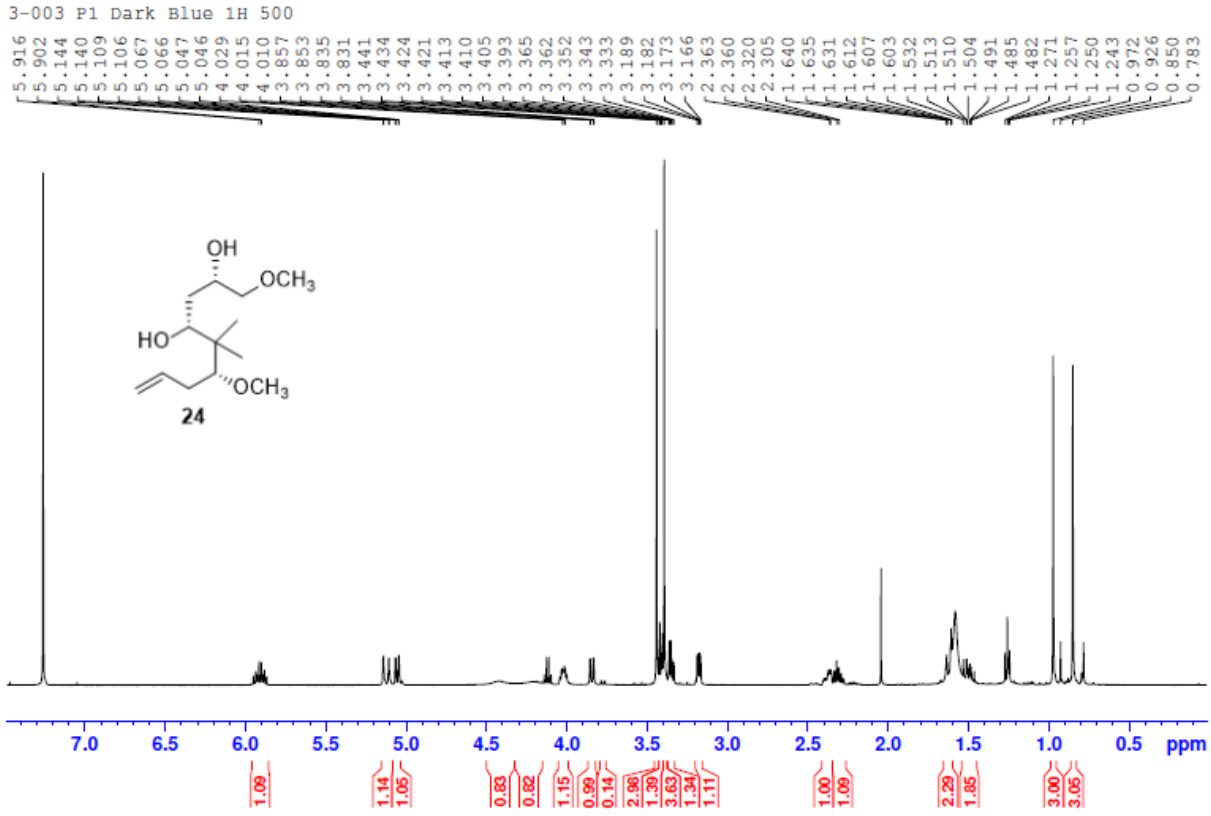
3-003 P1 Dark Blue 1H 500
5.916
5.902
5.144
5.140
5.109
5.106
5.067
5.066
5.047
5.046
4.029
4.015
4.010
3.857
3.853
3.835
3.831
3.441
3.434
3.424
3.421
3.413
3.410
3.405
3.393
3.365
3.362
3.352
3.343
3.333
3.189
3.182
3.173
3.166
2.363
2.360
2.320
2.305
1.640
1.635
1.631
1.612
1.607
1.603
1.532
1.513
1.510
1.504
1.491
1.485
1.482
1.271
1.257
1.250
1.243
0.972
0.926
0.850
0.783
OH
OCH3
HO
OCH3
24
7.0 6.5 6.0 5.5 5.0 4.5 4.0 3.5 3.0 2.5 2.0 1.5 1.0 0.5 ppm
1.09
1.14
1.05
0.83
0.82
1.15
0.99
0.14
2.96
1.39
3.63
1.34
1.11
1.00
1.08
2.29
1.85
3.00
3.05

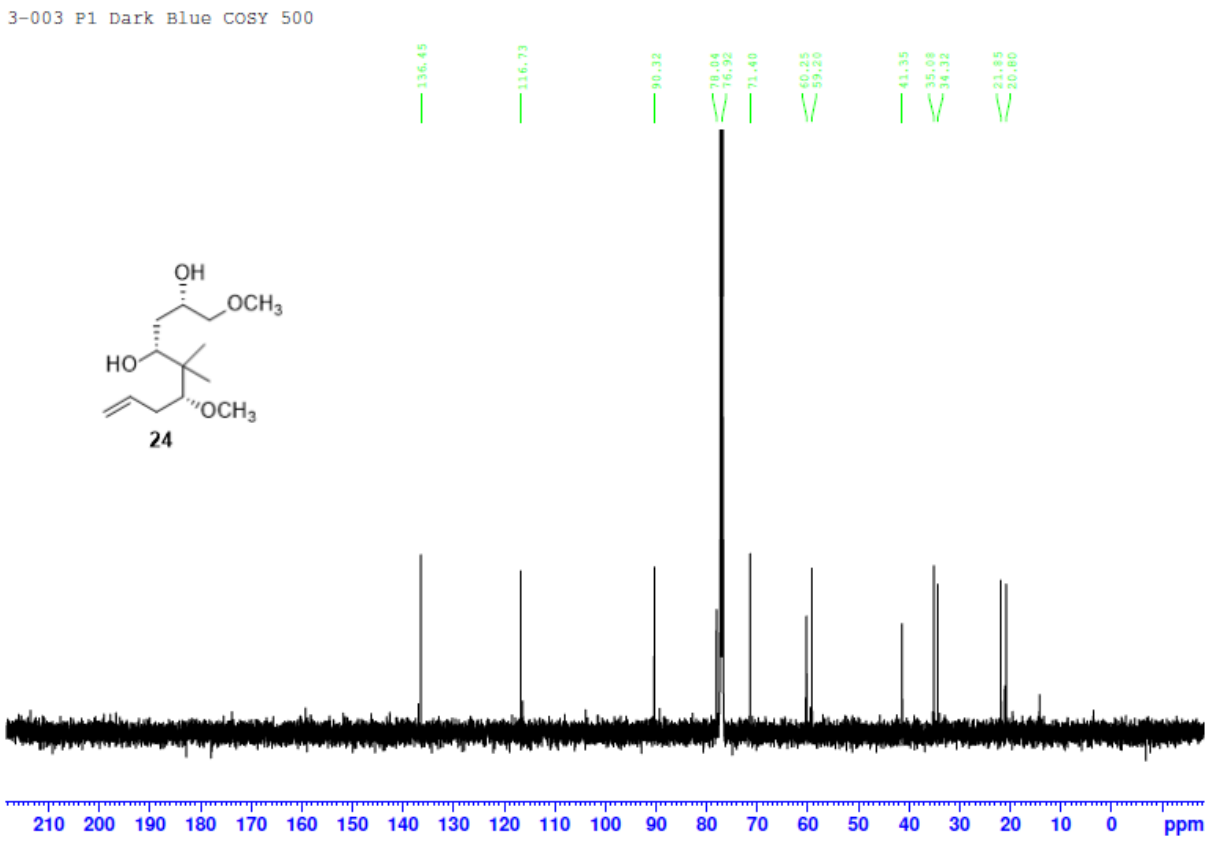
3-003 P1 Dark Blue COSY 500
136.45
116.73
90.32
78.04
76.92
71.40
60.25
59.20
41.35
35.08
34.32
21.85
20.80
OH
OCH3
HO
OCH3
24
210 200 190 180 170 160 150 140 130 120 110 100 90 80 70 60 50 40 30 20 10 0 ppm

3-032 P1 1H 500

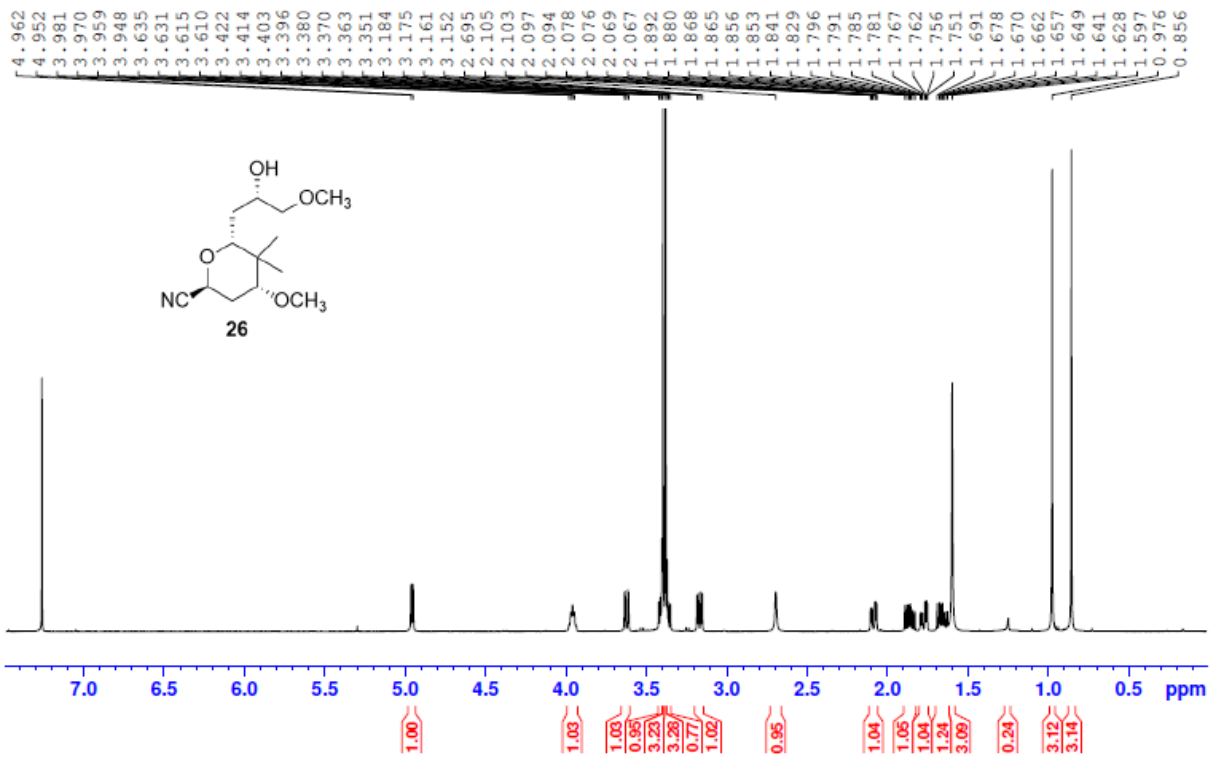

3-032 P1 13C 125

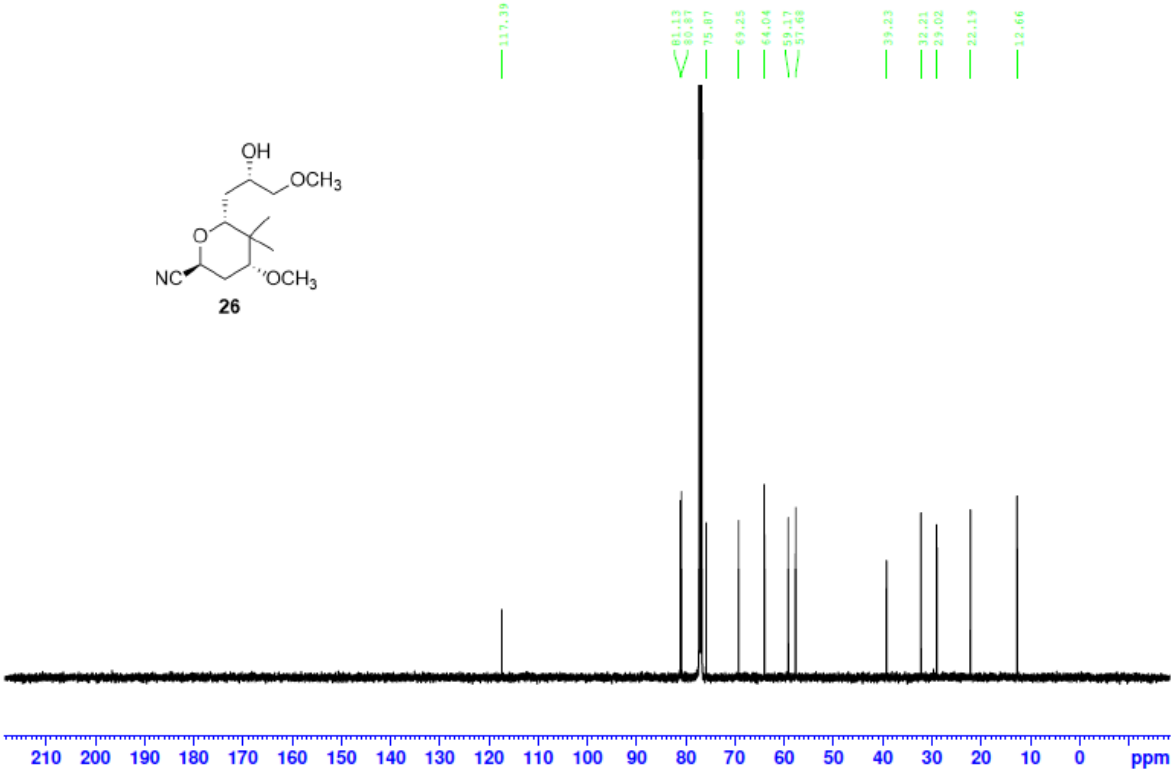

3-033 1H 500

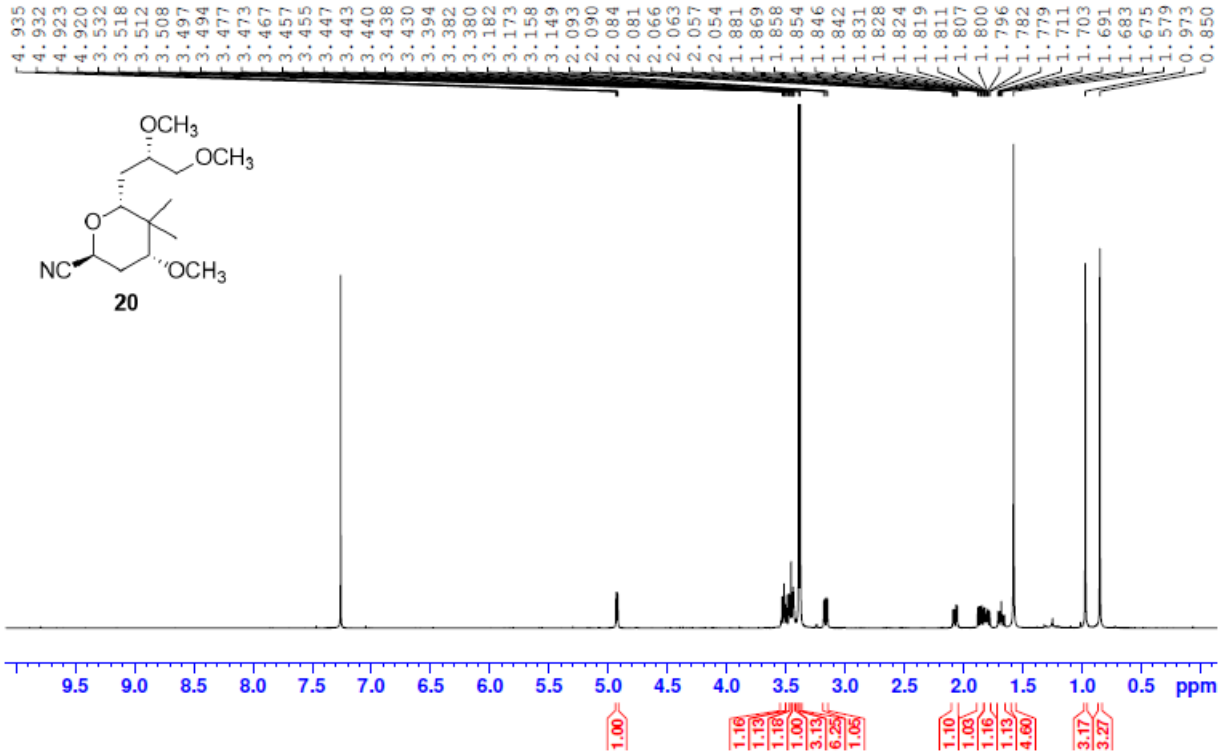
4.935
4.932
4.923
4.920
3.532
3.518
3.512
3.508
3.497
3.494
3.477
3.473
3.467
3.457
3.455
3.447
3.443
3.440
3.438
3.430
3.394
3.382
3.380
3.182
3.173
3.158
3.149
2.093
2.090
2.084
2.081
2.066
2.063
2.057
2.054
1.881
1.869
1.858
1.854
1.846
1.842
1.831
1.828
1.824
1.819
1.811
1.807
1.800
1.796
1.782
1.779
1.711
1.703
1.691
1.683
1.675
1.579
0.973
0.850
OCH3
OCH3
O
NC
OCH3
20
9.5
9.0
8.5
8.0
7.5
7.0
6.5
6.0
5.5
5.0
4.5
4.0
3.5
3.0
2.5
2.0
1.5
1.0
0.5
ppm
1.00
1.16
1.13
1.18
1.00
3.13
6.25
1.05
1.10
1.08
1.16
1.13
4.60
3.17
3.27

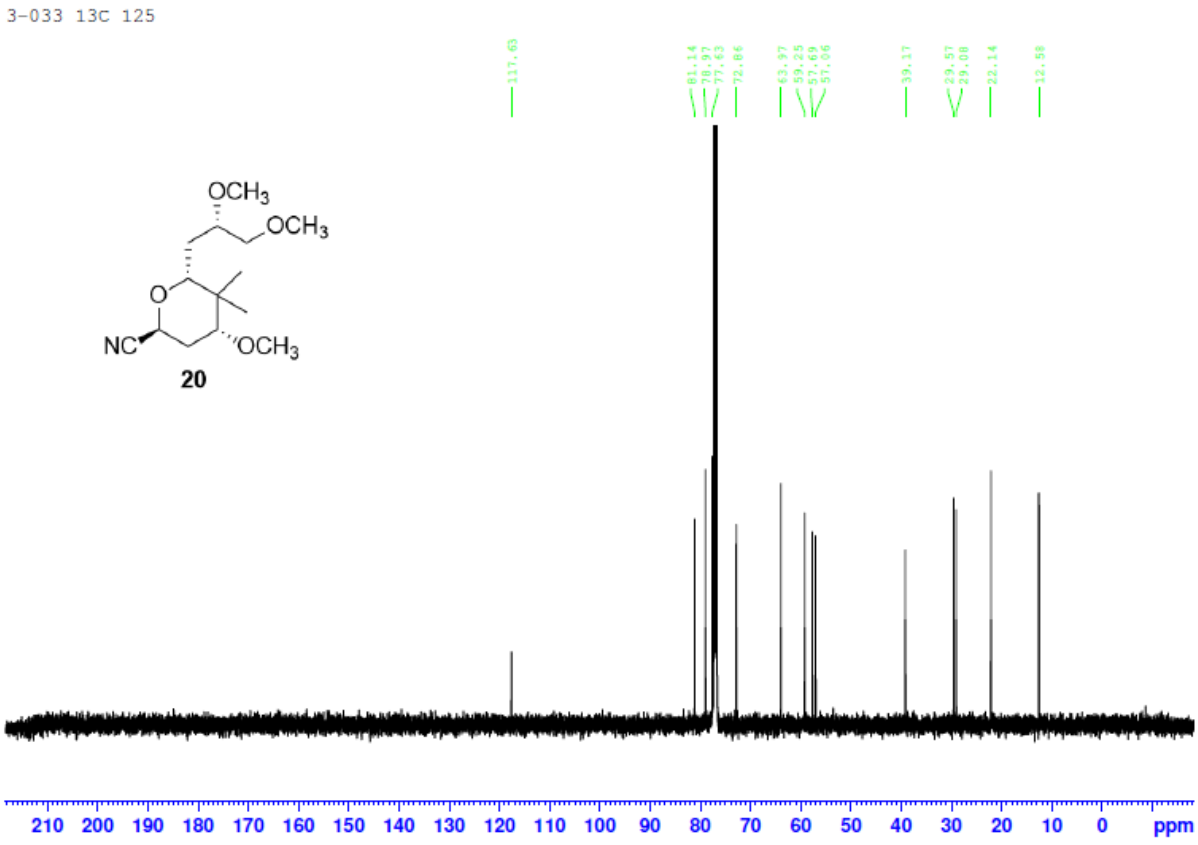
3-033 13C 125
117.63
81.14
78.97
77.63
72.66
63.97
59.25
57.69
57.06
39.17
29.57
29.08
22.14
12.58
OCH3
OCH3
O
NC
OCH3
20
210 200 190 180 170 160 150 140 130 120 110 100 90 80 70 60 50 40 30 20 10 0 ppm

3-055 Recrystallized 1H 500

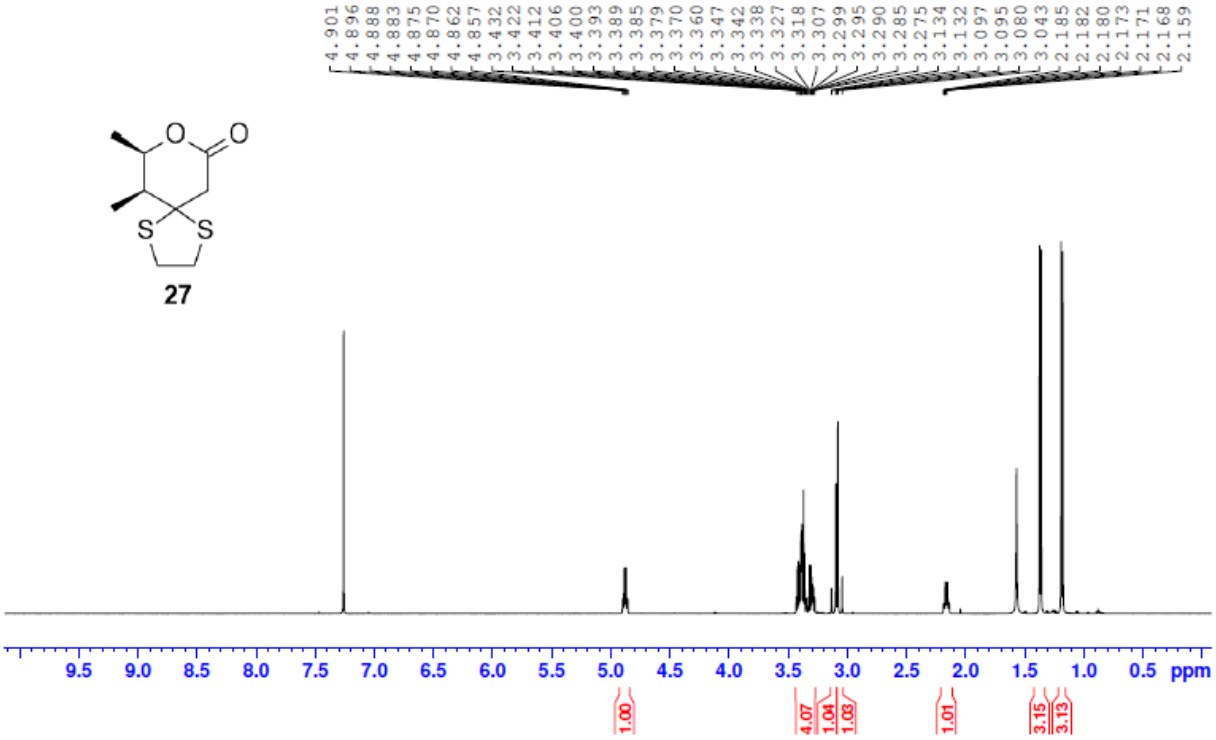

27

3-055 Recrystallized 13C 125

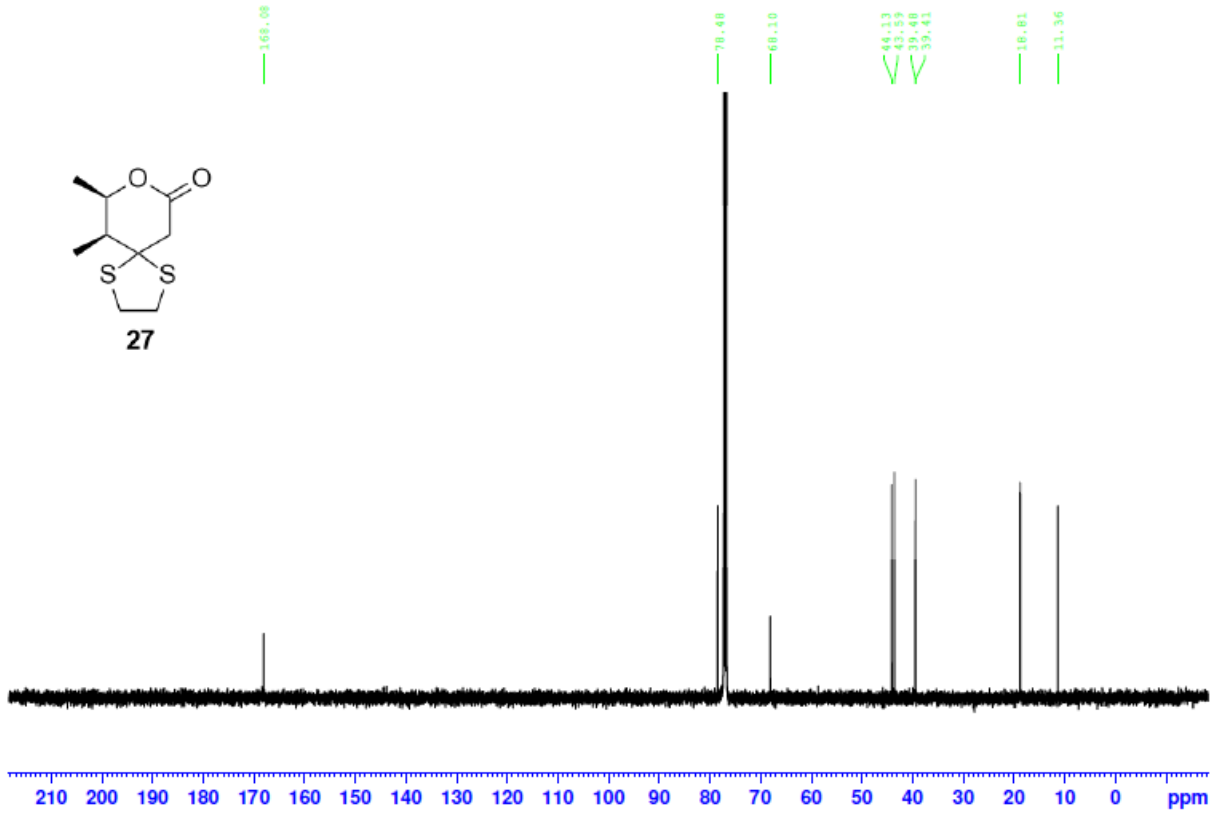

27

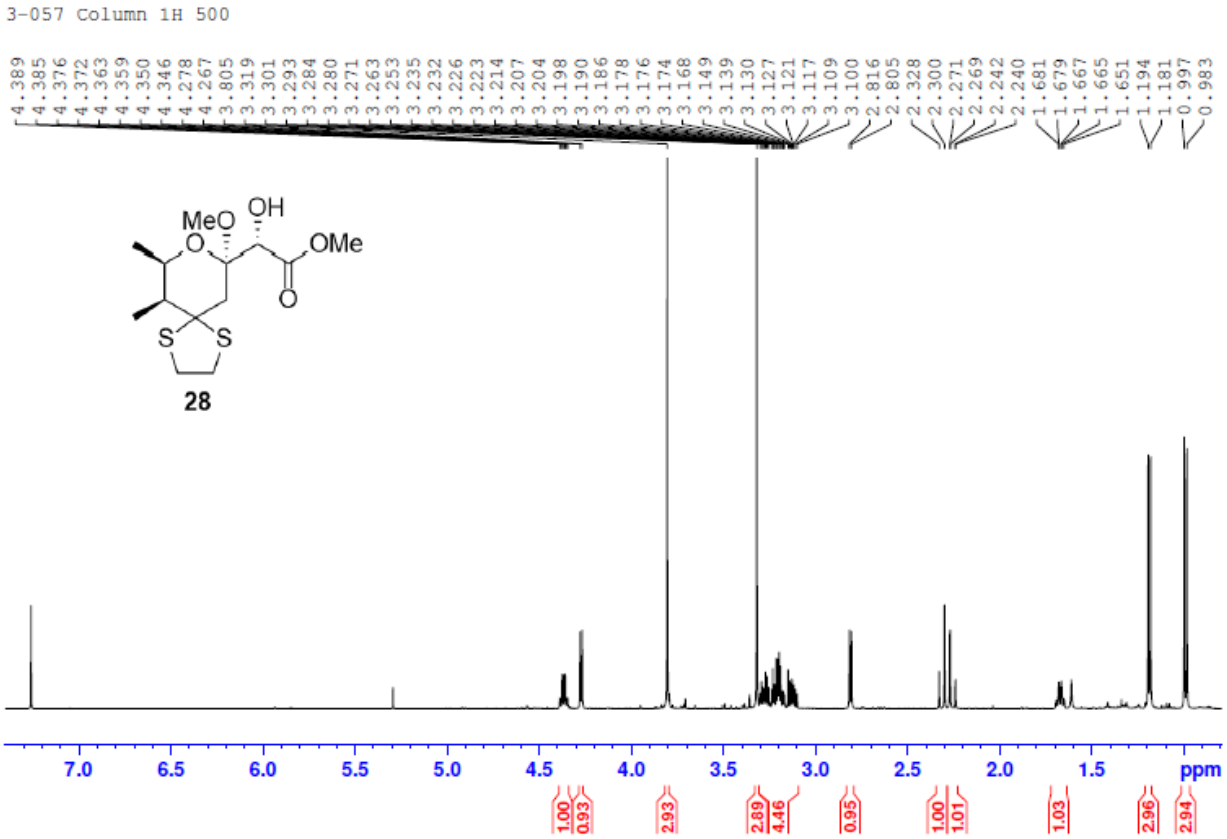
3-057 Column 1H 500
4.389
4.385
4.376
4.372
4.363
4.359
4.350
4.346
4.278
4.267
3.805
3.319
3.301
3.293
3.284
3.280
3.271
3.263
3.253
3.235
3.232
3.226
3.223
3.214
3.207
3.204
3.198
3.190
3.186
3.178
3.176
3.174
3.168
3.149
3.139
3.130
3.127
3.121
3.117
3.109
3.100
2.816
2.805
2.328
2.300
2.271
2.269
2.242
2.240
1.681
1.679
1.667
1.665
1.651
1.194
1.181
0.997
0.983
MeO
OH
OMe
O
O
S
S
28
7.0
6.5
6.0
5.5
5.0
4.5
4.0
3.5
3.0
2.5
2.0
1.5
ppm
1.00
0.93
2.93
2.89
4.46
0.95
1.00
1.01
1.03
2.96
2.94

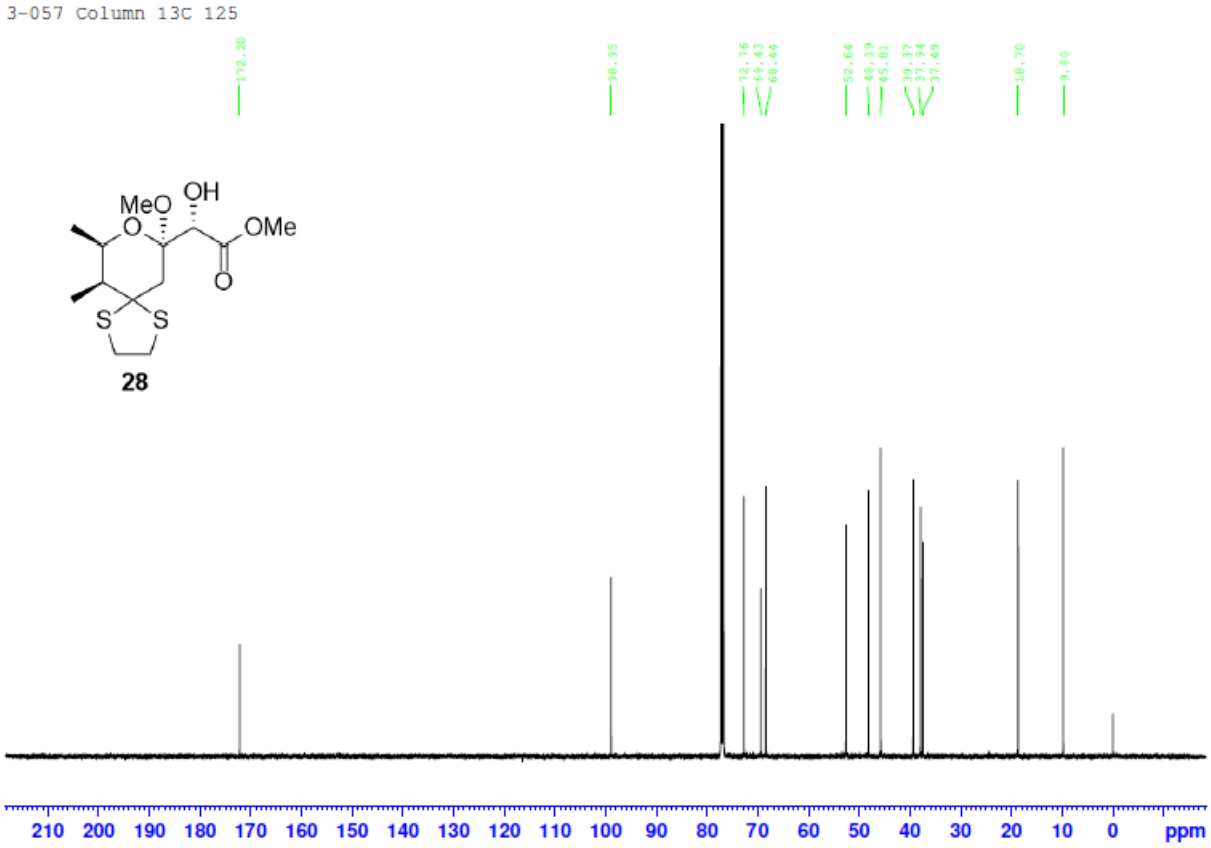
3-057 Column 13C 125
172.20
90.95
72.76
69.43
68.44
52.64
48.19
45.81
39.37
37.94
37.49
18.70
9.80
MeO
OH
OMe
O
O
S
S
28
210 200 190 180 170 160 150 140 130 120 110 100 90 80 70 60 50 40 30 20 10 0 ppm

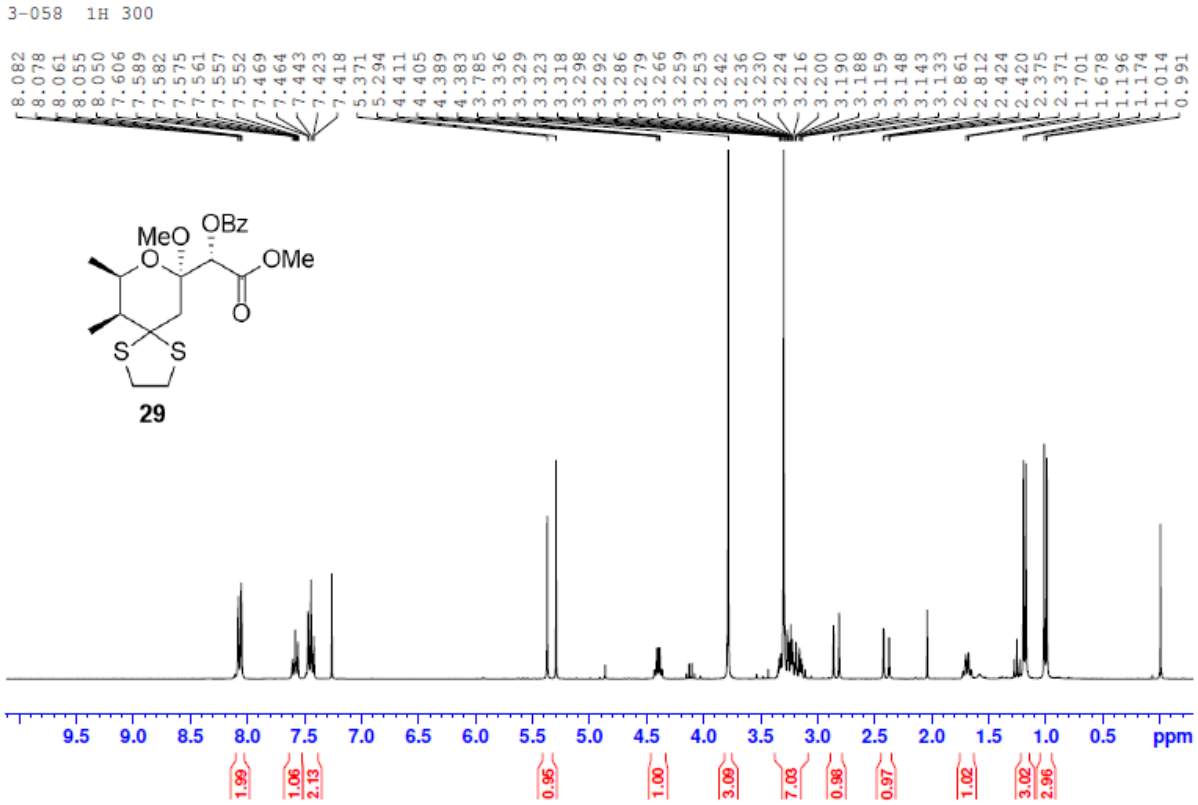
3-058 1H 300
MeO
OBz
OMe
S
S
29
ppm

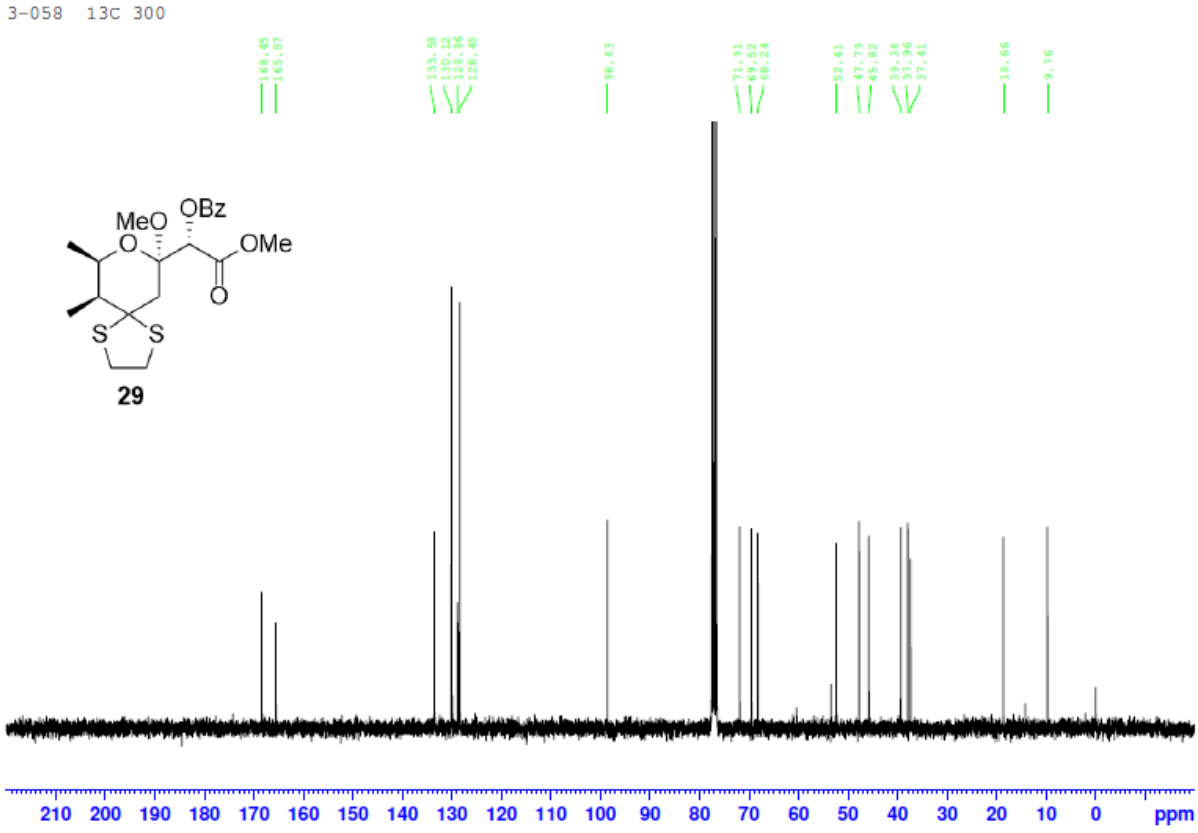
3-058 13C 300
MeO
OBz
OMe
S
S
29
ppm

3-060 Ketone 1H 400

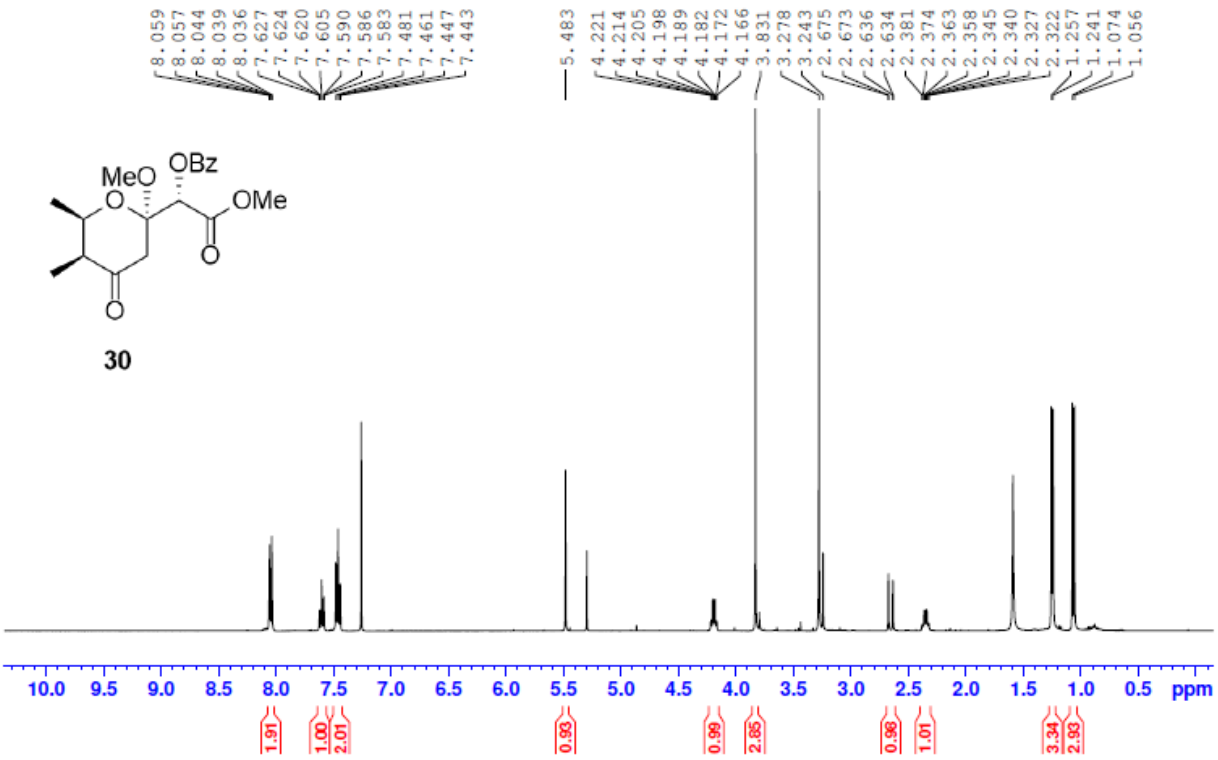

30

3-060 Ketone 1H 400

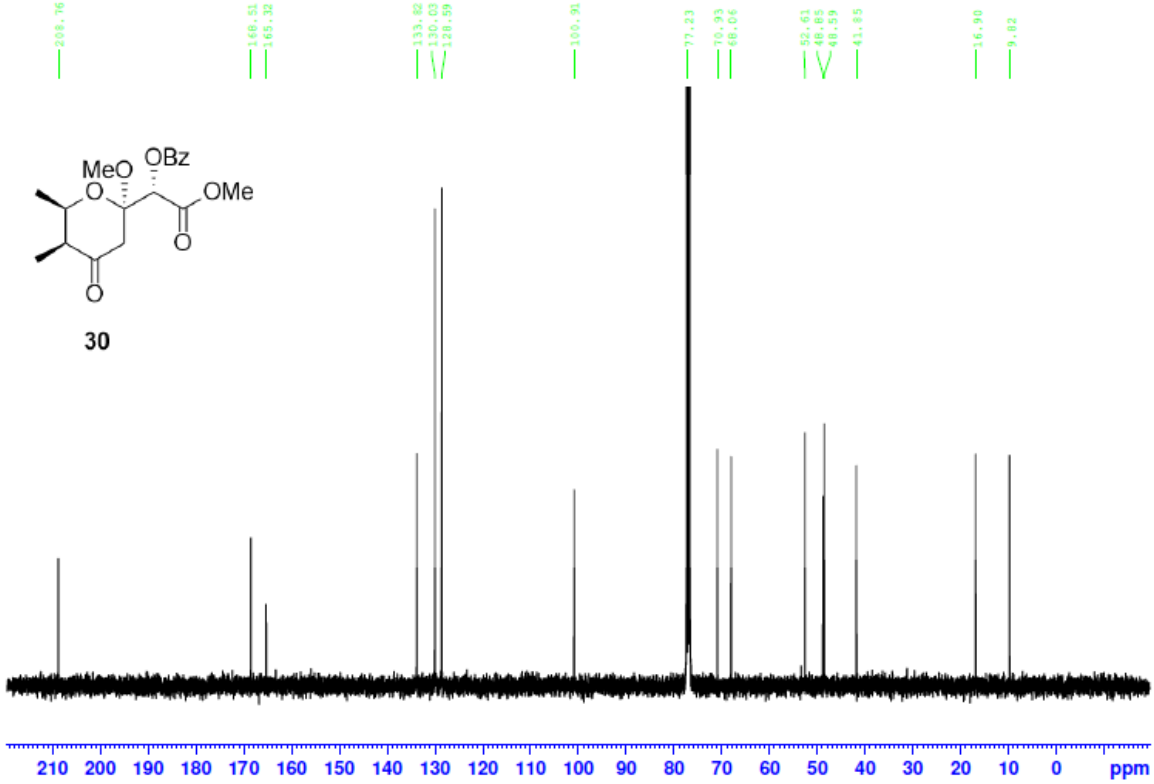

30

3-061 Alkene 1H 400

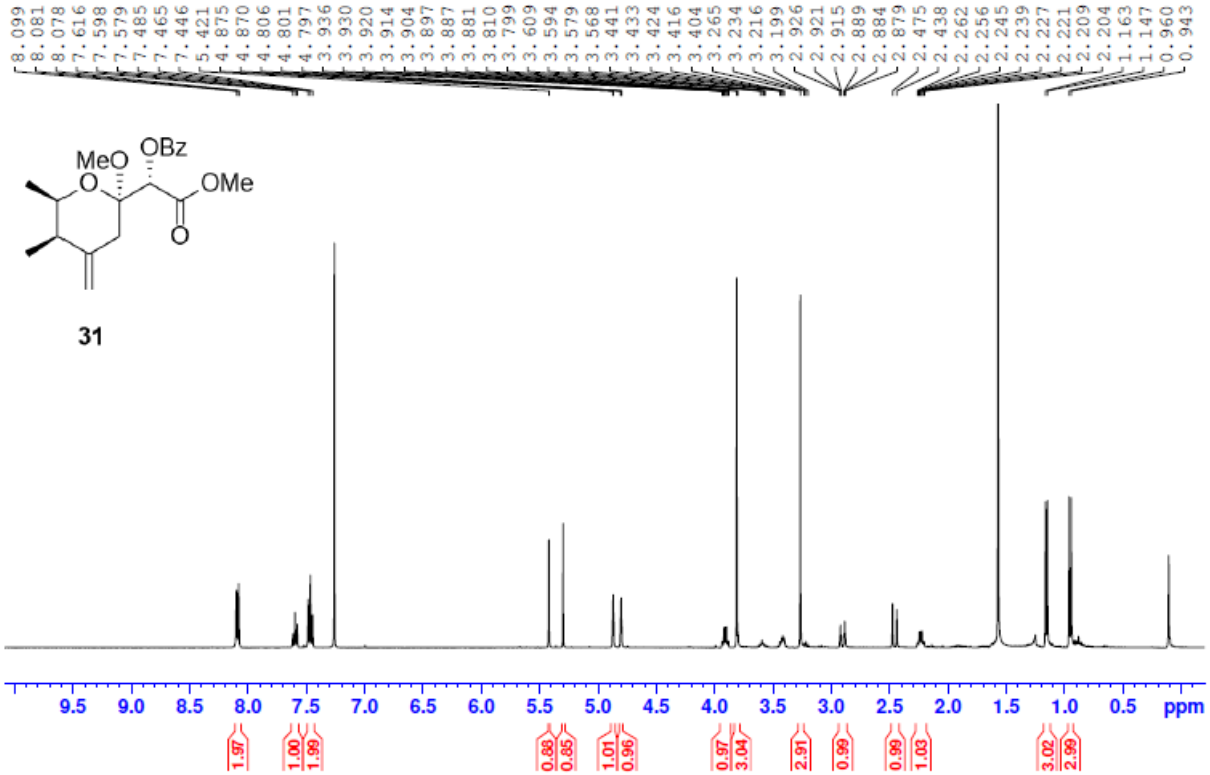

3-061 Alkene 13C 400

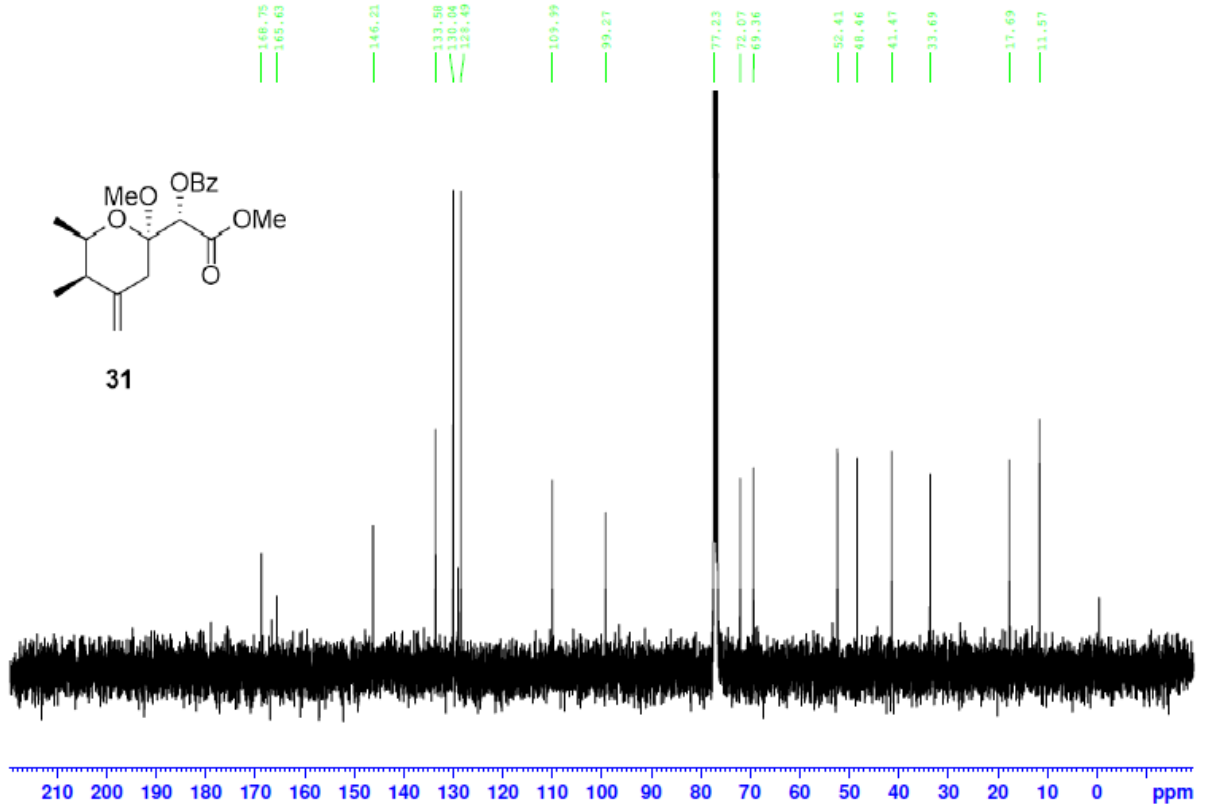

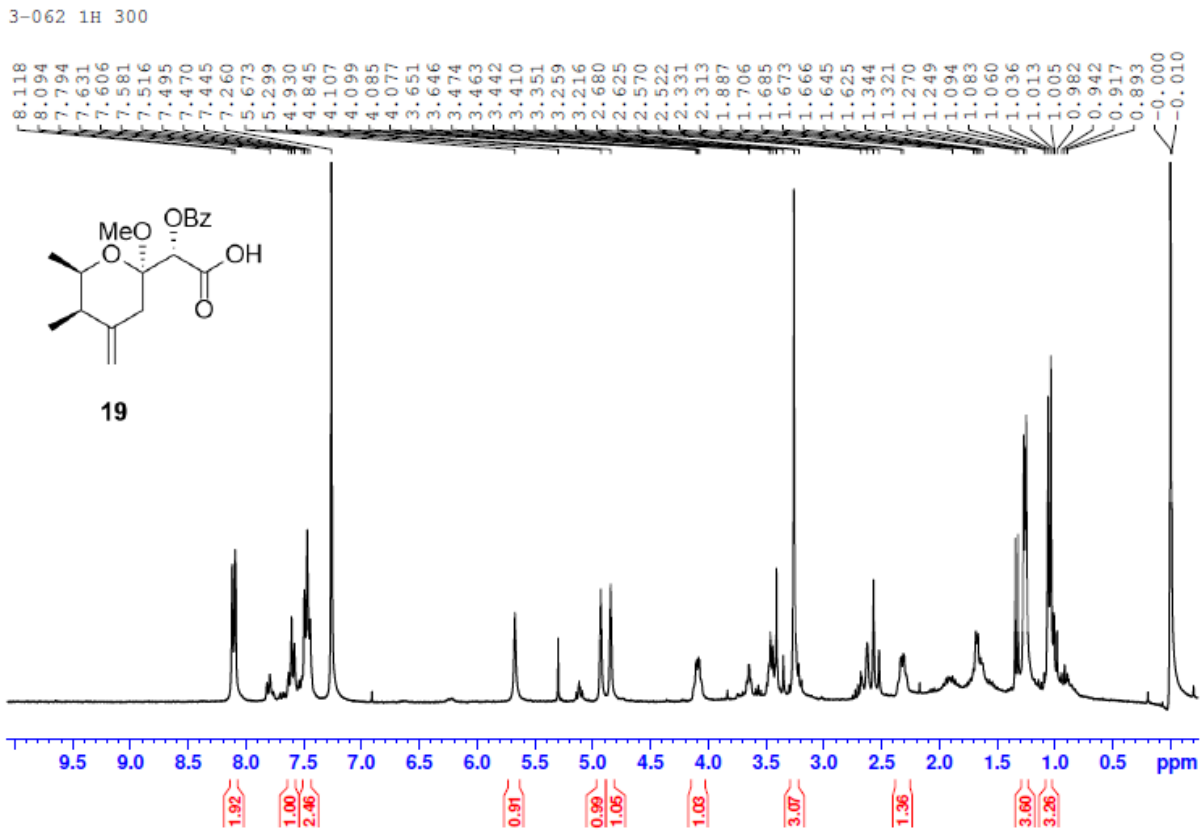
3-062 1H 300
MeO
OBz
OH
O
O
19
ppm

COA-3-102 1H 400 Benzoylated Pdt

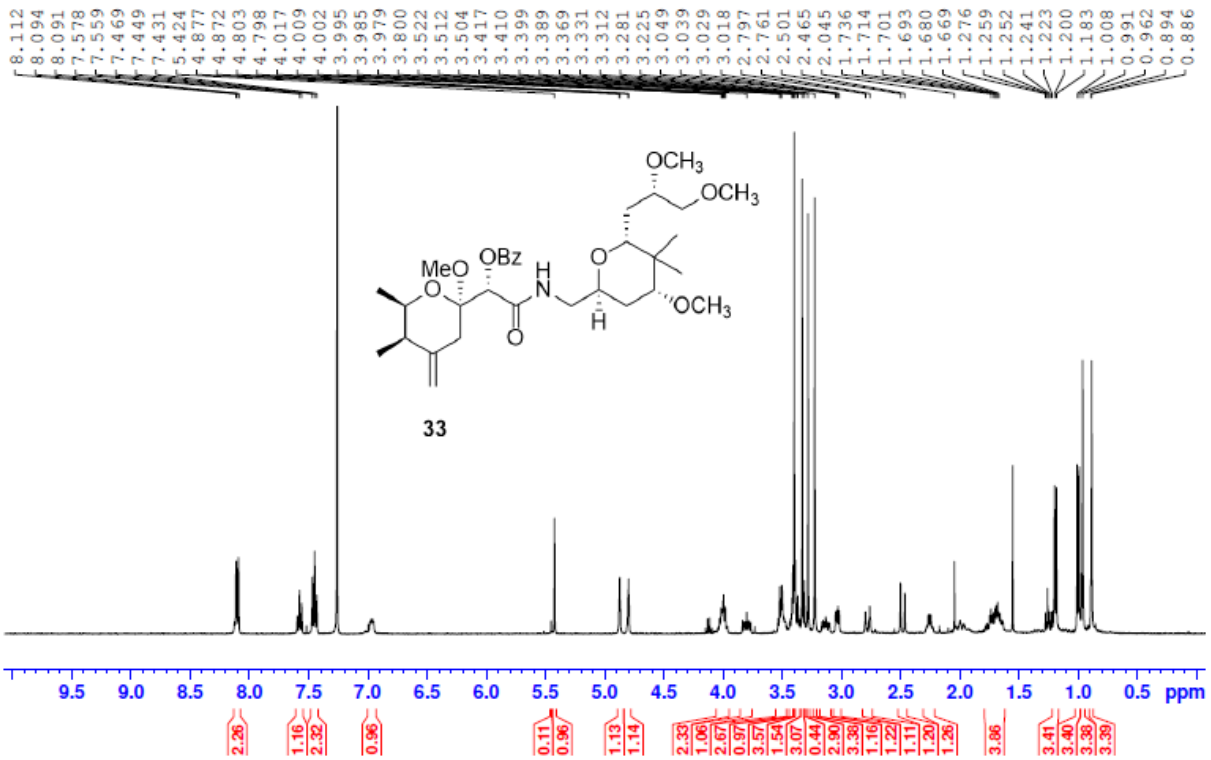

COA-3-102 13C 400 Benzoylated Pdt

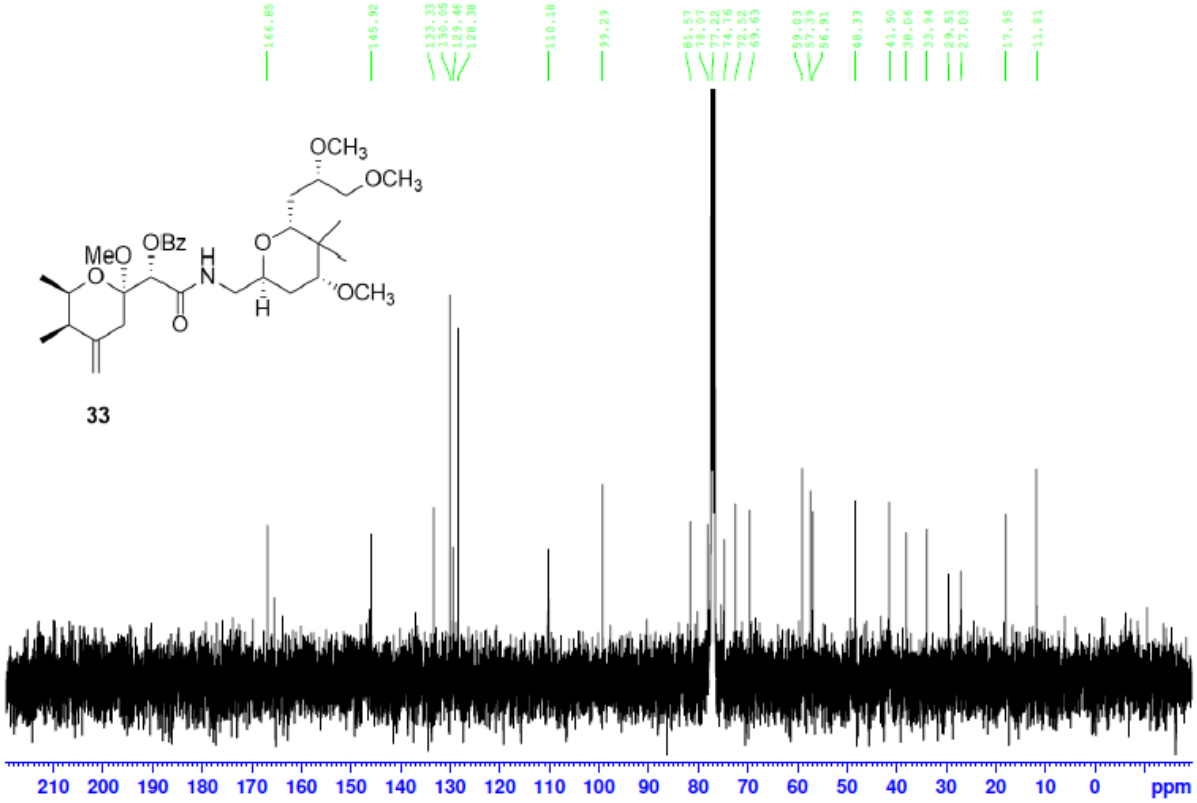

3-217 Ped Analogue 1H

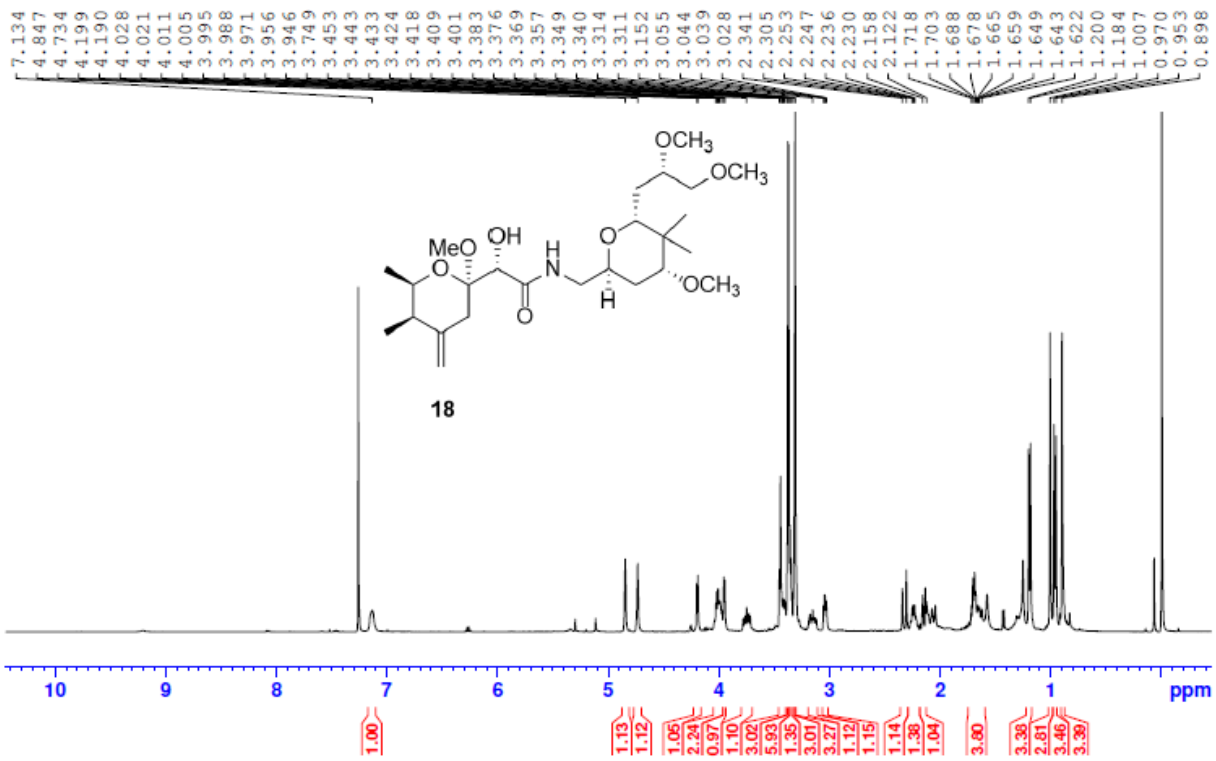

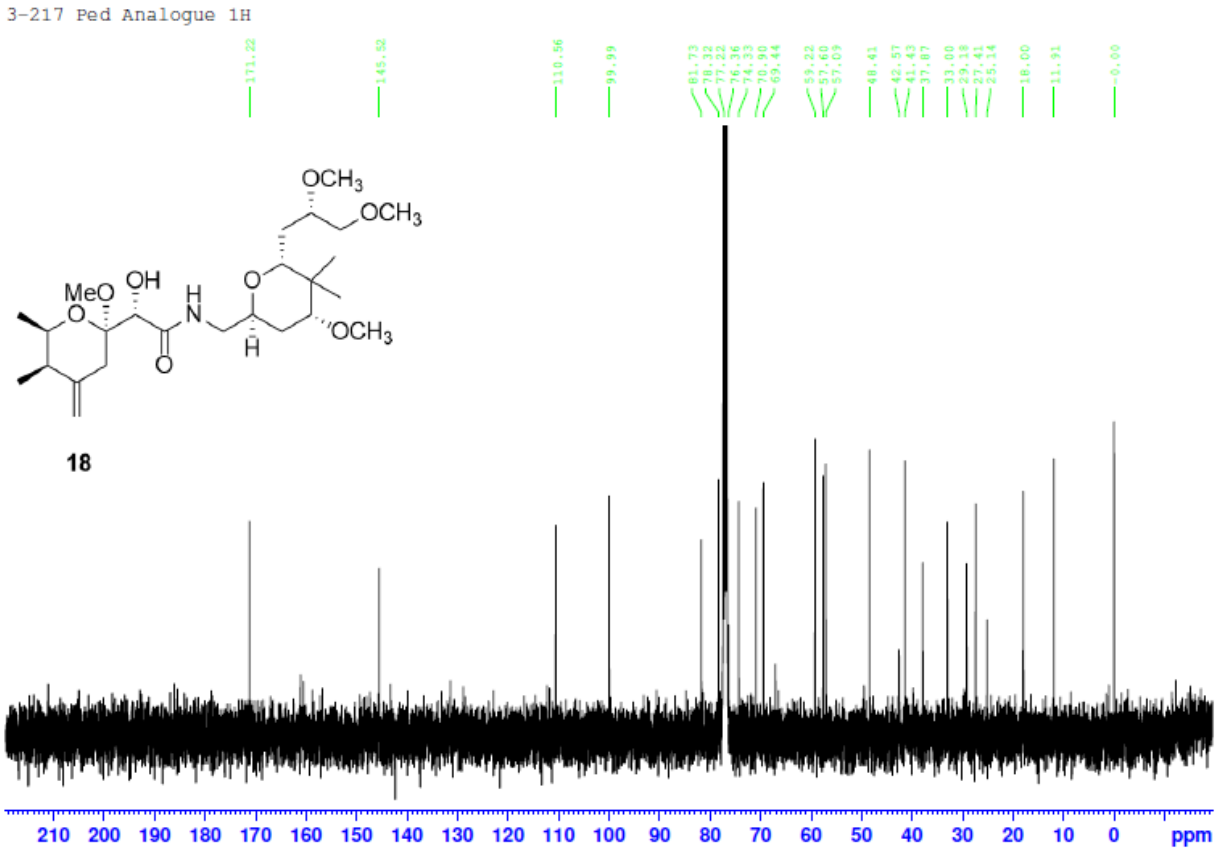
3-217 Ped Analogue 1H
171.22
145.52
110.56
99.99
81.73
78.32
77.22
76.36
74.33
70.90
69.44
59.22
57.60
57.09
48.41
42.57
41.43
37.87
33.00
29.18
27.41
25.14
18.00
11.91
-0.00
OCH3
OCH3
MeO
OH
H
N
O
O
O
H
OCH3
18
210 200 190 180 170 160 150 140 130 120 110 100 90 80 70 60 50 40 30 20 10 0 ppm

COA-3-212 Ped-Allyl C 1H

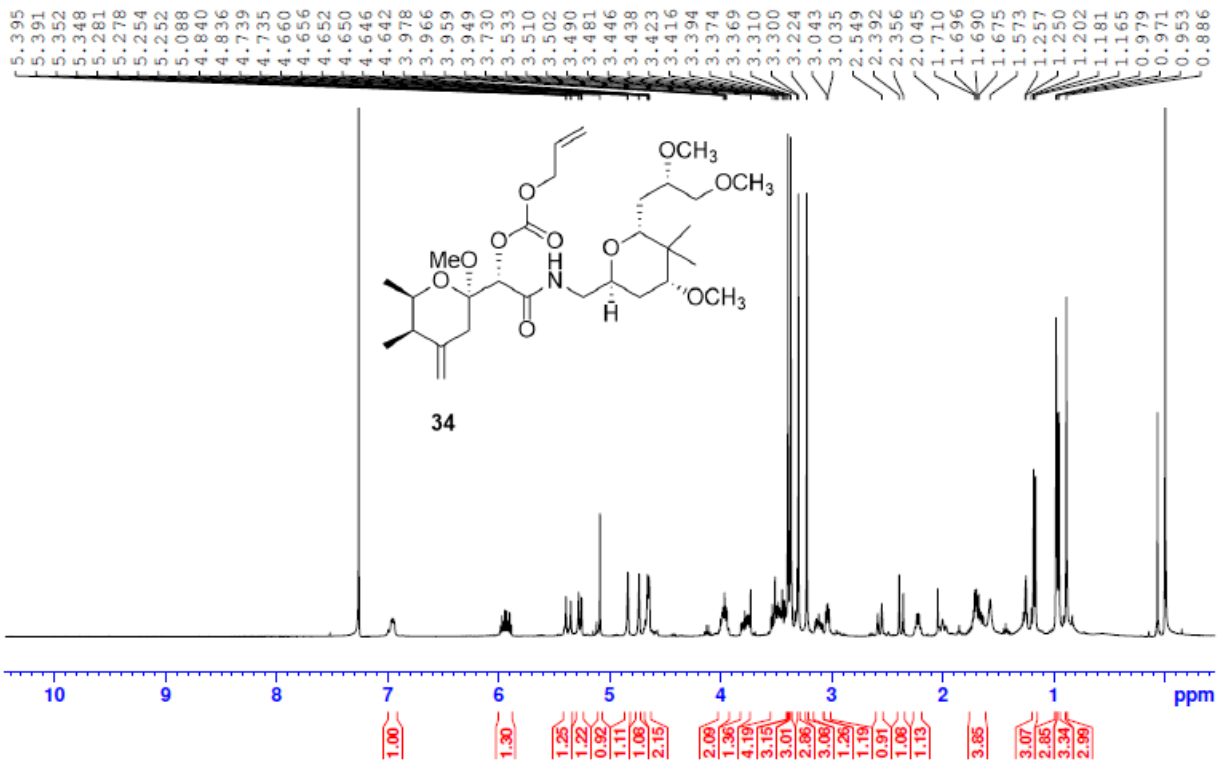

3-Chloroformate

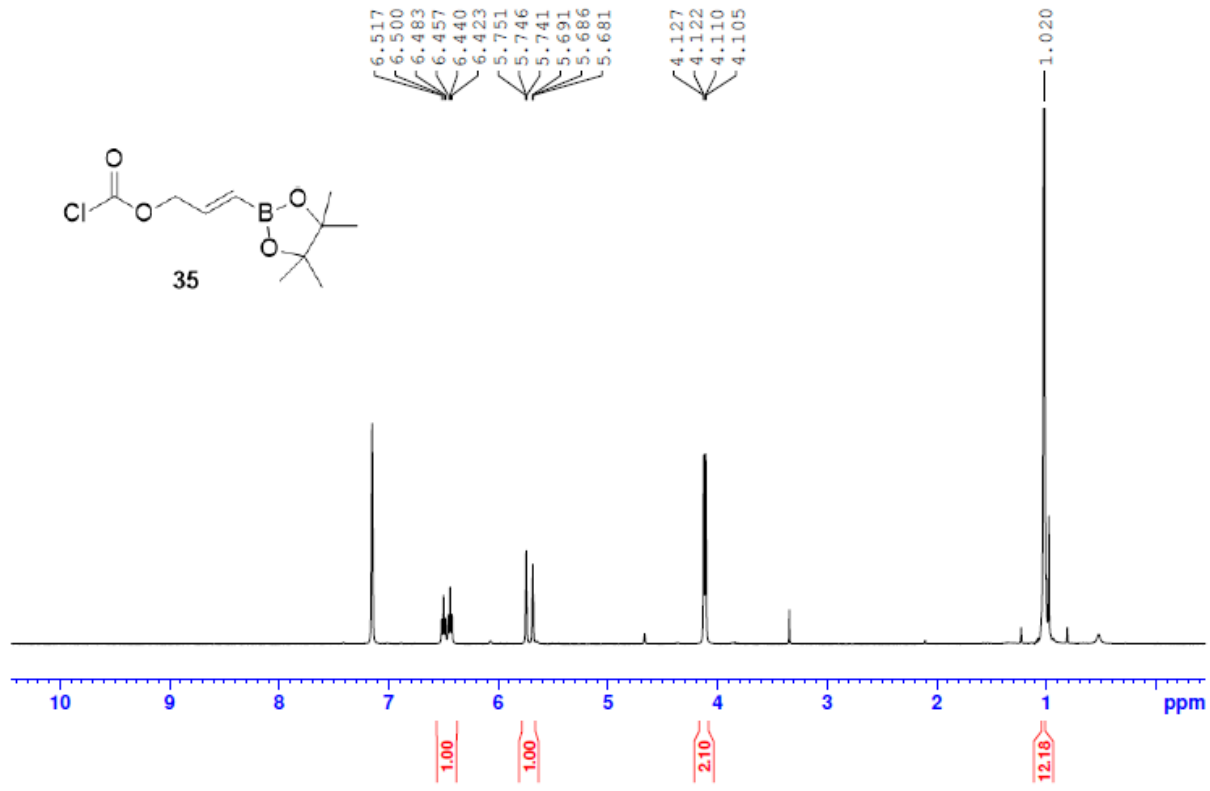

3-220 Ped-Bpin 1H 400

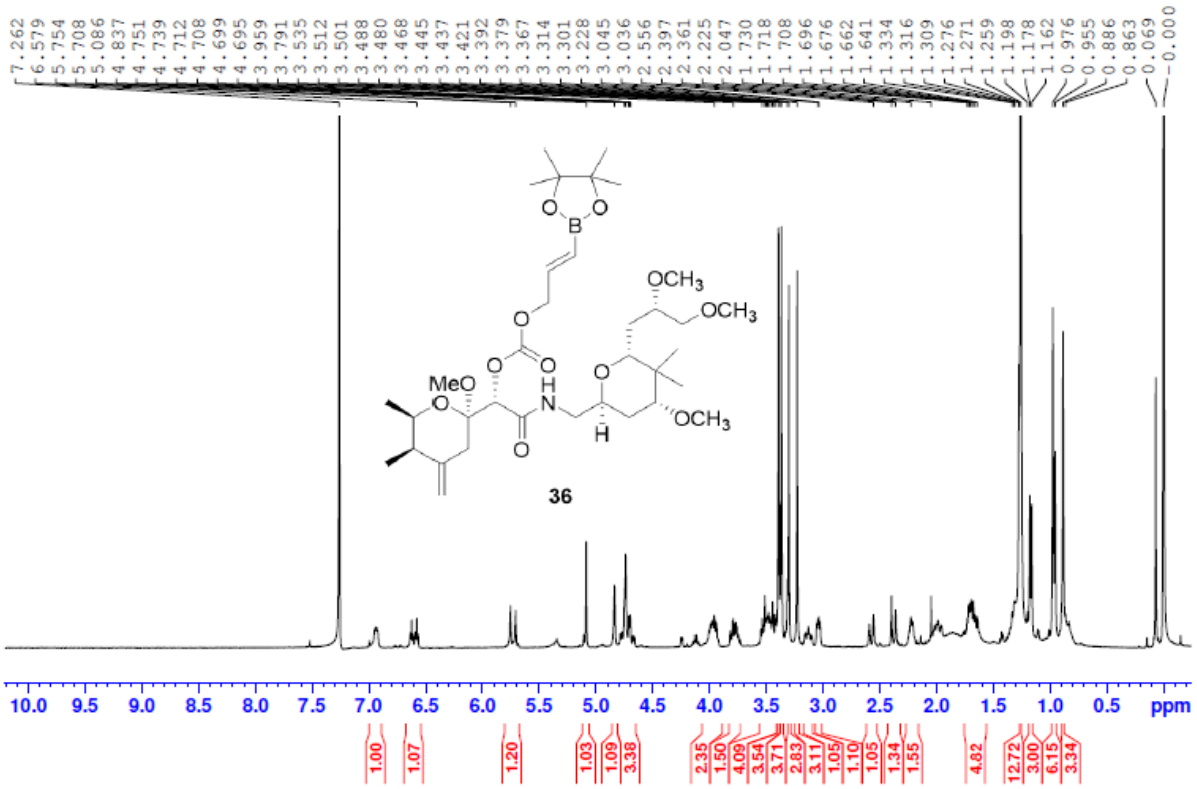

3-211 (2) in C6D6 13C

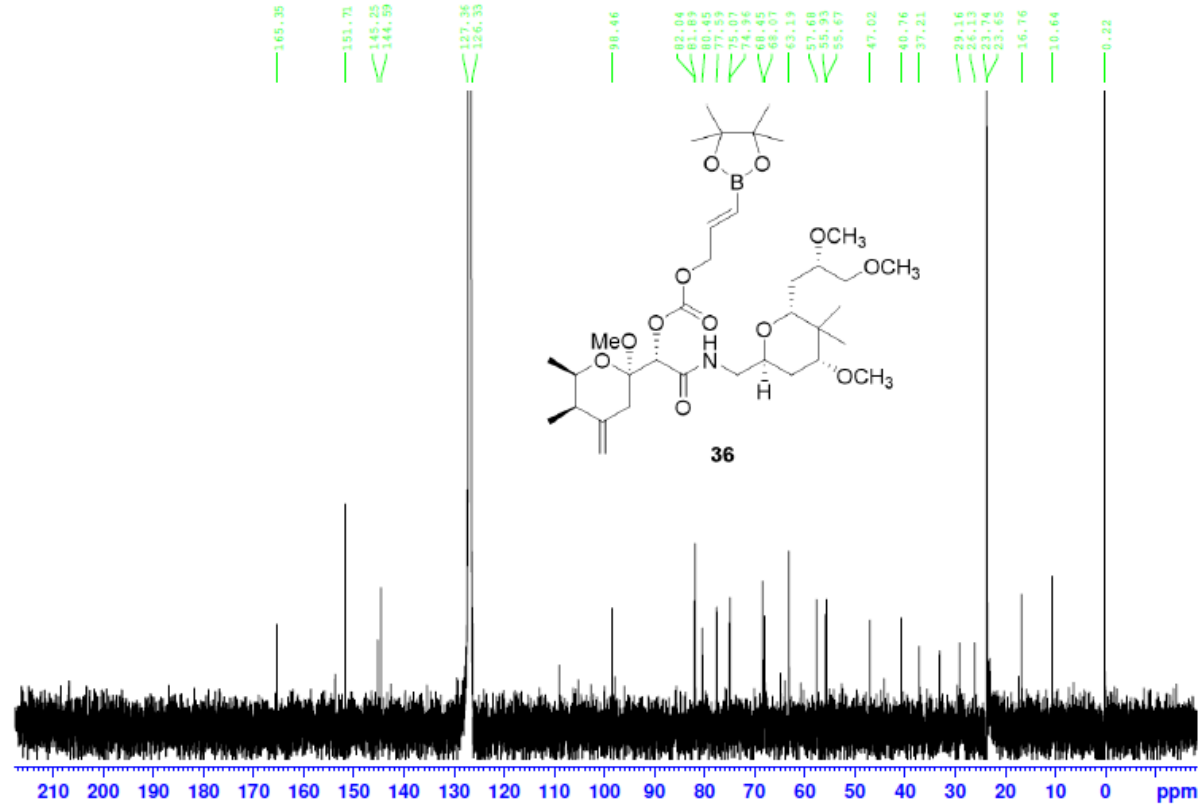

BIBLIOGRAPHY

1. (a) Lovering, F.; Bikker, J.; Humblet, C. *J. Med. Chem.* **2009**, *52*, 6752-6756. (b) Lovering, F. *MedChemComm* **2013**, *4*, 515-519. (c) Hann, M.M.; Leach, A. R.; Harper, G. *J. Chem. Inf. Comput. Sci.*, **2001**, *41*, 856−864.
2. Roughley, S. D.; Jordan, A. M. *J. Med. Chem*. **2011**, *54*, 3451-3479.
3. Allu, T. K.; Oprea, T. I. *J. Chem. Inf. Model*. **2005**, *45*, 1237-1243.
4. Barone, R.; Chanon, M. *J. Chem. Inf. Comput. Sci.* **2001**, *41*, 269-272.
5. Rucker, C.; Rucker, G.; Bertz, S.H. *J. Chem. Inf. Comput. Sci*. **2004**, *44*, 378-386.
6. Whitlock, H. W. *J. Org. Chem*. **1998**, *63*, 7982-7989.
7. Han, X.; Floreancig, P. E. *Angew. Chem., Int. Ed*. **2014**, *53*, 11075-11078.
8. Peh, G. R.; Floreancig, P. E. *Org. Lett.* **2015**, *17*, 3750-3753.
9. Hanna, R. D.; Naro, Y.; Deiters, A.; Floreancig, P. E. *Chem. - Eur. J.* **2018**, *24*, 16271-16275.
10. Caplan, S. M.; Floreancig, P. E. *Angew. Chem., Int. Ed*. **2018**, *57*, 15866-15870.
11. Baxendale, I.R.; Smith, L.K. *Org. Biomol. Chem*., **2015**, *13*, 9907–9933.
12. Zheng, Y.; Tice, C.M.; Singh, S.B. *Bioorg. Med. Chem. Lett.*, **2004**, *24*, 3673–3682.
13. Veber, D. F.; Johnson, S. R.; Cheng, H.-Y.; Smith, B. R.; Ward, K. W.; Kopple, K. D. *J. Med. Chem.*, **2002**,*45*, 2615-2623.
14. (a) Palmes, J. A.; Aponick, A. *Synthesis*, **2012**, *44*, 3699-3721. (b) Raju, B. R.; Saikia, A. K. *Molecules*, **2008**, *13*, 1942-2038. (c) Aho, J. E.; Pihko, P. M.; Rissa, T. K. *Chem. Rev*., **2005**, *105*, 4406-4440. (d) Mead, K. T.; Brewer, B. N. *Curr. Org. Chem*. **2003**, *7*, 227-256.
15. Ley, S. V.; Schucht, O.; Thomas, A. W.; Murray, P. J. *J. Chem. Soc., Perkin Trans. 1*, 1999, 1251–1252.

16. .Falomir, E.; Álvarez-Bercedo, P.; Carda, M.; Marco, J. A. *Tetrahedron Lett.* **2005**, *46*, 8407–8410.

17. McCrae, D.; Dolby, L. *J. Org. Chem*., **1977**, *42*, 1607–1610.

18. Martin, S.; Chou, T. *J. Org. Chem*., **1978**, *43*, 1027–1031.

19. (a) Mongrain, M.; Lafontaine, J.; Bélanger, A.; Deslongchamps, P. *Can. J. Chem*., **1970**, *48*, 3273–3274. (b) Lafontaine, J.; Mongrain, M.; Sergent-Guay, M.; Ruest, L.; Deslongchamps, P. *Can. J. Chem.*, **1980**, *58*, 2460– 2476.

20. Zhang, F.-M.; Zhang, S.-Y.; Tu, Y.-Q. *Nat. Prod. Rep*., **2018**, *35*, 75–104.

21. Rosenberg, S.; Leino, R. *Synthesis*, **2009**, *16*, 2651-2673.

22. Young, J.-j.; Jung, L.-j.; Cheng, K.-m. *Tetrahedron Lett.*, **2000**, *41*, 3411-3145.

23. (a) Paquette, L. A.; Lord, M. D.; Negri, J. T. *Tetrahedron Lett.* **1993**, *34*, 5693-5696. (b) Lord, M. D.; Negri, J. T.; Paquette, L. A. *J. Org. Chem*. **1995**, *60*, 191-195.

24. Osborn, J.A.; Le Ny, J.P.; Gisie, H.; Bellemin-Laponnaz, S., *Angew. Chem. Int. Ed,* **1997,** *36(9)*, 976-978.

25. Grubbs, R.H; Beutner, G.L.; Morrill, C., *J. Org. Chem.*, **2006**, *71*, 7813-7825.

26. Grubbs, R.H; Morrill, C., *J. Am., Chem. Soc*., **2005**, *127*, 2842-2843.

27. Jung, H. H.; Seiders, J. R., II; Floreancig, P. E. Angew. Chem., Int. Ed. 2007, 46, 8464-8467.

28. Wang, Y.; Janjic, J.; Kozmin, S. A., *J. Am., Chem. Soc*., **2002**, *124*, 13670-13671.

29. Xie, Y.; Floreancig, P. E. *Chem. Sci*. **2011**, *2*, 2423-2427.

30. Xie, Y.; Floreancig, P. E. *Angew. Chem., Int. Ed*., **2013**, *52*, 625-628.

31. Xie, Y.; Floreancig, P.E., *Angew. Chem. Int. Ed.* **2014**, *53*, 4926 –4929.

32. Xie, Y, *Ph.D. Dissertation - University of Pittsburgh*, **2014**, pp. 54-69.

33. Arundale, E.; Mikeska, L.A., *Chem. Rev*., **1952**, *51 (3)*, 505–555.

34. Rychnovsky, S.D.; Tadpetch, K., *Org. Lett.*, **2008**, *10(21)*, 4839-4842.

35. (a) Zheng, Y-J.; Tice, C. M., *Expert Opinion on Drug Discovery*, **2016,** *11*(9), 831-834: (b) Rios, R., *Chem. Soc. Rev.*, **2012**, *41*, 1060–1074.

36. : (a) Han, X.; Peh, G. R.; Floreancig, P. E. *Eur. J. Org. Chem.* **2013**, *2013*, 1193-1208. (b) Crane, E. A.; Scheidt, K. A. *Angew. Chem., Int. Ed.* **2010**, *49*, 8316-8326. (c) Olier, C.; Kaafarani, M.; Gastaldi, S.; Bertrand, M. P. *Tetrahedron*, **2010**, *66*, 413-445.

37. Jasti, R.; Vitale, J.; Rychnovsky, S. D. *J. Am. Chem. Soc.* **2004**, *126*, 9904-9905.

38. See the experimental section for details on substrate synthesis.

39. Seeman, J. I. *Chem. Rev.* **1983**, *83 (2)*, 83-134.

40. Johnson, F. *Chem. Rev.* **1968**, *68*, 375-413.

41. Lightstone, F. C.; Bruice, T. C. *J. Am. Chem. Soc.* **1996**, *118*, 2595-2605.

42. "Reprinted (adapted) with permission from {Afeke, C.; Xie, Y.; Floreancig, P. E., *Org. Lett.* **2019**, *21*, 13, 5064-5067.}. Copyright {2019} American Chemical Society."

43. Bardaweel, S. K. et al., *Eurasian J Med,* **2018**, *50(3),* 193-201.

44. Amer, J.; Ghoti, H.; Rachmilewits, E.; Koren, A.; Levin, C.; Fibach, E., *British Journal of Haematology*, **2005** *132*, 108–113.

45. (a) Sabharwal, S.S.; Schumacker, P.T., *Nat Rev Cancer*, **2014**, *14*, 709. (b) Park, I.; Hwang, J.; Kim, Y.; Ha, J.; Park, O., *Ann. N. Y. Acad. Sci.*, **2006**, *1091*, 102. (c) Sandström, M.E.; Zhang, S.J.; Bruton, *J. et al.*, *J. Physiol.*, **2006**, *575*, 251.

46. Najjar, A.; Najjar, A.; Karaman, R., *Molecules*, **2020**, *25*, 884.

47. Schieber, M.; Chandel, N. S., *Curr Biol.*, **2014**, *24(10)*, 453–462.

48. (a) Ja Kim, S., Min Joh, H. & Chung, T. H., *Appl. Phys. Lett*., **2013**, *103*, 153705. (b) Yang, N.; Xiao, W.; Song, X.; Wang, W.; Dong, X., *Nano-Micro Lett*., **2020**, *12(15)*,1-27.

49. (a) Peng, X.; Gandhi, V., *Ther. Deliv.* **2012**, *3*, 823-833. (b) Cadahia, J.P.; Previtali, V.; Troelsen, N.S.; Clausen, M.H., *Med. Chem. Commun*., **2019**, *10*, 1531-1549.

50. Major Jourden, J. L.; Cohen, S. M., *Angew. Chem., Int. Ed*., **2010**, *49*, 6795–6797.

51. Labruere, R.; Pethe, S.; Skarbek, C.; Maslah, H., *Eur. J. Med. Chem*., **2020**, *207*, 112670.

52. (a) Chang, M. C. Y.; Pralle, A.; Isacoff, E. Y.; Chang, C. J. *J. Am. Chem. Soc.* **2004**, *126*, 15392. (b) Lippert, A. R.; Van De Bittner, G. C.; Chang, C. J. *Acc. Chem. Res*. **2011**, *44*, 793.

53. Lo, L.-C.; Chu, C.-Y. *Chem. Commun*., **2003**, *39*, 2728.

54. (a) Srikun, D.; Miller, E. W.; Domaille, D. W.; Chang, C. J. *J. Am. Chem. Soc*. **2008**, *130*, 4596. (b) Lippert, A. R.; Gschneidtner, T.; Chang, C. J. *Chem. Commun*. **2010**, *46*, 7510.

55. Broaders, K. E.; Grandhe, S.; Frechet, J. M. J. *J. Am. Chem. Soc*. **2011**, *133*, 756-758.

56. Mosey, R. A.; Floreancig, P. E., *Org. Biomol. Chem*., **2012**, *10*, 7980–7985.

57. Barhoumi, R.; Burghardt, R. C.; Thompson, D. C., *Toxicology and Applied Pharmacology*, **1998**, *149*, 55–63.

58. Hanna, R. D.; Naro, Y.; Deiters, A.; Floreancig, P.E., *J. Am. Chem. Soc*. **2016**, *138*, 13353−13360.

59. a) Wu, F.; Green, M. E.; Floreancig, P. E., *Angew. Chem. Int. Ed*. **2011**, *50*, 1131 –1134; b) Furusaki, A., Watanab, T.; Matsumoto, T.; Yanagiya, M., *Tetrahedron Lett*. **1968**, *9*, 6301.

60. Pavan, M.; Bo, G., *Physiol. Comp. Oecol*. **1953**, *3*, 307.

61. a) Soldati, M.; Fioretti, A.; Ghione, M., *Experientia* **1966**, *22*, 176; b) Richter, A.; Kocienski, P.; Raubo, P.; Davies, D. E., *Anti-Cancer Drug Des*. **1997**, *12*, 217.

62. Nishimura, S.; Matsunaga, S.; Yoshda, M.; Hirota, H.; Yokoyama, S.; Fusetani, N., *Bioorg. Med. Chem*. **2005**, *13*, 449.

63. Carrasco, L.; Fernandez-Puentes, C.; Vasquez, D., *Mol. Cell. Biochem*, **1976**, *10*, 97

64. Wan, S.; Wu, F.; Rech, J.C.; Green, M.E.; Balachandran, R.; Horne, W. S.; Day, B. W.; Floreancig, P. E., *J. Am. Chem. Soc*. **2011**, *133*, 16668–16679.

65. (a) Matsunaga, S.; Fusetani, N.; Nakao, Y. *Tetrahedron* **1992**, *48*, 8369; (b) Simpson, J. S.; Garson, M. J.; Blunt, J. W.; Munro, M. H. G.; Hooper, J. N. A. *J. Nat. Prod*., **2000**, *63*, 704.

66. Huang, X.; Shao, N.; Huryk, R.; Palani, A.; Aslanian, R.; SeidelDugan, C. Org. Lett. 2009, 11, 867.

67. Rech, J. C.; Floreancig, P. E., *Org. Lett*. **2005**, *7(23)*, 5175–5178.

68. Rech, J.C.; Green, M.E., *Angew. Chem. Int. Ed*. **2008**, *47*, 7317 –7320.

69. Berger, R.; Rabbat, P. M. A.; Leighton, J. L. *J. Am. Chem. Soc*. **2003**, *125*, 9596–9597. Kinnaird, J. W. A.; Ng, P. Y.; Kubota, K.; Wang, X.; Leighton, J. L. *J. Am. Chem. Soc.* **2002**, *124*, 7920–7921.

70. a) Paterson, I.; Goodman, J. M.; Isaka, M. *Tet. Lett*. **1989**, *30*, 7121-7124. b) Paterson, I.; Wallace, D. J.; Cowden, C. J. *Synthesis* **1998**, 639-652.

71. Takai, K.; Kakiuchi, T.; Kataoka, Y.; Utimoto, K. *J. Org. Chem*. **1994**,*59*, 2668-2670.

72. Estrada, A. A.; Zak, M.; Lee, S. H.; Safina, B. S.; Nicolaou, K. C., *Angew. Chem. Int. Ed.* **2005**, *44*, 1378 –1382.

73. Special acknowledgement to Amy Ryan from the research group of Prof. Alexander Deiters (University of Pittsburgh), who performed the cell viability studies for this research.

74. See experimental section for details.

75. Adams, M.A.; Duggan, A.J.; Smolanoff, J.; Meinwald, J.; *J. Am. Chem. Soc*. **1979**, *101*(18), 5364-5370.

76. (a) Nuñez, S. A.; Yeung, K.; Fox, N. S.; Phillips, S. T. *J. Org. Chem*. **2011**, *76*, 10099. (b) Schmid, K. M.; Jensen, L.; Phillips, S. T. *J. Org. Chem*. **2012**, *77*, 4363.

77. Fernandes, G.F.S.; Denny, W.A.; Dos Santos, J.L. *Eur. J. Med. Chem.*, **2019**, *179*, 791-804.

78. Nocentini, A.; Supuran, C.T.; Winum, J.-Y., *Expert Opin. Ther. Pat.*, **2018**, *28*, 493-504.

79. Freund, Y.R., et al., *FEBS Lett*, **2012**, *586*, 3410-3414.

80. Akama, T., et al., *Bioorg. Med. Chem. Lett.*, **2009**, *19*, 2129-2132.

81. Richardson, P.G.; Hideshima, T.; Anderson, K.C., *Cancer Control*, **2003**, *10*, 361-369.